CIRCULARLY POLARIZED RESONATOR ANTENNA

USING AN ELECTROMAGNETIC

BAND GAP MATERIAL

Nuchanart Fafiem

A Thesis Submitted in Partial Fulfillment of the Requirements for the

Degree of Doctor of Philosophy in Telecommunication Engineering

Suranaree University of Technology

Academic Year 2014

สายอากาศเรโซเนเตอร์ที่มีโพลาไรซ์แบบวงกลม
โดยใช้วัสดุช่องว่างแถบความถี่แม่เหล็กไฟฟ้า

นางสาวนุชนาฏ ฝาเฟี้ยม

CIRCULARLY POLARIZED RESONATOR ANTENNA

USING AN ELECTROMAGNETIC BAND GAP MATERIAL

Suranaree University of Technology has approved this thesis submitted in partial fulfillment of the requirements for the Degree of Doctor of Philosophy.

Thesis Examining Committee

_____

(Prof. Dr. Prayoot Akkaraekthalin)

Chairperson

_____

(Asst. Prof. Dr. Piyaporn Mesawad)

Member (Thesis Advisor)

_____

(Assoc. Prof. Dr. Rangsan Wongsan)

Member

_____

(Assoc. Prof. Dr. Peerapong Uthansakul)

Member

_____

(Assoc. Prof. Dr. Chuwong Phongcharoenpanich)

Member

_____   _____

(Prof. Dr. Sukit Limpijumnong)   (Assoc. Prof. Flt. Lt. Dr. Kontorn Chamniprasart)

Vice Rector for Academic Affairs   Dean of Institute of Engineering

and Innovation

นุชนาฏ ฝาเฟี้ยม : สายอากาศเรโซเนเตอร์ที่มีโพลาไรซ์แบบวงกลมโดยใช้วัสดุช่องว่าง
แถบความถี่แม่เหล็กไฟฟ้า (CIRCULARLY POLARIZED RESONATOR ANTENNA
USING AN ELECTROMAGNETIC BAND GAP MATERIAL) อาจารย์ที่ปรึกษา :
ผู้ช่วยศาสตราจารย์ ดร.ปิยาภรณ์ มีสวัสดิ์, 163 หน้า.

ในปัจจุบันการสื่อสารไร้สายได้ถูกพัฒนาขึ้นอย่างรวดเร็ว ซึ่งนับได้ว่ามีความสำคัญเป็น
อย่างยิ่งที่จะเพิ่มประสิทธิภาพการส่งสัญญาณของสายอากาศ ให้สามารถตอบสนองความต้องการ
ของผู้ใช้ที่อยู่ในพื้นที่ให้บริการได้อย่างไม่มีข้อผิดพลาด เพื่อให้ผู้ใช้สามารถรับสัญญาณได้ในทุก
กรณี ไม่ว่าสายอากาศภาครับจะวางตัวในแนวใดก็ตาม จึงเป็นที่มาของความต้องการสายอากาศ
โพราไรซ์แบบวงกลมที่มีเพิ่มมากขึ้น ดังนั้นงานวิจัยนี้จึงได้ออกแบบสายอากาศสำหรับสถานีฐาน
เพื่อรองรับเทคโนโลยีในยุค 3.9G ซึ่งควรที่จะมีอัตราขยายสูง เนื่องจากที่ความถี่ที่ 2.1 GHz สามารถ
เกิดการสูญเสียระหว่างการเดินทางของคลื่นได้สูงขึ้น โดยที่สายอากาศประกอบด้วย
2 องค์ประกอบหลัก ได้แก่ (1) สายอากาศสตริปไดโพลโค้ง (curved strip dipole) ซึ่งมีข้อดีหลาย
ประการ อาทิเช่น มีความกว้างลำคลื่นครึ่งกำลังสูง ราคาถูกและออกแบบง่าย และ (2) ช่องว่างแถบ
ความถี่แม่เหล็กไฟฟ้า (Electromagnetic Band Gap หรือ EBG) ถูกนำมาประยุกต์ใช้สำหรับเพิ่ม
อัตราขยายของสายอากาศโดยใช้ทำงานร่วมกับแผ่นตัวนำ เรียกว่า สายอากาศเรโซเนเตอร์
(resonator antenna) นอกจากนี้เพื่อให้เกิดโพลาไรซ์แบบวงกลม สายอากาศสตริปไดโพลโค้ง
จึงถูกนำมาวางเอียง 45° บนแผ่นตัวนำ โดยให้ช่องว่างแถบความถี่แม่เหล็กไฟฟ้าเป็นตัวโพลาไรซ์
(polarizer) สายอากาศถูกจำลองแบบและวิเคราะห์ด้วยโปรแกรมสำเร็จรูป CST ค่า S_{11} อัตราส่วน
แกน (axial ratio) รูปแบบการแผ่กระจายกำลังงาน (radiation pattern) และอัตราขยาย (gain) จะถูก
แสดงผล เทคนิคการออกแบบสายอากาศสามารถยืนยันได้ด้วยผลวัดสายอากาศต้นแบบ พบว่า
มีความสอดคล้องกับผลการจำลองแบบ โดยสายอากาศที่ถูกนำเสนอมีความกว้างแถบความถี่
ครอบคลุมตั้งแต่ 1.87 - 2.17 เมกะเฮิรตซ์ และมีอัตราขยาย 15.11 dB

สาขาวิชาวิศวกรรมโทรคมนาคม   ลายมือชื่อนักศึกษา _____

ปีการศึกษา 2557   ลายมือชื่ออาจารย์ที่ปรึกษา _____

NUCHANART FAFIEM : CIRCULARLY POLARIZED RESONATOR
ANTENNA USING AN ELECTROMAGNETIC BAND GAP MATERIAL.
THESIS ADVISOR : ASST. PROF. PIYAPORN MESAWAD, Ph.D.,
163 PP.

CURVED STRIP DIPOLE/CIRCULARLY POLARIZATION/RESONATOR
ANTENNA/ELECTROMAGNETIC BAND GAP

Nowadays, wireless communications are developing rapidly, which highlights the importance of increasing the transmission efficiency of antennas. The main responsibility towards mobile users is that the antenna should be totally free of error, irrespective of which way the receiving antenna is directed. For this reason, a circularly polarized antenna is widely required. Therefore, this research designs the base station antenna for 3.9G technology, which the antenna should have high gain. In consideration of high frequency at 2.1 GHz, the path loss between transmitting and receiving antennas are increased. The antenna consists of two main components, (1) a curved strip dipole, with advantages such as its wide beamwidth, economical and simple design, (2) electromagnetic band gap (EBG) which has practical use for high gain antenna. When a curved strip dipole is fed and placed an between EBG and conductor plane, it is called a resonator antenna. Furthermore, the circularly polarized antenna is created by an EBG polarizer and a curved strip dipole placed on a conductor plane at 45˚. The antenna was designed and analyzed by using a computer simulation technology (CST), S_{11}, axial ratio, radiation pattern and gain are displayed. The designed technique has been confirmed by measurement results from our prototype antenna corresponding to simulation results. The proposed antenna has a

bandwidth covering the frequency range of 1.87 − 2.17 GHz, the gain of the antenna increases up to 15.11 dB.

School of <u>Telecommunication Engineering</u>   Student's Signature _____

Academic Year 2014   Advisor's Signature _____

ACKNOWLEDGEMENTS

Nuchanart Fafiem

TABLE OF CONTENTS

TABLE OF CONTENTS (Continued)

TABLE OF CONTENTS (Continued)

TABLE OF CONTENTS (Continued)

TABLE OF CONTENTS (Continued)

LIST OF TABLES

LIST OF FIGURES

LIST OF FIGURES (Continued)

LIST OF FIGURES (Continued)

LIST OF FIGURES (Continued)

LIST OF FIGURES (Continued)

LIST OF FIGURES (Continued)

CHAPTER I

INTRODUCTION

1.1 Background of problems

Nowadays, wireless communications have been developed for entertainment, education, economic, health, industry, and so on. The most popular wireless communication technology is the mobile communication system, especially mobile phones. It is an electronic instrument, where communication with a mobile base station is by using the radio wave. Mobile communications have changed dramatically during the last decades due to the growth of mobile capabilities. The first generation (1G) cellular systems for mobile communication had only analogue voice facility. These were replaced by second generation (2G) digital phones with added fax, data, and messageing services. The 2G systems have been developed to support higher data rate using HSCSD (High Speed Circuit Switch Data), GPRS (General Packet Radio Services), and EDGE (Enhanced Data rates for Global Evolution) technologies. The third generation (3G) system has added multimedia facilities to 2G phones, that are presently utilized in Thailand. The applications of 3G are mobile TV, video on demand, video conferencing, telemedicine, GPS (Global Positioning System), and so on. In addition, the 3.9G is developed to use in Thailand at 2.1 GHz, it is pre-4G technology which provides an information transfer rate of 42 Mbps. The advantage of 3.9G technology is to provide a higher speed internet than 3G technology. Moreover, the fourth generation (4G) mobile technology is expected to make available more advance features such as all-IP packet-switched networks, mobile ultra-broadband

(gigabit speed) access, and multi-carrier transmission. The data rates are expected to grow up to around 100 Mbps. For that reason, mobile base station antenna techniques also have been rapidly developed to keep up with the increased number of users within a service area. The antenna requirement for these system properties are high gain and high efficiency. Therefore, the proposal of this research is to design a high gain antenna for mobile base stations. Futhermore, the proposed antenna should have high power handing capability and coverage of a broad area.

Dual polarization antennas with sector-shaped radiation patterns are often required for mobile communication systems. To radiate the dual polarized wave, two dipole antennas need to be used with dual feeding (Liu, et. al, 2004; Mak, Wong, and Luk, 2007; Abas, et. al, 2013). They are placed at $\pm45°$ angle and arrayed to improve the gain, but it is hard to fabricate the feed system. However, the dipole antenna is still interesting in wireless communication systems because it has an elementary structure, simple concept, and broadband characteristics (Han, et. al, 2012; Azad and Ali, 2008; Zhang, et. al, 2004). If the dipole is bent to half curved, it has a wider beamwidth than a straight dipole (Fhafhiem, et. al, 2009). One solution to enhance the antenna gain of an antenna is to use a metallic reflector which is located at the back of dipole with the gap as a quarter wavelength (Thumvichit and Takano, 2006; Zhan and Rahmat-Samii, 2000). Unfortunately, the main disadvantage of an antenna on a metallic plane is that it results in the overall size of the antenna too big and bulky for the low frequency range of operation. Besides, the reflector plane cannot suppress the surface wave, so the antenna gain and efficiency will then be greatly decreased.

In recent years, metamaterials based on electromagnetic band gap (EBG) structures have been widely investigated in the antennas domain to enhance gain and radiation efficiency (Yang, F. and Rahmat-Samii, 2008). The metamaterials classified by a permittivity and permeability are primarily dependent on the geometrical properties of an inclusion shape and mutual distance between the lattices constant. The EBG can be applied to grating, frequency selective surface (FSS), and so on. It is not only used as a reflector plane (Grelier M., et. al, 2012; Nakano H., et. al, 2009), but also adapted for a superstrate of the primary radiator with the reflector plane (Rodes, et. al, 2007; Hajj, et. al, 2009; Fhafhiem N., et. al, 2013; Trentini G. V., 1956). The main advantage of the EBG resonator is enhancing gain and efficiency. In any case, there are only a few papers that have really proposed the EBG structures for polarization adjustment (Lin Peng, et. al, 2010; Wu, et. al, 2013).

In this thesis, the high directive gain of the dual and circularly polarized antenna for mobile base station is presented. The proposed resonator antenna consists of two main components, a curved strip dipole as a primary radiator mounted on a U-shaped reflector plane and the metallic rod type metamaterial as a superstrate. The gain and polarization of the antenna are adjusted by using the metallic rod type metamaterial demonstrated a double positive medium behavior which acts as partially reflective surface. If the horizontal polarization of the EBG (in x axis) is placed above a primary radiator, it can only improve the gain in horizontal polarization. Therefore, the gain in vertical polarization is improved by using the vertical polarization of the EBG (in y axis). Consequently, two layers of the metamaterial, in horizontal and vertical polarizations, are combined for the dual polarized antenna with high gain enhancement. In addition, the polarizer is added and placed on the top of the EBG

polar H and V, it is possible to generate a 90˚ phase shift between the electric field in *x* and *y* axises. The circularly polarized resonator antenna could be obtained as revealed in Figure 1.1.
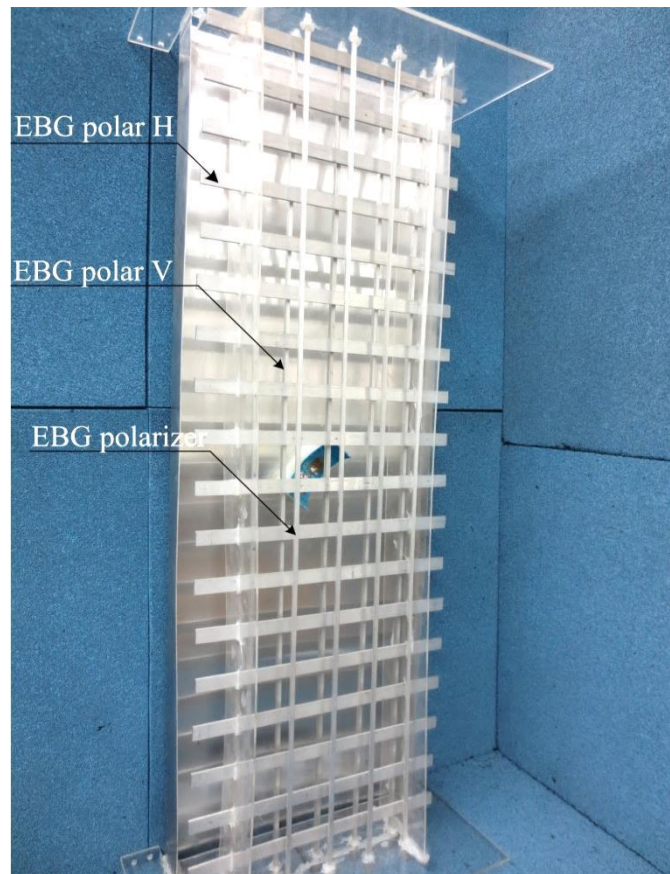
Figure 1.1 Circularly polarized resonator antenna using an EBG material.

1.2 Research objectives

The objective of this research is organized as follows:

1.2.1 To study mobile base station antenna at the frequency band of 2.1 GHz.

1.2.2 To design and simulate the dual and circularly polarizations of a resonator antenna by using a 45˚ oriented curved strip dipole and metallic rod type metamaterial.

       1.2.3   To verify the performance of the antenna, the prototype is fabricated and tested.

1.3   Scope and limitation of the study

       1.3.1   To characterize circularly polarization antenna by using a curved strip dipole antenna and electromagnetic band gap.

       1.3.2   To simulate the resonator antenna by using CST Microsoft Studio.

       1.3.3   To develop and design the antenna for mobile communication systems at 2.1 GHz.

1.4   Expected Benefits

       1.4.1   To enhance the performance of mobile base station antenna at 2.1 GHz.

       1.4.2   To achieve a prototype of the antenna at 2.1 GHz.

1.5   Thesis organization

       The remainder of this thesis is organized as follows. Literature review is discussed in Chapter 2. This chapter presents several types of antenna for wireless communications found in the literatures from text book and academic publications. In addition, we briefly overview the dipole antenna, electromagnetic band gap, dual polarization antenna, and circularly polarization antenna.

       Chapter 3 presents the principle of cellular systems and choosing a mobile base station antenna. Furthermore, the theory of dipole antenna and metamaterials are described.

       In Chapter 4, the analysis and design of the base station antenna is presented. The dual and circularly polarization of resonator antenna is studied by using CST

Microwave Studio. A 45˚ oriented curved strip dipole and metallic rod type EBG is considered.

Having confirmed the validity of this base station antenna approach, the antenna prototype is fabricated and tested which are given in Chapter 5. Then, the performances obtained from experimental results are compared with the ones from simulation results.

In the last chapter, chapter 6 provides conclusions of the research work and suggestion for future studies.

CHAPTER II

LITERATURE REVIEW

2.1 Introduction

Due to the rapid development of mobile communication systems, the study of an antenna design for cellular system has been improved. The aim of this thesis is as follows: the dual polarized resonator antenna is designed by using a 45˚ oriented curved strip dipole on reflector plane and double polarizing metallic EBG layers. Furthermore, the circularly polarized resonator antenna is improved from the dual polarized resonator antenna by simply adding the metallic EBG which is called polarizer. This antenna is applied for 3rd and 4th generations of cellular network. Therefore, the open literature about the antenna for mobile communication systems, electromagnetic band gap evolution for antenna design, dual polarized antenna and circularly polarized antenna are researched at the present moment.

2.2 Literature research

2.2.1 Dipole antenna in mobile communication systems

In mobile communication systems, the bridge between user terminal and the Base Station Controller (BSC) is a base station antenna. The development of antennas with new performances becomes currently imperatively essential for the new services and network of telecommunication. To achieve the requirements, the basic antenna such as the dipole antenna is widely applied in the cellular mobile communication systems because it has elementary structure, simple concept, and broadband characteristics. Firstly research, the literature about modified shape of dipole antenna is researched. In 2004, a dipole antenna was remodeled for S-shaped (Elkamchouchi and Abu Nasr, 2004) as shown in Figure 2.1. An S-shaped dipole

antenna has wide beamwidth and it radiates elliptically polarized waves. In addition, the optimum shape of a symmetrical wire antenna for maximum directive gain has been obtained by using a pricewise parabolic approximation (Cheng and Liang, 1982) as displayed in Figure 2.2. Apart from this, the various structures of V-shaped dipole are compared and shown in Figure 2.3. When the arm of dipole is optimized and the dipole is turned to upside down. Its side lobe is reduced (Paez, 2009). The next technique of the gain enhancement is a V-shaped antenna using two arc-curved dipoles located on the reflector plane (Krishnan and Leong, 2005) as denoted in Figure 2.4. In (Thumvichit and Takano, 2007; Dubost, 1981), a straight dipole is closed to the reflector plane for high gain. In addition, a curved dipole is shorted ends on reflector plane for wide beamwidth and gain enhancement. The structures are demonstrated in Figure 2.5. All of above mentioned, a dipole antenna is popularly applied for various shapes in wireless communication.
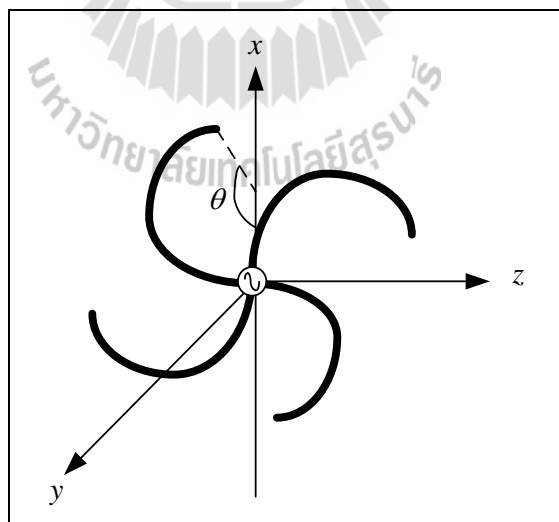
Figure 2.1 S-shaped dipole antenna.
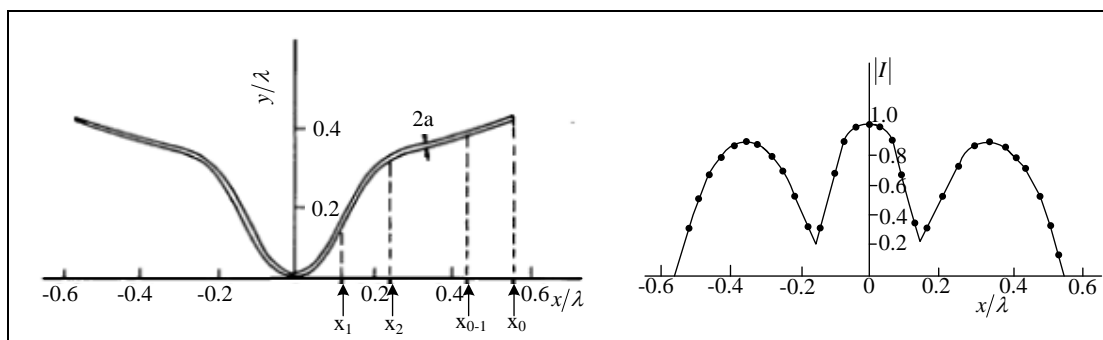
Figure 2.2 Shaped symmetrical wire antenna.
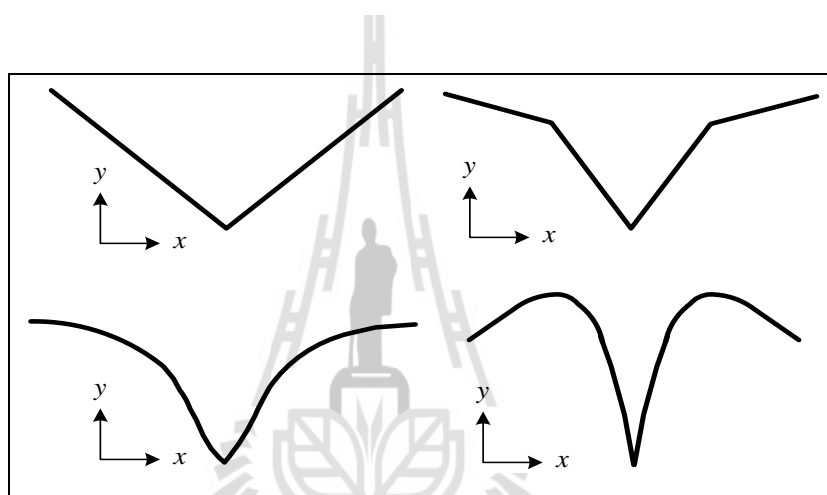
Figure 2.3 Four different types of curved dipole antenna optimum.
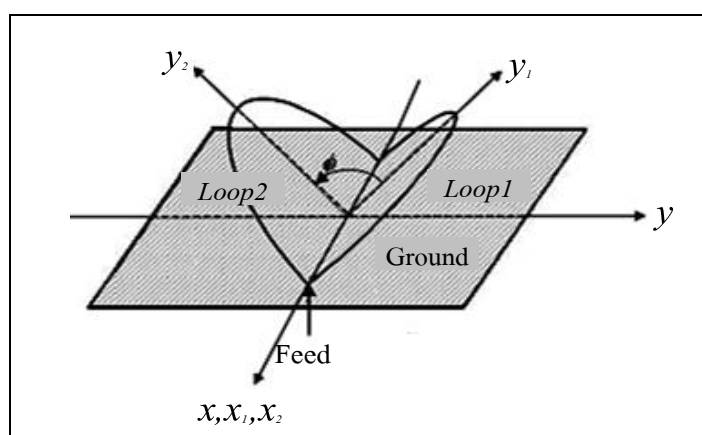
Figure 2.4 V-shape antenna.
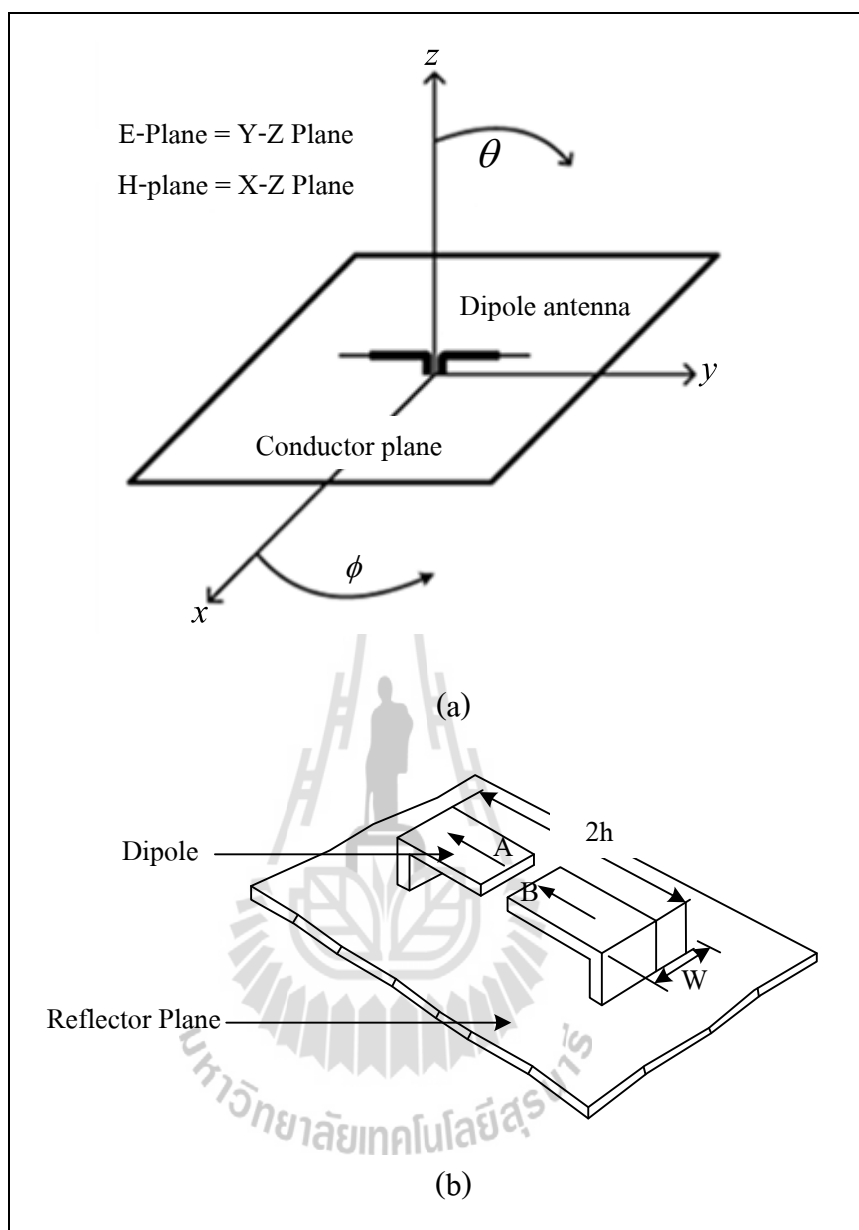
Figure 2.5 Antenna on conductor plane (a) the strength dipole antenna

and (b) shorted end dipole antenna.

Furthermore, this thesis attentively presents the papers about base station antenna trend that the initial 3G sector antenna is maintained the performance (Stephen, et. al, 2003). The dipole antenna has become one of the most common and widely used in base station antennas such as a wideband dipole antenna for 3G base

station, consisting of two dipole arms which are only connected through a parallel strip line as shown in Figure 2.6 (Wu Di, et. al, 2005). Moreover, the novel dual-broadband planar antenna is proposed for 2G/3G/LTE base station. This antenna consists of one element for the lower band and two elements for the upper band, making it possible to be arrayed as shown in Figure 2.7 (YueHui Cui, et. al, 2013). In addition, the dipole linear arrays that are aligned in parallel with compact size was presented for next generation mobile communication base station application (Young Bae Jung, 2013) as shown in Figure 2.8. All above literatures seem that the dipole antenna is most commonly used for mobile base station antenna and the average directive gain is around 10 – 18 dBi. At the frequency band of 1.92 – 2.17 GHz, the broadband dipole and the dual polarization techniques were presented (Zhen Qi Kuai, 2005) for WCDMA base station as appeared in Figure 2.9. If we could design the antenna to increase the directive gain, it will have more efficiency for field radiating. Therefore, many new technologies have appeared in the current antenna design and one exciting discovery is the development of Electromagnetic Band Gap (EBG) structures as illustrated in next topic.
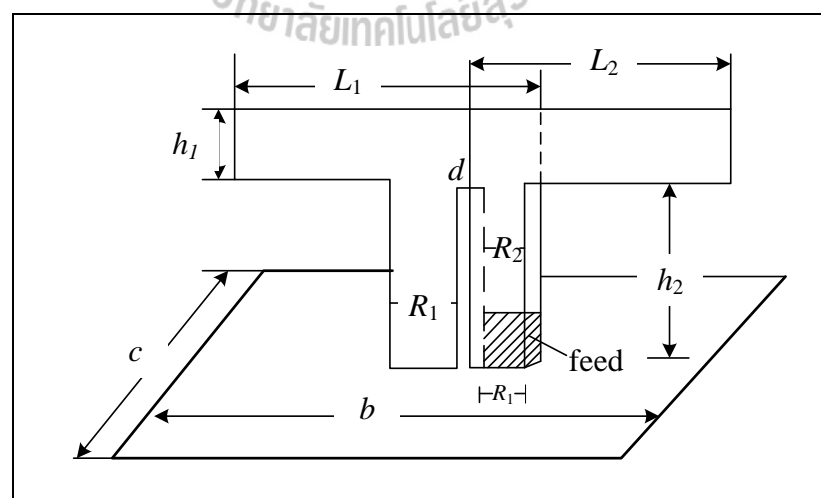
Figure 2.6 Wideband dipole antenna for 3G base station.
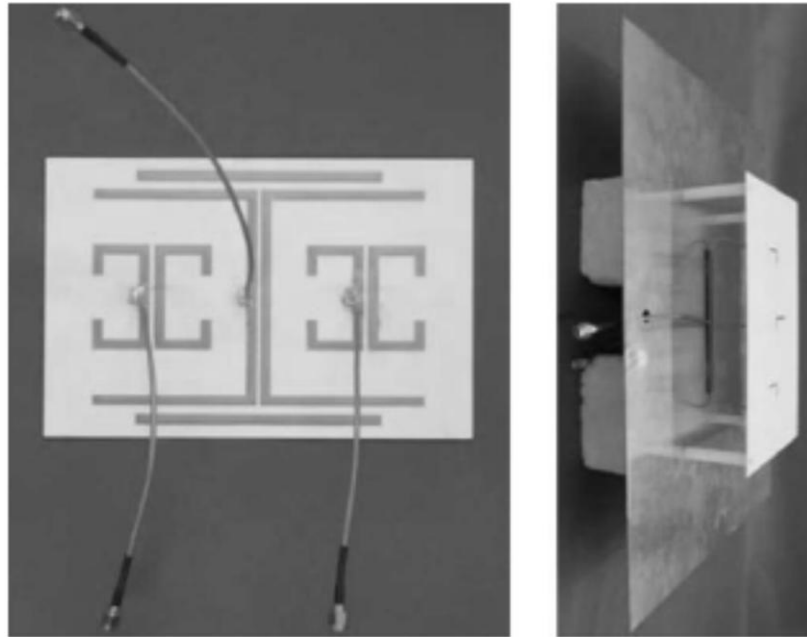
Figure 2.7 Dual-broadband base-station antenna.
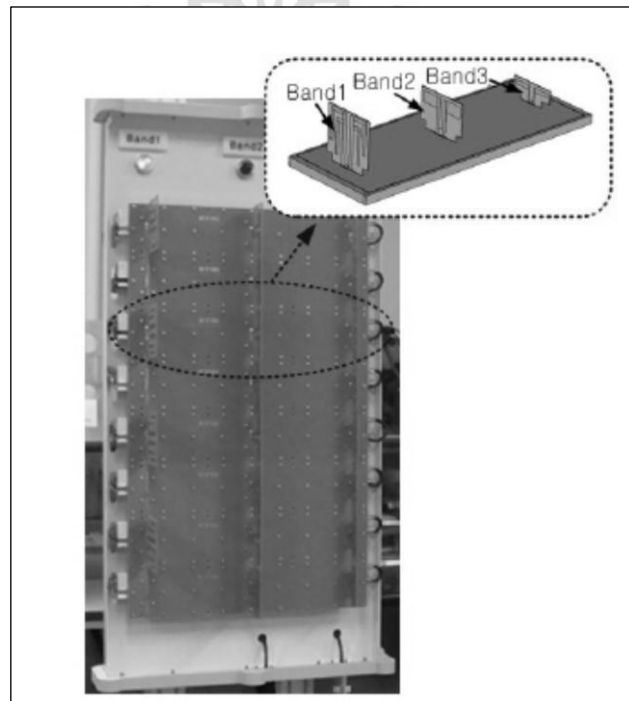
Figure 2.8 Multi-band reconfigurable base station antenna.
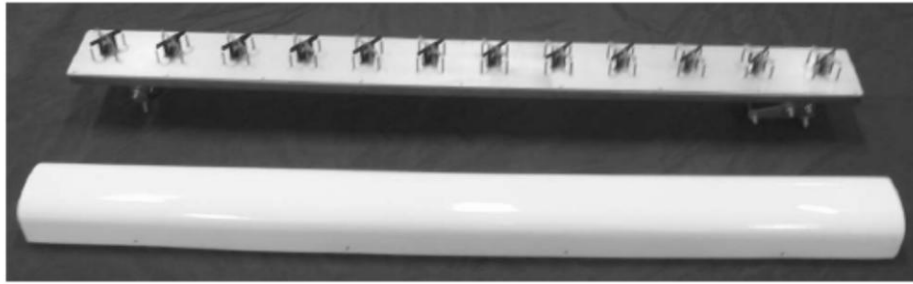
Figure 2.9 Broadband printed dipole base station antenna.

2.2.2 Antenna with Electromagnetic Band Gap (EBG)

The EBG structures applications in the antenna designs have become a thrilling topic for antenna engineering. It is a matter of the EBG structure technology, a new technology for the improvement of the antenna performances, applicable on an extremely wide frequency spectrum covering from the acoustic to the optical frequencies. In addition EBG structures, also known as photonic crystals, are also used to improve the performance of the antenna. The EBG can be applied to grating, frequency selective surface (FSS), and so on. Moreover, the EBG is not only used to a reflector plane (Fhafhiem, et. al, 2010; Huan Yi and Shi-Wei, 2013; Abkenar, et. al, 2011) as shown in Figure 2.10, but also adapted for a superstrate of the primary radiator with reflector plane (Rodes, et. al, 2011; Hajj, et. al, 2009; Pirhadi A., et. al, 2007; Farahani H.S, et. al, 2010) as shown in Figure 2.11.

(a)

(b)

(c)
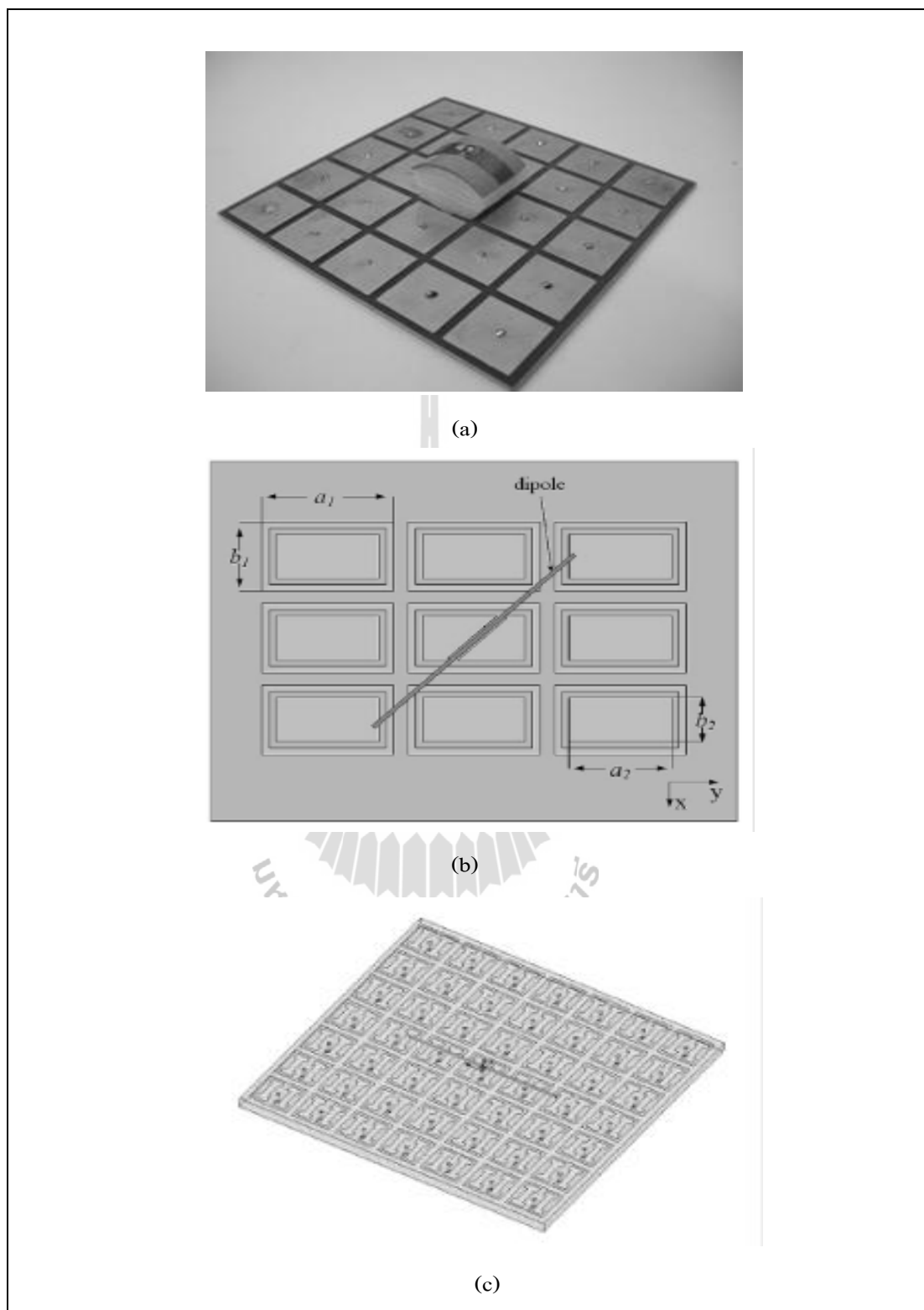
Figure 2.10 The antenna over EBG reflector plane (a) curved strip dipole, (b) printed

dipole, and (c) straight dipole.

When EBG is performed as a reflector plane, it can control the reflection phase to become a low profile antenna and moderately improve gain performance, when EBG is used to superstrate on excitation feed with reflector plane. The advantage of an EBG resonator antenna is that it increases the gain of the antenna and can vastly increase the radiation efficiency (Yuehe Ge, et. al, 2012) because it is the resonator antenna as illustrated in Figure 2.12.
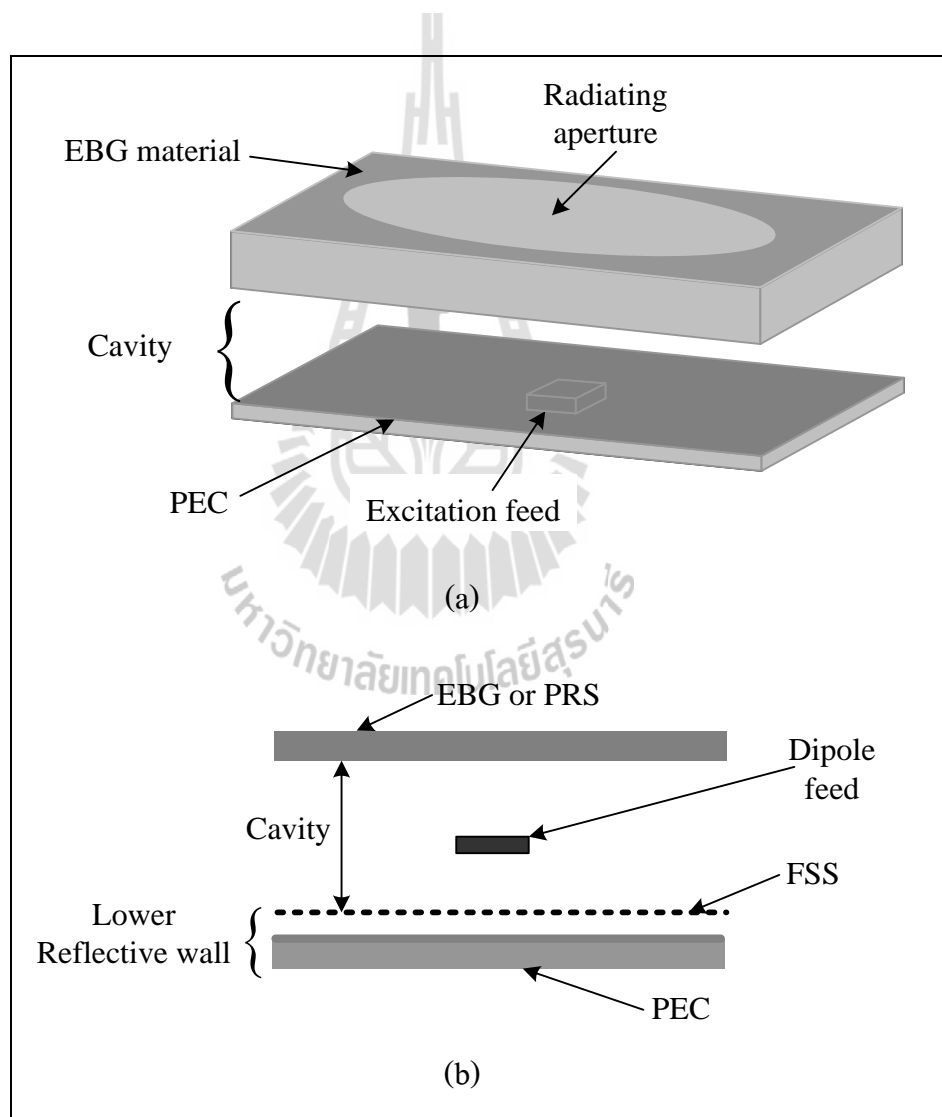
Figure 2.11 EBG superstrate on excitation feed (a) patch antenna, (b) dipole antenna, (c) HIS and patch antenna, and (d) arrayed patch antenna.
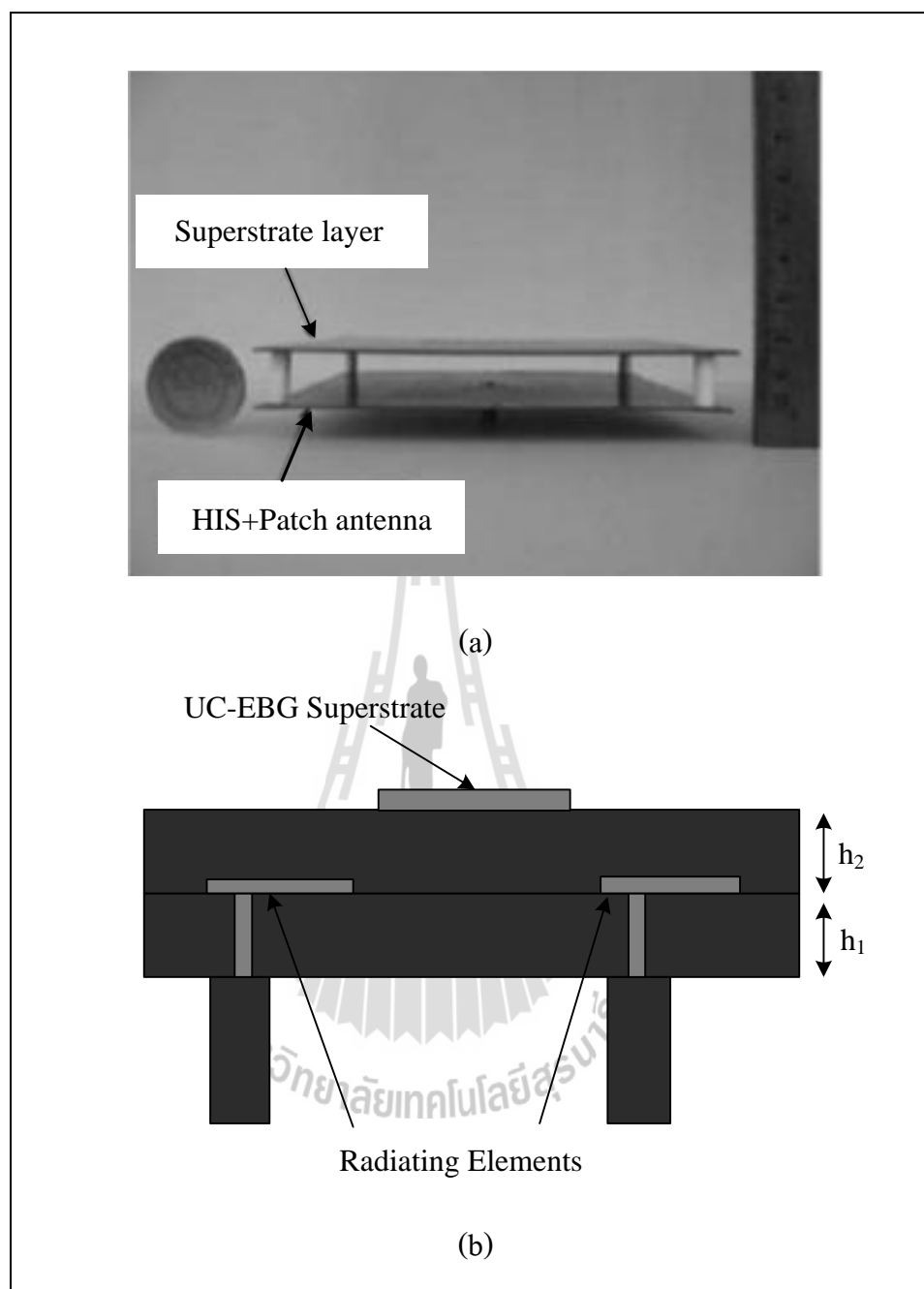
Figure 2.11 EBG superstrate on excitation feed (a) patch antenna, (b) dipole antenna,

(c) HIS and patch antenna, and (d) arrayed patch antenna (cont.).
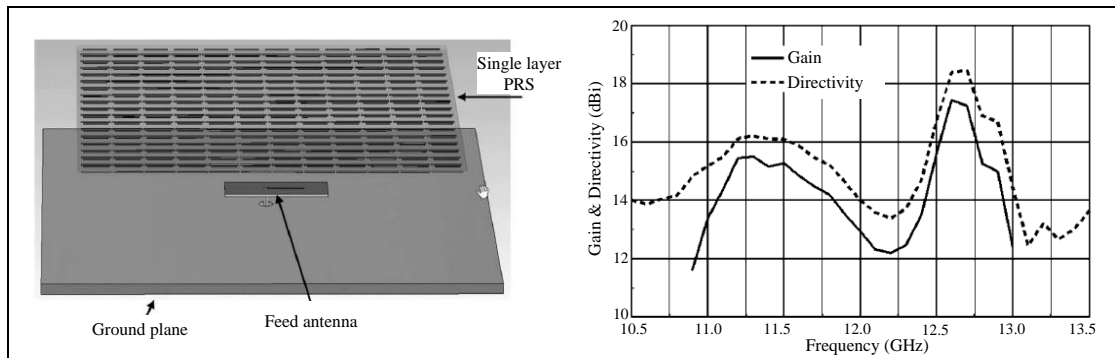
Figure 2.12 High gain resonator antenna.

2.2.3   Dual polarization antenna

Dual polarization antennas with sector-shaped radiation pattern are often required for mobile communication systems. To radiate the dual polarized wave, a microstrip patch antenna is excited by using two SMA connectors for orthogonal polarization and also added double layer printed orthogonal dipole arrays for the gain enhancement (Moghadas, et. al, 2011). In this letter, the feeder has complicated mechanisms: similarly, a dual polarization patch antenna double fed by an L-shaped probe (Yong-Xin, et. al, 2002). Figures 2.13 and 2.14 show the mechanism of feeder which is radiated dual polarization. Additionally, a dual polarized dipole antenna is designed by using two pairs of radiating arms providing orthogonally polarized radiator (Ying Liu, et. al, 2013) as shown in Figure 2.15.
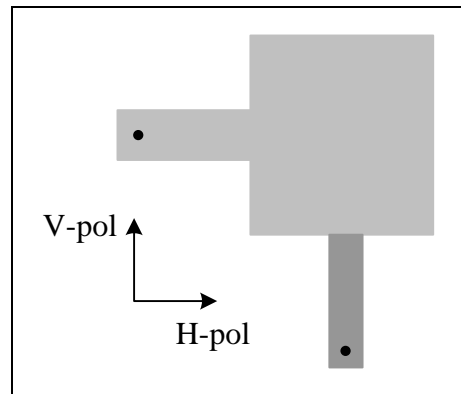
Figure 2.13 Dual-band and dual polarized microstrip antenna fed

by two SMA connectors.
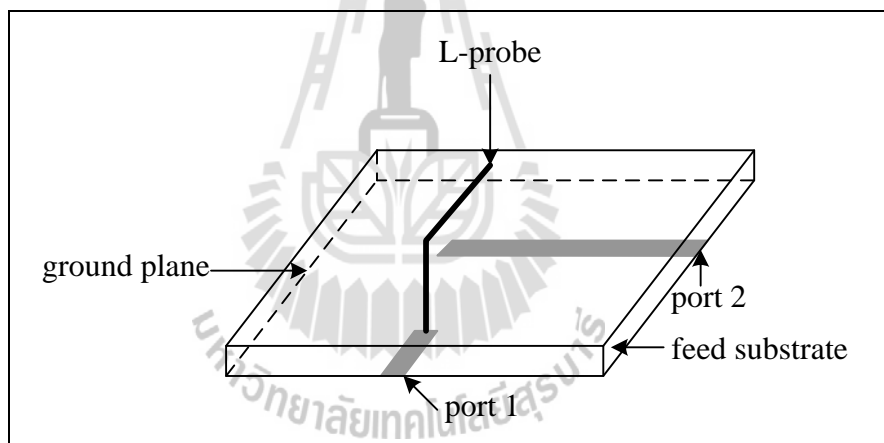
Figure 2.14 Feed system of dual polarization patch element for cellular phone

base station.
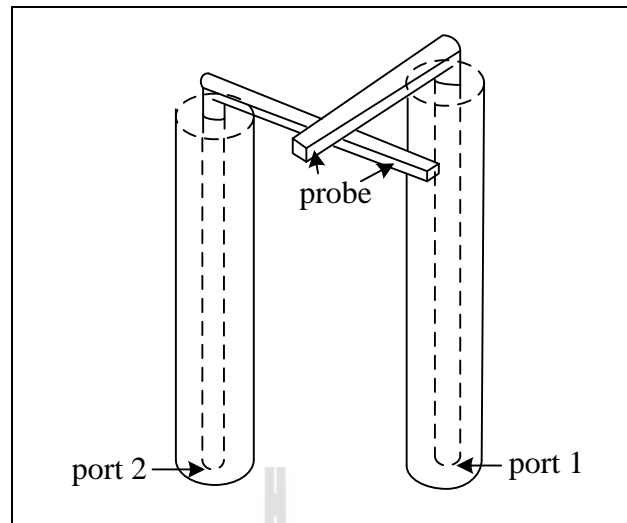
Figure 2.15 Geometry of L-shaped probes.

2.2.4 Circularly polarization antenna

The circularly polarized antenna has various types in wireless communication system. For example, a low profile single dipole antenna radiating circularly polarized wave (Yang and Rahmat-Samii, 2005) and a novel design of circularly polarized sectoral M-PRS antenna (Hajj, et. al, 2010) are studied. Firstly, a dipole antenna is used for exciting feed and placed on EBG reflector plane. It is placed on EBG at a 45˚ angle. When a gap between dipole and EBG is proper high, the reflected field becomes perpendicular to the directly radiating field with a 90˚ phase difference. Therefore, a right hand circularly polarization electromagnetic wave is obtained. The geometry is illustrated in Figure 2.16. Secondly, a circular polarization is occurred by using a collaboration between a patch microstrip antenna and an EBG because of a patch microstrip antenna fed on its diagonal for controlling and switching horizontal and vertical polarizations as exhibited in Figure 2.17. Furthermore, the gain is escalated by using EBG polar H and V, so two perpendicular electromagnetic plane waves are equal and 90˚ phase different.
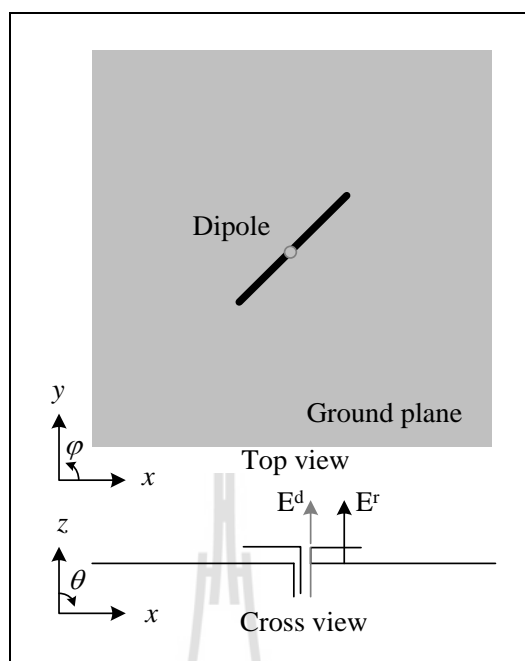
Figure 2.16 Circularly polarized antenna by using dipole antenna with 45˚ angle

on EBG reflector plane.
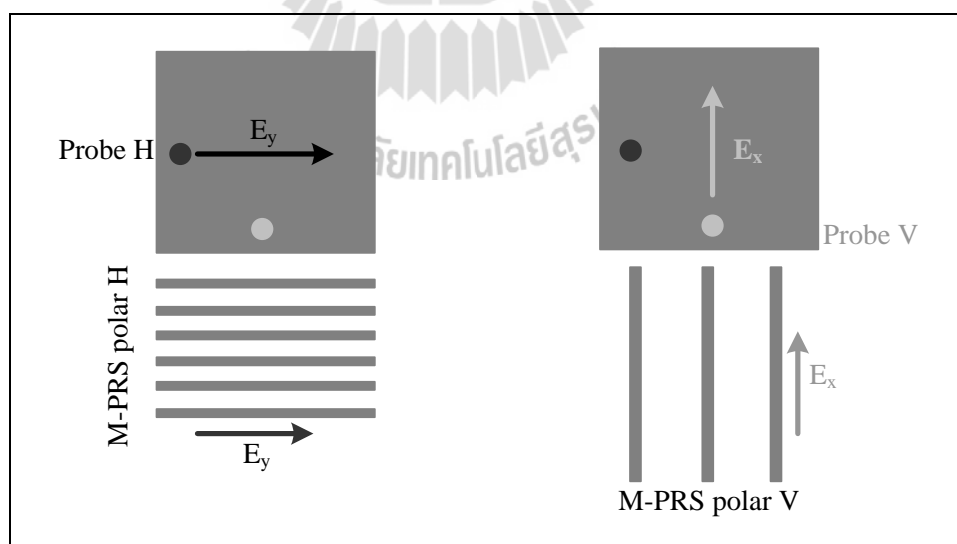
Figure 2.17 Circularly polarized antenna by using dual feeder.

2.3   Chapter summary

The content of this Chapter presents information about the shape modification of dipole antenna in wireless communication and 3G sector antenna performance. Moreover, the design of the high gain, dual polarization, and circular polarization are studied and discussed. Therefore, we conclude that when a 45° oriented dipole antenna is placed on EBG reflector plane, it has unsuitable gain for mobile base station antenna. If we use a patch microstrip antenna with dual feed, the circularly polarization antenna is rather complicated feeding, when compared to one feeder. Therefore, this research presents a curved strip dipole antenna placed on the metallic reflector plane at 45° angle. Furthermore, the primary radiator enhances the gain in x and y axis by using EBG. The elementary aim, a dual polarization resonator antenna using EBG material is occurred. Finally, when the EBG polarizer is placed on the top of double layers EBG, it is possible to generate a 90° phase shift between the electric field in x and y axis. Hence, this antenna is said to be a high directivity circularly polarized antenna. All above the prediction is researched in Chapter 3 and also will be simulated in Chapter 4.

CHAPTER III

BACKGROUD THEORY

3.1 Introduction

The antenna is a device for converting electromagnetic radiation in space into electrical currents in conductors, depending on whether it is being used for receiving or transmitting. The majority of the antenna characteristics such as its radiation pattern and gain are important to study. In this chapter describes the antenna characteristics for mobile communication system. In addition, a dipole theory, matching technique, metamaterials classification, electromagnetic band gap, electromagnetic wave propagation, and polarization of plane wave are illustrated in this chapter.

3.2 Antenna in cellular system

Antennas are a key in a cellular phone system; an antenna converts guided radio wave energy to energy that is radiated into free space. An antenna also does the reverse, it receives radio waves from the air and feeds them into the devices that detect, decode and amplify them. In cell phone system, there are one antenna in the handset and another in the base station tower. Both of these antennas transmit and receive waves. Base station antennas are the rectangular devices, usually in groups of three, mounted high on a base station tower. The base station can be thought of as the command center that both sends and receives signals to the consumer's hand set. The base station performs a router function to property direct incoming and outgoing calls, and a repeater function to enable the consumer to communicate from cell to cell

within the terrestrial cellular network. The base station antenna is mounted on tall towers because from this high point it is easier to stay in communication with cell phone users, who are often near the ground.

When designing cellular phone antennas, especially balance several different is concerned. The first, all transmitting antennas radiate energy in a particular pattern that depends on the shape of the antenna and other factors. It is the best for a cellular system if the pattern is roughly parallel to the ground, where most cell phone users are located. Another important concern is called gain, which refers to the fact that an antenna does not transmit (or receive) waves from every direction with equal sensitivity. A third factor is physical size, because of an antenna have to be placed along roads and in other public places. They cannot be too tall and large. A cellular handset antenna is the small component embedded in the handset case and is not visible to the user. The cell phone handset antennas pose a different set of the problem than the base station. Since a cell phone user is constantly changing his or her position and moving from cell to cell, the mobile phone requires an antenna that transmits and receives equally well in all direction.

All of above mentioned a mobile base station antenna is important for efficiency of mobile cellular system.

3.3   Choosing a mobile base station antenna

An antenna is a communication system bridge between a user terminal and base station control equipment, widely applying to cellular mobile communication system. As the communication technology is developing, antennas will be on progress consequentially. The mobile communication system in the seventies adopted

omnidirectional antennas or angle reflector antenna, for the reason that a few carriers and base stations can meet the demands of few users in a mobile communication system of a city. As the economy goes forward, the amount of mobile terminals, whose demands cannot be met by the old base stations, is boosting so rapidly. Especially as the development of digital cellular technology goes, new antennas are required to be configured to improve the multi-path fading, site assignment and multi-channel network in metropolis. Therefore, the several options to choose mobile base station typical antenna base on the following principles:

1.)   Properly choosing half-power beamwidth and gain of an antenna based on the number of base station sectors, traffic density and coverage requirements.

2.)   Adopting duplexer to save antenna locations

3.)   Adopting dual polarization antennas in the dense urban areas.

Furthermore, the main lobe direction and angle of tilt of the directional antennas should be properly adjusted to the traffic distribution and communication quality requirements. When setting antennas, the isolation between antennas should meet the requirements of horizontal and vertical isolation to avoid interference. The setting height of antenna is up to the coverage, interference, isolation, and future development requirements. The antennas used in mobile base station, whose requirements are as follow:

- Sector antenna gain : 13 − 18 dBi

- Sector antenna half power beamwidth : 60 - 65 degree

- Impedance : 50 Ohm

When the cell is usually divided into six sectors, the base station demands six antennas for covering the cell side. So, the antennas should be set in a cell. However,

too many antennas will result in many problems, such as high setting cost. In addition, the optimum diversity reception antennas set, saying nothing of that the antennas are unable to be set in some base stations. In that case, the technology of dual polarized antennas emerges as the time require. Besides, the technology of circularly polarized antennas is required too.

In 3G phase, as the wireless technology grows and the signal detection varies, the cellular network should be adjusted and optimized, which demands new base station antenna, such as self-adapting control antenna and intellectualized antenna.

3.4 Dipole antenna

The dipole is the most widely used antenna for wireless communication systems because it has elementary structure, simple concept, and broadband characteristics (L. Han, 2012).

3.4.1 Basic dipole antenna

Figure 3.1(a) shows the dipole antenna consists of two conductive elements such as metal wires or rods which are fed by a signal source or feed energy that has been picked up to a receiver. The current on radiating element vary along the length of the dipole. This occurs because standing waves are set up along the length of the radiating element and as result peaks and troughs are found along the length. The current fall to zero at the end and rises towards the middle. The current on the dipole antenna vary in a sinusoidal manner, meaning that there may be other peaks and troughs along the length of the radiating sections dependent upon their length as indicated in Figure 3.1(b).
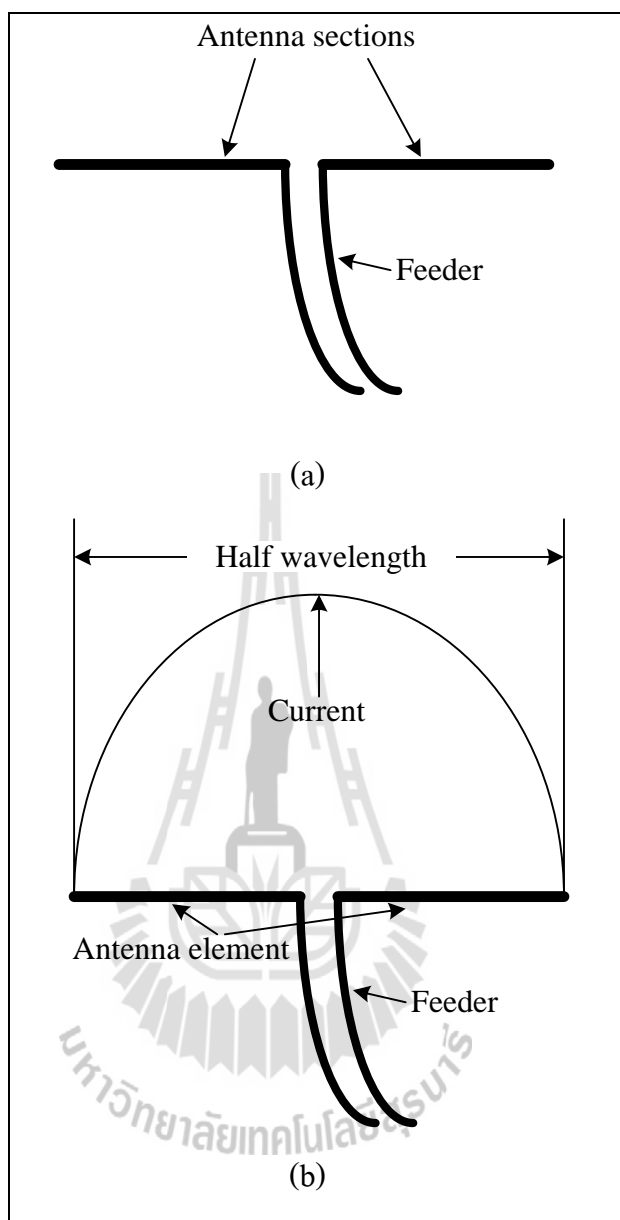
Figure 3.1 Basic dipole antenna (a) antenna section and (b) current distribution.

An interesting type of dipole antenna is an inverted V dipole, it is a dipole with both legs slanting down towards the ground in the shape of an upside down V. The obvious advantages of this design, it takes up less horizontal space than a horizontal dipole. Therefore, a strip dipole antenna is bended to half curved, it can be increased the antenna beamwidth.

3.4.2 Dipole antenna polarization

In addition, we study the dipole antenna polarization, which the electric and magnetic fields radiate from the dipole in the manner shown in Figure 3.2. The magnetic field always surrounds the conductors and is perpendicular to them. The electric field is parallel to the conductors. In right hand of Figure 3.3, the conductors of the dipole are horizontal to the earth, it is an electric field. For that reason, we call this a horizontally polarized antenna. The dipole in left hand of Figure 3.3 is located in vertical to the earth. It is the vertically polarized antenna.
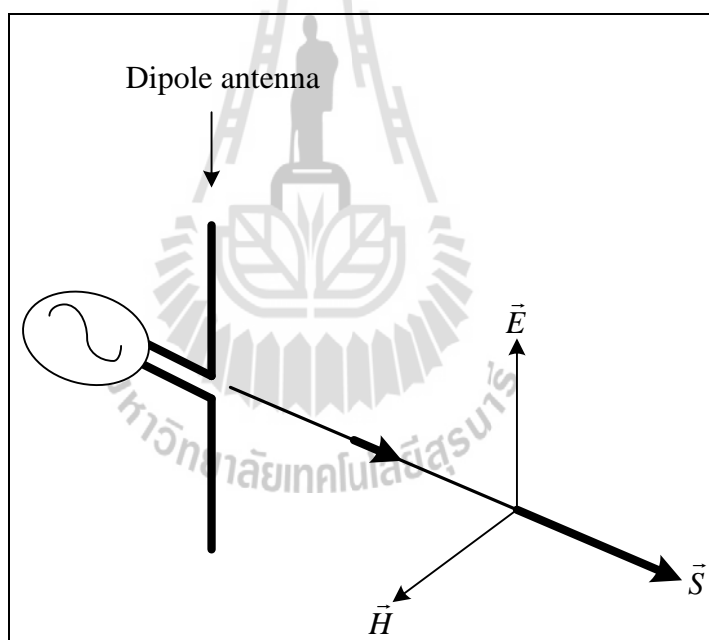
Figure 3.2 Electromagnetic field of dipole antenna.
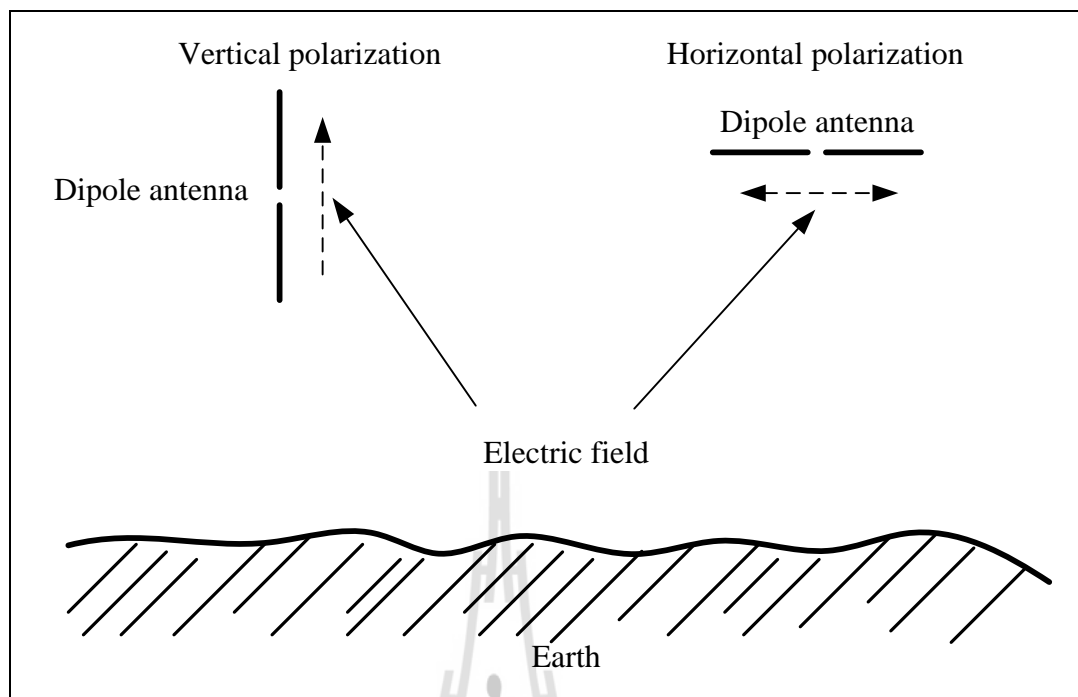
Figure 3.3 Polarization of dipole antenna.

In this research, a dipole antenna is applied for a circularly polarized antenna by using 45° slant dipole antenna on reflector plane with multi layers of metamaterials based on metallic rod EBG.

3.5 Coaxial balun

The original of the word balun is balance and unbalance. A balun is used to balance an unbalanced systems, it is a device that joins a balance line to unbalance line. A balanced line is one that has two conductors with equal currents in opposite directions such as dipole antenna. On the other hand, an unbalance line is one that has just on conductor and ground plane such as coaxial cable. Since, the disparate characteristic of dipole and coaxial is produced balance and unbalance current mode, respectively. Figure 3.4 displays the current flow, when the currents on both arms of

the dipole should be equal in magnitude. A coaxial cable is connected directly to the dipole; however, the currents are not necessary equal. The current on the center conductor (I_1) flows along the dipole arm that is connected from the center conductor. The current on inside surface of the shield has two directions, they flow down the outside surface of the shield (I_3) and flow up to an antenna feed point (I_2). Consequently, the maximum magnitude of the current is only occurred on the left arm. On the right arm, a magnitude of the current is reduced because this is an unbalance system.
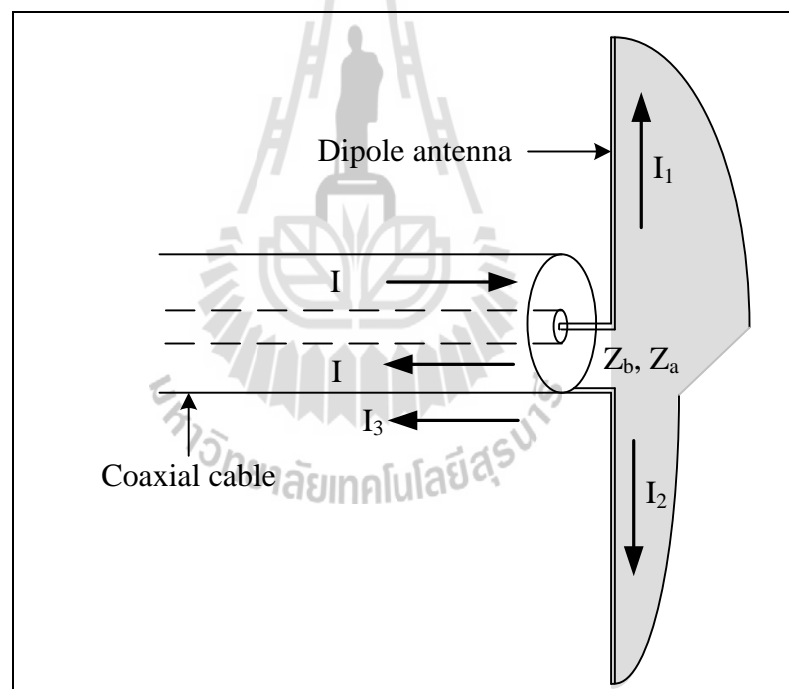
Figure 3.4 Unbalance to balance system.
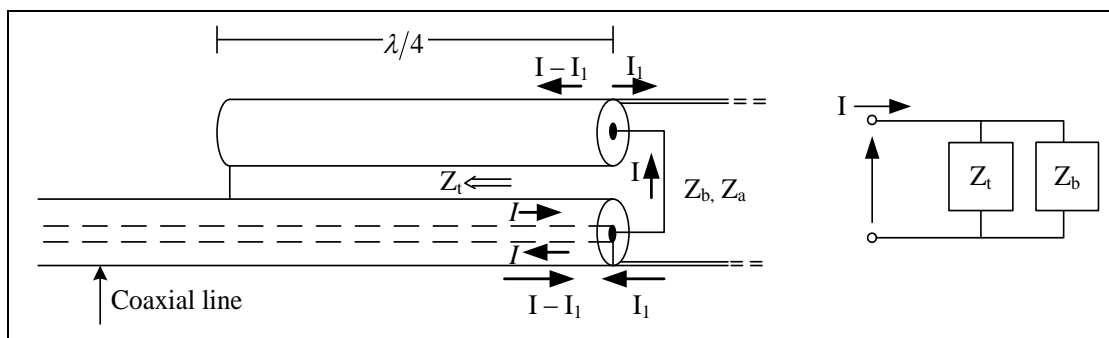
Figure 3.5 Parallel conductor balun.

Enter the balun to solve an unbalance system is illustrated in Figure 3.5. This balun is used the coaxial line with length of $\lambda/4$, it is placed parallel with the $3\lambda/4$ coaxial line. The end of $\lambda/4$ parallel coaxial line is connected to inner conductor of $3\lambda/4$ coaxial line and the other one side is connected to outer shield. If Z_t is a balun impedance which is infinity, the current is flown into only parallel line. In addition, the currents (I_1) are equal and have opposite direction, so, it is called 1:1 balun.

3.6 Metamaterials

Metamaterials are artificial structures to have properties that may not be found in nature. All natural materials such as glass, diamond, and such have positive electrical permittivity, magnetic permeability and an index of refraction. It comprises of periodic or non-periodic structure. Metamaterials are generally specified by the parameter of structure design. The characteristic of metamaterials are shown in the effective macroscopic behavior. Early stage researchers researches a negative refraction index, based on super lens technique. It can magnify a picture that its resolution is higher than a limited of general lens. In addition, negative refraction index is also called left hand metamaterials. Moreover, the antenna is another possible

application which uses metamaterials to increase performance of the antenna system. The metamaterials are classified by permittivity (ε) and permeability (μ), the equivalent permittivity and permeability are primarily dependent on the geometrical properties of an inclusion shape and mutual distance between the lattices constant. Therefore, it is possible to tailor the electromagnetic response of the inclusions almost arbitrarily and achieve exotic values of equivalent permittivity and permeability that cannot be found in nature. A part from natural double-positive materials (DPS), there are also materials that have either negative permittivity or negative permeability (SNG). Whereas, the negative permittivity materials are called epsilon negative medium (ENG) and the negative permeability materials are called mu negative medium (MNG). Furthermore, zero refractive index or near zero refractive index materials are described in antenna engineering that are classified in three types.
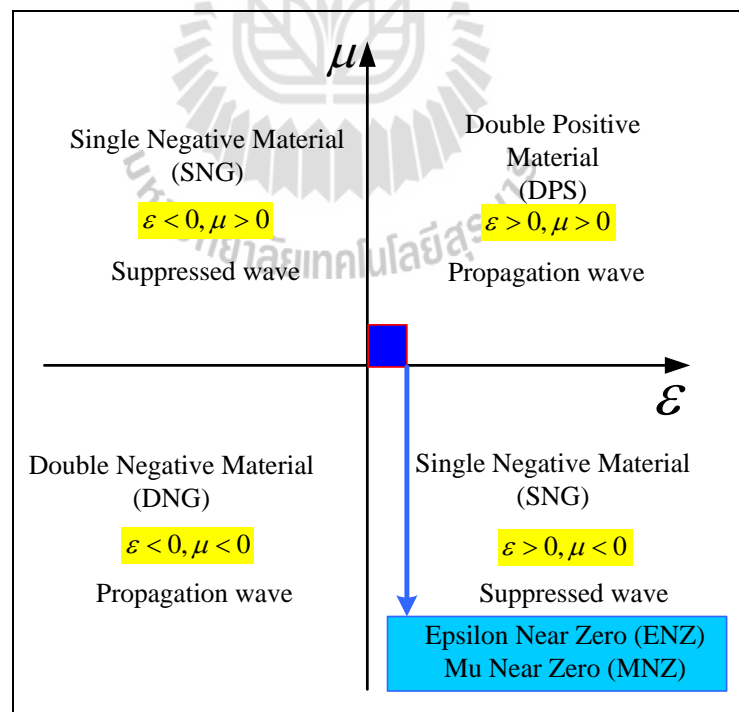
Figure 3.6 Classification of metamaterials.

1) When a permeability greater than or equal to one ($\mu \geq 1$), this case is called epsilon near zero (ENZ).

2) When a permittivity greater than or equal to one ($\varepsilon \geq 1$), this case is called mu near zero (MNZ).

3) When a permeability and a permittivity are zero ($\mu = \varepsilon = 0$), this case is called double zero index or mu-epsilon near zero.

The classification of metamaterials is illustrated in Figure 3.6. Beside this the electromagnetic band gap and partially reflective surface based on electromagnetic metamaterials are studied.

3.6.1   Electromagnetic band gap (EBG)

EBG is a periodic structure, consists of dielectric and metallo-dielectric materials. It is capable of the radiation deterrence in a specific direction and frequency. The diversity of the EBG structure that is applied for the antenna application can be also divided in three categories.

3.6.1.1 High impedance surface

High impedance surface is a new type of metallic electromagnetic structure. It is a planar array of continuous metallic periodic cell surfaces able to suppress surface waves, which case multipath interference and backward radiation in a narrow bandwidth near the cell resonance. This structure is referred to as the 2D structure that can be applied with a microstrip antenna to suppress the surface wave, as shown in Figure 3.7 (Agi, et. al, 2005).
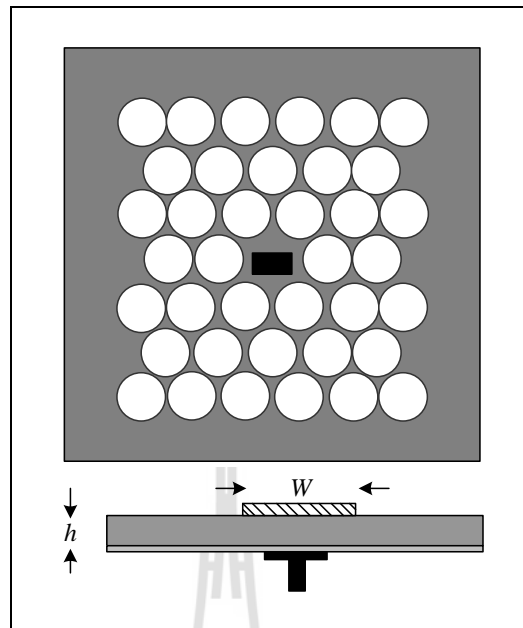
Figure 3.7 2D electromagnetic band gap and microstrip antenna.

3.6.1.2 Artificial surface

Artificial surfaces are artificial magnetic conductors (AMC) and reactive surfaces to design low profile antenna, as shown in Figure 3.8 (Alireza Foroozesh and Lotfollah Shafai, 2011).
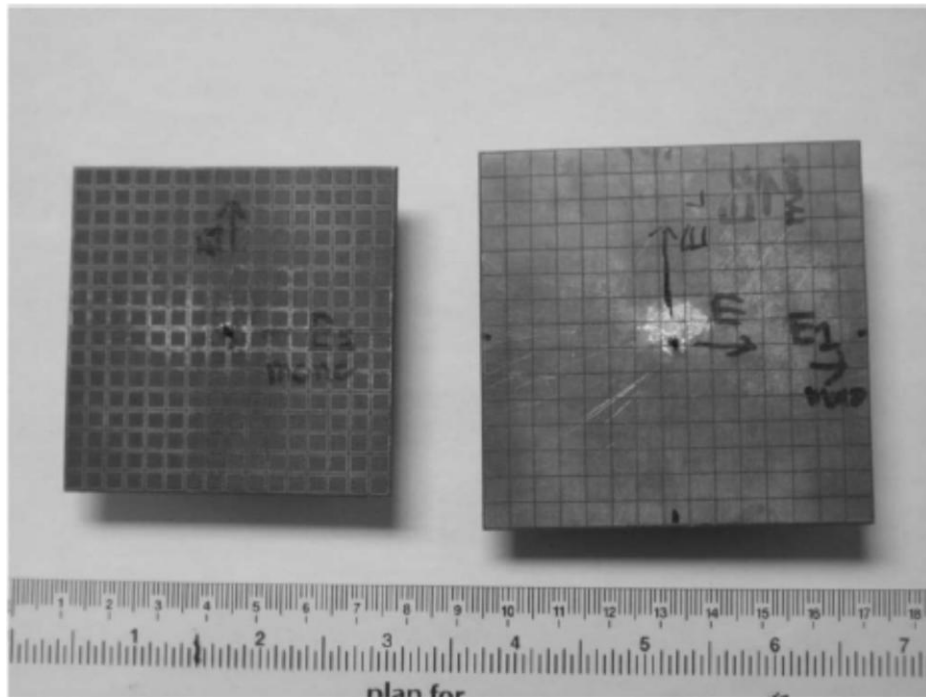
Figure 3.8 Fabricated VMAs over reduced-size AMC.

3.6.1.3 High Directive resonator antenna

A resonator antenna are designed base on the basis of creating detects in a uniform EBG structure. It is composed of a complex artificial surface and a metallic ground plane. Moreover, a primary radiation source such as microstrip patch antennas, horn antennas, dipole antennas, and so on, the EBG structure can be configured as a superstrate. The main goal of using EBG is to improve the primary radiating efficiency. The structure of various forms of EBG can be used in the design of high directive gain resonator antenna. For example, multiple layers of metallic dielectric and multiple layers of frequency selective surface (FSS) are shown in Figures 3.9 (Weily, et. al, 2005) and 3.10 (Young Ju Lee, et. al, 2005), respectively.
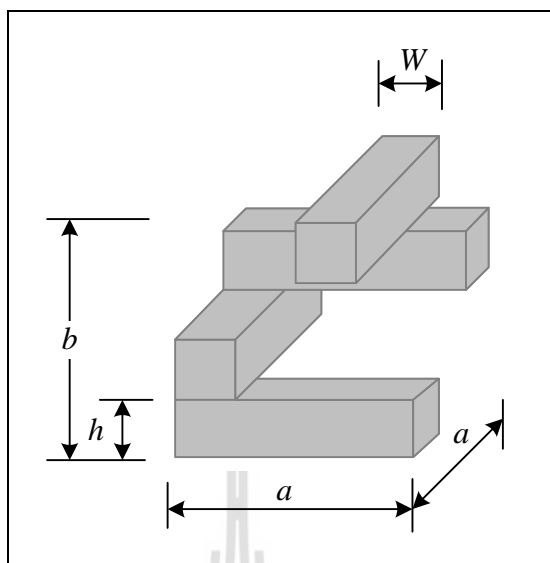
Figures 3.9 Woodpile EBG.
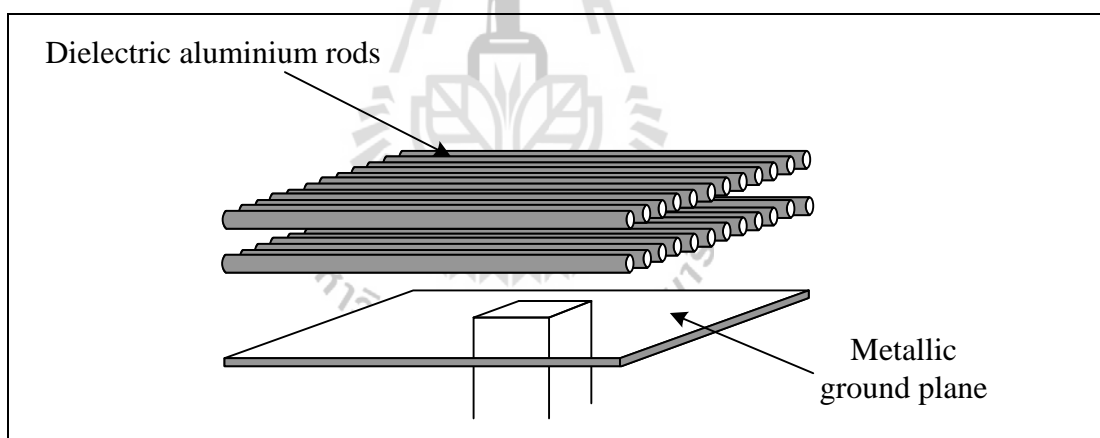
Figure 3.10 1D EBG using dielectric aluminium rods.

3.6.2 Partially Reflective Surface (PRS)

Whenever the EBG becomes one of the several aluminium rod functions, it works as a medium in form of a superstrate. Figure 3.11 demonstrates the propagation of electromagnetic fields which are passed through the medium, the

reflection and refraction wave occurs. In this case, the electromagnetic waves propagates along *x* direction. To concern about the polarization mode where the medium is worked of partially reflective surface (PRS), it has two polarization modes as follow.
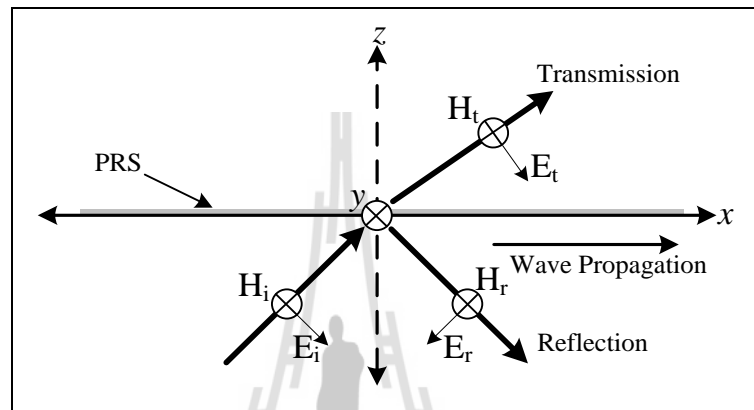
Figure 3.11 Electromagnetic propagation when passed the medium.

3.6.2.1 Transverse electric polarization (TE) mode

Figure 3.12 indicates the transverse electric polarization mode. The metamaterials based on EBG rod are set up along *y* axis, so the electromagnetic waves propagate in *y* direction. Because of a dipole antenna is located along *x* axis, the electric field direction is propagated along *x* axis. Therefore, TE polarization mode have only magnetic field in the direction of EBG polarization. In this case, the propagation of transmitted wave can be propagated more than reflected wave.
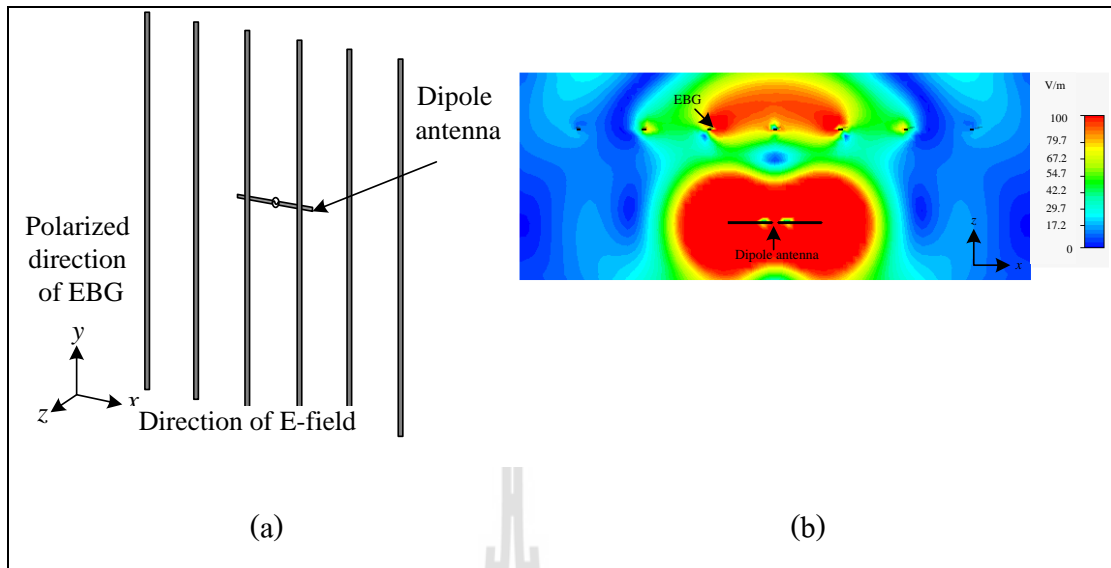
Figure 3.12 Simulation of transverse electric polarization mode (a) structure and

(b) near-field distribution.

3.6.2.2 Transverse magnetic polarization (TM) mode

The metamaterials based on EBG rod are set up along x axis,
so the electromagnetic waves propagate in x direction. Futuremore, the electric field
of a primary radiator is propagated along x axis because a dipole antenna is placed
along x direction. Consequently, the direction of EBG polarization has only electric
field, it is the transverse magnetic polarization mode as shown in Figure 3.13. In this
case, the propagation of transmitted wave can be propagated less than reflected wave.
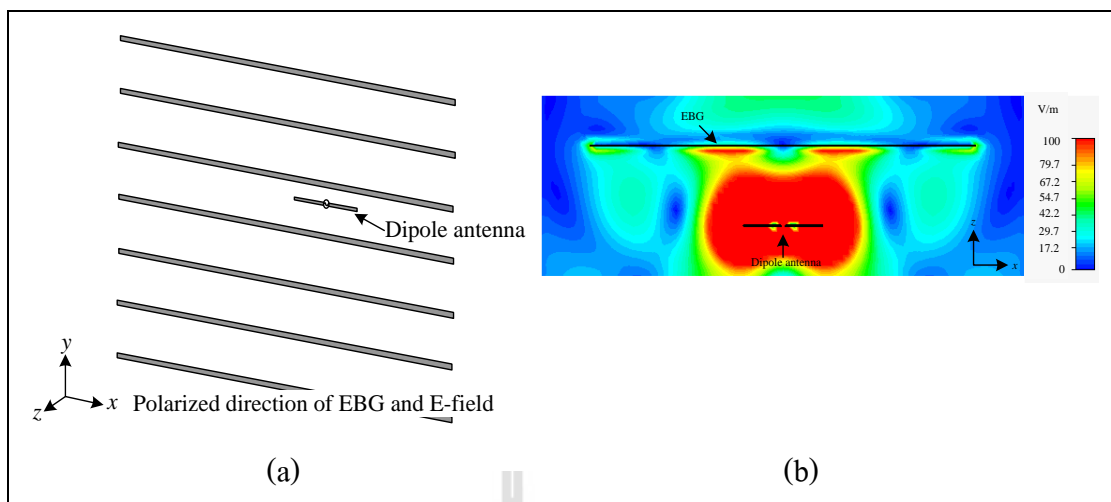
Figure 3.13 Simulation of transverse magnetic polarization mode (a) structure and

(b) near-field distribution.

From the theory above, the wave propagation is obstructed wave propagation by the metamaterial based on EBG rods along *x* and *y* directions in TE and TM polarization mode, respectively. If electric field of a primary radiator is propagated along the direction of EBG polarization mode, the minority of wave can be transmitted and the wave propagation is mostly reflected. In this case, if metamaterials based on EBG rods are used as superstrate and metallic plate is applied to reflector plane, the high directive gain resonator antenna can be obtained at the resonant frequency band of EBG and primary radiator.

3.7 Polarization of plane wave

Polarization is the orientation of an electric field. An electromagnetic wave can be polarized to restrict its electric field to one direction; this principle is also behind polarized sunglasses, which block all light wave components that are oriented

in a certain direction. The polarization is categorized into three types, which are linear polarization, circularly polarization, and elliptical polarization.

Consideration on wave polarization, an electric field has a component in x and y axises and electromagnetic field is propagated in $+z$ direction. So, wave equation is defined by

$$\vec{E} = \left(E_{x0}\hat{a}_x + E_{y0}e^{j\varphi}\hat{a}_y\right)e^{-j\beta z}e^{j\omega t} = \left(E_{x0}e^{j(\omega t-\beta z)}\hat{a}_x + E_{y0}e^{j(\omega t-\beta z+\varphi)}\hat{a}_y\right),$$ (3.1)

Where φ is phase different between E_x and E_y and, E_{x0} and E_{y0} are an amplitude of E_x and E_y, respectively.

And also display a magnetic field equation is

$$\vec{H}(z) = \frac{1}{\eta}\left(-E_{x0}\hat{a}_x + E_{y0}e^{j\varphi}\hat{a}_y\right)e^{-j\beta z}e^{j\omega t}.$$ (3.2)

Hence, the real part of electric field is

$$\vec{E} = E_{x0}\cos(\omega t - \beta z)\hat{a}_x + E_{y0}\cos(\omega t - \beta z + \varphi)\hat{a}_y,$$ (3.3)

or $\quad E_x = E_{x0}\cos(\omega t - \beta z),$ (3.4)

and $\quad E_y = E_{y0}\cos(\omega t - \beta z + \varphi).$ (3.5)

From law of cosine, it seem that cos (A+B) = cos A cos B − sin A sin B, is capable of

$$E_y = E_{y0}\cos\left[(\omega t - \beta z) + \varphi\right] = E_{y0}\cos(\omega t - \beta z)\cos\varphi - E_{y0}\sin(\omega t - \beta z)\sin\varphi. \quad (3.6)$$

When $\sin^2 A = 1 - \cos^2 A$, equation (2.4) can be arranged as follow;

$$\sin(\omega t - \beta z) = \sqrt{1 - \left(\frac{E_x}{E_{xo}}\right)^2}. \quad (3.7)$$

So, the electric field in y direction is

$$E_y = \left(\frac{E_{y0}}{E_{x0}}\right)E_x\cos\varphi - E_{y0}\sqrt{1 - \left(\frac{E_x}{E_{x0}}\right)^2}\sin\varphi. \quad (3.8)$$

Finally, the polarization equation could be achieved,

$$\sin^2\varphi = \left(\frac{E_x}{E_{x0}}\right)^2 - 2\frac{E_x E_y}{E_{x0}E_{y0}}\cos\varphi + \left(\frac{E_y}{E_{y0}}\right)^2. \quad (3.9)$$

Consideration of equation (3.9) concludes that the polarization type is depended on

the phase (φ) and amplitude (E_{x0} and E_{y0}).

3.7.1 Linear polarization

From equation (3.9), if the phase different is $\varphi = 0$ or $\varphi = \pm n\pi$,

$$0 = E_{y0}^2 E_x^2 \pm 2E_{x0}E_{y0}E_x E_y + E_{x0}^2 E_y^2 = \left(E_{y0}E_x \pm E_{x0}E_y\right)^2 \quad (3.10)$$

$$E_{y0}E_x = \pm E_{x0}E_y \quad (3.11)$$

Equation shows linearly polarization, which is displayed in Figure 3.14. In addition,

$$\alpha = \tan^{-1}\left(\frac{E_y}{E_x}\right).$$
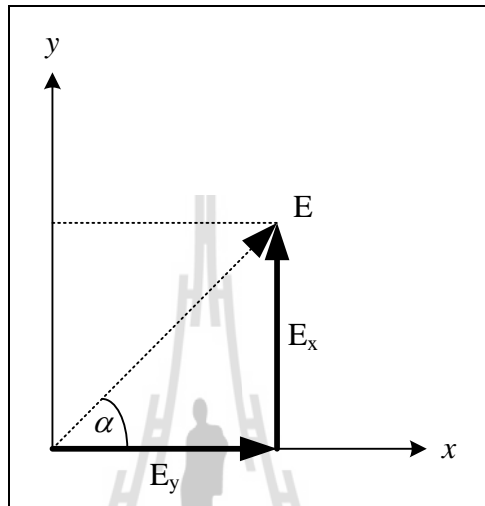
Figure 3.14 Linear polarization.

3.7.2 Circularly polarization

From equation (3.9), if $E_{x0} = E_{y0}$ and the phase different is $\varphi \pm \dfrac{\pi}{2}$,

$$1 = \frac{E_x^2}{E_{x0}^2} + \frac{E_y^2}{E_{y0}^2} \text{ or } E_x^2 + E_y^2 = \left(E_{x0}\right)^2 = \left(E_{y0}\right)^2 \tag{3.12}$$

Equation (3.12) is circular equations, its middle point is (0,0) and the radius is $E_{x0} = E_{y0}$. Figure 3.15 plots the circularly polarization.
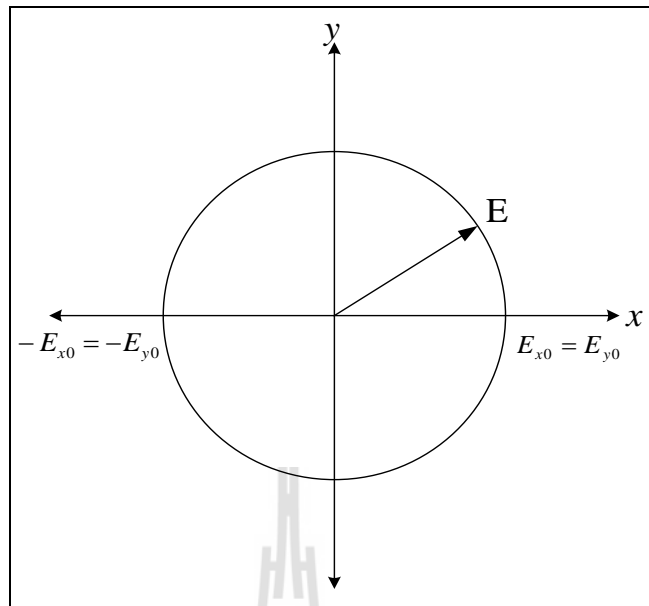
Figure 3.15 Circular polarization.

Consideration of the left and right hand circularly polarization, assume that the phase convention is looked at the direction of propagation and note from phasors that a factor of j is equivalent to a +90 degree phase shift. For RHCP, E_y "lags" E_x, and a factor of j would rotate the phasor of E_y onto that of E_x. Another way of looking at it is that after a quarter wavelength of propagation, E_y would have the phase that E_x start with, as revealed in Figure 3.16 (traveling of wave in the positive z-direction). Hence,

$$E_R = E_x - jE_y \tag{3.13}$$

and

$$E_L = E_x + jE_y, \tag{3.14}$$

when E_R is a Right Hand Circular Polarization (RHCP : clockwise) and E_L is a Left

Hand Circular Polarization (LHCP : counter clockwise).
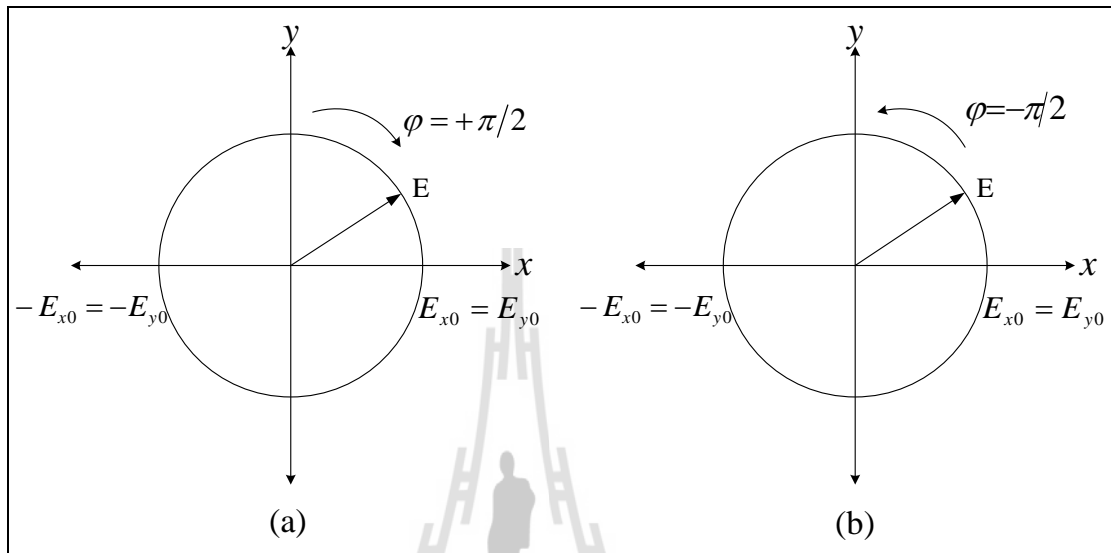
Figure 3.16 (a) Left-hand circular polarization and (b) right-hand circular polarization.
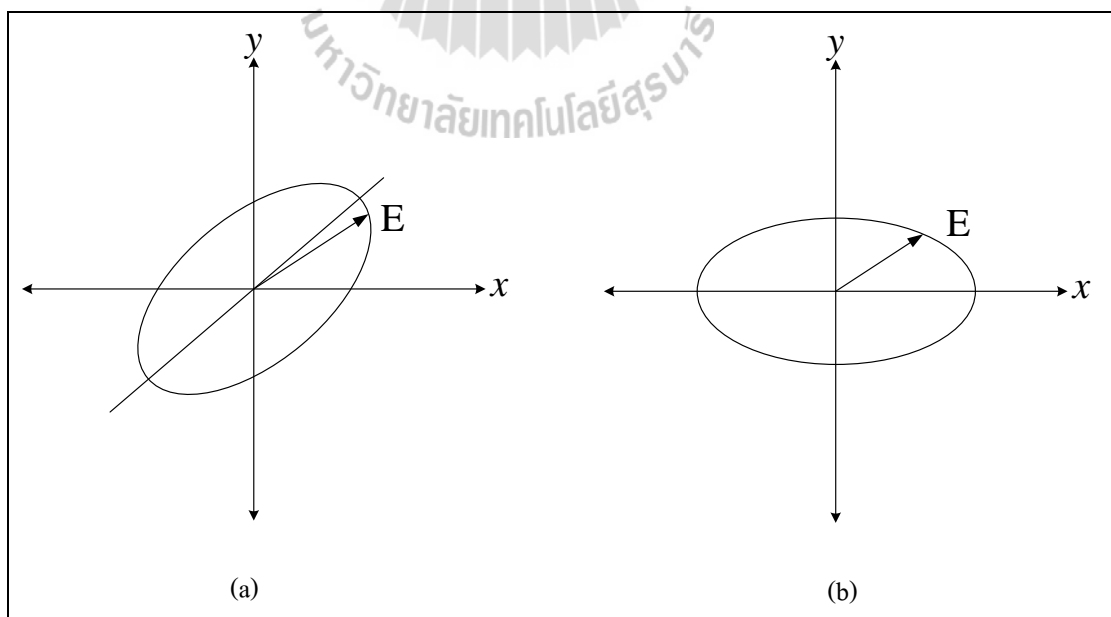
Figure 3.17 Elliptical polarization.

3.7.3 Elliptical polarization

In this polarization can be divided into two cases, Figure 3.17(a) demonstrated the elliptic polarization when phase different $\varphi \neq 0$ or $\varphi \neq \pm \dfrac{\pi}{2}$ and $E_x \neq E_y$. It describes that the elliptic is not located in major and minor axis. Beside this is shown in Figure 3.17(b), if phase different $\varphi = \pm \dfrac{\pi}{2}$ and $E_x \neq E_y$, the elliptic is located in major and minor axis.

3.8 Chapter summary

In this chapter, several theories have been proposed to improve the performance of mobile base station antenna. Firstly, the antenna in cellular system has been proposed and how to choose a mobile base station antenna is discussed. From the review literature the dipole antenna is widely used to modify the performance, so, the basic theory of the dipole antenna is considered in this Chapter. Moreover, coaxial balun is studied to join a dipole antenna to coaxial feed line. After that the EBG rod based on metamaterials is researched and EBG superstrate is discovered to enhance the gain performance. To achieve the dual and circularly polarization, the polarization of plane wave is also studied. All above theories are important understanding to design the proposed antenna.

CHAPTER IV

ANTENNA DESIGN AND ANALYSIS

4.1   Introduction

In a previous work, an antenna design of high directive gain using a curved strip dipole on electromagnetic band gap (EBG) was studied (Fhafhiem, Krachodnok, and Wongsan, 2010). The resonant EBG structure was been used as a reflector for directive gain increment by utilizing the good performance of a mushroom-like EBG structure, which is capable of providing a constructive image current within a certain frequency band. Therefore, when a wide beam curved strip dipole is appropriated located horizontally on a resonant EBG reflector, high directive gain can be obtained of 7.6 dBi for RFID reader. The purpose of this thesis is to design the antenna for mobile base station, so the antenna performance is developed to perform the resonator antenna by using EBG structure. In this design, the EBG structure can partially reflect the wave of a primary radiator. This chapter proposes the design and analysis of the circularly polarized resonator antenna by using curved strip dipole placed on U-shaped reflector plane and multi layers EBG. The results indicate that the antenna can also generate a circular polarization. The proposed antenna has a beamwidth covering the frequency range of 1.85 – 2.23 GHz, the gain is increased up to 15.53 dBi. In addition, an interesting sectoral 60˚ pattern is presented in horizontal plane.

4.2   Curved strip dipole antenna design

At the desired frequency of 2.1 GHz, the initial dimension of a curved strip dipole antenna is calculated based on the total length (L_d) of $\lambda/2$, then radius (a) is found from (4.3):

$$L = \lambda_{2.1GHz}/2,\tag{4.1}$$

when the length of semicircle is

$$L = \pi a.\tag{4.2}$$

Therefore,

$$a = \left(\lambda_{2.1GHz}/2\right)/\pi\tag{4.3}$$

The geometry of a curved strip dipole is mounted over an inexpensive curved polyvinyl chloride (PVC) with the dielectric constant of 3.4 as shown in Figure 4.1(a). The radius of PVC is determined by 18, 20, 24, and 34 mm, consequently the curved strip dipole with various radius of PVC is simulated. It seems that when the length of the curved strip dipole is decreased from 0.5 λ, the S_{11} is varied as plotted in Figures 4.1(b) and (c). Consideration of the radius and width of the curved strip dipole are 34 mm and 15 mm, respectively, these results can obtain a good match with 50 ohms transmission line. The optimal parameters are concluded in Table 4.1. Referring to Figure 4.1(d) that is illustrated the best performance of a curved strip dipole antenna. It has the maximum gain of 2 dBi and S_{11} is -14 dB at the resonant frequency of 2.1 GHz. The omnidirectional pattern of the curved strip dipole in E-plane provides the half power beamwidth (HPBW) around 92.4°because the dipole is bent to be a half annular.

Table 4.1 Parameters of curved strip dipole antenna

Parameters	Size (mm)
a : radius of curved strip dipole	34
L : length of curved strip dipole	82.81
w_1 : width of curved strip dipole	15
w_2 : width of PVC	30
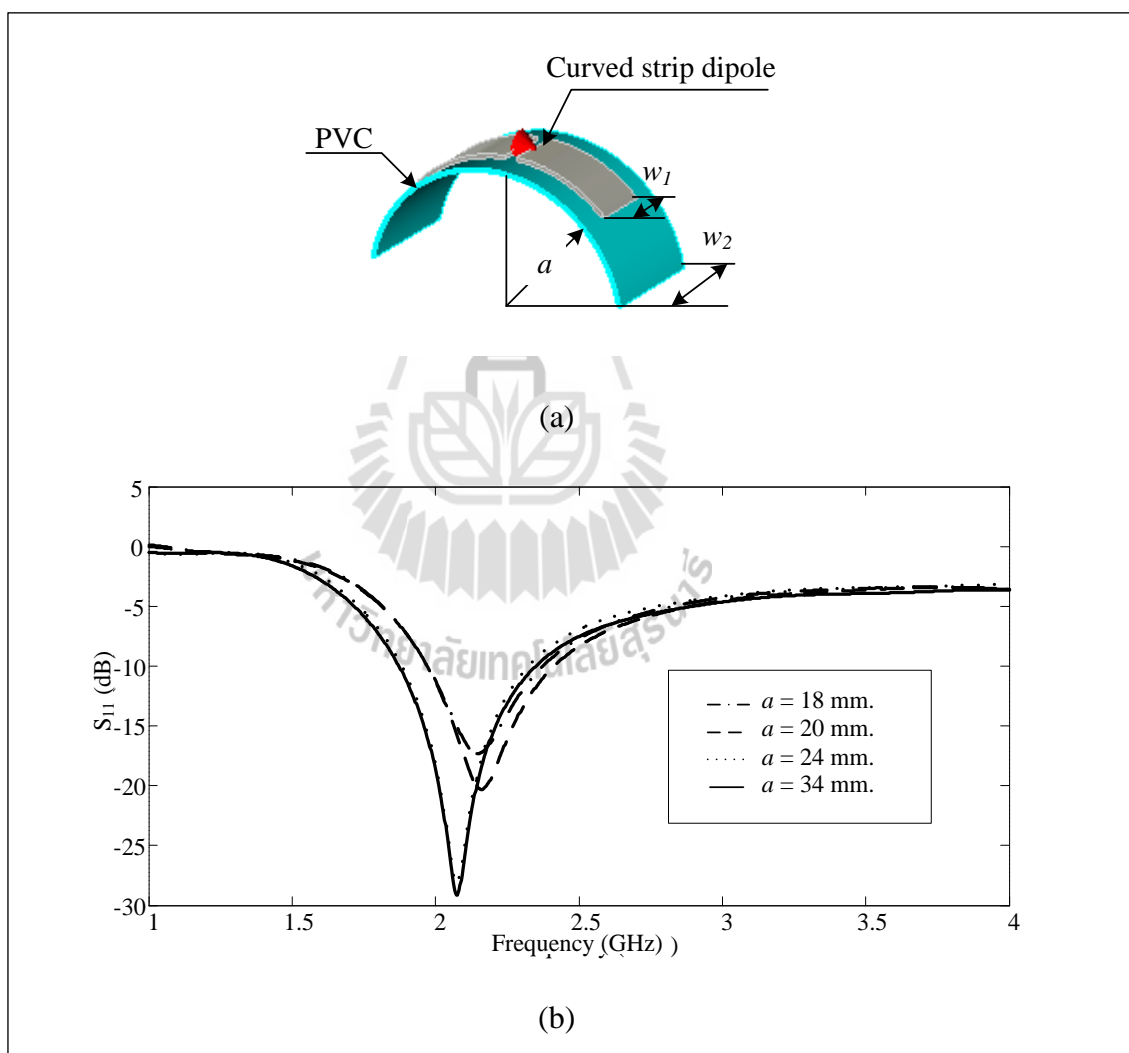
(a)

(b)

Figure 4.1 Simulated results of curved strip dipole antenna (a) structure, (b) S_{11} when

a is varied, (c) S_{11} when w_1 is varied, and (d) radiation pattern.

(c)

(d)
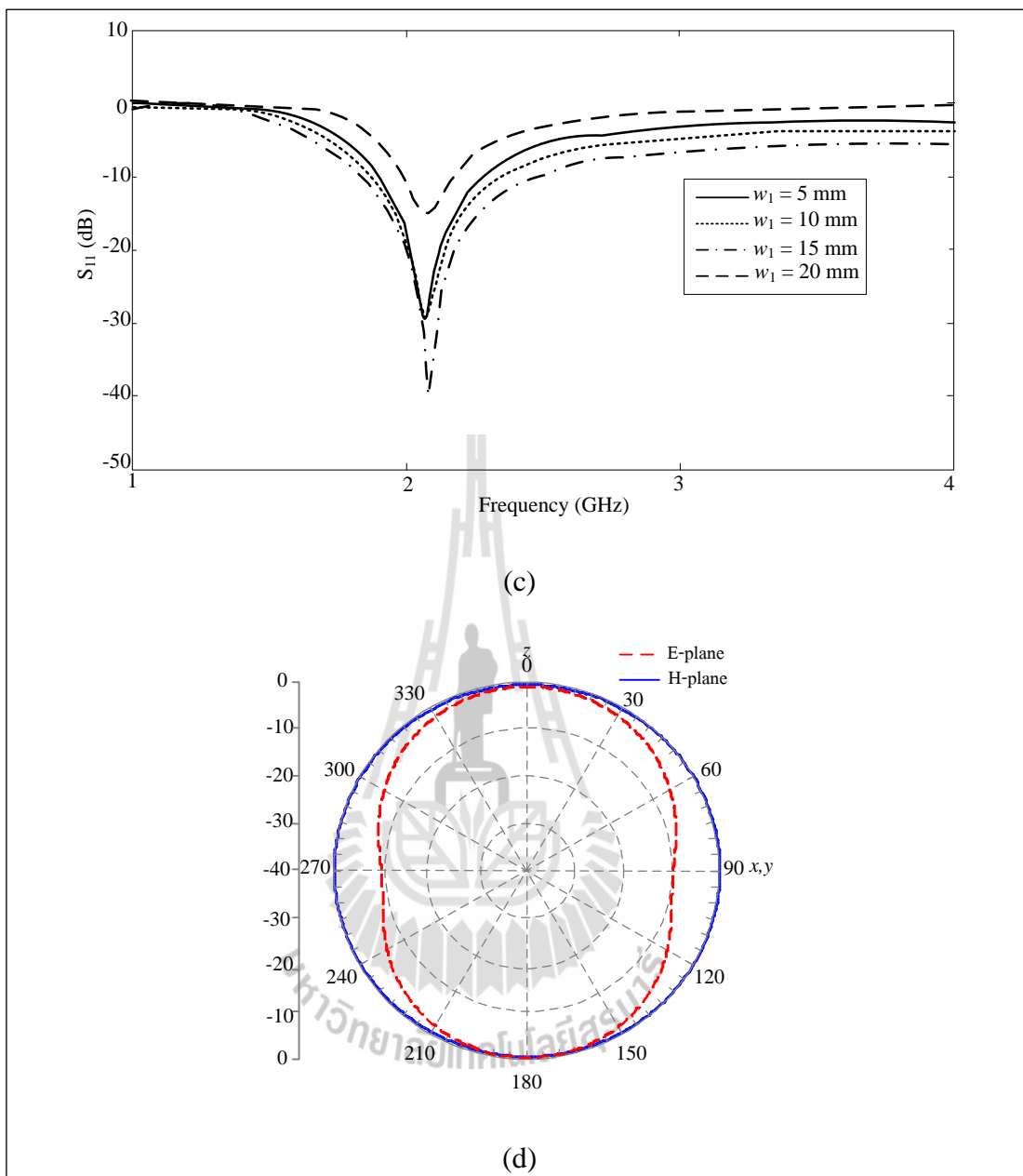
Figure 4.1 Simulated results of curved strip dipole antenna (a) structure, (b) S_{11} when a is varied, (c) S_{11} when w_1 is varied, and (d) radiation pattern (cont.).

One solution to enhance the gain of an antenna is using metallic reflector plane as shown in Figure 4.2 (a). The metallic reflector is located at the back of a dipole antenna with gap as a quarter wavelength. Usually, the main disadvantage of an

antenna on metallic plane is that it makes the overall size of the antenna too big and bulky for the low frequency range of operations. Moreover, the reflector plane cannot suppress the surface wave, so an antenna gain and efficiency will then be greatly decreased. Figure 4.2(b) shows radiation patterns of a curved strip dipole on reflector plane in E- and H- plane with the maximum gain of 7.6 dBi at 2.1 GHz.
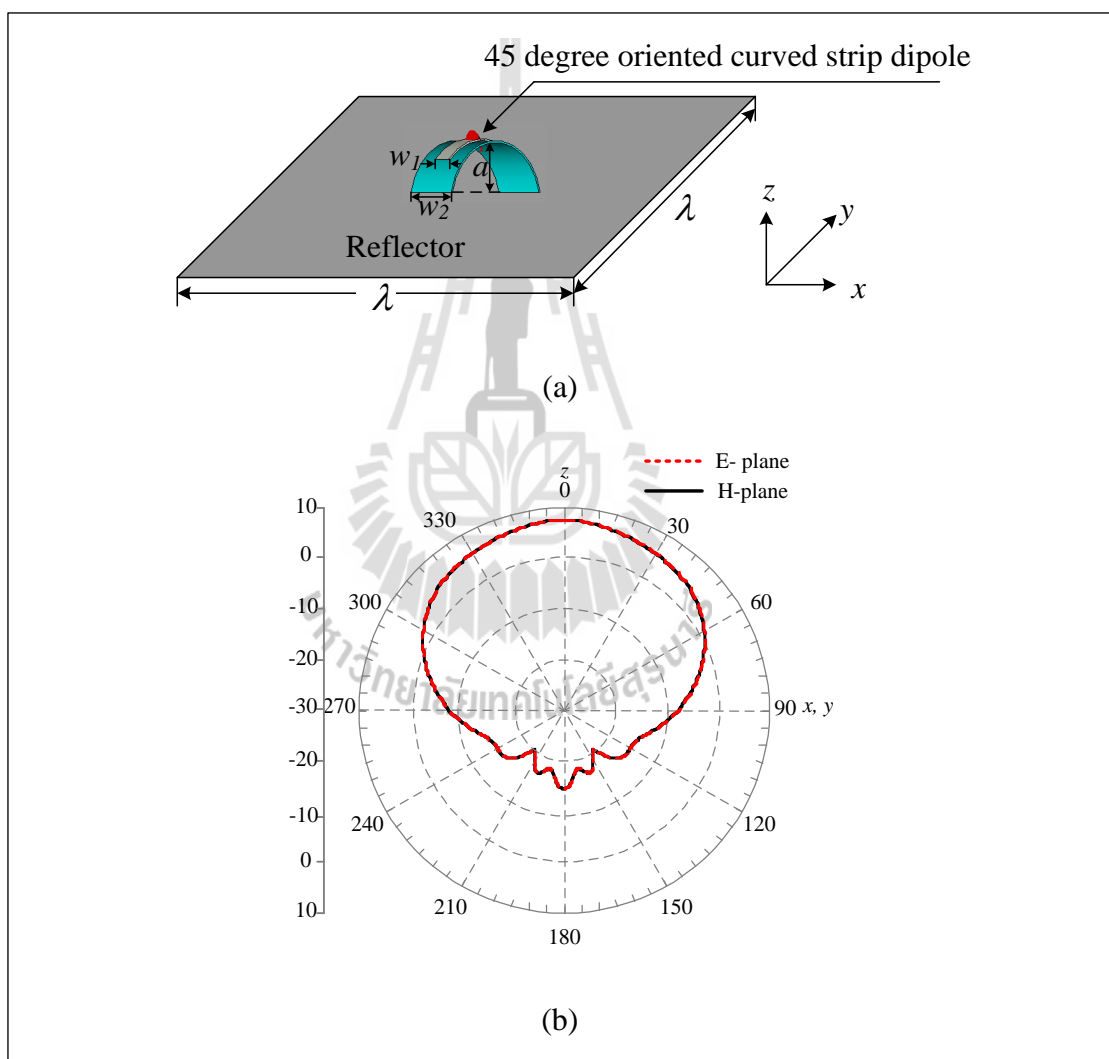
Figure 4.2 Simulated results of curved strip dipole on reflector plane with gap as

a quarter wavelength (a) structure and (b) radiation pattern.

Consideration of the gain of the curved strip dipole on reflector plane concludes that it is unsuitable to be utilized in mobile base station systems owing to the face that base station antenna must have unidirectional pattern, high directive gain, and wide beamwidth in horizontal plane, and dual polarization. The technique to meet the requirement is the resonant antenna using the resonant metamaterials structure as a superstrate of the curved strip dipole which is located on PEC reflector plane.

4.3   Study of metallic rod type metamaterials

To design the EBG superstrate for resonator antenna the image theory is applied. A cavity consisted of the EBG superstrate and its image will resonate at the same frequency as the antenna. Because the size of the exciting feed is considered much smaller than that the EBG superstrate and the reflector plane, the effect of the small feed antenna on the resonant cavity can be ignored (Ge, Essellec, and Bird, 2010). Therefore, a unit cell is surrounded by four periodic boundaries and a unit cell model is shown in Figure 4.3(a). This model can be used to evaluate the transmission and reflection amplitude and phase of the EBG, under the normal incidence. Figure 4.3(b) illustrates the cavity model that it has a single cell of the periodic superstrate and its image surrounded by four periodic boundaries. For normal incidence, the periodic boundaries surrounding the unit cell or the unit cavity can be replaced by the PEC (perfect electric conductor) and PMC (perfect magnetic conductor) walls.

In the case shown in Figure 4.3(a), a metallic rod performs as a unit cell. The boundary perpendicular to axis x should be set as PEC walls and those perpendicular to axis y should be PMC walls. Waveguide ports are located on two sides of the model. To analyze the transmission and reflection coefficient through the equivalent

cavity model, shown in Figure 4.3(b), the EBG and its image are included in the cavity model.
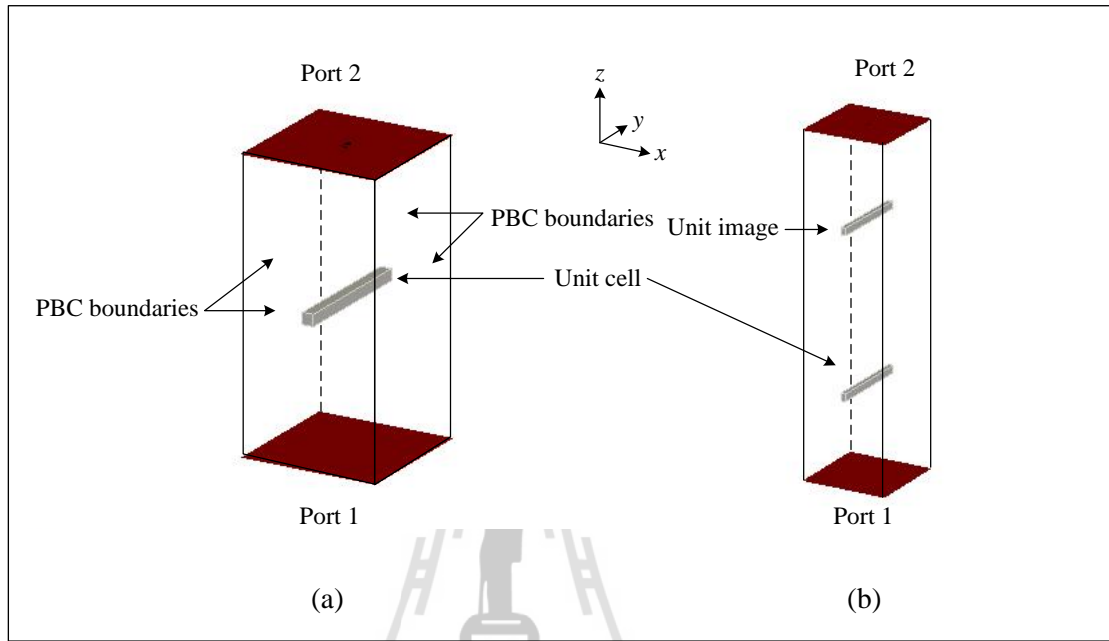
Figure 4.3 (a) A unit cell model for the EBG and (b) a cavity model composed

of a unit cell and its image.

Furthermore, metallic rod unit cell is classified in three cases which are single layer, double layers, and three layers as follows.

4.3.1 Single layer of metallic rod

Unit cell of metallic rod is a primary simulation of the metamaterials design as shown in Figure 4.4. A unit cell defined by parameters A_0, g_0, and t_0 and an aluminium rod is surrounded by four periodic boundaries. The parameters are optimized as plotted in Figure 4.5 to analyze the reflection phase that can be reflected partial wave, so A_0, g_0, and t_0 are 0.09λ, $0.25\ \lambda$, and 0.5λ, respectively. It seems that the resonant frequency is determined by the parameter of the aluminium rod structure,

especially by the A_0 and g_0 of rod structure. This model can be estimated the transmission and the reflection coefficient of the aluminium rod structure as plotted in Figure 4.6. Consideration of S_{11} and S_{21} at 2.1 GHz concludes that the aluminium rod can be partially reflected wave. The reflection phase in Figure 4.6(b) is performed that the allowed bandwidth is mostly narrow, thus limiting the EBG antenna bandwidth.
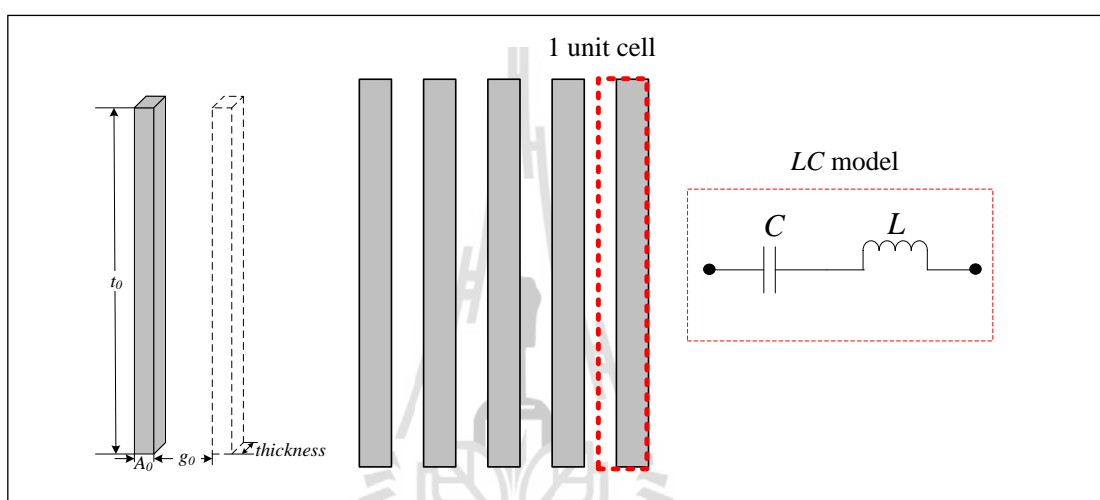
Figure 4.4 A unit cell of single layer.
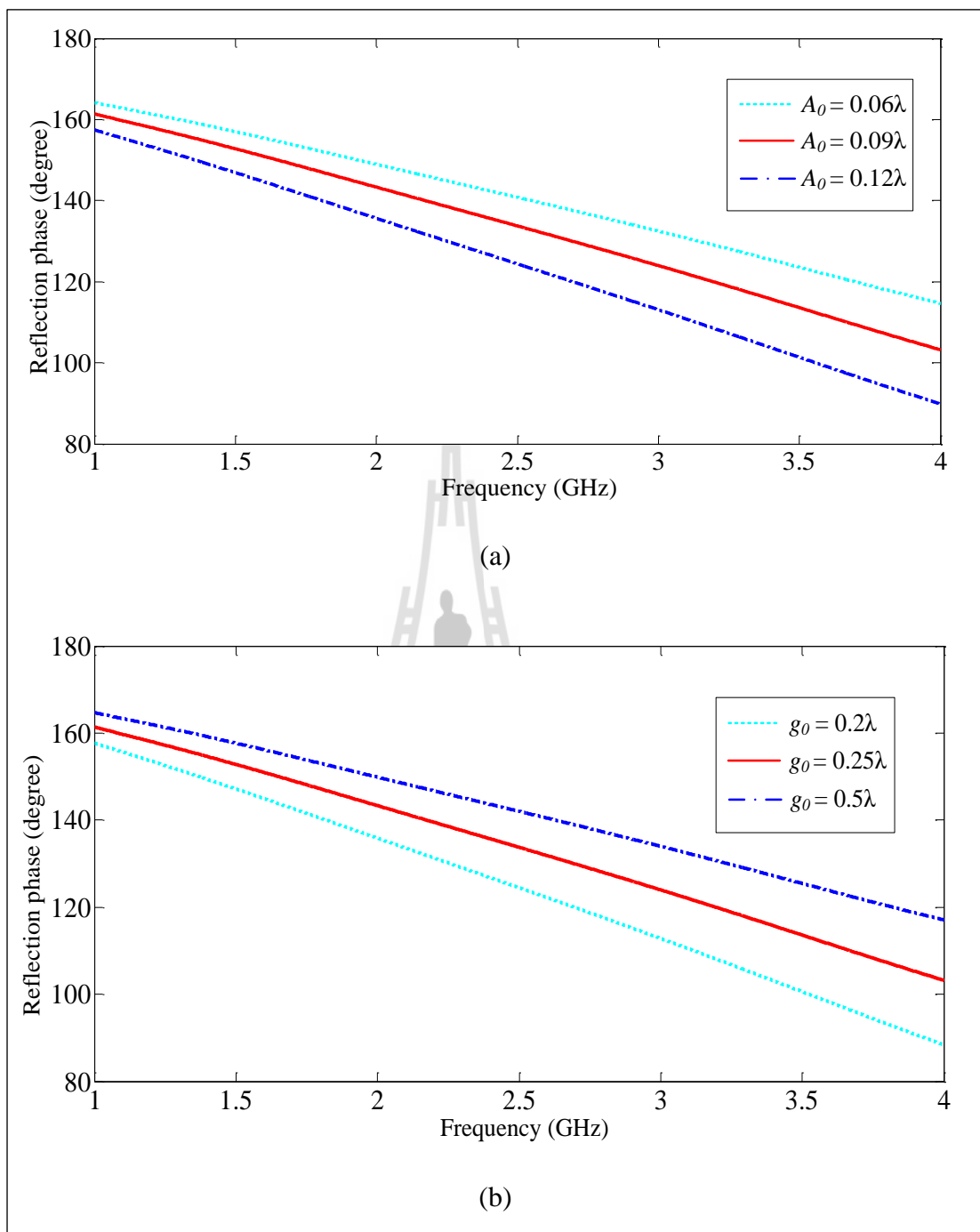
Figure 4.5 Optimization of EBG parameters (a) A_0, (b) g_0, (c) t_o, and (d) thickness.
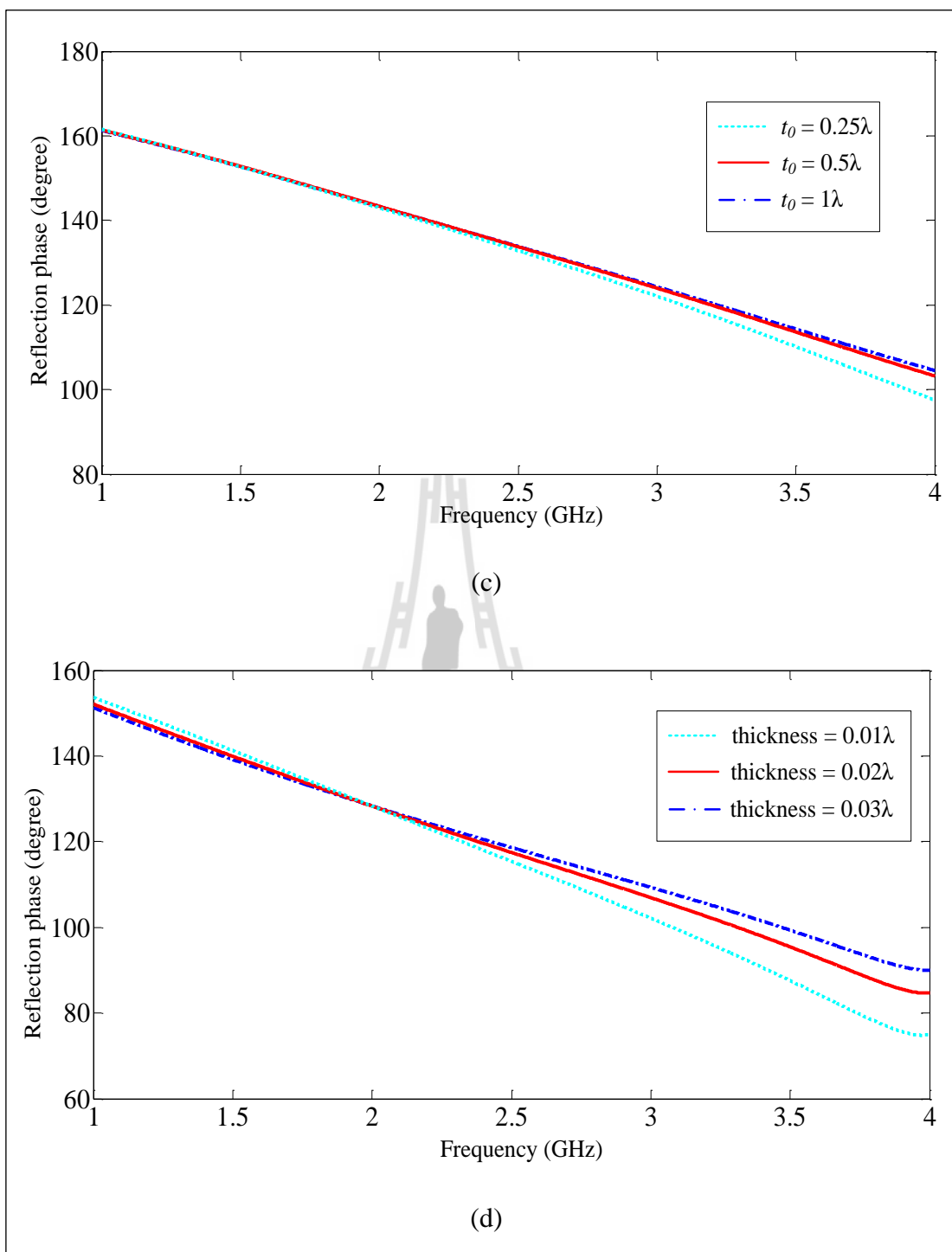
Figure 4.5 Optimization of EBG parameters (a) A_0, (b) g_0, (c) t_o, and

(d) thickness (cont.).
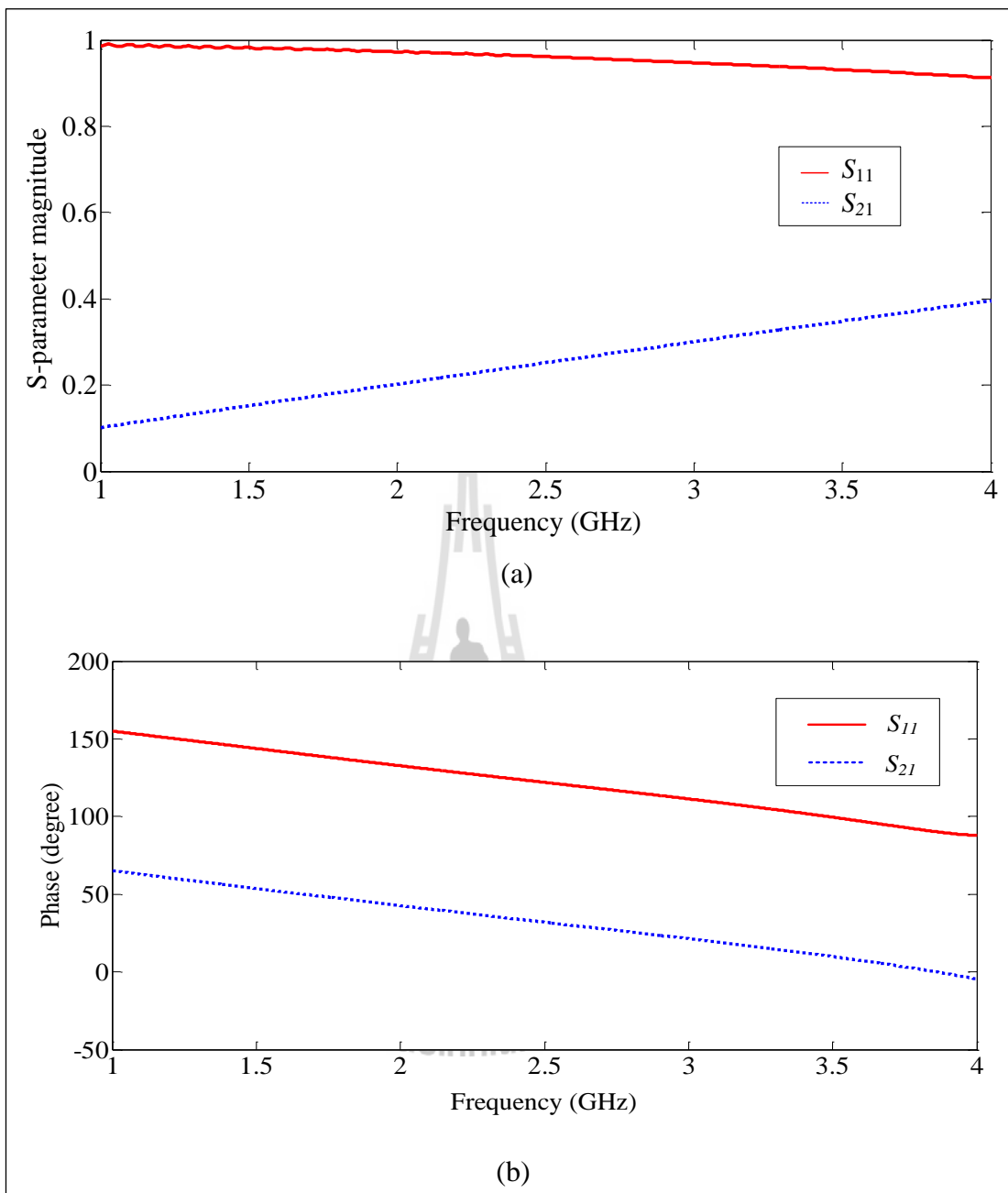
Figure 4.6 S-parameter of single layer (a) magnitude and (b) phase.

More interestingly, the S-parameters are used to calculate the permittivity (ε), permeability (μ), and refraction index (*n*) of the aluminium rod

structure, and the results. Initially, the basic equations used to determine the ε, μ, and n are shown below (Majid, et. al, 2009):

$$\varepsilon_r \approx \frac{2}{jk_0 d} \frac{1-v_1}{1+v_1} \tag{4.4}$$

$$\mu_r \approx \frac{2}{jk_0 d} \frac{1-v_2}{1+v_2} \tag{4.5}$$

$$n = \pm\sqrt{\varepsilon\mu} \tag{4.6}$$

where:

$v_1 = S_{21} + S_{11}$,

$v_2 = S_{21} - S_{11}$,

$k_0 = \omega/c$,

ω = radiation frequency,

d = dielectric thickness,

c = speed of light.

The permittivity and permeability at the resonant frequency of this structure is depicted in Figure 4.7 with the value of 11.46 and 1.4, respectively. The aluminium rod is classified in a medium with both permittivity and greater than zero (ε>0, μ>0). Referring to Figure 4.7 (c) concluded that the refraction index is 4.01. Therefore, the wave propagation incident upon a plane surface separating two media is refracted upon entering the second medium if the incident wave is oblique to the

surface. The incident angle is related to the refraction angle by the simple relationship known as Snell's law.
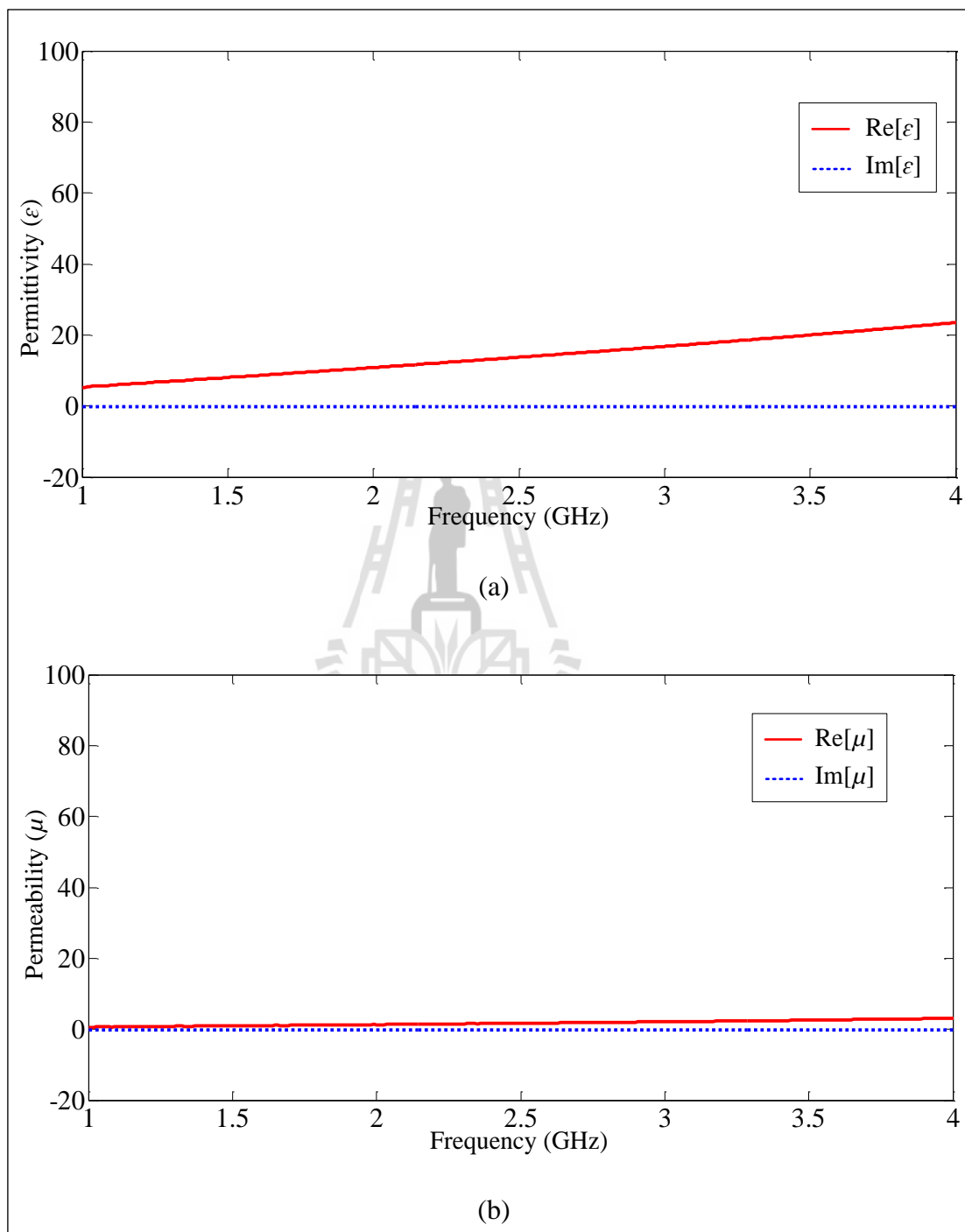
(a)

(b)

Figure 4.7 Calculated results of single layer unit cell aluminium rod

(a) ε_r, (b) μ_r, and (c) n.
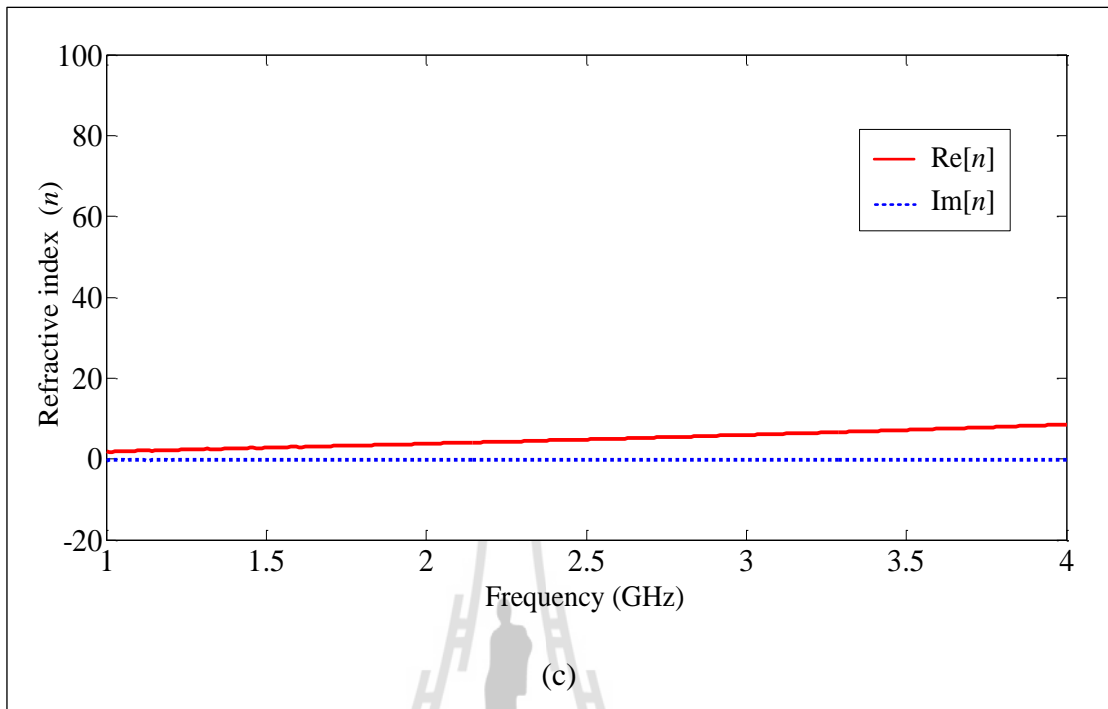
Figure 4.7 Calculated results of single layer unit cell aluminium rod

(a) ε_r, (b) μ_r, and (c) n (cont.).

One characteristic of the EBG material is to prohibit the wave propagation whose frequency belongs to the material band gap. The second characteristic property is to allow electromagnetic modes to exist within the forbidden frequency band by using the cavity model. Let us now analyze the transmission and reflection coefficient, assuming the cavity height (h) is adjusted to control the band gap of EBG which is 67.46 mm. This S-parameter is plotted in Figure 4.8 and indicated that the cavity resonance frequencies is 2 GHz to 2.1 GHz.
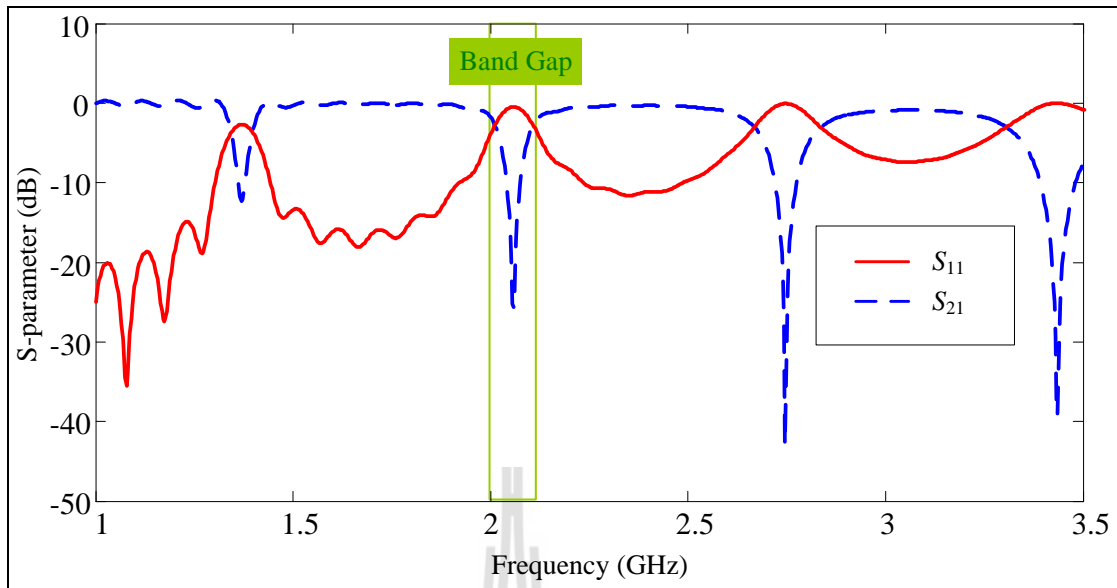
Figure 4.8 The band gap of single layer.

4.3.2 Double layers of metallic rod

In this thesis double layers of EBG superstrate are divided into two cases which are cross polarization of EBG and co-polarization of EBG.

Case 1 : Cross polarization of EBG

Both the EBG polar H and EBG polar V are considered and shown in Figure 4.9. This model can estimate the transmission and the reflection wave of the EBG structure as plotted in Figure 4.10(a). It concludes that the aluminium rod can be partially reflected wave. The reflection phase in Figure 4.10(b) is performed that the allowed bandwidth is mostly narrow. Referring to Figure 4.11 that shows the aluminium rods which are classified in a medium with epsilon near zero (ENZ). The permittivity and permeability at the resonant frequency are 0.14 ($0<\varepsilon<1$) and 6.5, respectively, so the reflection index of double layers EBG with cross polarization is about 0.95. From Equation (4.5), if the permittivity is near zero and the reflection

index is closed to zero, so the directivity enhancement in this medium is based on the phenomenon of geometrical optics and Snell's law (R. Zhou, et. al, 2010). The exiting ray from the substrate will be normal to the surface.
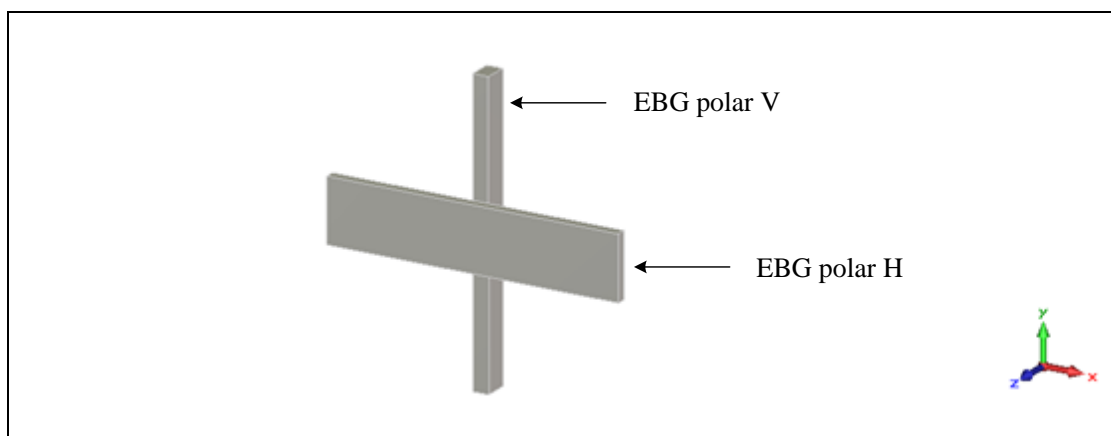
Figure 4.9 A unit cell of double layers with cross polarized EBG.
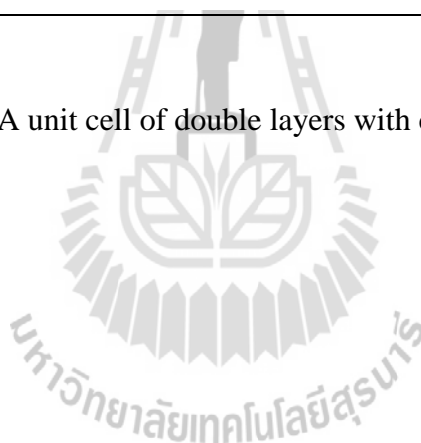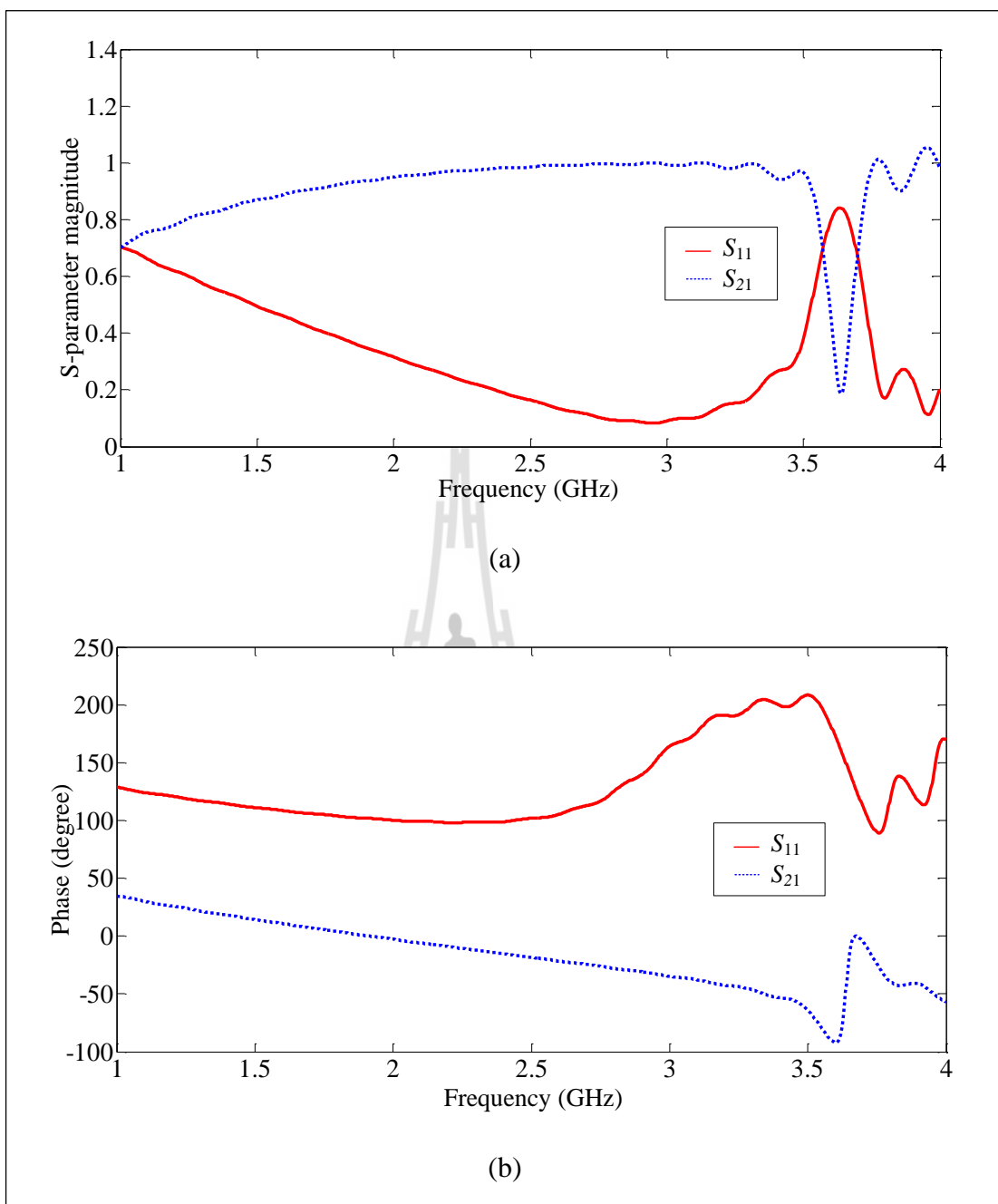
Figure 4.10 S-parameter of a cross polarized double layer EBG

(a) magnitude and (b) reflection phase.
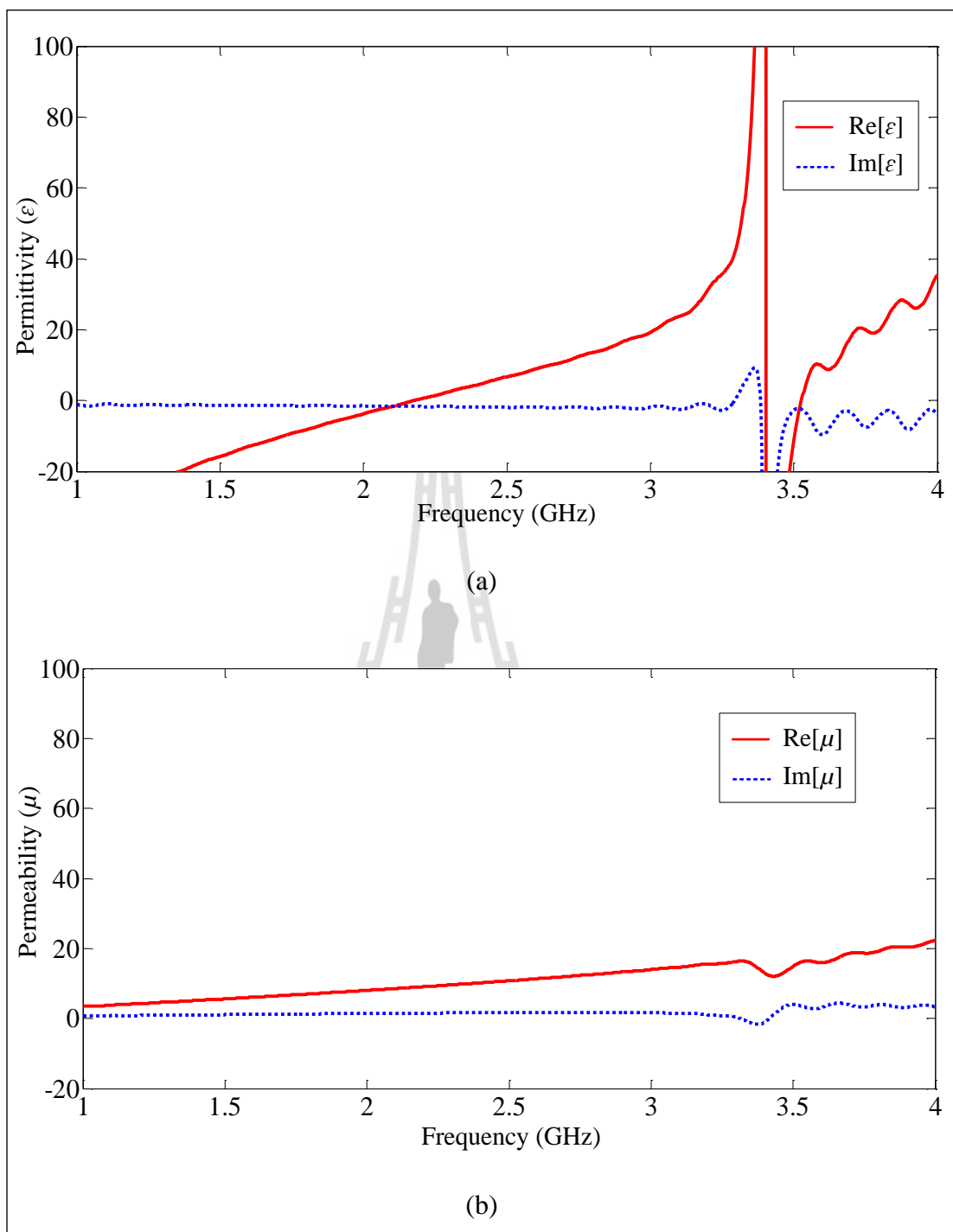
Figure 4.11 Calculated results of the double layers with cross polarized EBG
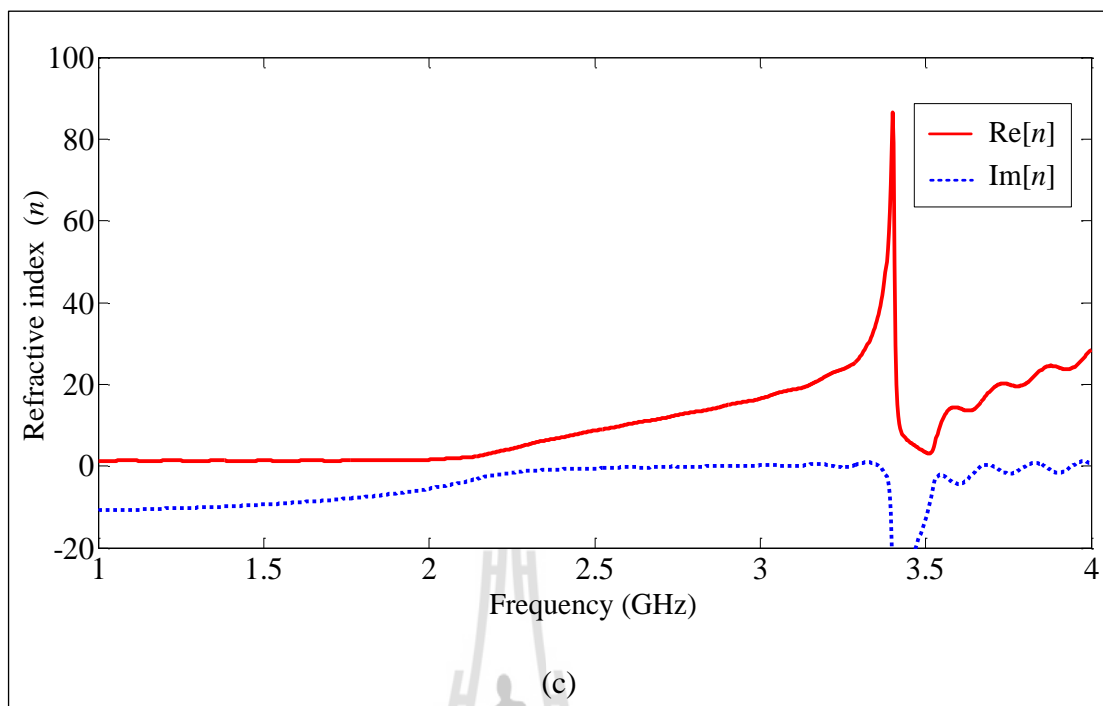
(a) ε_r, (b) μ_r, and (c) n.

Figure 4.11 Calculated results of the double layers with cross polarized EBG

(a) ε_r, (b) μ_r, and (c) n (cont.).
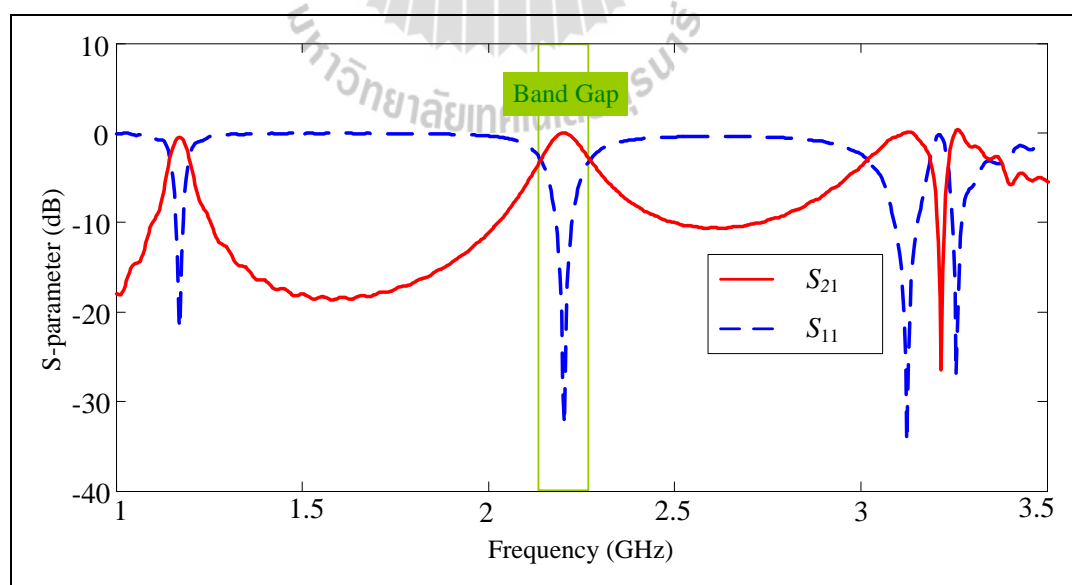
Figure 4.12 The band gap of double layers with cross polarization

The band gap of the cross polarized EBG is obtained by using

the cavity model. Assuming the cavity height (h) is adjusted to control the band gap of

EBG which is 60 mm. This S-parameter is plotted in Figure 4.12 and shown the band

gap at frequency 2.21 GHz to 2.31 GHz.

Case 2 : Co-polarization of EBG
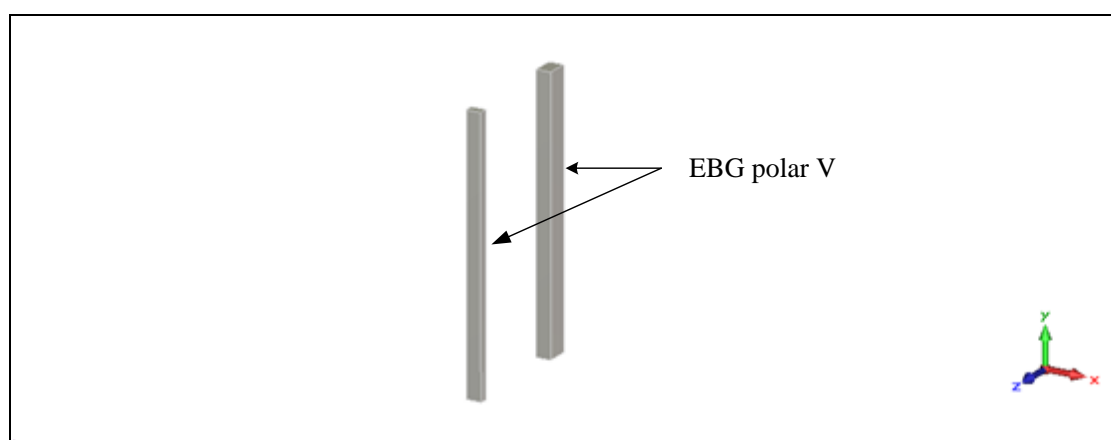
Figure 4.13 A unit cell of double layers with co-polarization.

The double EBG polar V is considered, a unit cell is

surrounded by four periodic boundaries as shown in Figure 4.13. This model can

estimate the transmission and the reflection wave of the EBG structure as plotted in

Figure 4.14(a) Consideration of S_{11} and S_{21} at 2.1 GHz concludes that the aluminium

rod can be partially reflected wave. The reflection phase in Figure 4.14(b) is

performed that larger phase inversion has been obtained, thus the allowed bandwidth

can be increased. Referring to Figure 4.15 denoted that the aluminium rods are

classified in a medium with epsilon near zero (ENZ) with the permittivity,

permeability and refraction index of 0.01, 22.29 and 0.47, respectively. The band gap

of the co-polarized EBG is obtained by using the cavity model. Let us now analyze

the transmission and reflection coefficient, assuming the cavity height (h) is adjusted to control the band gap of EBG which is 60.3 mm. The band gap is covering the frequency of 1.83 GHz to 2.25 GHz.
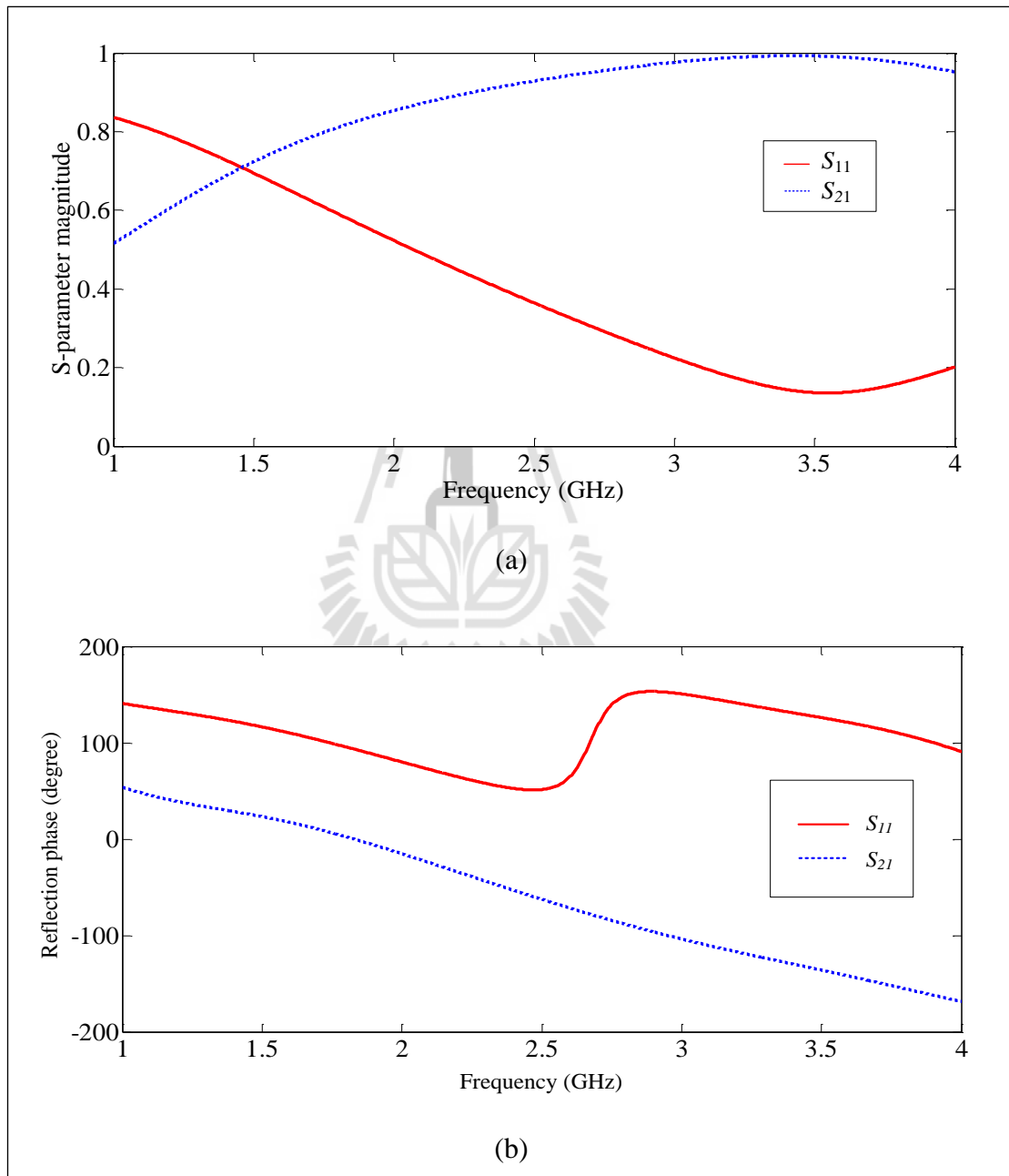
Figure 4.14 S-parameter of double layers with co-polarization (a) magnitude and (b) phase.
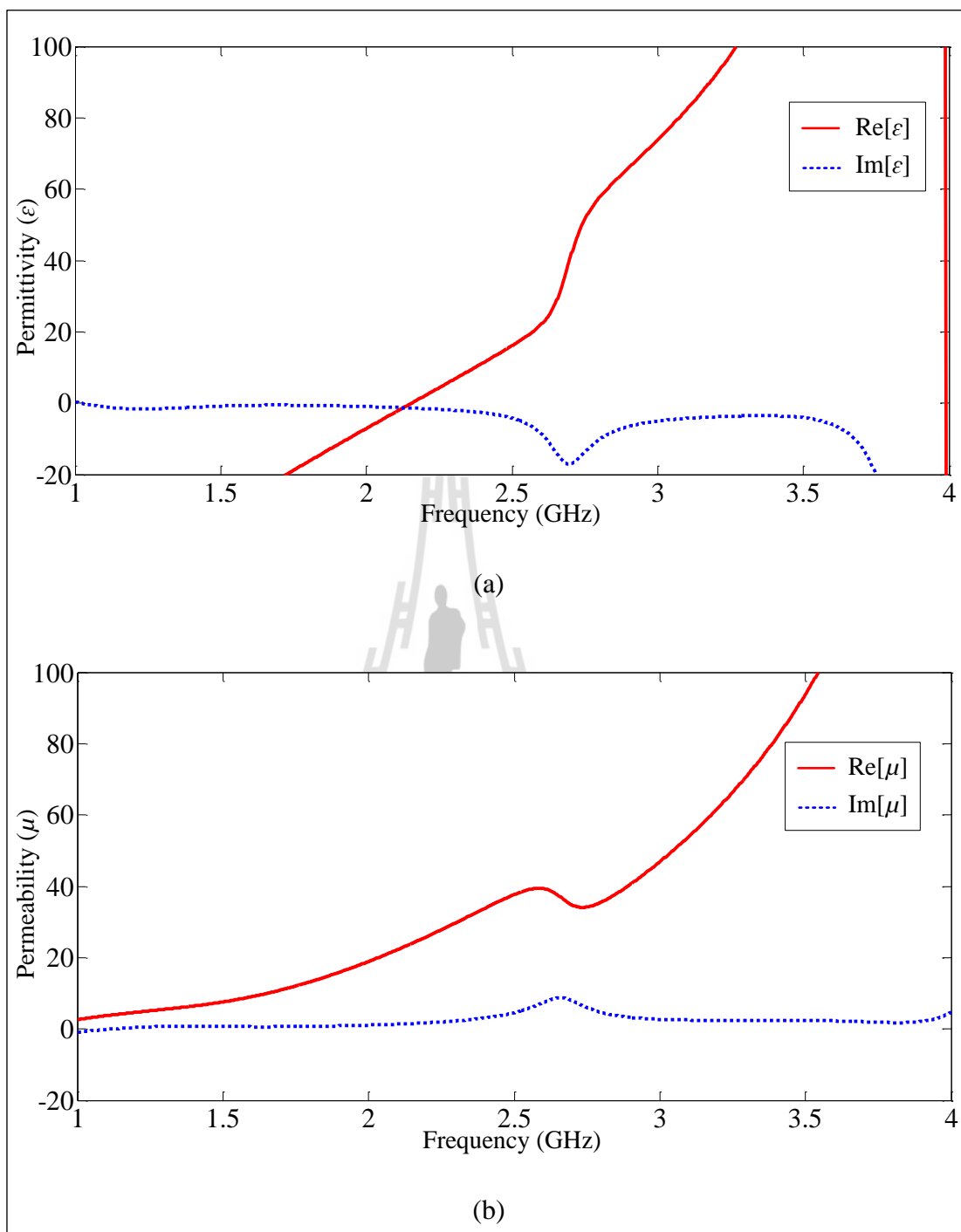
Figure 4.15 Calculated results of the double layers with co-polarization
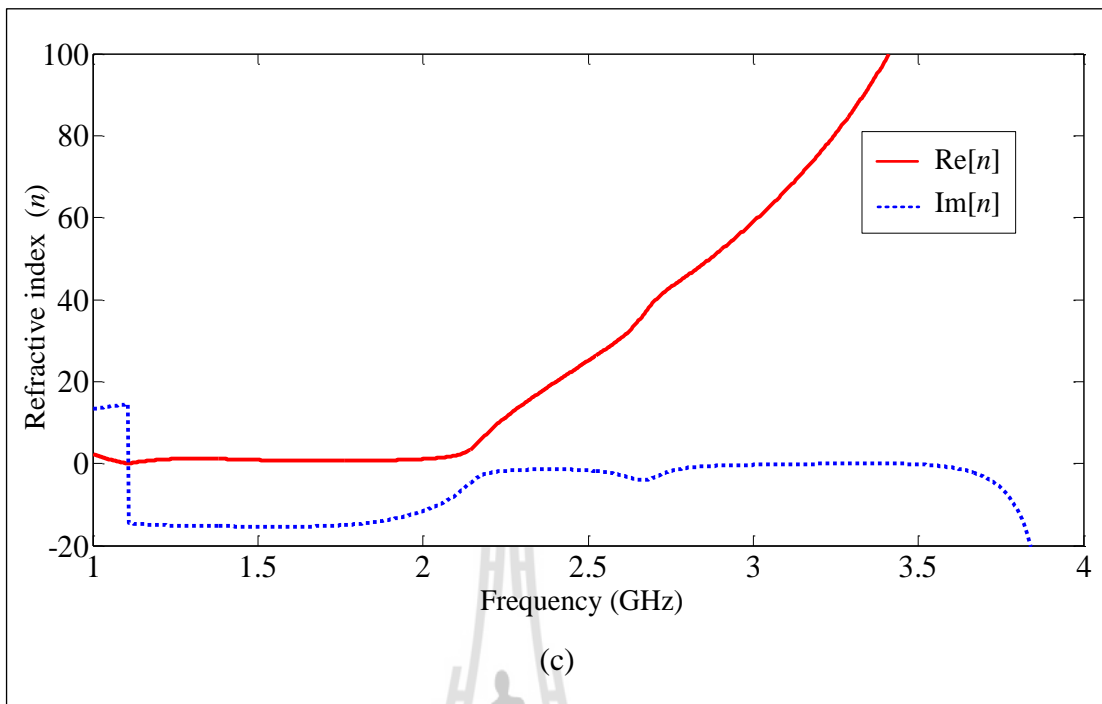
(a) ε_r, (b) μ_r, and (c) n.

Figure 4.15 Calculated results of the double layers with co-polarization

(a) ε_r, (b) μ_r, and (c) n (cont.).
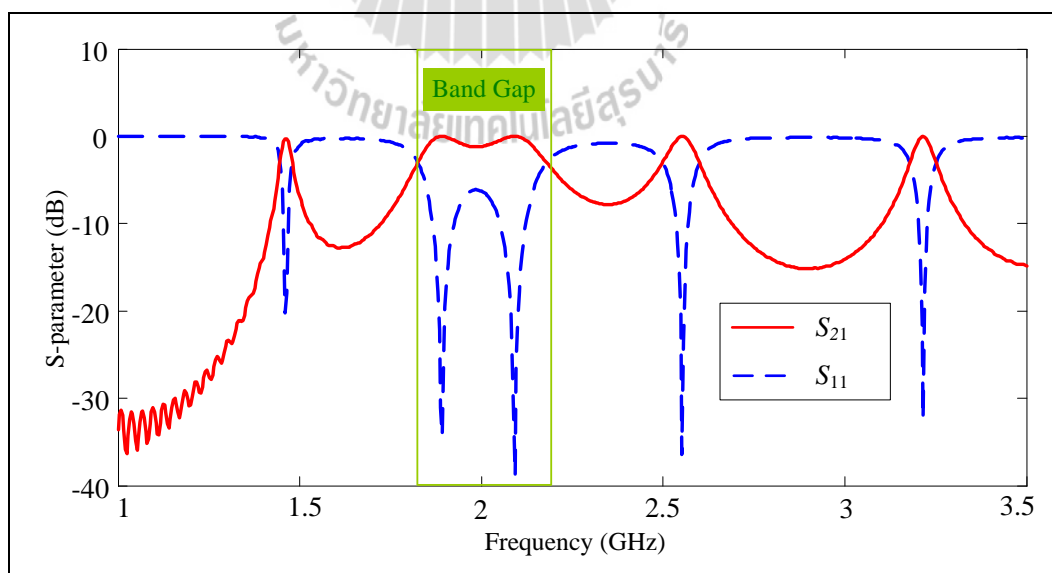
Figure 4.16 The band gap of double layers with co-polarization.

4.3.3 Three layers of metallic rod
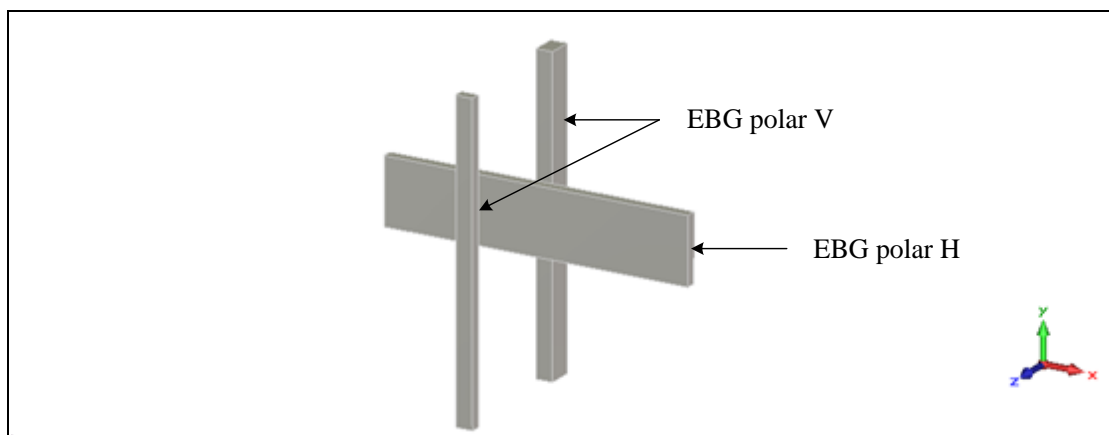
Figure 4.17 A unit cell of three layers.

Three layers are considered and a unit cell is surrounded by four periodic boundaries as shown in Figure 4.17. This model can estimate the transmission and the reflection wave of the EBG structure as plotted in Figure 4.18(a) Consideration of S_{11} and S_{21} at 2.1 GHz concludes that the aluminium rod can be partially reflected wave. The reflection phase in Figure 4.18(b) is performed that larger phase inversion has been obtained, thus the allowed bandwidth can be increased. Figure 4.15 illustrates the electromagnetic properties of three layers EBG, it is classified in a medium with epsilon near zero (ENZ) with low refraction index of 2.6. The band gap of the three layers EBG is obtained by using the cavity model. Let us now analyze the transmission and reflection coefficient, assuming the cavity height (*h*) is adjusted to control the band gap of EBG which is 60.31 mm. This S-parameter is plotted in Figure 4.20, indicate one partially reflected band gap at frequency 1.65 GHz to 2.5 GHz. This band is satisfied for mobile base station in 3G and 4G technology.
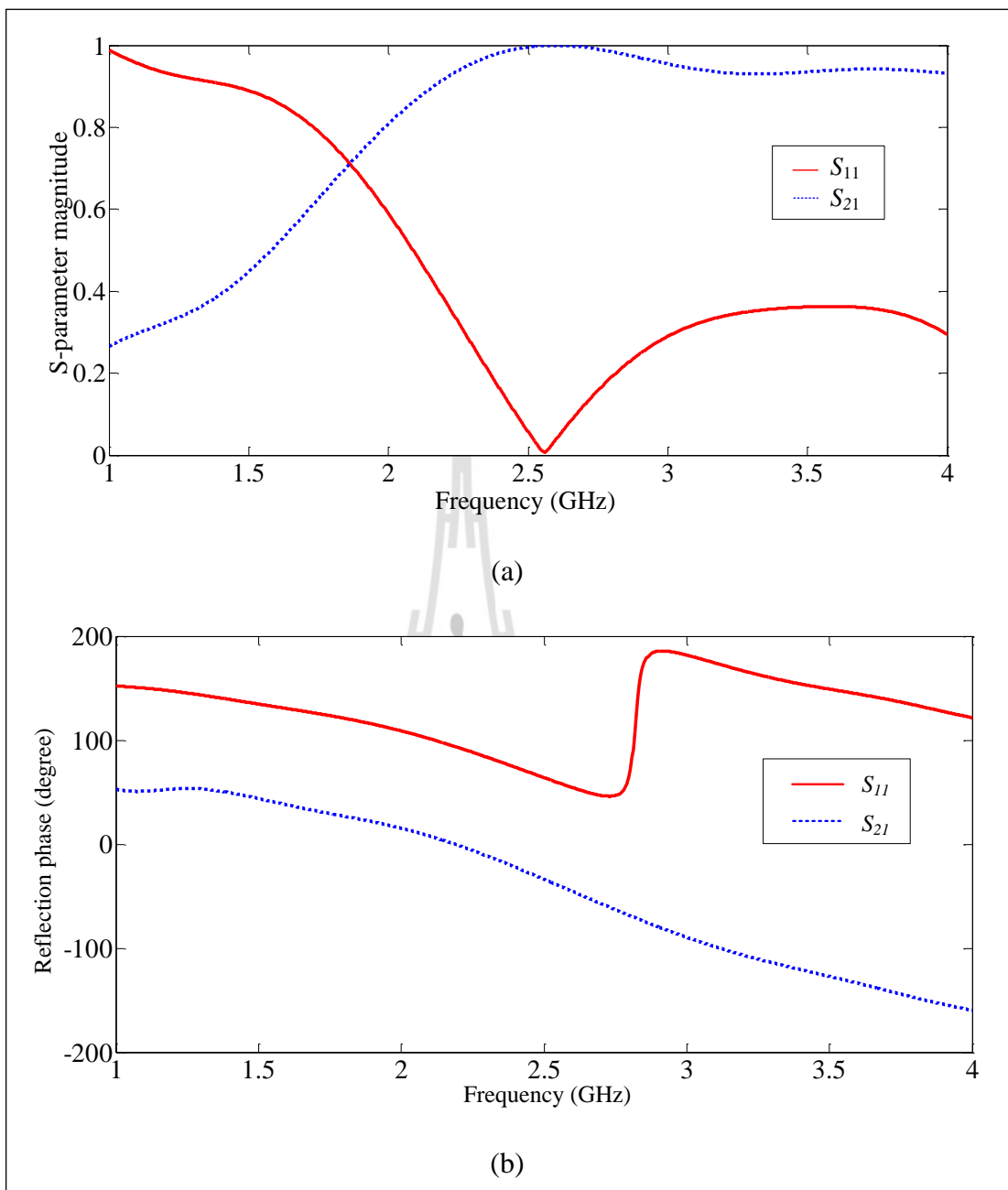
Figure 4.18 S-parameter of three layers (a) magnitude and (b) phase.
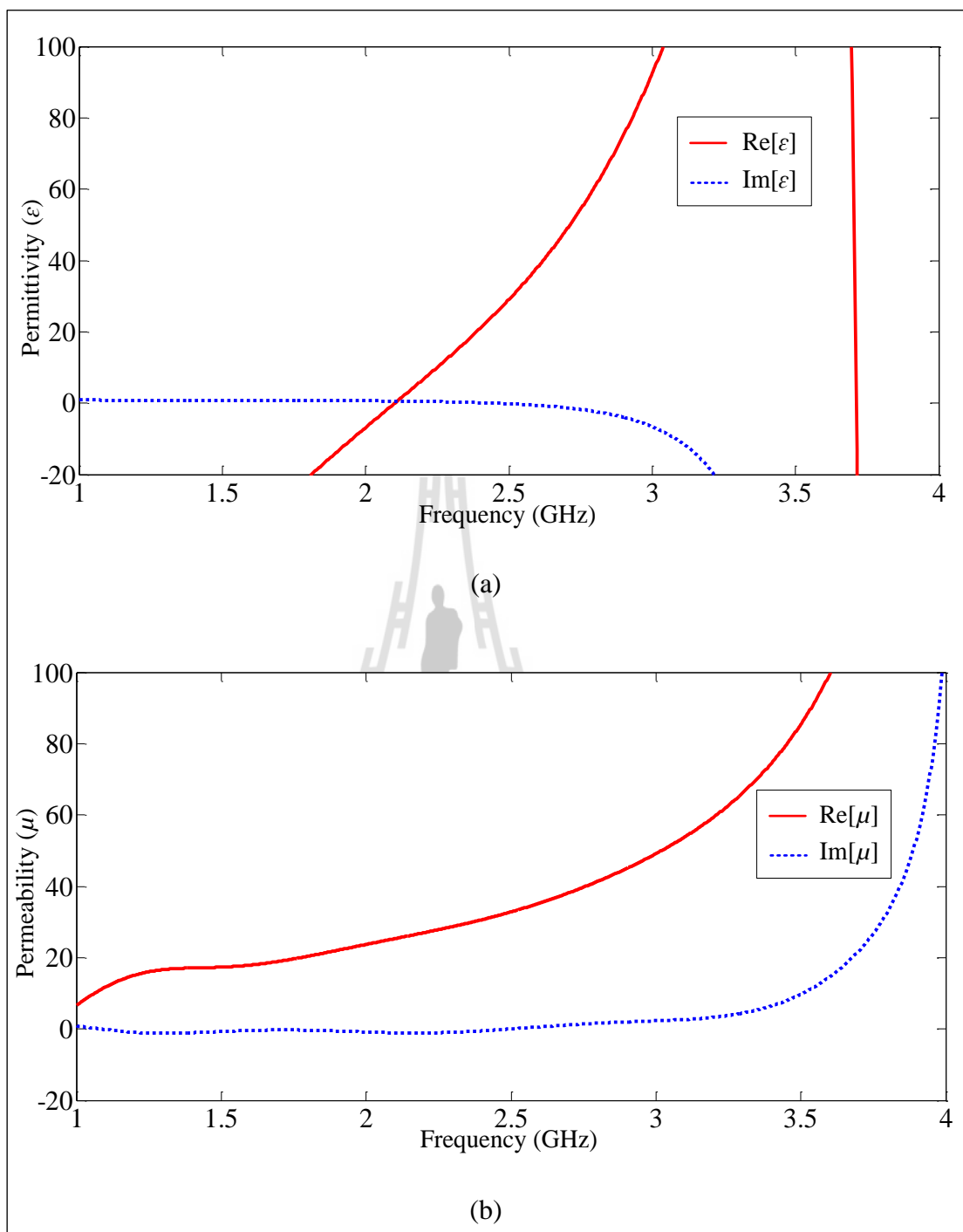
Figure 4.19 Calculated results of three layers (a) ε_r, (b) μ_r, and (c) n.
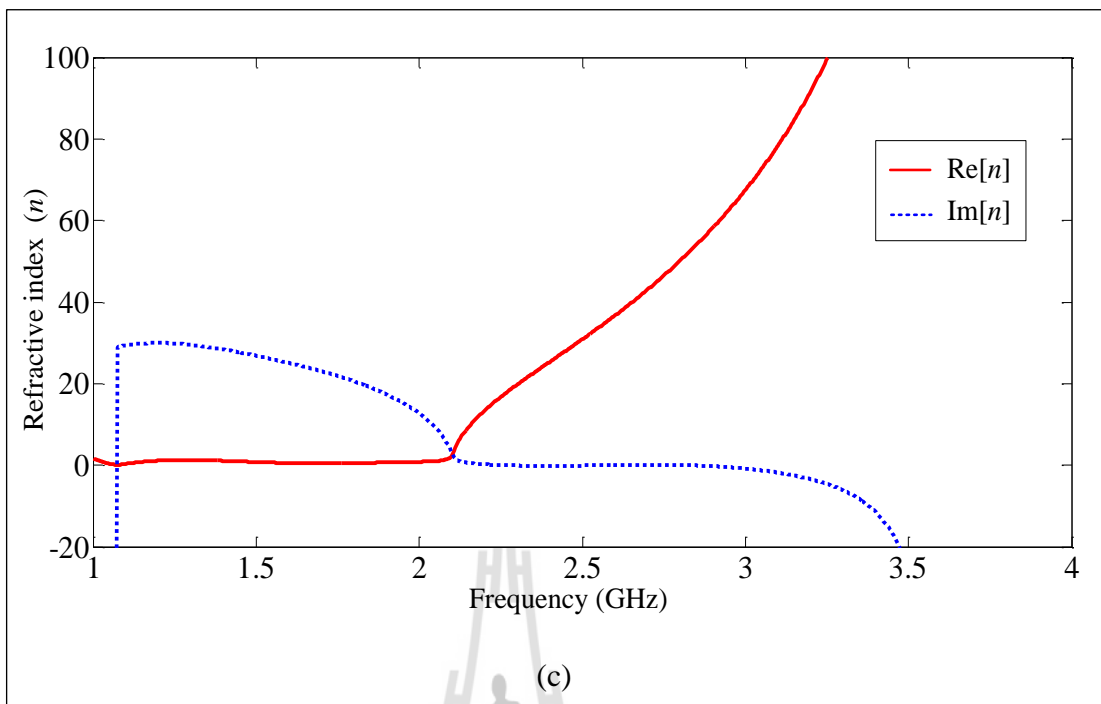
Figure 4.19 Calculated results of three layers (a) ε_r, (b) μ_r, and (c) n. (cont.)
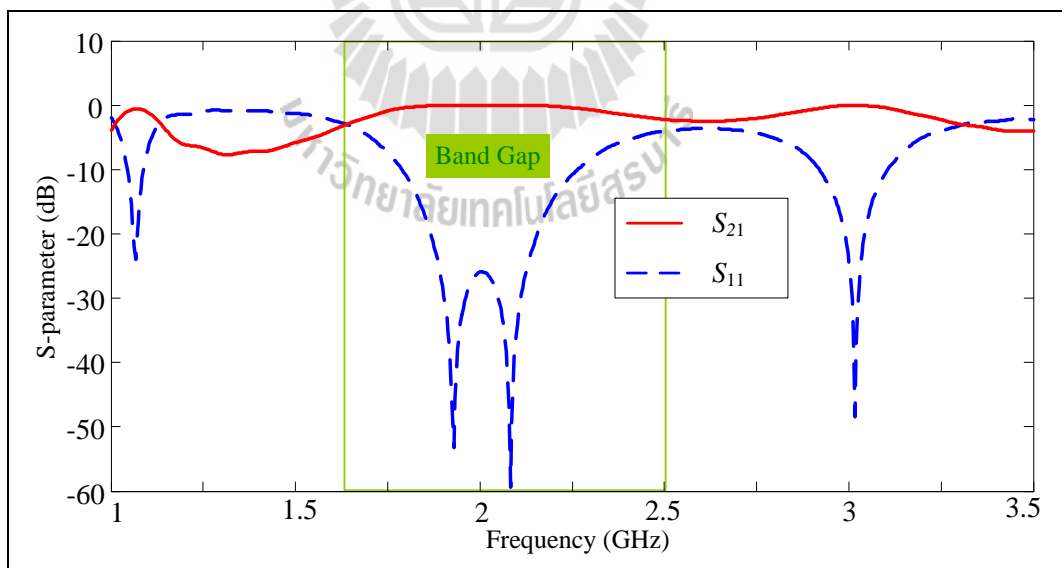
Figure 4.20 The band gap of three layers.

Metamaterial antenna is a class of antennas which use metamaterials to enhance or increase performance of the system. In this study, thirteen aluminium rods are arrayed in y axis that it is EBG horizontal polarization (EBG polar H) as shown in Figure 4.21(a). The EBG polar H structure is fed by using the plane wave with the gap as a half wavelength to concentrate the reflection phase parameter. The parameters are optimized by using CST microwave studio as concluded in Table 4.2 and the reflection phase of EBG polar H ($\varphi_{EBGpolarH}$) is plotted in Figure 4.21(b). This result can be applied for the EBG resonator antenna that will be described in next section.

Table 4.2 Parameters of EBG horizontal polarization

Parameters	Size (mm)
A_1 : width of EBG polar H	13.26
g_1 : gap between EBG polar H	29.83
t_1 : length of EBG polar H	530

t_1

A_1

g_1

y

x

Top

1 mm

Bottom

$\lambda/2$

plane wave

y

x

z

(a)

(b)
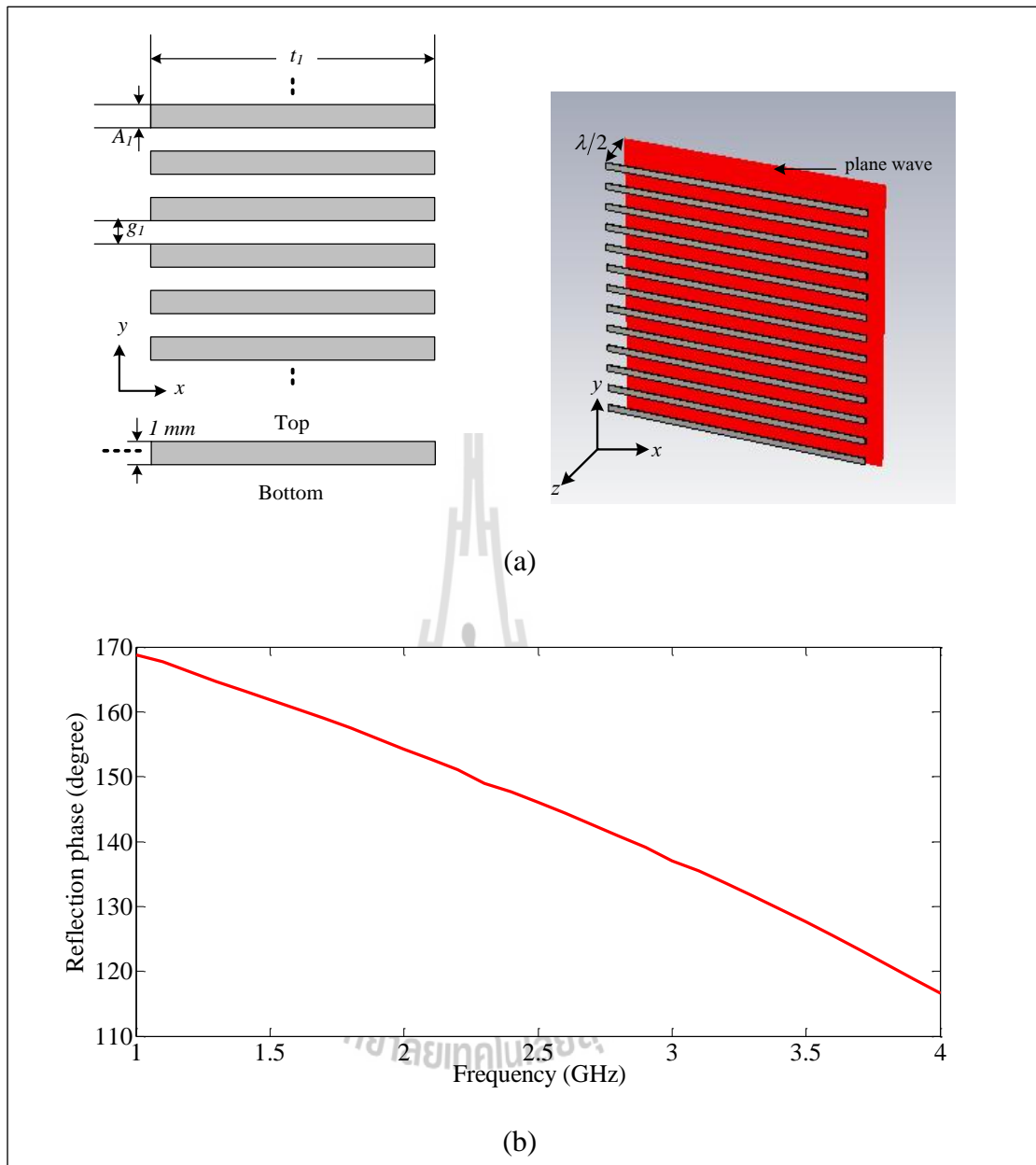
Figure 4.21 Simulation of the EBG horizontal polarization (a) structure

and (b) reflection phase.

4.4   The linearly polarized resonator antenna

This section shows EBG resonator antenna, which consists of three components. There are a superstrate, a reflector plane, and a curved strip dipole

antenna for the excitation source. The superstrate forms a 1-D EBG structure where periodic conducting pattern is metallic rods. It behaves as a PRS array at the antenna operating frequencies. A curved strip dipole antenna is placed between PEC reflector plane and 1-D EBG as shown in Figure 4.22. The radiation of feeding antenna has a center point at P, whereas the radiation pattern of a curved strip dipole antenna is $f(\theta)$. In addition, the distance between the PEC reflector plane and EBG is h, and reflection coefficient of EBG is $\gamma e^{j\varphi_{EBG}}$.
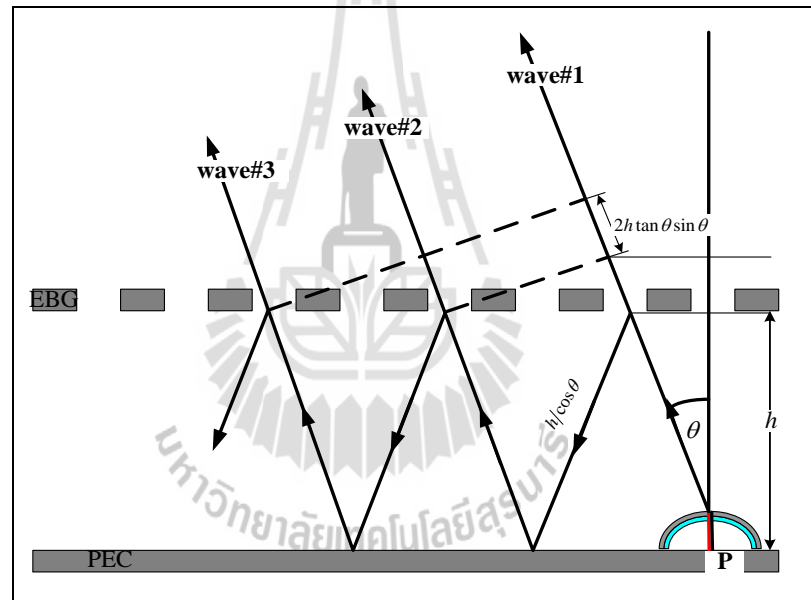
Figure 4.22 Reflection wave between PEC and EBG.

Assume that the transmission is lossless, the amplitude of the direct wave 1 is $\sqrt{1-\gamma^2}$, the amplitude of the once-reflected wave 2 is $\gamma\sqrt{1-\gamma^2}$, in the same way the amplitude of the twice- reflected wave 3 is $\gamma^2\sqrt{1-\gamma^2}$, etc. Therefore, summation of electric field is examined from

$$\overline{E} = \sum_{n=0}^{\infty} f(\theta) E_0 \gamma^n \sqrt{1-\gamma^2}\, e^{j\Delta\varphi_n}, \tag{4.6}$$

where, $\Delta\varphi$ is the phase variations. When the phase difference between wave 2 and wave 1 is

$$\Delta\varphi_1 = \frac{2\pi}{\lambda} 2h \tan\theta \sin\theta - \frac{2\pi}{\lambda} \frac{2h}{\cos\theta} - \varphi_{PEC} + \varphi_{EBG}, \tag{4.7}$$

the phase difference between wave 3 and wave 1 is

$$\Delta\varphi_2 = \frac{2\pi}{\lambda} 4h \tan\theta \sin\theta - \frac{2\pi}{\lambda} \frac{4h}{\cos\theta} - 2\varphi_{PEC} + 2\varphi_{EBG}. \tag{4.8}$$

If the direct wave has n number, so the phase difference is

$$\Delta\varphi_n = n\left[-\frac{4\pi}{\lambda} \cos\theta - \varphi_{PEC} + \varphi_{EBG} \right]. \tag{4.9}$$

When $\gamma < 1$, we obtain

$$\sum_{n=0}^{\infty} \left(\gamma e^{j\Delta\varphi} \right)^n = \frac{1}{1 + \gamma e^{j\Delta\varphi}}. \tag{4.10}$$

Therefore, we can represent the electric field as followed;

$$|E| = |E_0| f(\theta) \sqrt{\frac{1-\gamma^2}{1+\gamma^2 - 2\gamma \cos\Delta\varphi}}, \tag{4.11}$$

and the power pattern is

$$\overline{S} = \frac{1 - \gamma^2}{1 + \gamma^2 - 2\gamma \cos\left(\varphi_{EBG} - \varphi_{PEC} - \frac{4\pi}{\lambda} h \cos\theta\right)} f^2(\theta). \tag{4.12}$$

However, the amplitude (γ) and phase (φ_{EBG}) of the EBG reflection coefficient are a function of the angle θ. Maximum power in the normal direction is obtained, when

$$\varphi_{EBG} - \varphi_{PEC} - \frac{4\pi}{\lambda} h = 0, \tag{4.13}$$

so, the distance between PEC reflector plane and EBG is

$$h \cong \left(\frac{c}{2f}\right)\left(\frac{\varphi_{EBG} - \varphi_{PEC}}{2\pi}\right) + N\frac{\lambda}{2}, \tag{4.14}$$

where, $N = 0, 1, 2, 3, \ldots$

From equation (4.14), the cavity height (h) depends on the resonant frequency which can be calculated by choosing the reflection phase in section 4.3 as plotted in Figure 4.23.
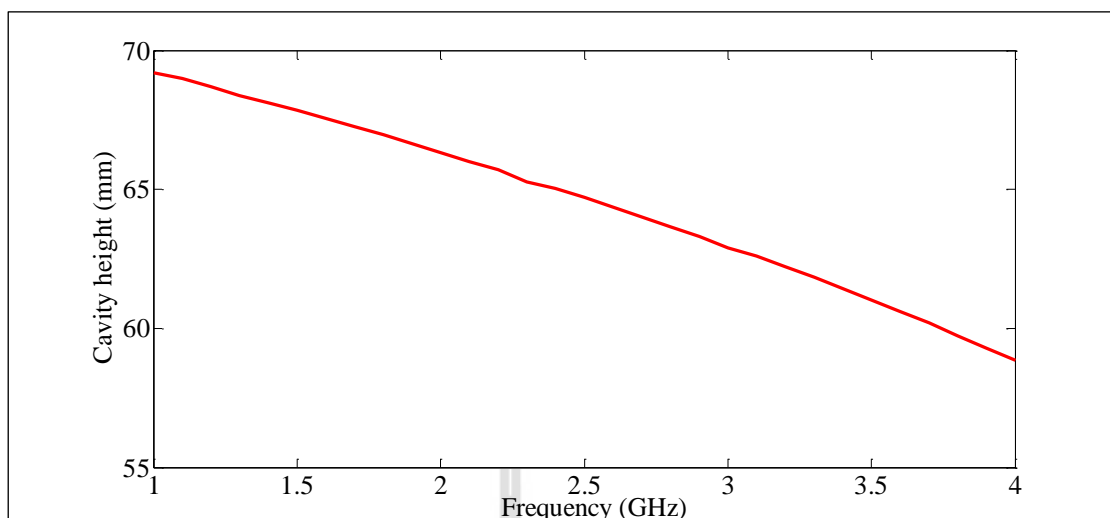
Figure 4.23 Cavity height (h_1) between the reflector plane and EBG.

The resonator antenna is classified in 2 cases through following the polarization, Transverse Electric (TE) polarization resonator antenna and Transverse Magnetic (TM) polarization resonator antenna.

4.4.1 Transverse Electric (TE) polarization resonator antenna

Chapter 3 shows that if the electric field of primary radiator does not propagate in the direction of EBG polarization, an antenna is proposed of TE polarization mode. Figure 4.24(a) shows the TE polarization resonator antenna model, which consists of the several aluminium rod array and PEC reflector plane. Moreover, a curved strip dipole antenna is fed between the cavity walls. A 1-D the several aluminium rod arrays is a simple example of PRS that can be employed for this design method afterward. For illustration, let us consider the single-layer EBG polar H. The several aluminium rods have a thickness of 1 mm and the unit cell has initial dimensions of 530 mm × 13.26 mm × 1 mm. The distance between aluminium rods (g_1) is 29.83 mm. When the reflection phase of the EBG polar H is 160˚ at 2.1 GHz, the cavity height (h_1) be obtained depended on the frequency can of 67.46 mm. Figure 4.24(b) shows the S_{11} value, it confirm that this antenna can be resonated in a band of

frequencies between 1.93 GHz and 2.16 GHz. The radiation patterns are illustrated in Figure 4.24(c), the HPBW in the vertical and horizontal plane is 103.7° and 69.5°, respectively. Furthermore, the near-field level is shown in Figure 4.8(d), the magnitude over EBG polar H is around 30.6 V/m. It seems that the transmitted wave occurs more often than the reflected wave because the reflection in the cavity walls is low. So, the simulation directive gain has a low of 8.5 dB, it is close to the gain of a curved strip dipole over PEC reflector plane.
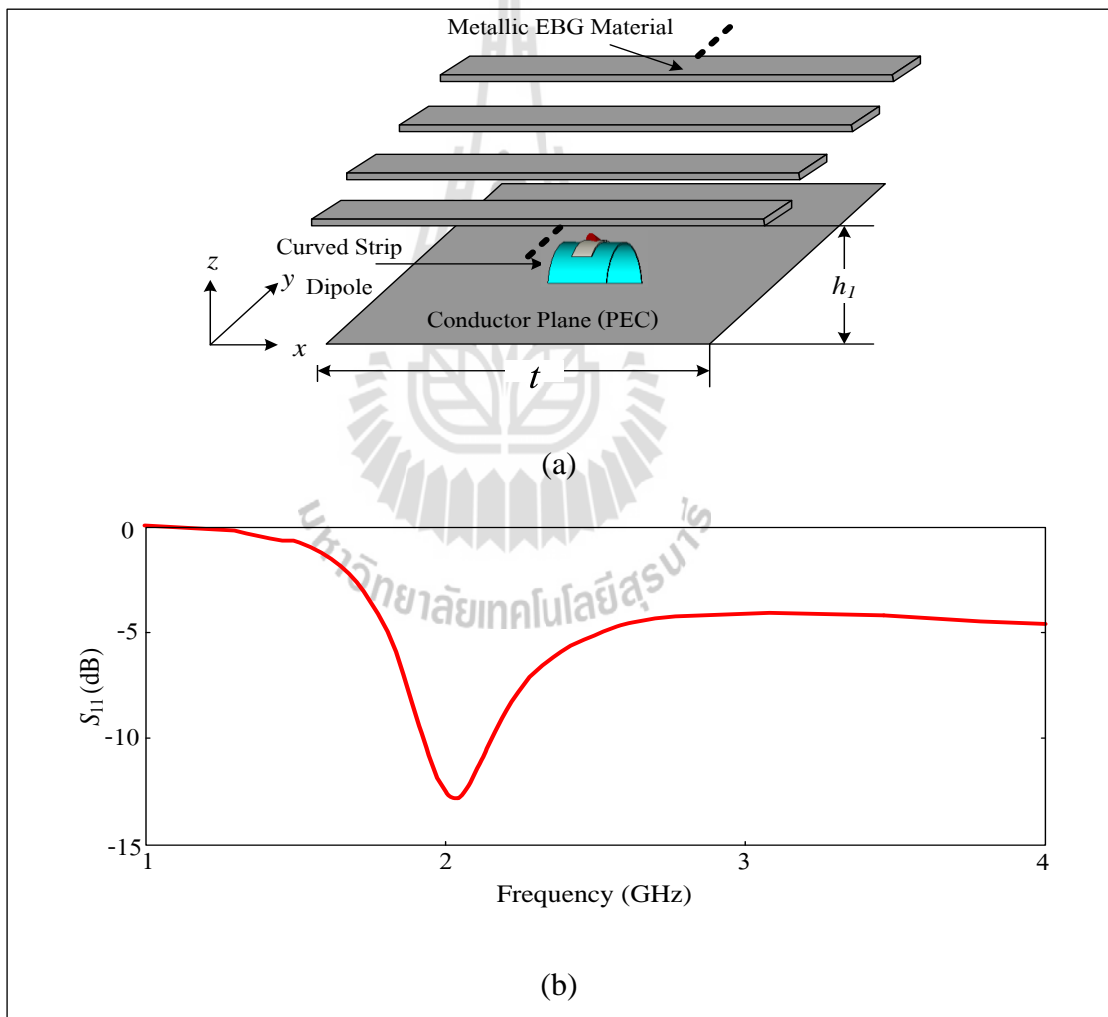
Figure 4.24 Simulation results of transverse electric polarization resonator antenna

(a) structure, (b) S_{11}, (c) radiation pattern, and (d) near-field distribution.

(c)

(d)
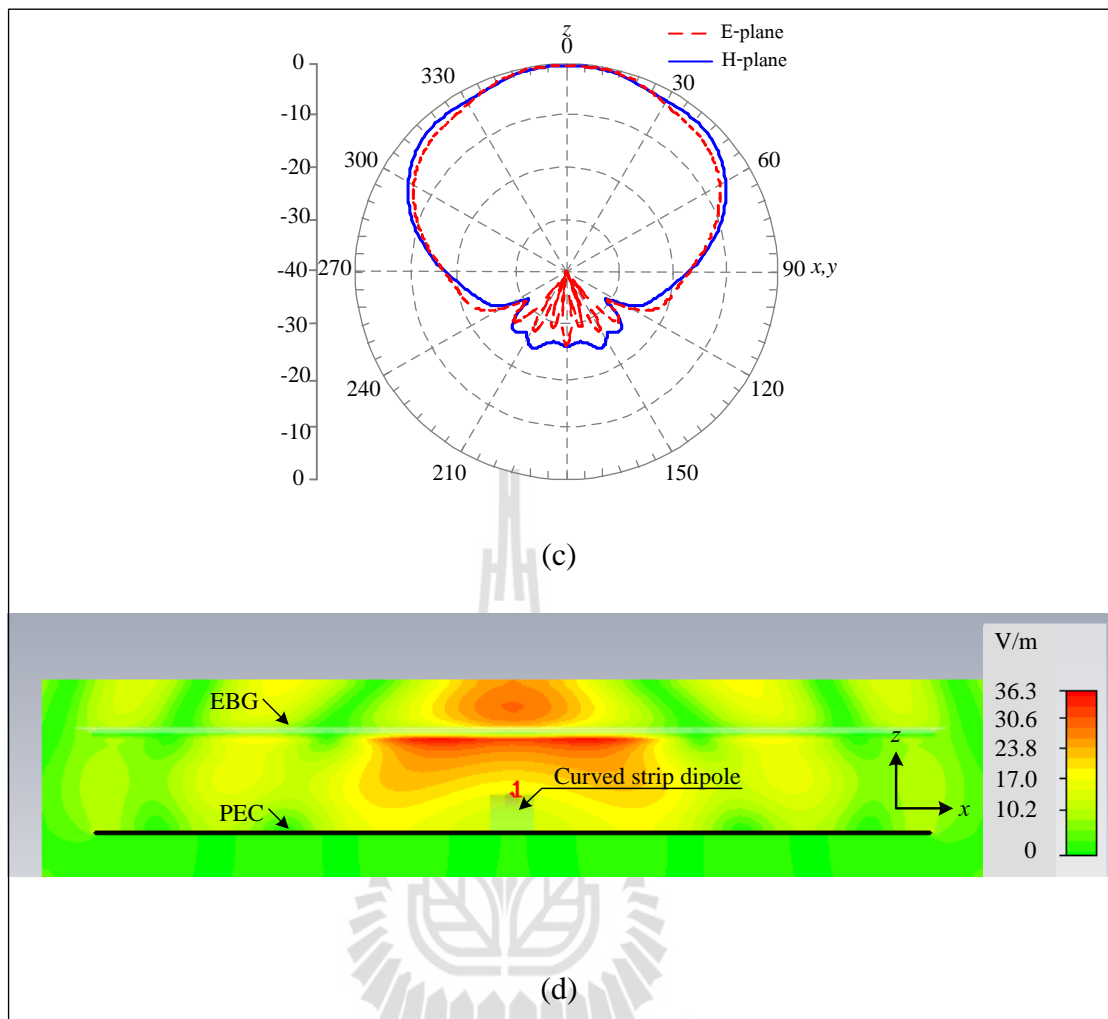
Figure 4.24 Simulation results of transverse electric polarization resonator antenna

(a) structure, (b) S_{11}, (c) radiation pattern, and (d) near-field

distribution (cont.).

4.4.2 Transverse Magnetic (TM) polarization resonator antenna

On the other hand, if the resonator antenna is set in TM polarization mode, it does not have a magnetic field in the direction of propagation waves, where the TM polarization antenna model is shown in Figure 4.25(a). In this case, we are unable to consider the S_{11} value because the reflection occurred in the cavity walls. Thus, the maximum gain at a varied frequency is plotted in Figure 4.25(b) together

with gain of 18 dBi. At -3 dB bandwidth, the TM polarization resonator antenna will resonate in a band of frequencies between 2.08 GHz and 2.2 GHz. Figure 4.25(c) shows the HPBW, which is 18.4° and 71.5° in vertical and horizontal planes, respectively. In consideration of the reflection wave, the magnitude over EBG polar H is around 20 V/m as shown in Figure 4.25(d). It seems that the transmitted wave occurs less than the reflected wave.
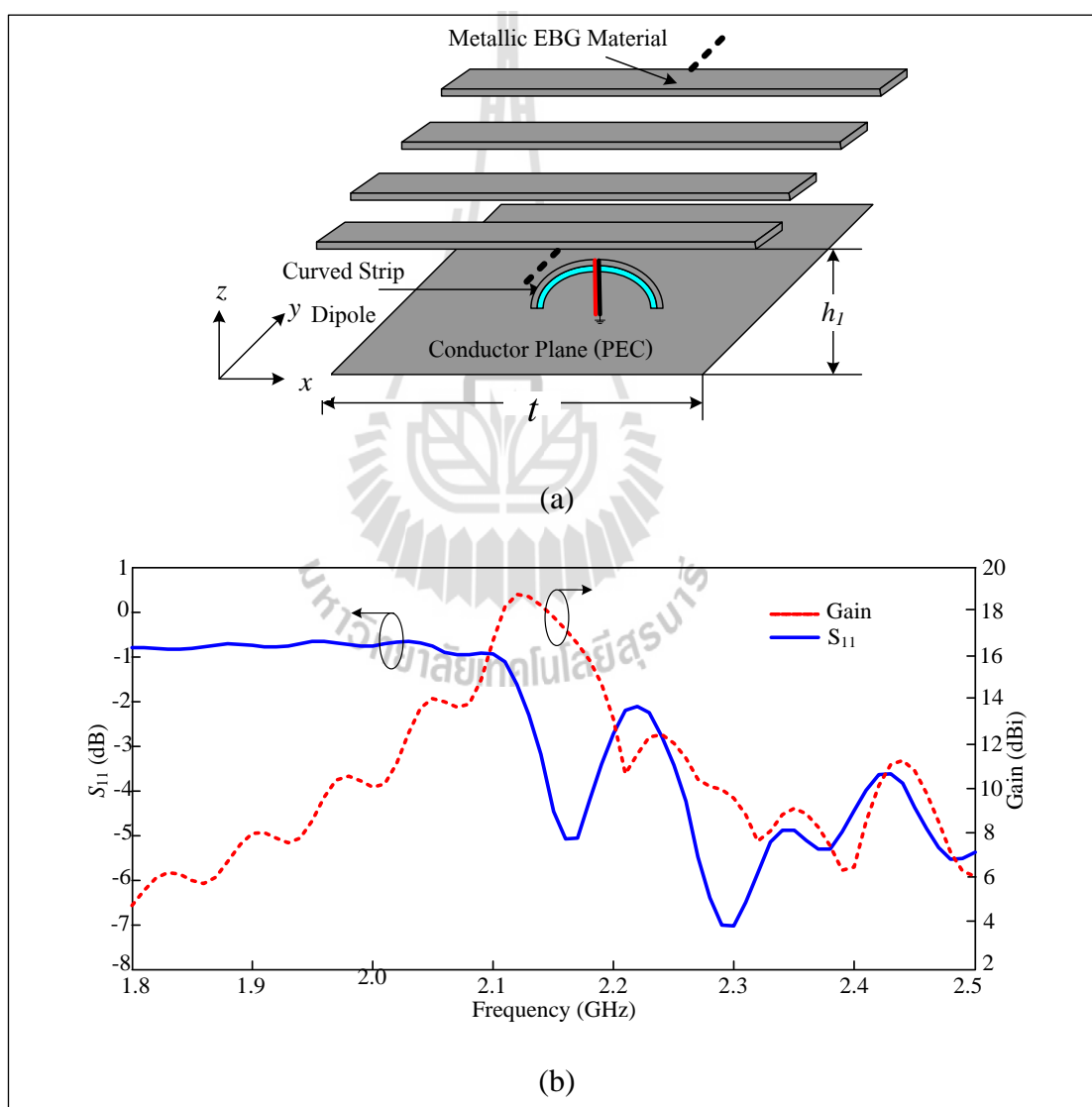
(a)

(b)

Figure 4.25 Simulation results of transverse magnetic polarization resonator antenna

(a) structure, (b) S_{11}, (c) radiation pattern, and (d) near-field distribution.
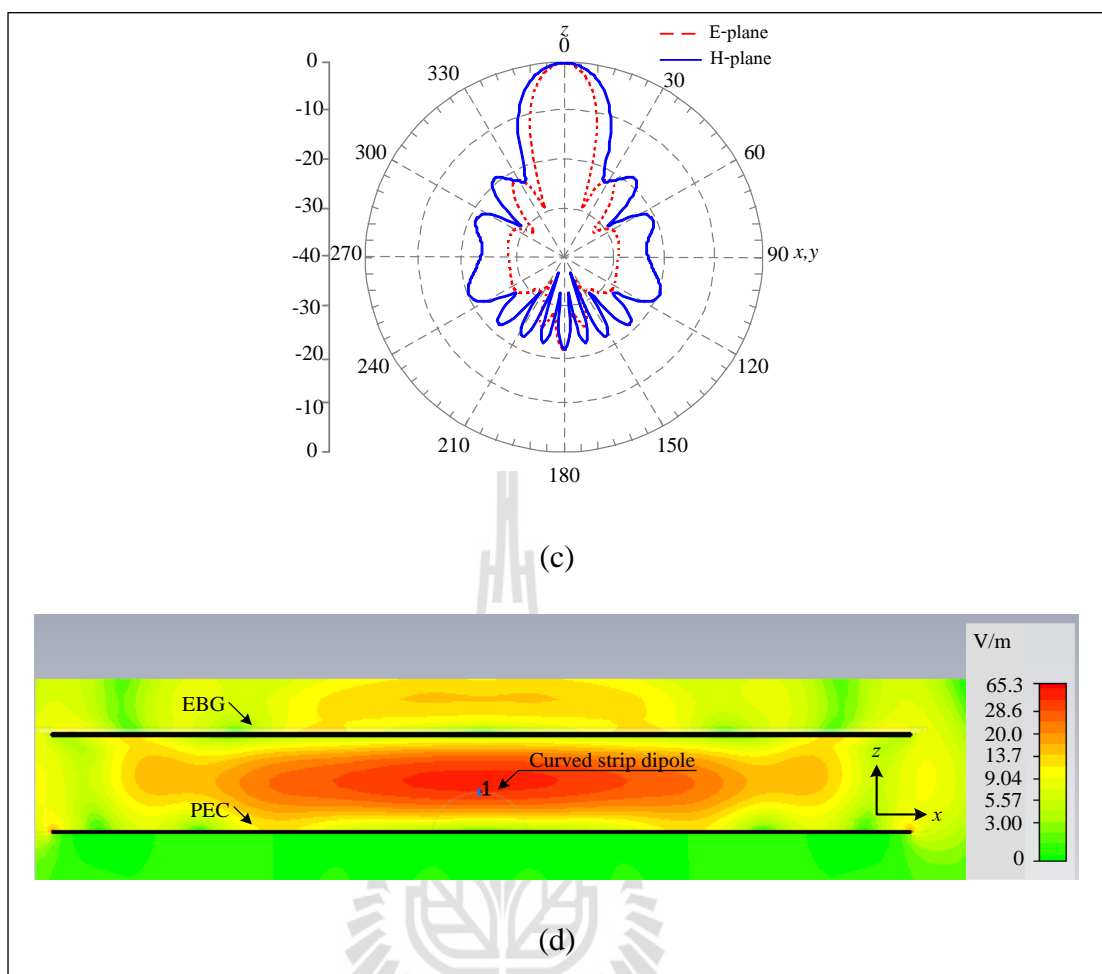
Figure 4.25 Simulation results of transverse magnetic polarization resonator antenna

(a) structure, (b) S_{11}, (c) radiation pattern, and (d) near-field

distribution (cont.)

4.5 Dual polarized resonator antenna

In all the above results, the directive gain of TM polarization mode is suitable for a mobile base station. But it is linear polarization because the magnitude of the electric field in the vertical polarization less than the horizontal polarization as shown in Figure 4.26.
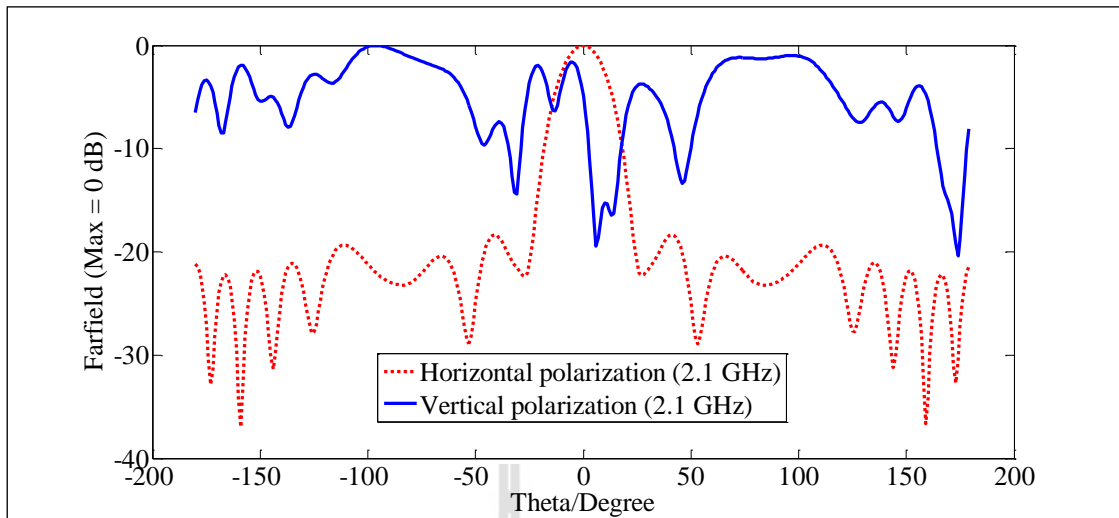
Figure 4.26 Electric field of transverse electric polarization resonator antenna.

This problem is resolved by using a 45° oriented curved strip dipole on PEC reflector plane. According to expectations of the high gain dual polarized antenna, EBG polar V is added to the lower reflective wall to increase the magnitude of the electric field in the vertical polarization. When the cavity height (h_2) between EBG polar V and PEC reflector plane is fixed of 60 mm, the reflection phase of EBG polar V is calculated of 122.4°. Furthermore, the EBG polar V is designed as shown in Figure 4.27(a) and the parameters are optimized by using CST microwave studio as concluded in Table 4.3. In this design, double layers EBG with 45 slant curved strip dipole on reflector plane does not include in TM and TE polarization mode. The primary wave from excitation feed is mostly reflected from the EBG superstrate. For this reason, the magnitude of the reflection coefficient is dramatically increased to achieve a high extra gain (Tomislav D., et. al, 2010). Referring to the reflection phase of the EBG polar V is plotted in Figure 4.27(b), it is satisfied with the calculation result. In addition, Figure 4.11(c) is illustrated the cavity height of the EBG polar V when the resonant frequency is varied.

Table 4.3 Parameters of EBG vertical polarization

Parameters	Size (mm)
A_1 : width of EBG polar V	3.85
g_1 : gap between EBG polar V	46.42
t_1 : length of EBG polar V	530
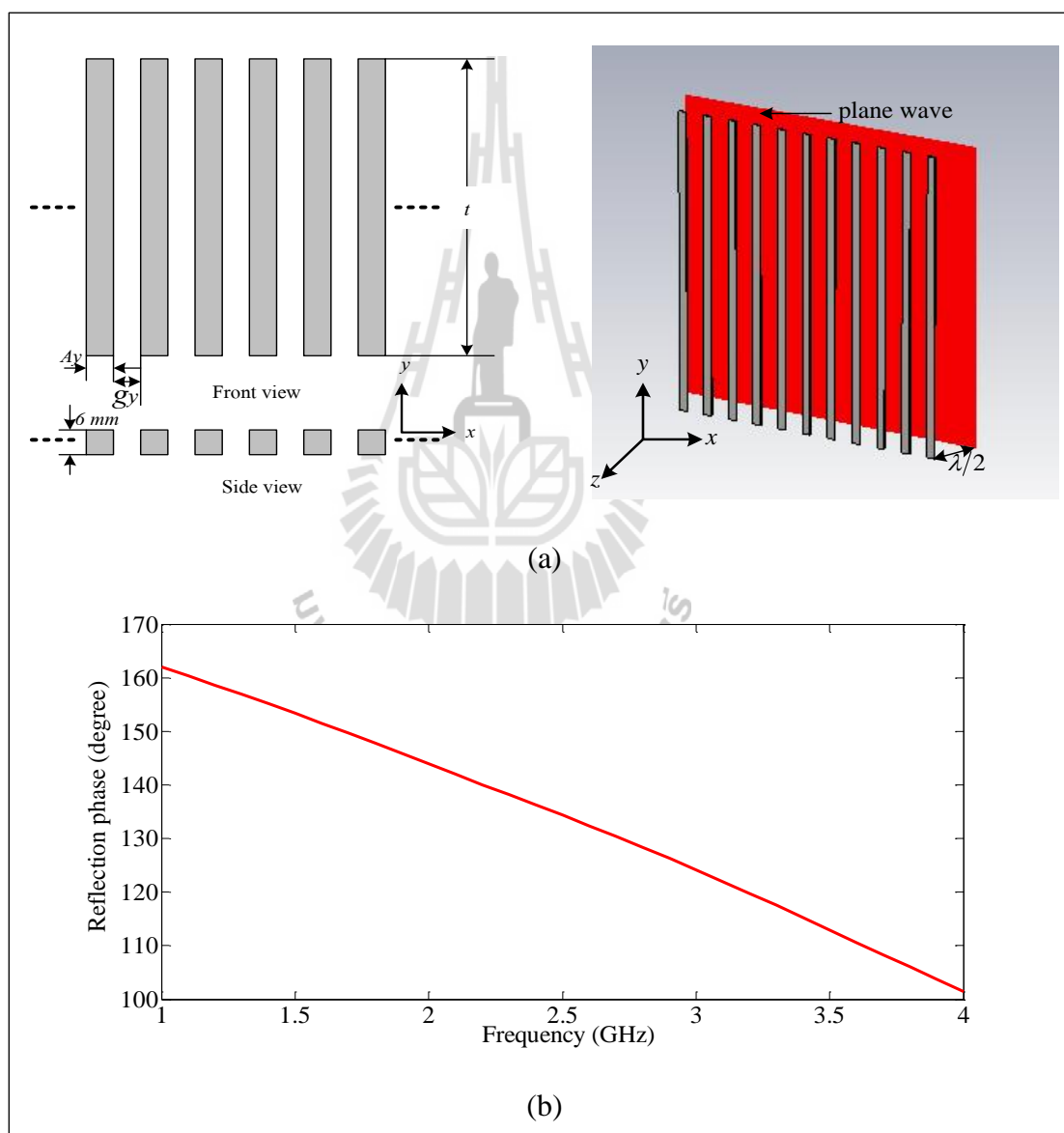
(a)

(b)

Figure 4.27 Simulation of the EBG vertical polarization (a) structure

and (b) reflection phase.
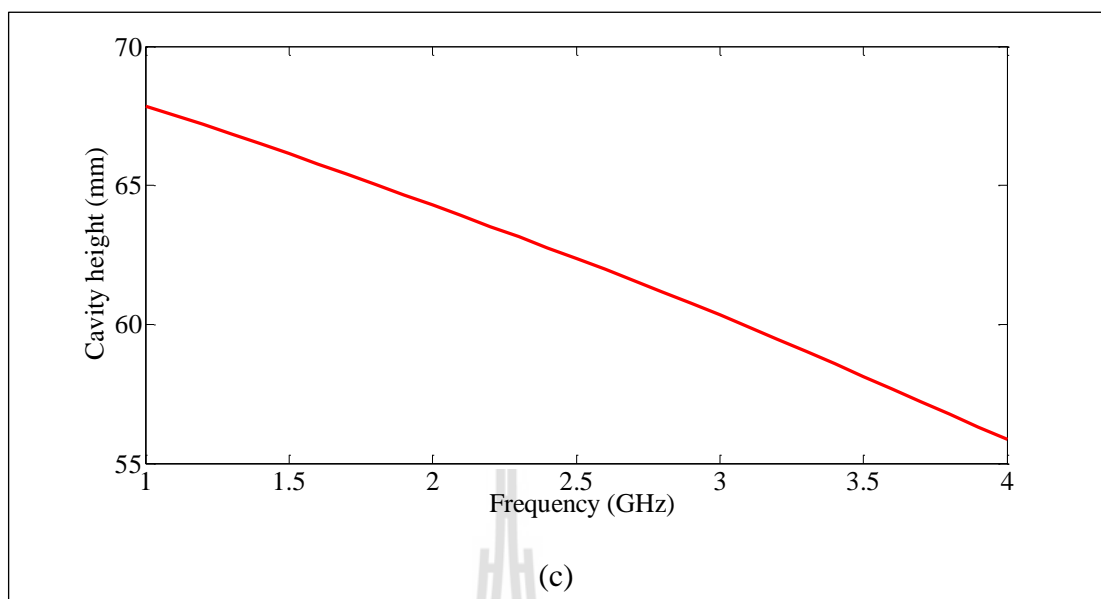
Figure 4.27 Simulation of the EBG vertical polarization (a) structure

and (b) reflection phase (cont.).

This section presents that there is a relationship between a 45° oriented curved strip dipole with double EBG layers and the electric field level in *x*- and *y*-axis is presented. The antenna can radiate the dual polarization. Almost all the parameters are taken from the antenna constructed for the experiment. Only the reflector plate size is assumed to be infinite and the geometry is shown in Figure 4.28. The calculated current is weak enough on the peripheral area out of 3λ×3λ. As the simulated gain, it is around 18.9 dBi at the frequency of 2.1 GHz as shown in Figure 4.29(a). In addition, over the whole frequency band (2.04 – 2.18 GHz), the -3 dB directive gain could be obtained. The near-field distribution behavior on the EBG surface of the dual polarization square antenna is studied and indicated in Figure 4.29(b). Studying the electric field behavior between superstrate and primary radiator with reflector plane reveals that waves are refracted and reflected by EBG surface;

therefore, the antenna can generate the high electric field level. The simulated radiation pattern of square resonator antenna is shown in Figure 4.29(c), which has low side lobes. Figure 4.30 shows the electric field in *x* and *y* axises where have the equivalent amplitudes.
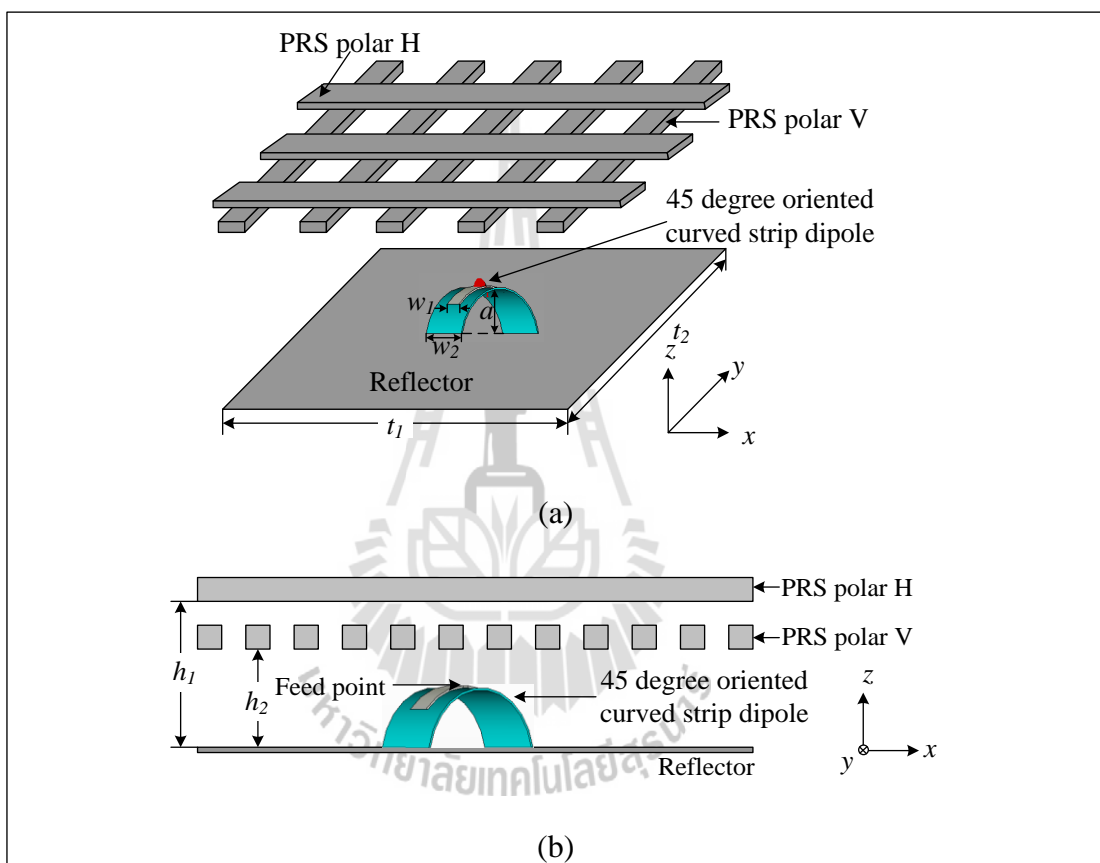
Figure 4.28 Configuration of dual polarization resonator antenna

(a) 3D view and (b) side view.

(a)

(b)

(c)
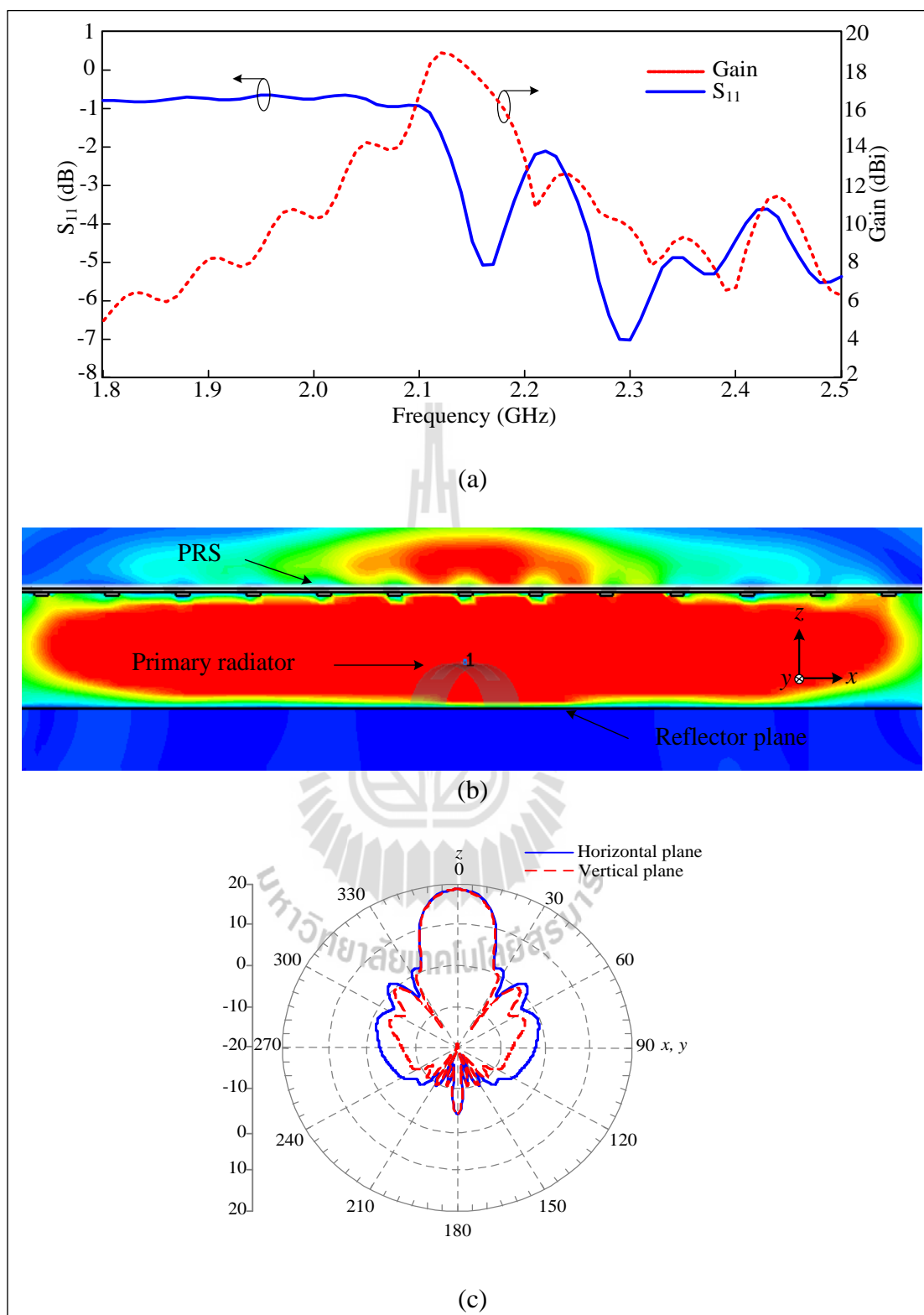
Figure 4.29 Simulated results of dual polarization resonator antenna (a) gain,

(b) near-field distribution, and (c) radiation pattern.
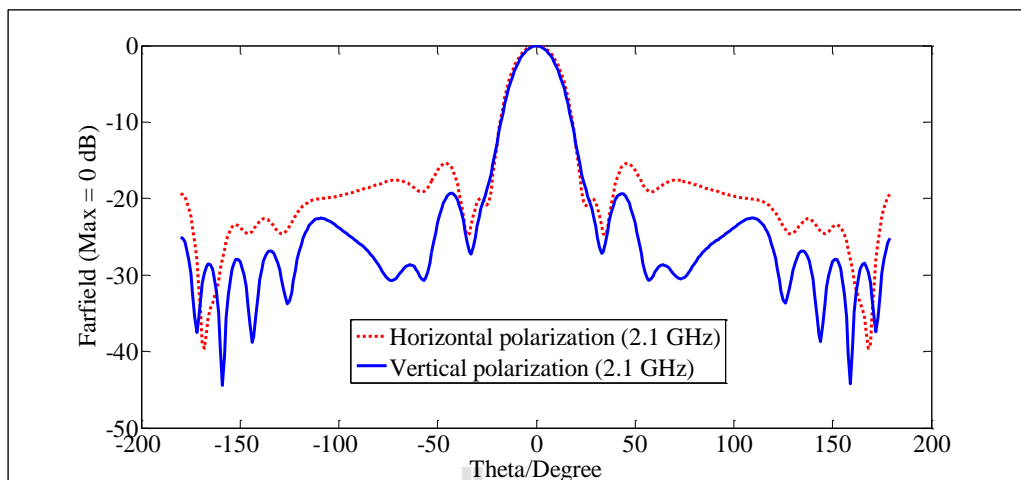
Figure 4.30 Maximum electromagnetic field of a dual polarized resonator antenna.

4.6 Circularly polarized resonator antenna

This paper studies the circularly polarized antenna, so two perpendicular electromagnetic plane waves are equal amplitude and 90° phase difference. From section 4.5, two perpendicular electromagnetic plane waves are equal. Therefore, the EBG polarizer is designed in this section to adjust the phase difference between two perpendicular electromagnetic plane waves as illustrated in Figure 4.31.
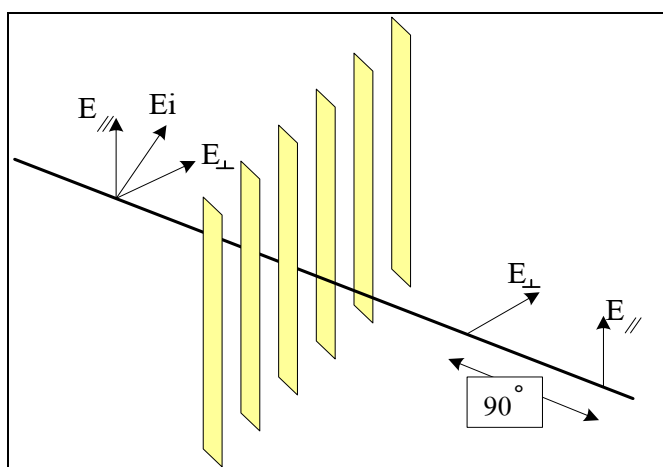
Figure 4.31 Metallic rods polarizer.

Therefore, 1-D metallic EBG is designed for the third layer of superstrate, which is called polarizer as shown in Figure 4.32(a). The transmission phase of polarizer is plotted as $\varphi_{S_{21}polarizer}$ about -6.24˚ as shown in Figure 4.32(b), and also the transmission phase of EBG polar H and EBG polar H are plotted as 53.65˚ and -15.74˚, respectively. Figure 4.33 shows the structure of EBG which is worked together with the polarizer. The requirement of phase difference is 90˚, where it is given by

$$k_0 d + \varphi_{S_{21}EBGpolarH} + \varphi_{S_{21}EBGpolarV} + \varphi_{S_{21}polarizer} = 90°,$$ (4.15)

where d is the distance between the EBG polar V and the polarizer and k_0 is $\dfrac{2\pi f}{c}$

$$d = \frac{90° - \varphi_{S_{21}EBGpolarH} + \varphi_{S_{21}EBGpolarV} + \varphi_{S_{21}polarizer}}{k_0},$$ (4.16)

$$d = \frac{90° - 53.65° - (-15.74°) - (-6.24°)}{2.52} = 23.14 mm.$$

Front view

Side view

A

g_y

2.4 mm

t

y

x

plane wave

1

y

x

z

(a)

(b)
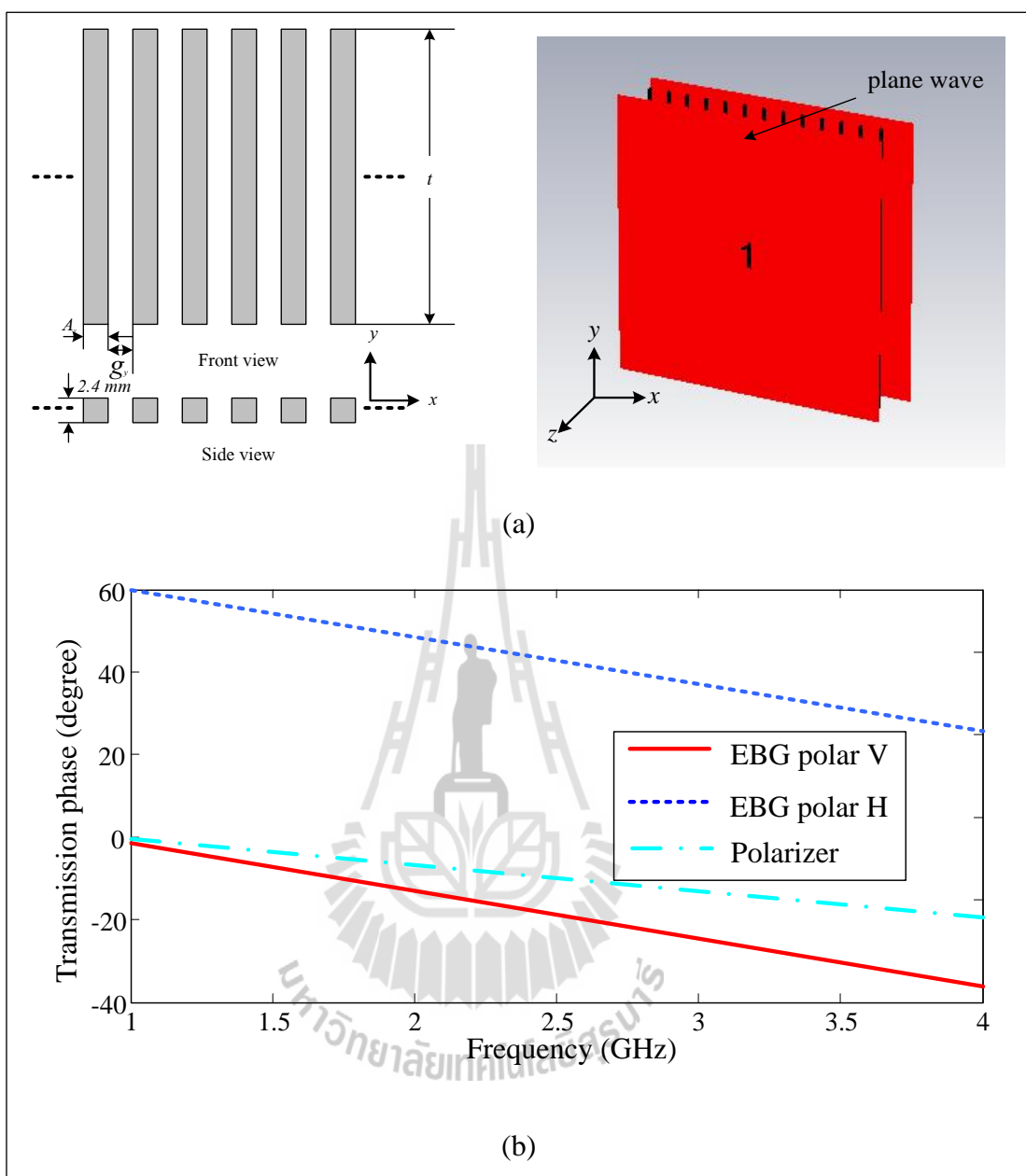
Figure 4.32 Simulation result of the metallic rods polarizer (a) structure and

(b) transmission phase.
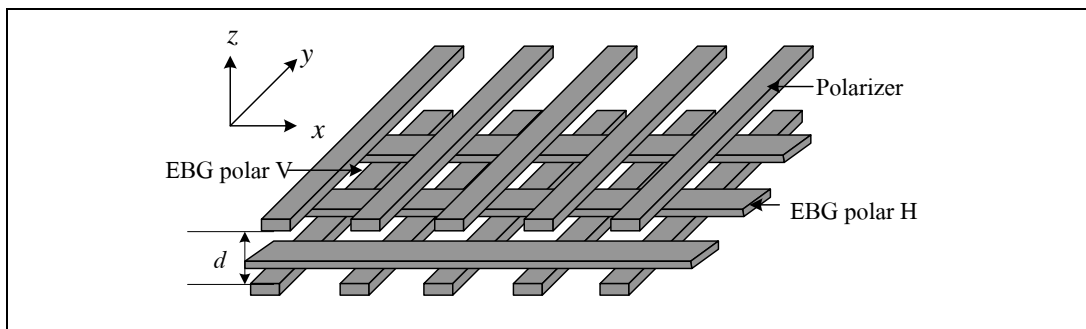
Figure 4.33 EBG superstrate.
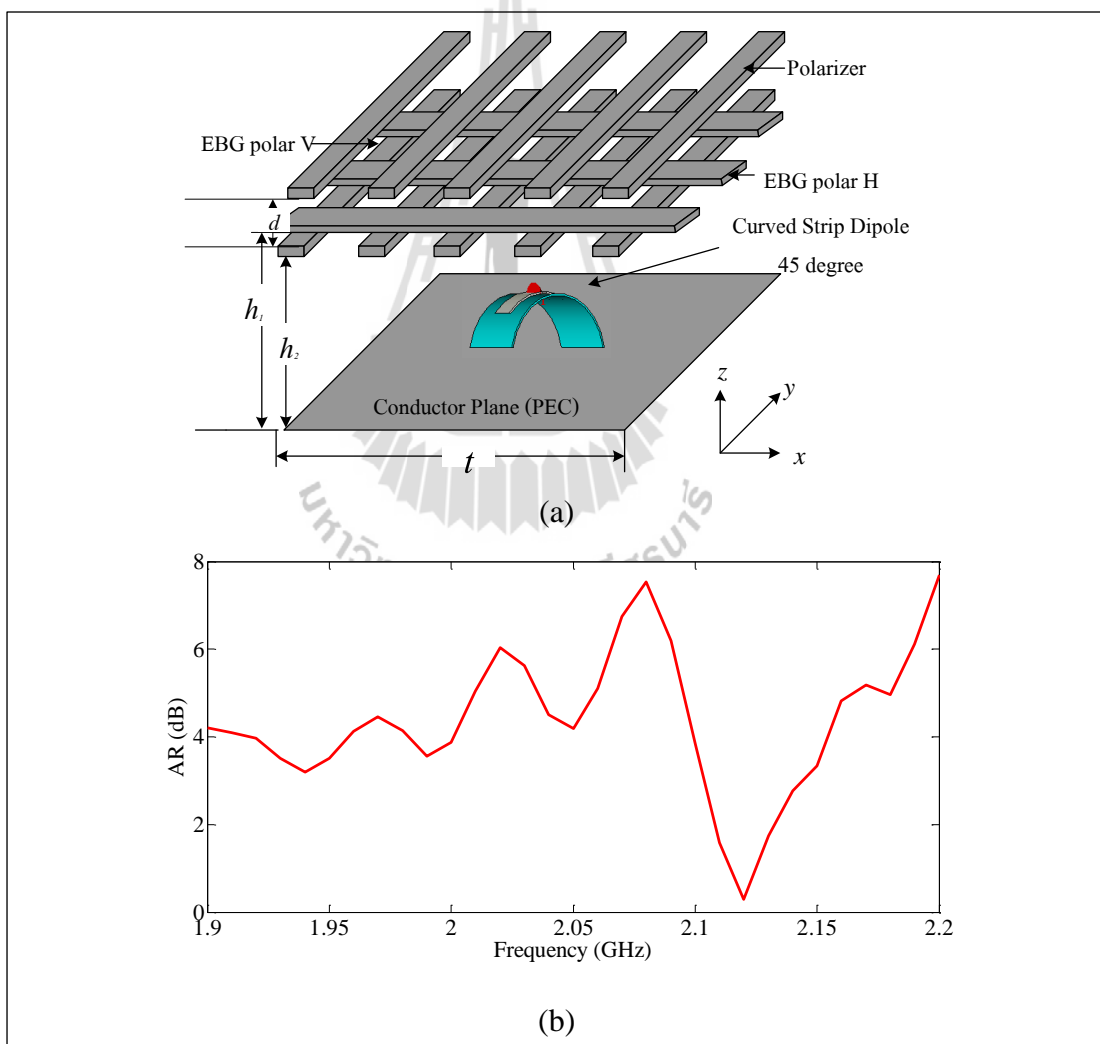
Figure 4.34 Simulation result of circularly polarized resonator antenna

when d_2 is 23.14 mm (a) structure and (b) AR.

When EBG and the polarizer structure are used for superstrate of a curved strip dipole antenna, which is placed on reflector plane at a 45˚ angle, the circularly polarized resonator antenna is achieved as shown in Figure 4.34(a). Figure 4.34(b) illustrates an axial ratio, which d is 23.14 mm. It seems that an axial ratio is unable to cover the frequency band because the mutual coupling between EBG layers occurs, so the d parameter is varied to optimize an axial ratio close to 0 dB at resonant frequency band. Consideration of Figure 4.35 concludes that at the gap between EBG polar V and the polarizer is 30 mm, an axial ratio close to 0 dB at 1.94 − 2.18 GHz because the phase difference is adjusted to 90˚. The maximum gain of 20.11 dBi could be achieved and the HPBW in vertical and horizontal plane are 18˚ and 18.1˚, respectively, as shown in Figure 4.36(a). Moreover, the electromagnetic vector is left-handed polarization because in Figure 4.36(b) the vector is circulated to left at the frequency of 2.1 GHz.
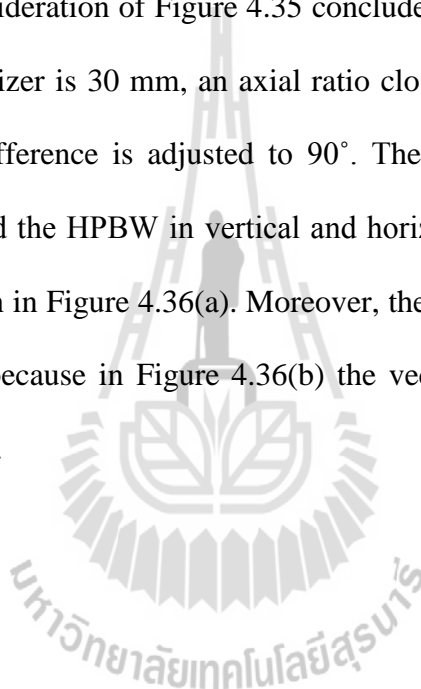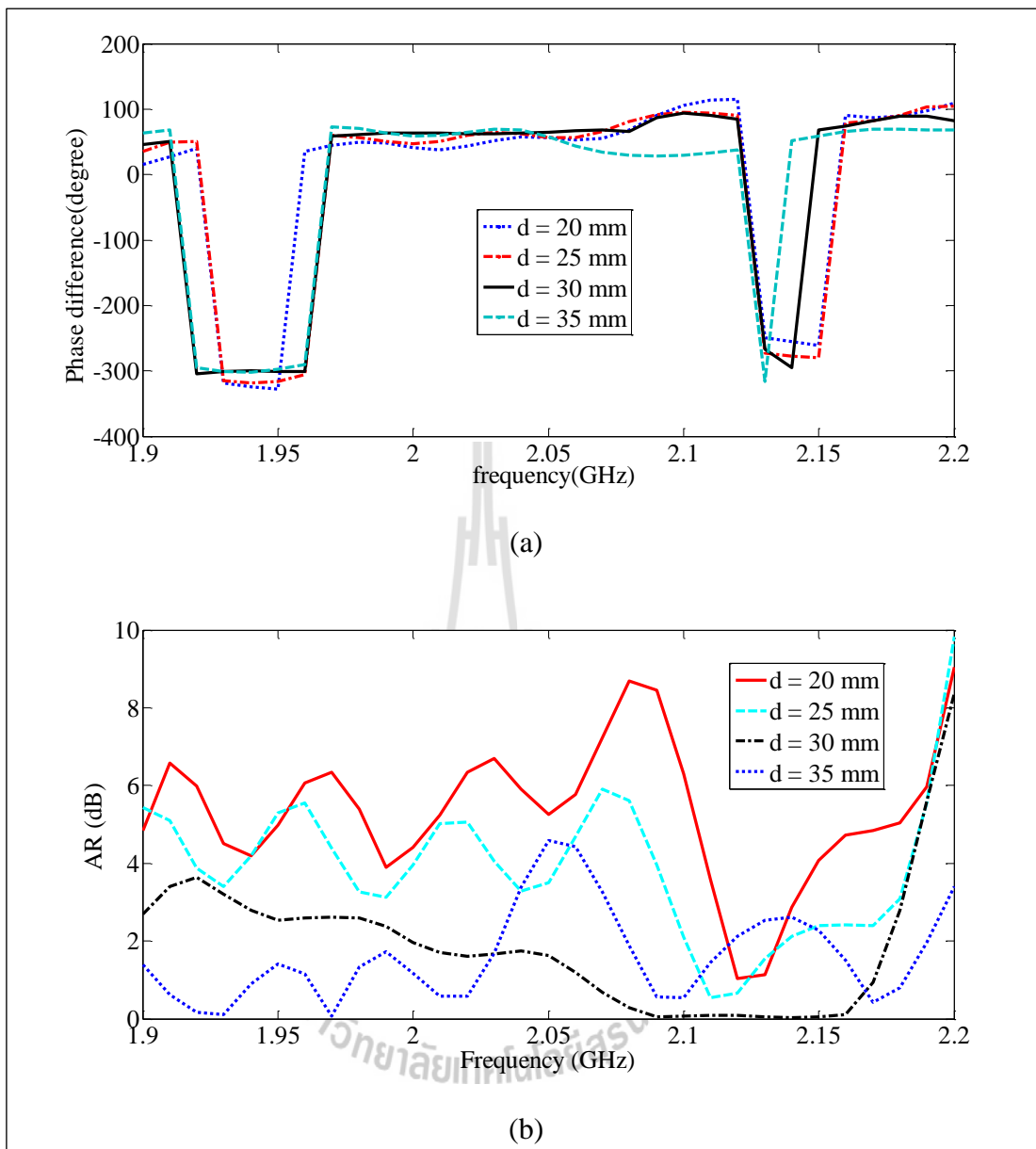
Figure 4.35 Simulation result of circularly polarized resonator antenna

when *d* is varied (a) phase different and (b) AR.
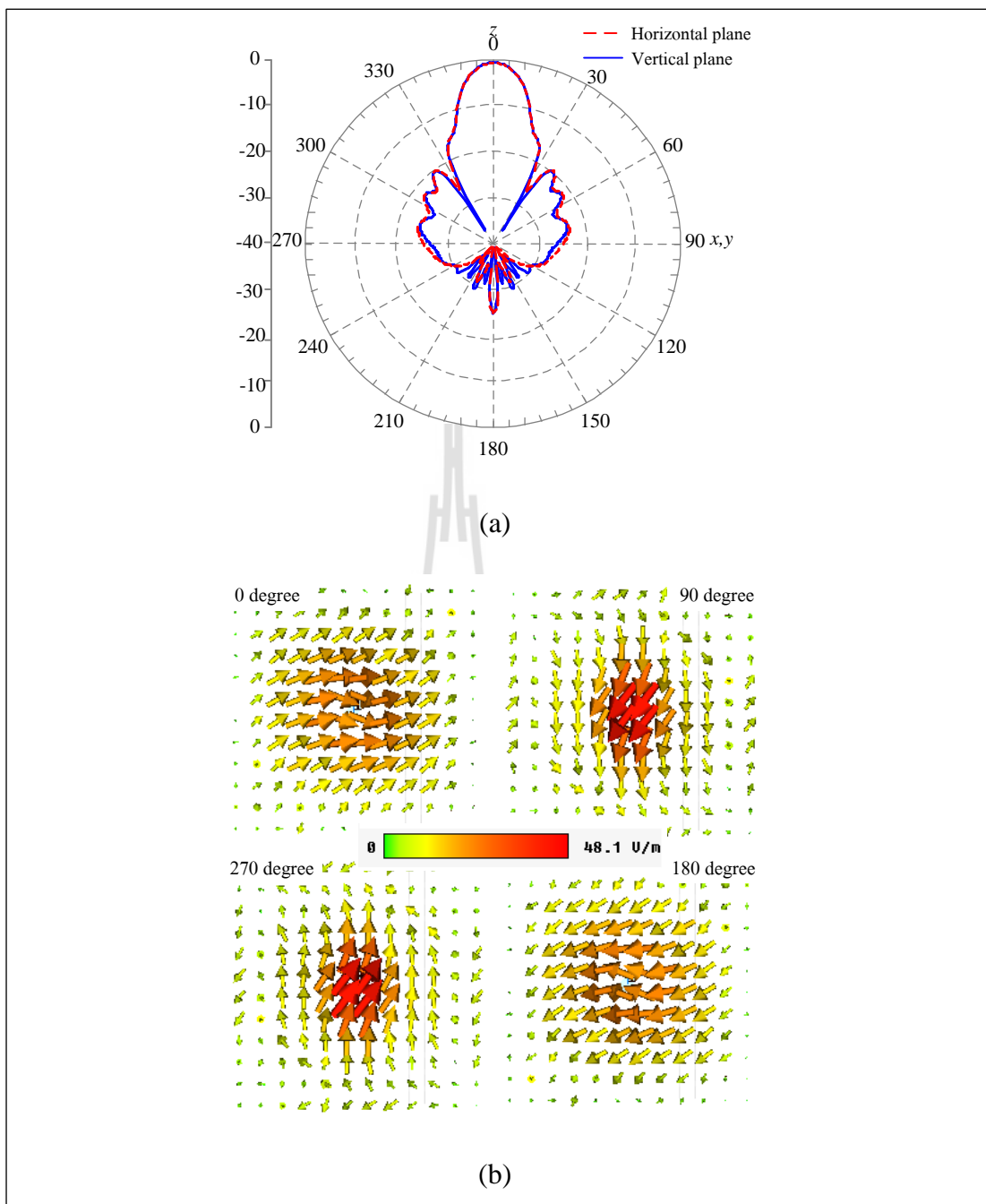
Figure 4.36 Simulation result of circularly polarized resonator antenna when *d*

is 30 mm (a) radiation pattern and (b) the electromagnetic vector

4.7 The effective directivity of resonator antenna using curved strip dipole

This section presents the optimum shape of a curved strip dipole antenna for maximum directive gain, which is used for excitation source of the circularly polarized resonator antenna. In this study, two difference shapes of curved strip dipole antenna located on conductor plane at 45˚ angle are appropriated, they have begotten the circularly polarized antenna. The curvature of a curved strip dipole have an effect on the efficiency of the circularly polarized resonator antenna, where a curved strip dipole is divided into two case studies, overturned and upturned curved strip dipoles. From previous section, an overturned curved strip dipole was studied and Figure 4.37(a) shows the circularly polarized resonator antenna using upturned curved strip dipole feeding. Figure 4.37(b) shows the simulated axial ratio for overturned and upturned curved strip dipole on conductor plane. As shown on this graph, the 3 dB AR at 2.1 GHz is found in the both cases. When the gain was plotted in varied frequency as shown in Figure 4.37(c), it found that the maximum gain of a resonator antenna using upturned curved strip dipole is 20.56 dBi at 2.1 GHz. In the other case, the gain is 20.11 dBi. Considering in a bandwidth of both cases, the resonator antenna using upturned curved strip dipole has a smaller band than the overturned curved strip dipole. From the radiation pattern simulation results in Figure 4.37 (d), the side lobe is reduced when the curved strip dipole is upturned. The radiation wave at the ends of curved strip dipole has high level because the electric field at the ends is closed. When the curved strip dipole is overturned in cavity wall, the reflection wave is too high. Moreover, the electromagnetic vector is left-handed polarization because in Figure 4.37(f) the vector is circulated to left.
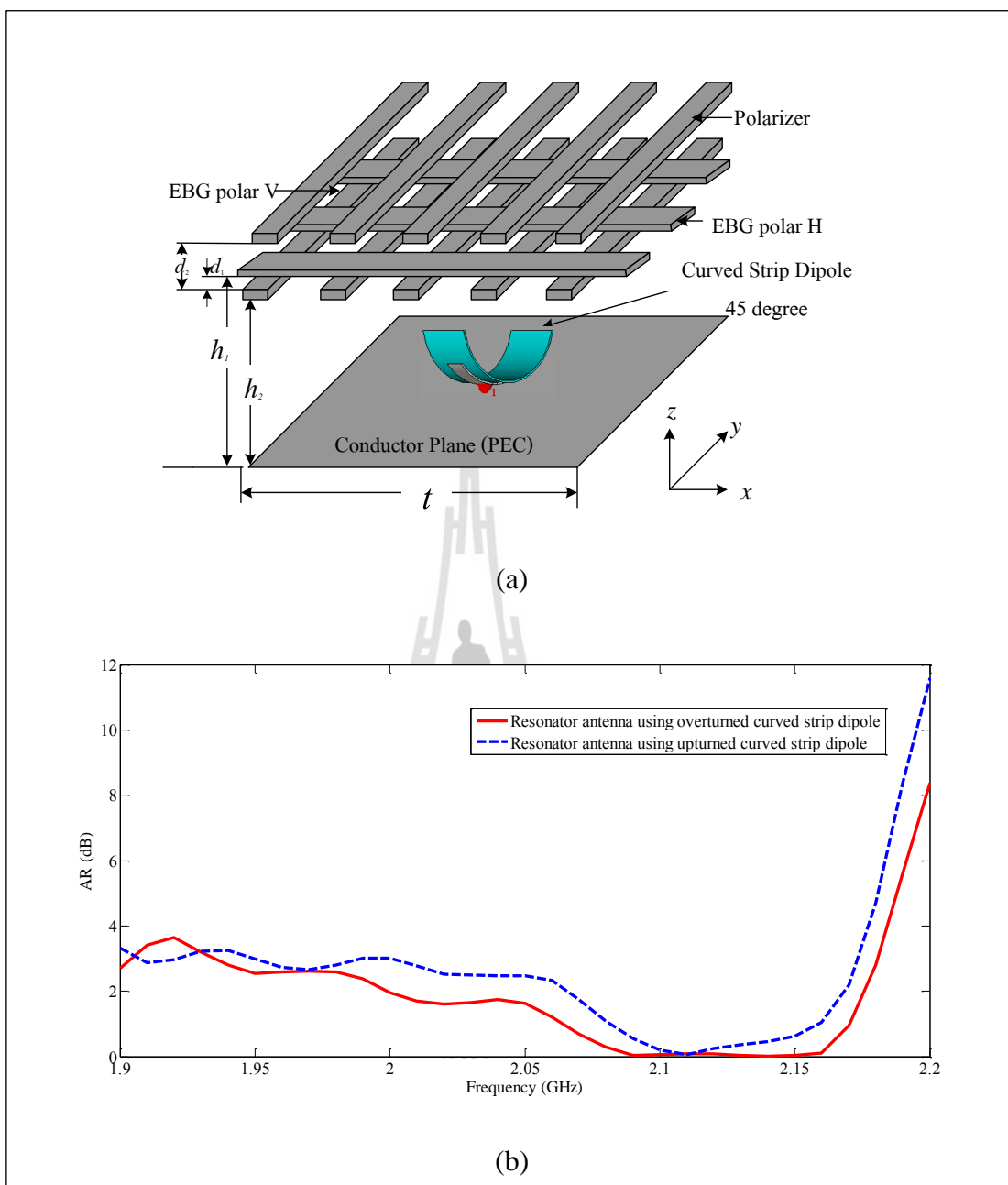
Figure 4.37 Simulation result of circularly polarized resonator antenna using an

upturned curved strip dipole (a) structure, (b) AR, (c) gain,

(d) *xz* plane, (e) *yz* plane, and (f) electromagnetic vector.

(c)

(d)

Figure 4.37 Simulation result of circularly polarized resonator antenna using an

upturned curved strip dipole (a) structure, (b) AR, (c) gain, (d)

xz plane, (e) *yz* plane, and (f) electromagnetic vector (cont.).

(e)

(f)
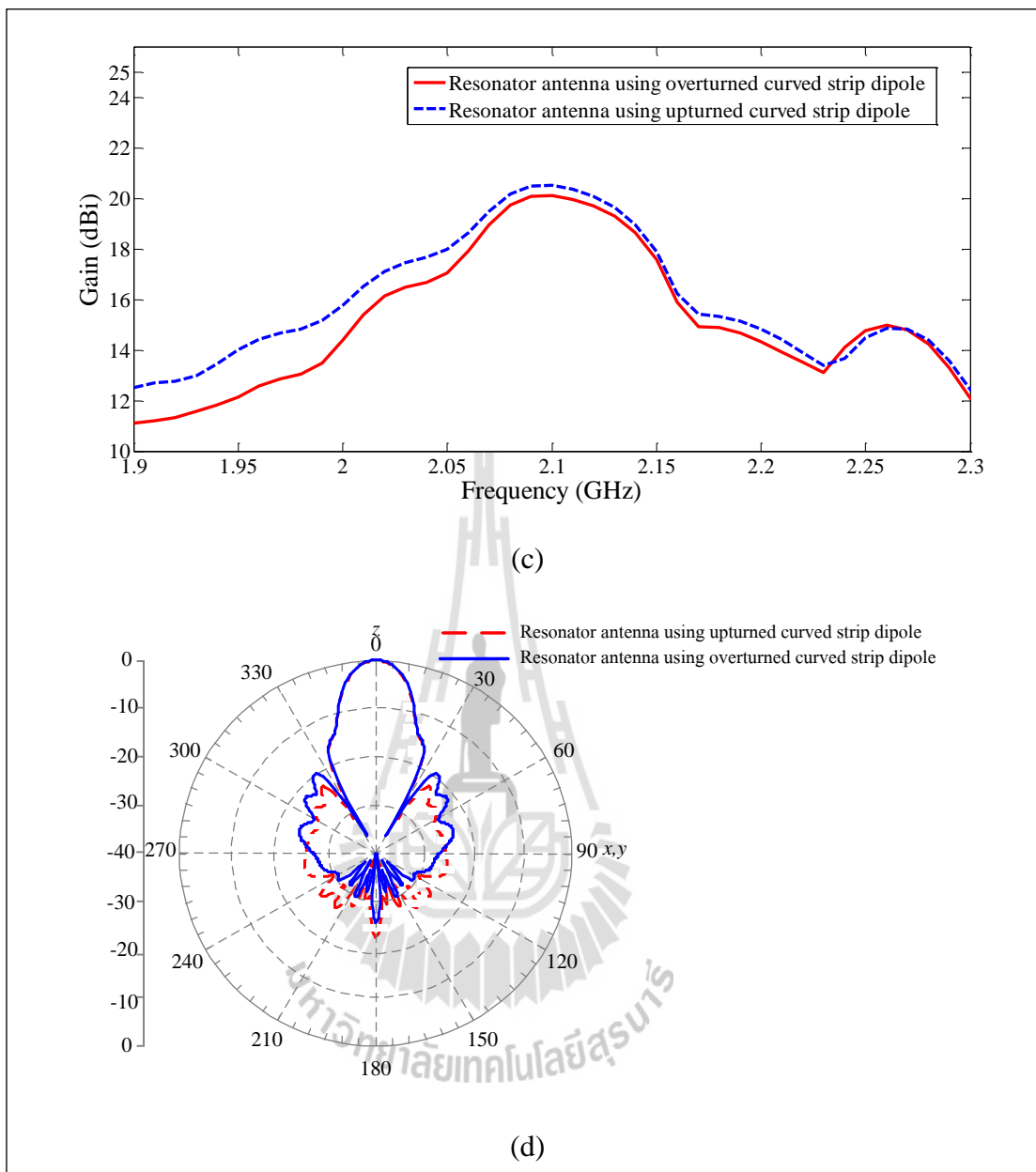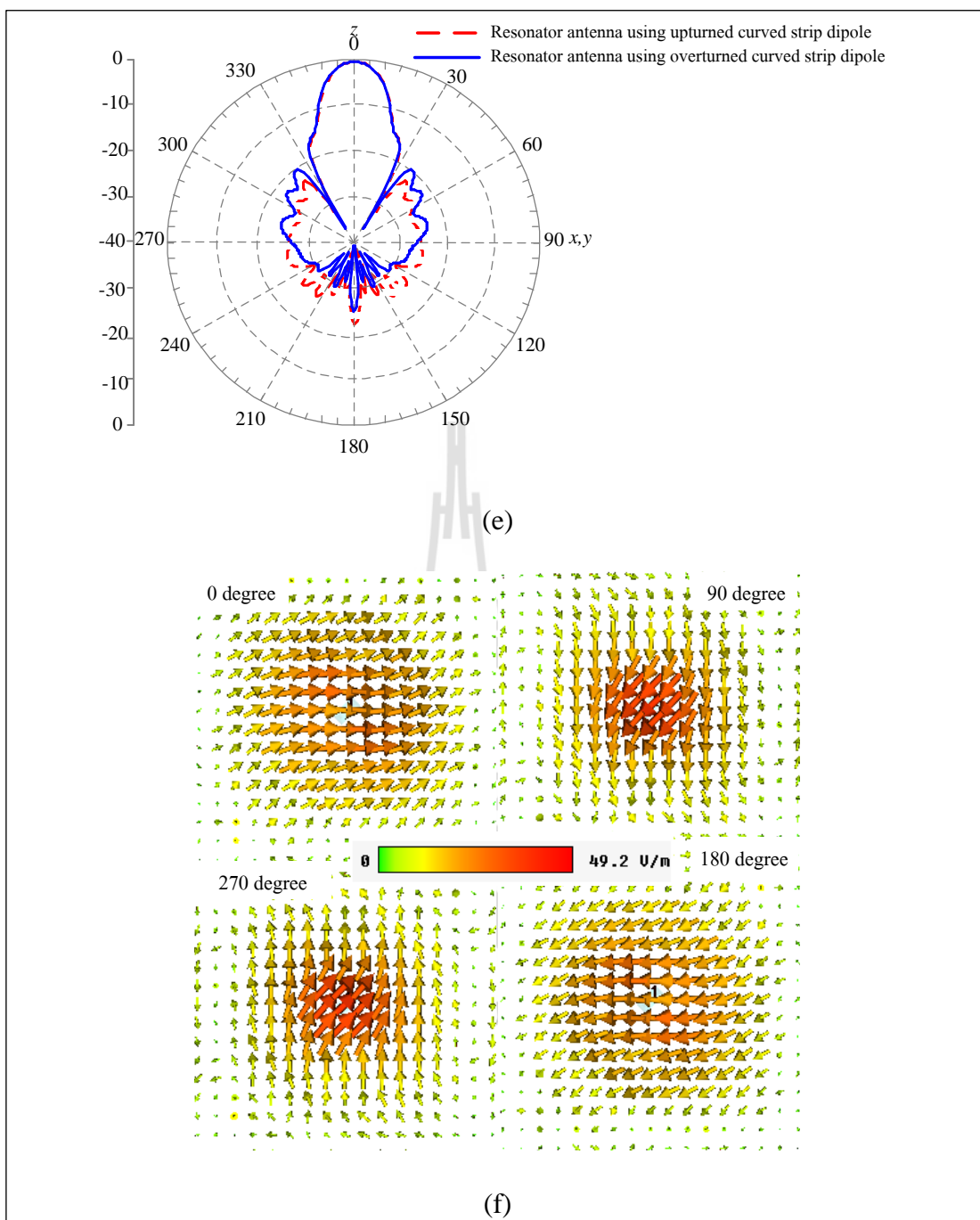
Figure 4.37 Simulation result of circularly polarized resonator antenna using an

upturned curved strip dipole (a) structure, (b) AR, (c) gain, (d)

xz plane, (e) *yz* plane, and (f) electromagnetic vector (cont.).

The optimum shape of a curved strip dipole antenna for maximum directive gain could be obtained. It shows that the shape of exciting source of resonator antenna can change the antenna performance. Moreover, the cavity wall, which consists of superstrate and conductor plane, improves the gain of traditional antenna from around 2 dBi to 20.11 dBi. In addition, the side lobe is reduced when the curved strip dipole is upturned the structure down on conductor plane.

Because of the high requirements on base station antenna in cellular network, the most popular choices are the antennas with horizontal half power beamwidth of 60°. The optimum horizontal and vertical beamwidth is decided by the network architecture and propagation environment.

4.8 Sector antenna design

As the square antenna is not suitable and does not meet the requirements of the sector antenna element, in this section; the antenna is reduced in size and the vertical walls in yz plane for wide beamwith in horizontal plane are added. First study is applied the square dual polarized antenna from section 4.5 to radiate the sectoral radiation pattern.

Consideration of Figure 4.38(a) concludes that if the resonator antenna size (t_1) is reduced to 400 mm because the near-field level is faded away at the width, the HPBW in horizontal plane of the resonator antenna is wider. While the pattern in horizontal plane is improved, the directive gain of the resonator antenna is certainly down. Simulated gain and HPBW in xz plane are concluded in Table 4.4. Although the pattern is symmetric at $t_1 = 400$ mm, the HPBW is not sufficient for the base station antenna. Therefore, the horizontal HPBW of 58.9° when $t_1 = 300$ mm is used.

A side from this the *yz* radiation pattern is plotted in Figure 4.38(c); it has been already symmetric. To solve a problem in *xz* plane, the U-shaped reflector is installed as shown in Figure 4.39 with parameter *h* of 50 mm. Five and nineteen metamaterial rods of EBG polar H and V structure, respectively, are used for a superstrate. To improve the directive gain, the length of antenna in *y* axis (t_2) is increased. Figures 4.40(a) and (b) show the radiation pattern when t_2 is varied. It illustrates that the HPBW and the gain are suitable for the sector antenna, when t_2 is 950 mm, the simulated gain and HPBW in *xz* plane are concluded in Table 4.5.
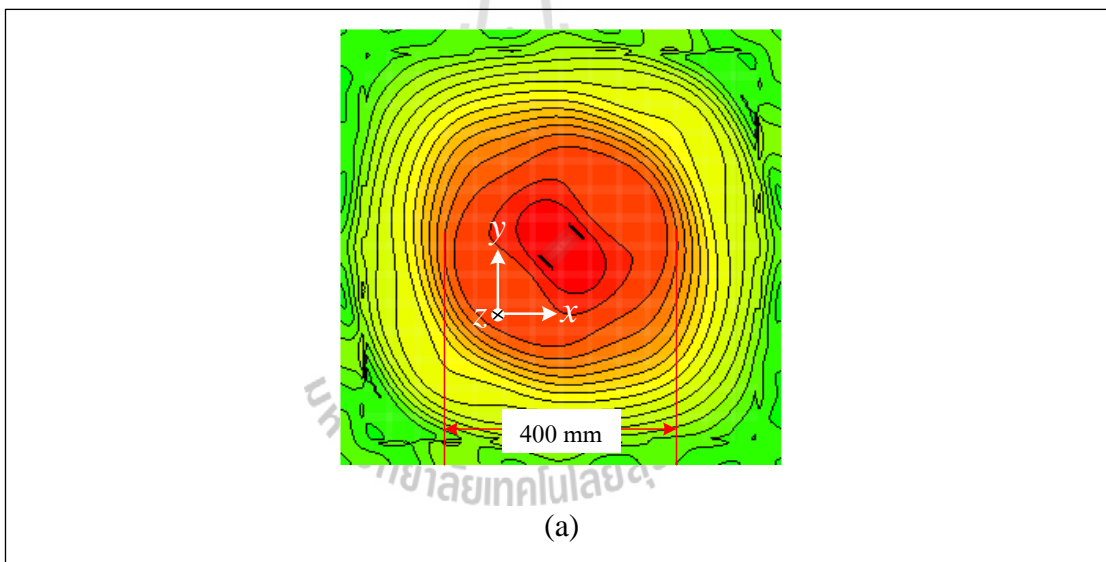
(a)

Figure 4.38 Simulated results when t_1 is varied (a) current distribution

on reflector plane, (b) radiation pattern in *xz* plane, and (c)

radiation pattern in *yz* plane.

(b)

(c)
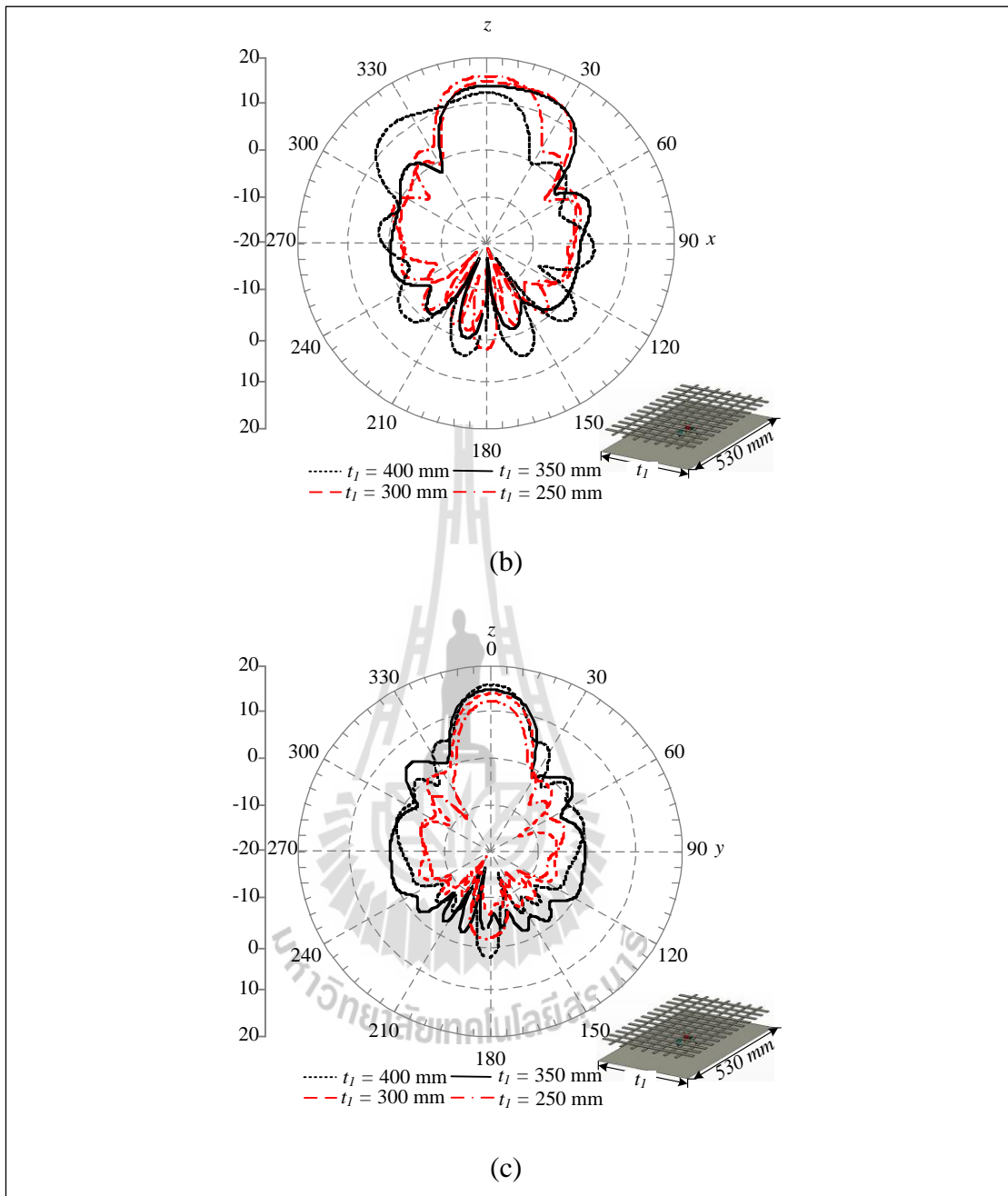
Figure 4.38 Simulated results when t_1 is varied (a) current distribution

on reflector plane, (b) radiation pattern in xz plane, and (c)

radiation pattern in yz plane (cont.).

Table 4.4 Simulated results when t_1 is varied.

t_1 (mm)	Gain (dBi)	HPBW (degree)
530	20.11	18
400	16.1	33.7
350	14.8	48.9
300	14.0	58.9
250	12.5	67.9
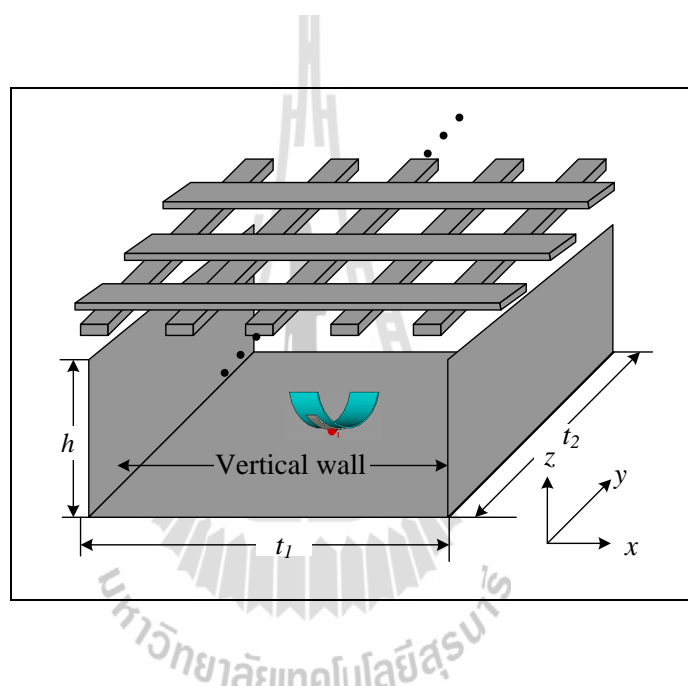
Figure 4.39 Dual polarization sector antenna structure.

Table 4.5 Simulated results when t_2 is varied.

t_2 (mm)	Gain (dBi)	HPBW (degree)
530	13.3	58.9
650	14.2	56.2
750	14.3	57.5
850	14.1	60.1
950	15.0	59.0
1050	14.2	59.6
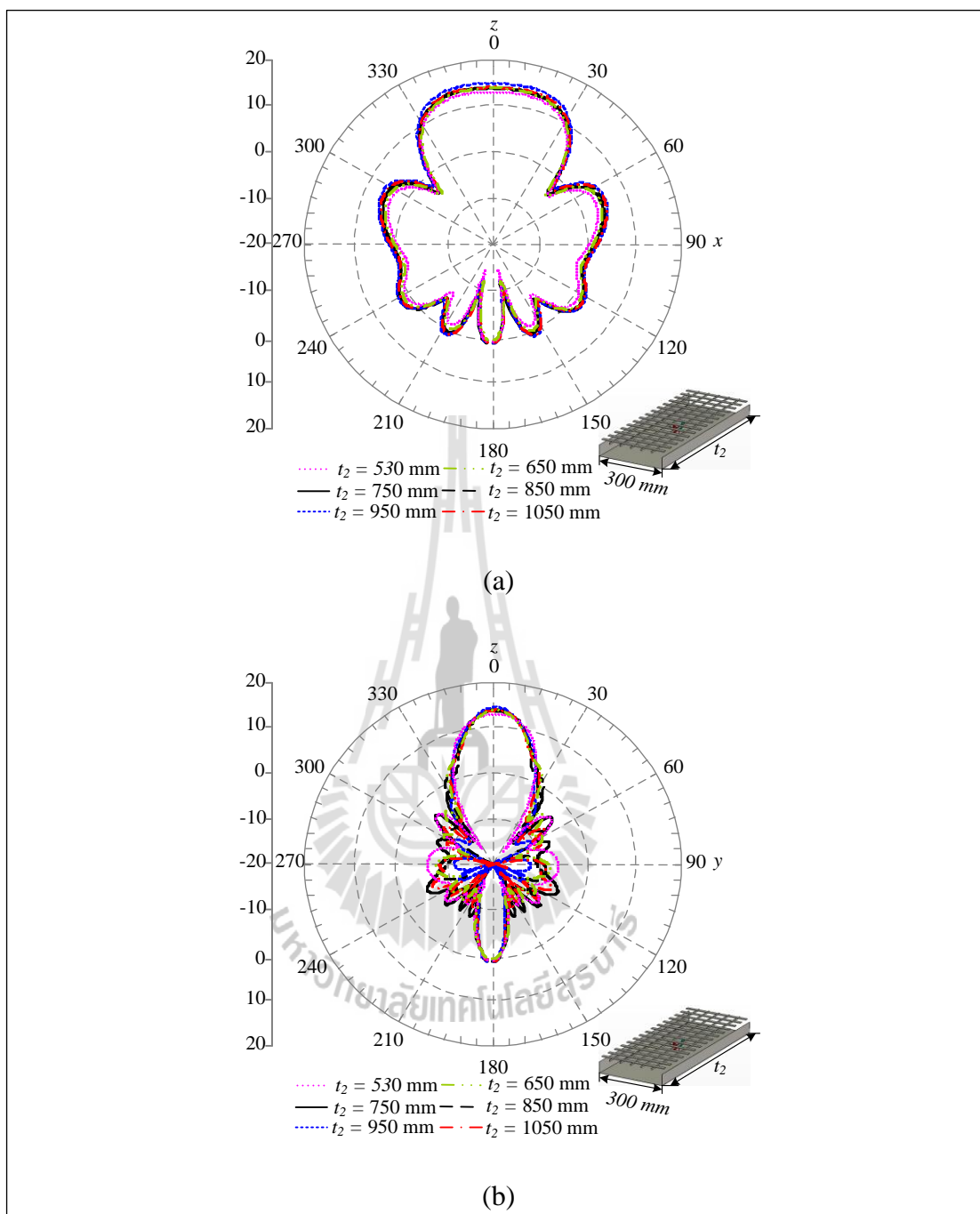
Figure 4.40 Radiation pattern when t_2 is varied (a) xz plane and (b) yz plane.
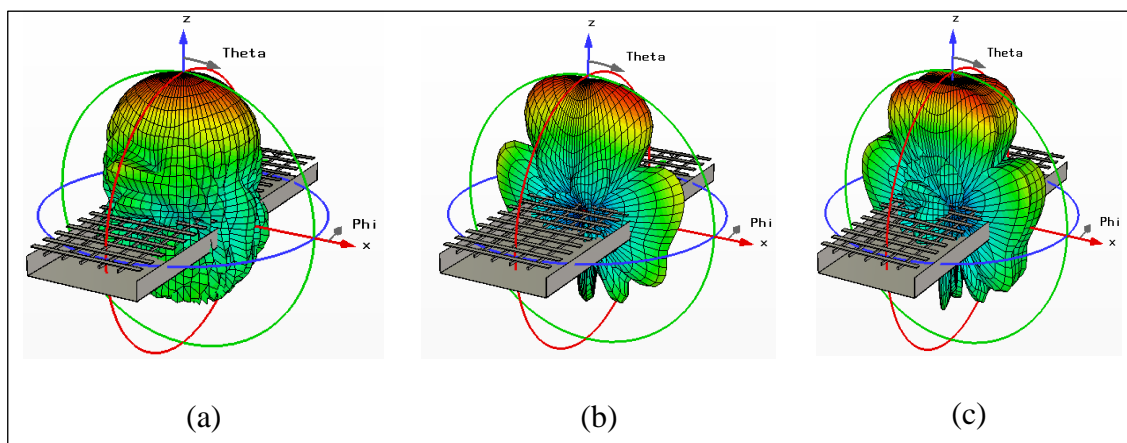
Figure 4.41 3D simulated radiation patterns of dual polarization antenna with U-

shaped reflector plane at (a) 1.92 GHz, (b) 2.1 GHz, and (c) 2.17 GHz.
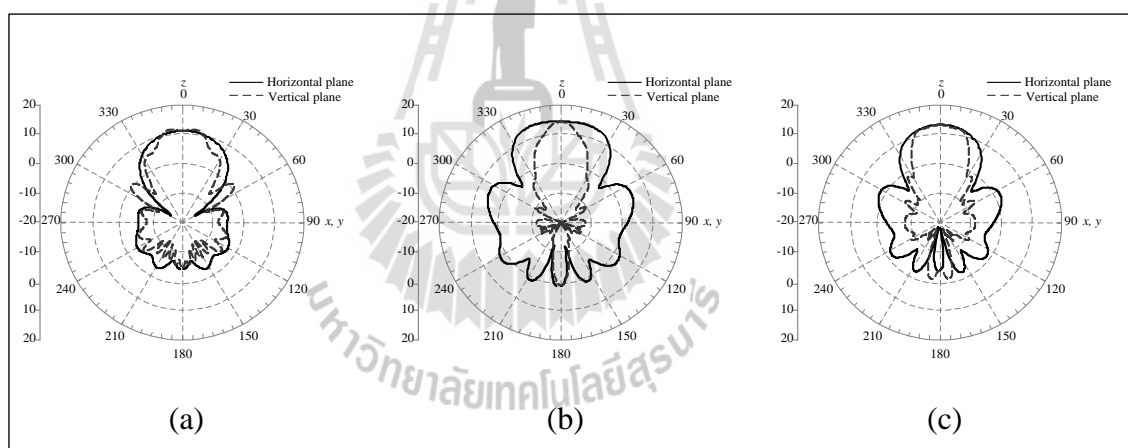
Figure 4.42 2D simulated radiation pattern of dual polarization antenna with

U-shaped reflector plane at (a) 1.92 GHz, (b) 2.1 GHz, and

(c) 2.17 GHz.

To reveal the radiation characteristic of dual polarization antenna in the whole operating bandwidth, the 3D radiation patterns of the proposed antenna at 1.92 GHz, 2.1 GHz, and 2.17 GHz are also simulated and shown in Figures 4.41 and 4.42. The antenna beam in horizontal plane (*xy* plane) is wide. These results illustrate the excellent sectoral properties of the antenna. In the vertical plane the radiation is directive with low side lobe, and in the horizontal plane these figures present an interesting sectoral pattern of 60°. The simulated gain is around 15 dBi at the frequency of 2.1 GHz as shown in Figure 4.43. In addition, over the whole frequency band (1.92–2.17 GHz), the -3 dB directive gain could be obtained. Moreover, the vertical walls can control the surface wave at the edge and corner, therefore the wave is redirected to the *z* direction, as shown in Figure 4.44.
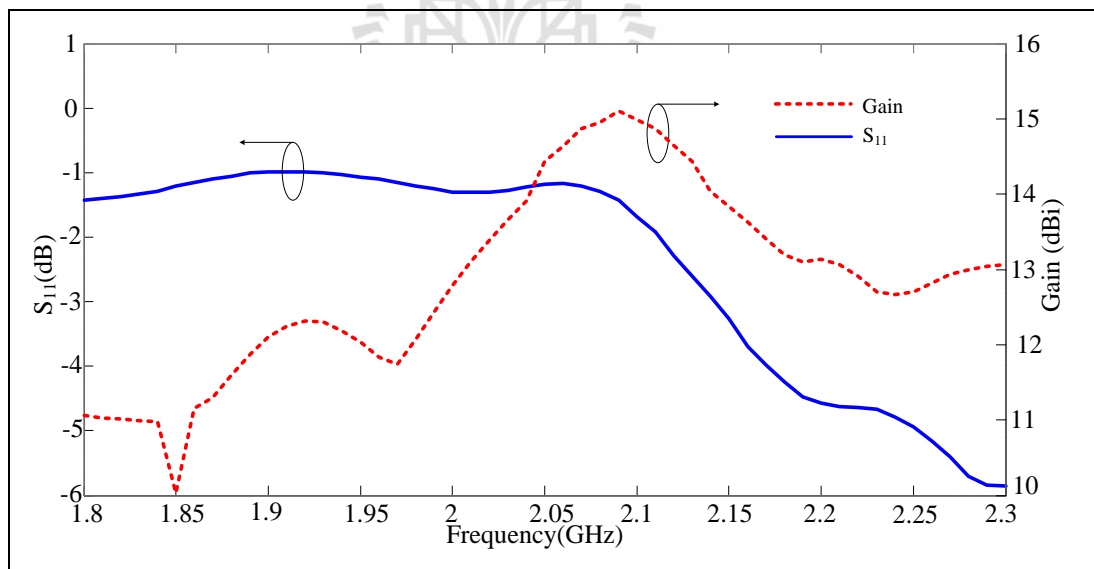
Figure 4.43 Simulated gain and S_{11} of the dual polarization antenna

with vertical walls.
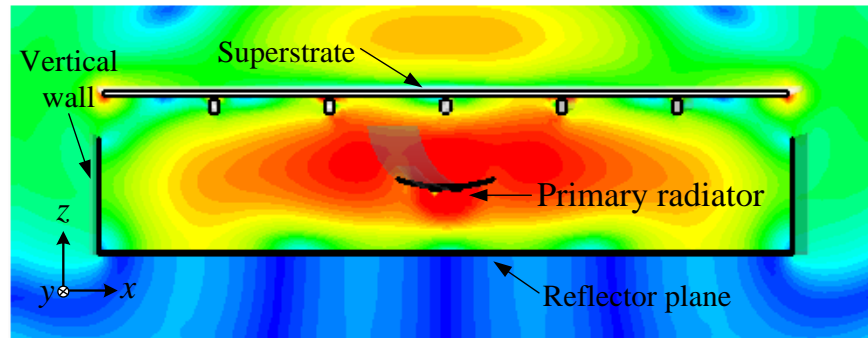
Figure 4.44 Near-field distribution of the dual polarization antenna

with vertical walls.

Furthermore, the circularly polarized sector antenna is created base on the dual polarized sector antenna by using the EBG polarizer. The EBG polarizer is placed over the double EBG layers with the gap (d_2) of 30 mm as shown in Figure 4.45. To reveal the radiation characteristic of circularly polarization antenna in the whole operating bandwidth, the 3D radiation patterns of the proposed antenna at 1.92 GHz, 2.1 GHz, and 2.17 GHz are also simulated and shown in Figures 4.46 and 4.47. The antenna beam in horizontal plane (xy plane) is wide. These results illustrate the excellent sectoral properties of the antenna. In the vertical plane the radiation is directive with low side lobe, and in the horizontal plane these figures present an interesting sectoral pattern of 60˚. The simulated gain is around 15.53 dBi at the frequency of 2.1 GHz as shown in Figure 4.48. In addition, over the whole frequency band (1.92–2.17 GHz), the -3 dB directive gain and axial ratio could be obtained. Moreover, the vertical walls can control the surface wave at the edge and corner, therefore the wave is redirected to the z direction, as shown in Figure 4.49. Moreover, the electromagnetic vector is left-handed polarization because in Figure 4.50 the vector is circulated to left.
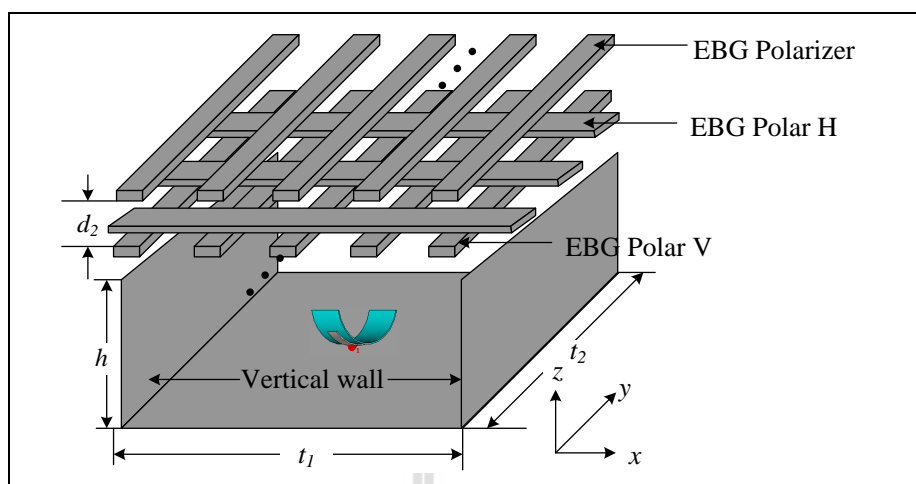
Figure 4.45 Sectoral circularly polarization antenna structure.

(a) (b) (c)
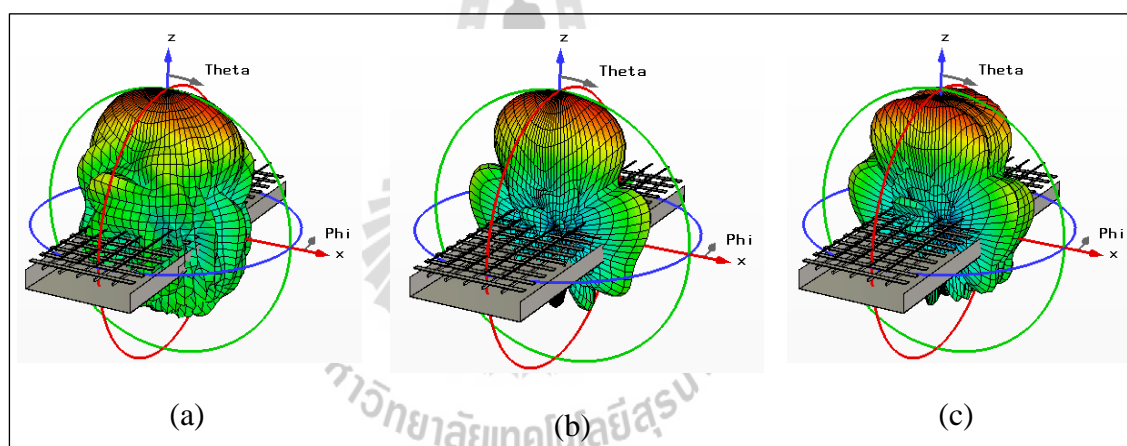
Figure 4.46 3D simulated radiation patterns of circularly polarization antenna with

U-shaped reflector plane at (a) 1.92 GHz, (b) 2.1 GHz, and
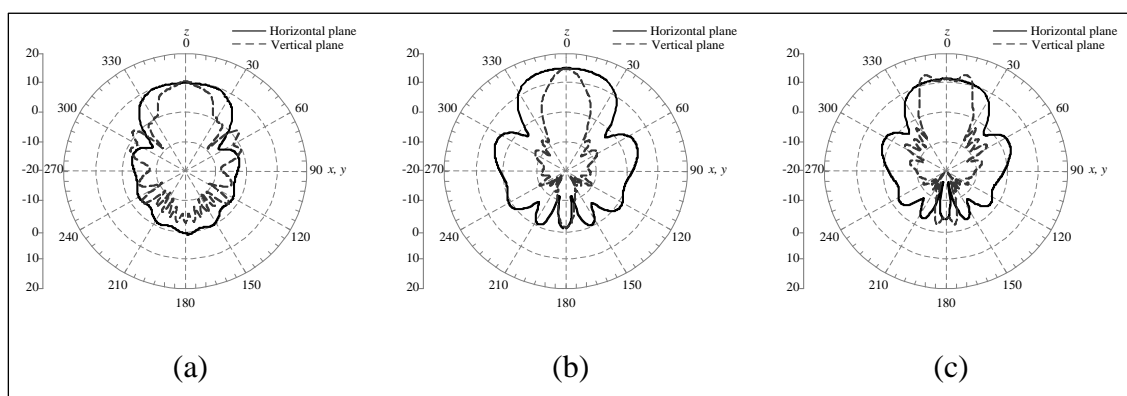
(c) 2.17 GHz.

Figure 4.47 2D simulated radiation pattern of circularly polarization antenna with

U-shaped reflector plane at (a) 1.92 GHz, (b) 2.1 GHz, and

(c) 2.17 GHz.
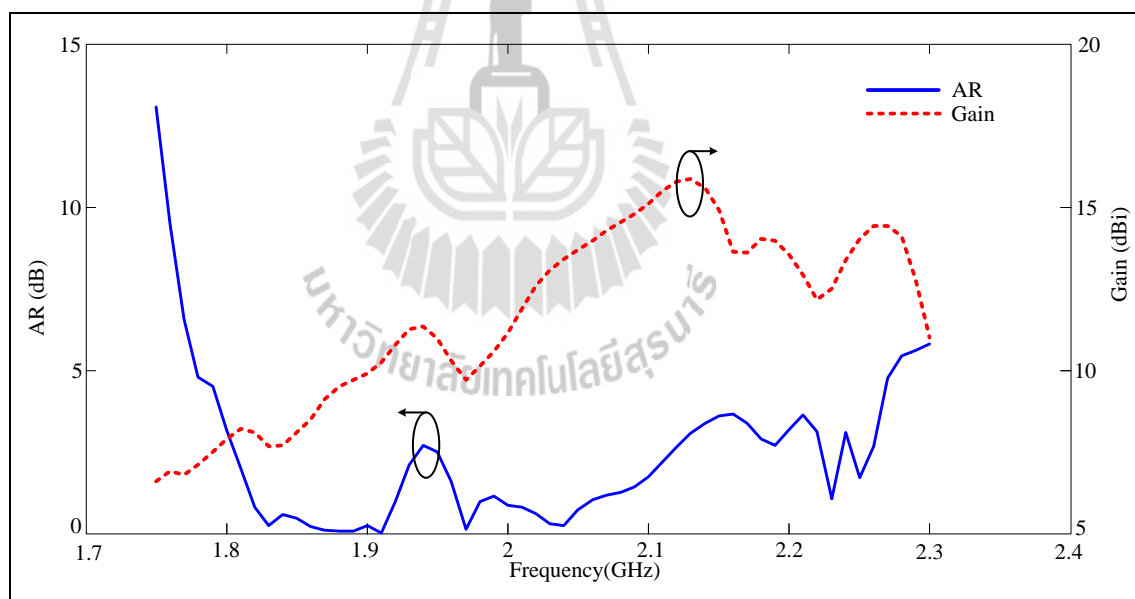
Figure 4.48 AR and gain of sectoral circularly polarization antenna structure.
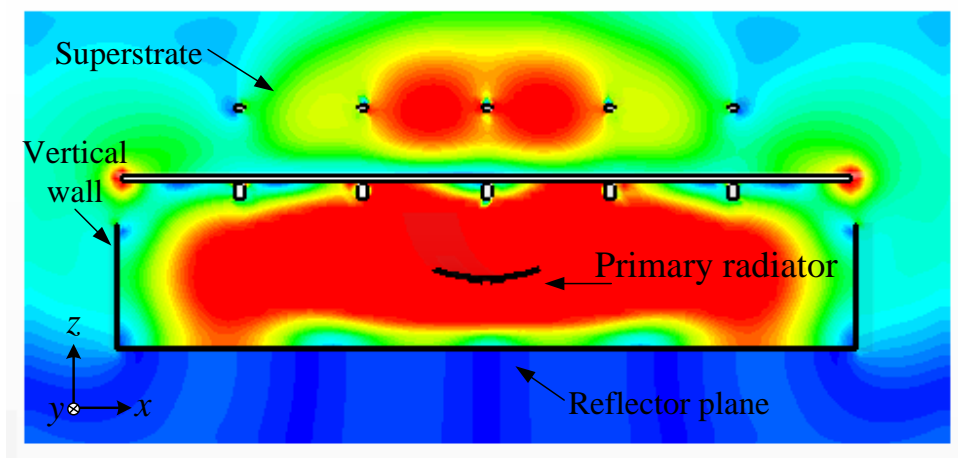
Figure 4.49 Near-field distribution of sectoral dual polarization antenna structure.
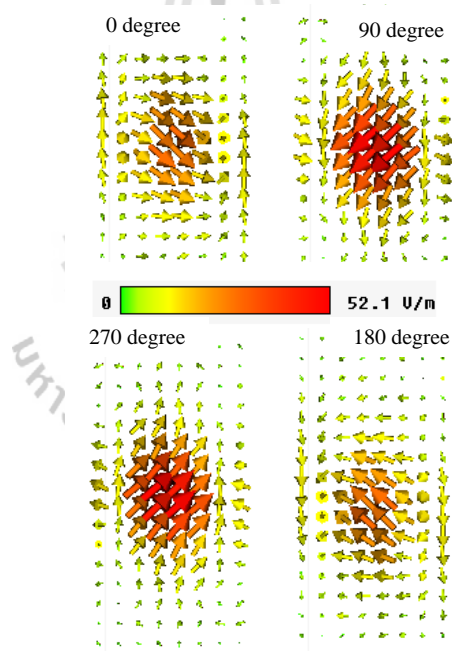
Figure 4.50 Electromagnetic vector of sectoral dual polarization antenna structure.

4.9   Chapter summary

This chapter presents analysis and design of a resonator antenna by using curved strip dipole to originate the exciting power over U-shaped reflector plane and three layers metallic rod EBG to improve the antenna performance. At the beginning, a previous feeding antenna is designed and it is placed over the reflector plane to enhance the directive gain. The antenna polarization and gain are unsuitable for mobile base station, though. Secondary design, when the metallic rod EBG is added with transverse magnetic polarization mode (TM mode), the antenna gain is extremely increased. Therefore, a curved strip dipole antenna is placed on the U-shaped conductor plane at a 45˚ angle to have a dual polarization. In this proposed antenna, the directive gain is increased in x and y axises by using double layers metallic rod EBG and the circular polarization is generated by using the EBG polarizer.
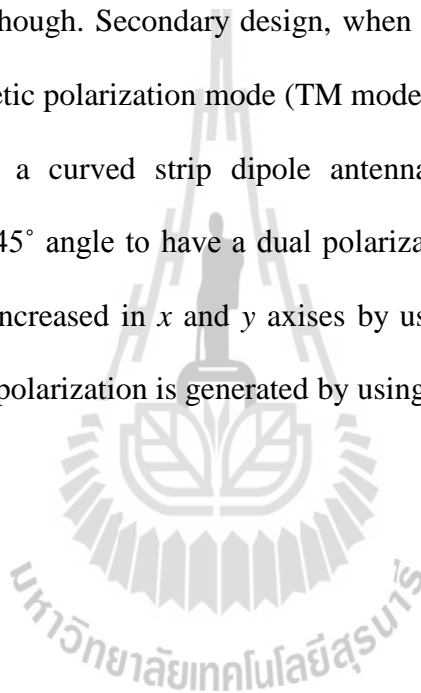
CHAPTER V

MESUREMENT AND DISCUSSION

5.1 Introduction

Having understood most of the general background and theory behind the resonator antenna, the development of a design procedure for the fabrication of dual and circularly polarized resonator antenna that meets the requirements of a mobile communication system will be conducted in this chapter, which dedicates to the overall development process of the resonator antenna by using the metamaterial superstrate. The fabrication of the antenna prototype will be measured and discussed. Table 5.1 depicts the required specifications of the antenna, which will be followed by achieving the performance required to construct the mobile base station antenna for six sectors.

Table 5.1 Design specification for antenna design

Parameters	Specification
Operating frequency (f_0)	2.1 GHz (1.92 – 2.17 GHz)
Polarization	Dual and Circular
HPBW (degree)	60 – 65 degree
Gain (dBi)	13 – 16 dBi
Antenna type	Directional antenna
Diamention (mm)	$1200 \times 300 \times 100$

In Chapter 3, a 2.1 GHz sectoral antenna using aluminium rods type metamateral was designed, and its predicted performance was discussed. The further simulations of key parameters such as radiation pattern, gain and half power beamwidth can also be evaluated. To verify the simulated results, the radiation patterns of antenna are tested under real circumstance using vector network analyzer HP8722D.

5.2   The proposed antenna components

5.2.1   How to fabricate a curved strip dipole antenna prototype

The first step in designing a curved strip dipole antenna is to choose an appropriate material such as copper plate and polyvinyl chloride (PVC). From simulated results of a curved strip dipole, the antenna prototype is fabricated by using the parameters size from chapter 4. A curved strip dipole antenna prototype is shown in Figure 5.1 and the parallel conductor balun is constructed to connect with both arms of curved strip dipole for feeder system. The configuration of the curved strip dipole antenna consists of two copper plates which are bent and upturned on half curved PVC. This provides the basis for the start of the design but finer adjustments have to be made to compensate and determine the best possible result. It can be seen invariably from Equation (4.3) that the resonant frequency is affected by the dipole length.
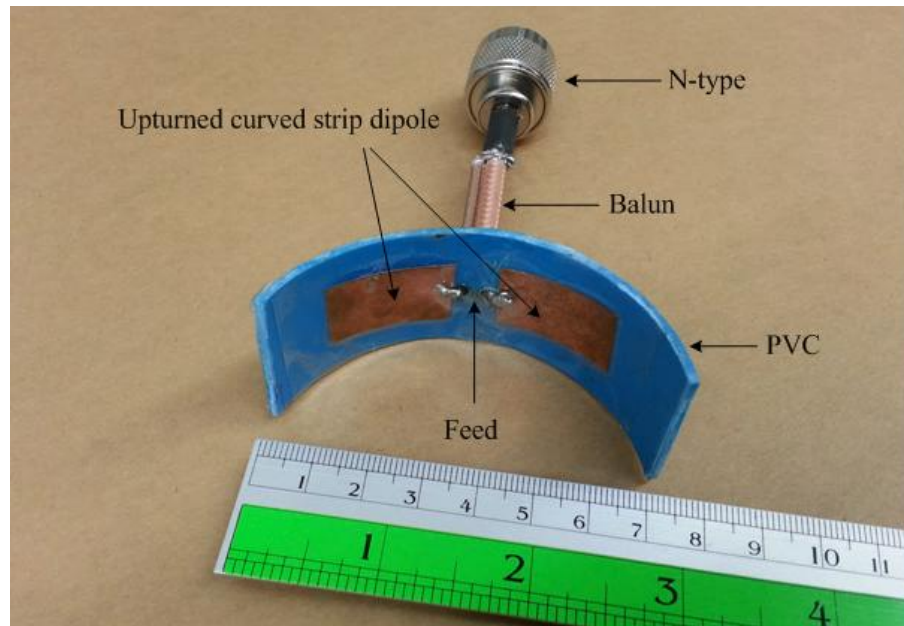
Figure 5.1 Upturned curved strip dipole antenna prototype.

5.2.2 A 45° oriented curved strip dipole separated by 1/4 wavelength from U-shaped reflector plane prototype

In this section a 45° oriented curved strip dipole antenna is placed on an aluminium reflector plane with thickness of 1.6 mm while the reflector plane is shaped up sectoral antenna. The metallic reflector is located at the back of a 45° oriented curved strip dipole antenna for dual polarization antenna with gap as a quarter wavelength as shown in Figure 5.2.
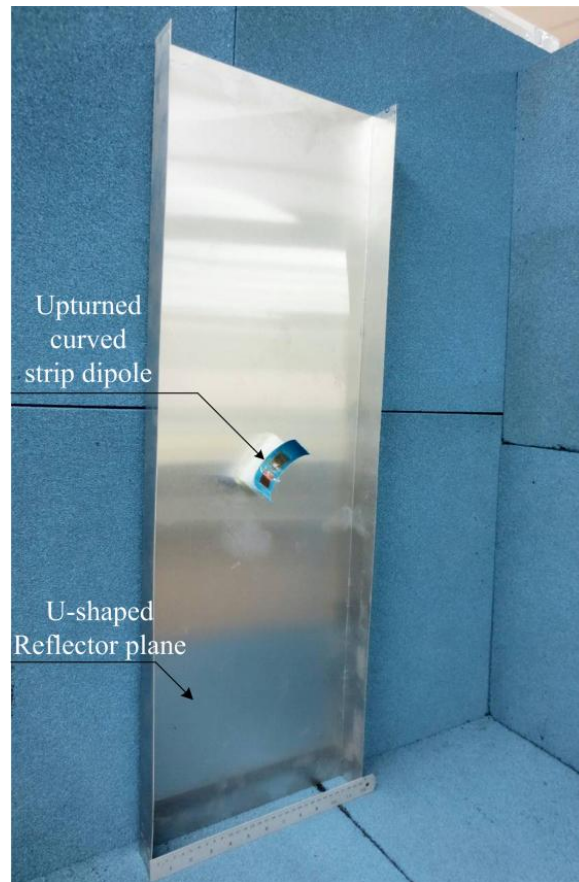
Figure 5.2 A 45˚ oriented upturned curved strip dipole antenna

on reflector plane prototype.

Therefore, the total round trip phase shift from the curved strip dipole, to the surface, and back to the antenna, equals one complete cycle, and the waves add constructively. The width of a metallic reflector is 300 mm while the other side that is length and the height of vertical wall are 950 mm and 50 mm, respectively. The antenna radiates efficiently, but the directive gain is not durable for applications.

5.2.3 Aluminium rod type metamaterial superstrste layers

An aluminium material is chosen to be metamaterial superstrate because it has light weight. Also, it is hard enough to be arranged to form a rod of tiny diameter. The fabricated prototype of aluminium rods are shown in Figure 5.3. A real structure based on the previous concept has been built.
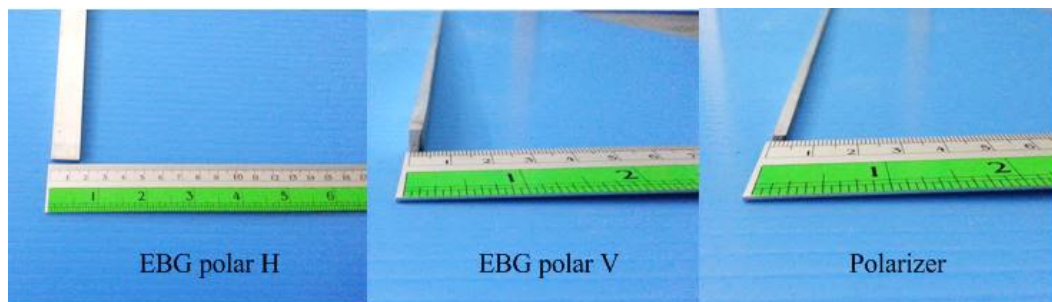
Figure 5.3 Aluminium rod type metamaterial.

For the design studied here, both lower EBG polar V and EBG polar H layers have been arranged as appeared in Figure 5.4(a). The lower EBG polar V layer is made up of five aluminium rods of 3.85×950 mm^2 and 6 mm periodicity. The upper EBG polar H layer is composed of nineteen aluminium rods of 300×13.26 mm^2 and 1 mm periodicity. Furthermore, the polarizer layer is constituted of five aluminium rods of 3.85×950 mm^2 and 2.4 mm periodicity and it has been located on the both layers as appeared in Figure 5.4(b).
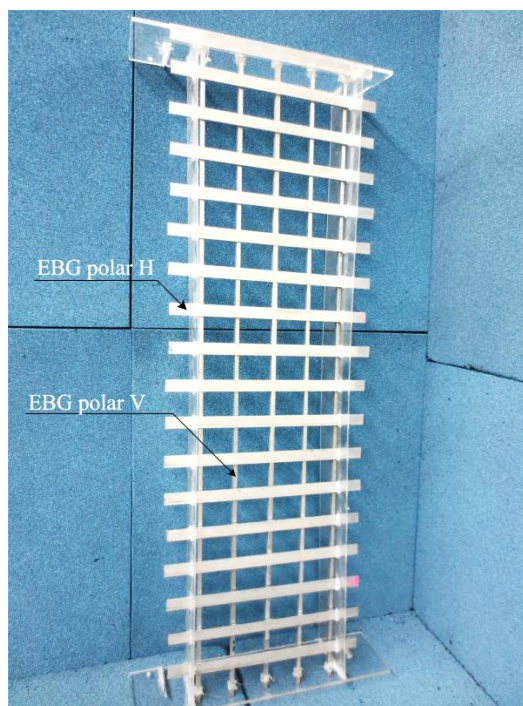
(a)
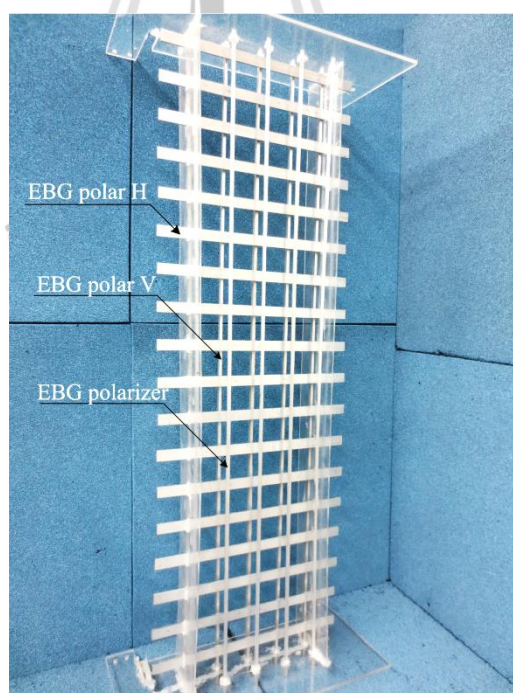
(b)

Figure 5.4 Superstrate layers (a) both layers of EBG polar V and H and

(b) EBG polarizer positioned on both layers of EBG polar V and H.

5.3   Dual polarized resonator antenna prototype

A real structure based on the previous concept has been built to verify the performance of the antenna. A dual polarization sectoral antenna prototype has been fabricated as shown in Figure 5.5, operating at 2.1 GHz by using a 45˚ oriented upturned curved strip dipole antenna on reflector plane, lower EBG polar V and upper EBG polar H layers. The dual polarized resonator antenna was designed using the components in Section 5.2. The both layers are mounted over reflector plane with the gap between reflector and upper layer about 60.4 mm.
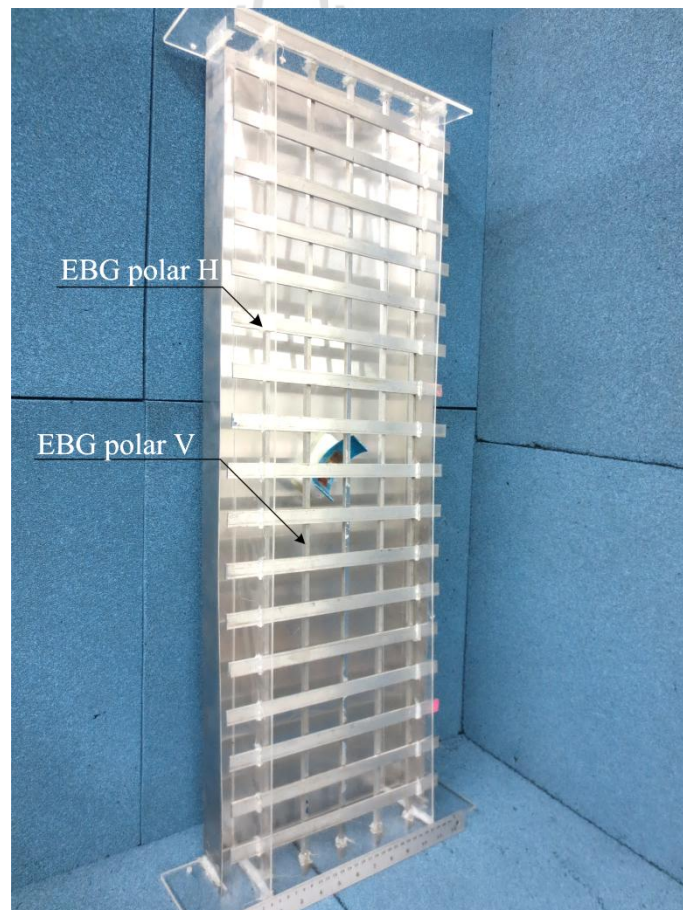
Figure 5.5 Photographs of dual polarized resonator antenna prototype.

5.4   Circularly polarized resonator antenna prototype

After the dual polarized resonator antenna was built, the circularly polarized resonator antenna was determined. The superstrate composes of EBG polar V, EBG polar H and EBG polarizer is positioned over reflector plane with the gap between reflector and upper layer of 62 mm. Also, the additional component that is EBG polarizer has the distance from EBG polar V of 30 mm. In this case, the feed system of the circularly polarization antenna is conveniently fabricated because it has only one feed point with a good matching coaxial balun as indicated in Figure 5.6.
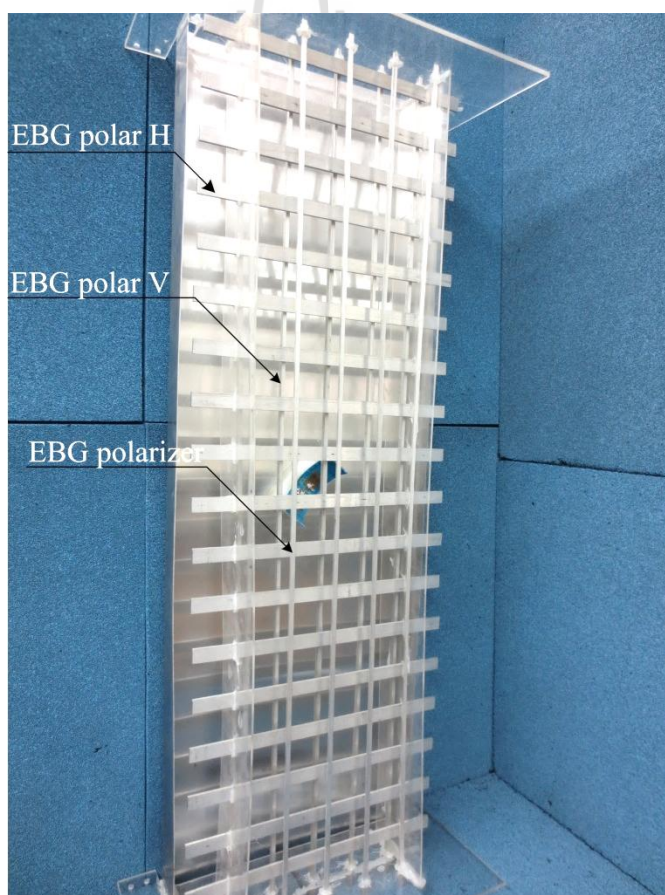
Figure 5.6 Photographs of circularly polarized resonator antenna prototype.

5.5   Antenna measurement

5.5.1   Far-field distance

The evaluation of the key antenna parameters such as radiation pattern, directivity, polarization, and gain can be performed in an outdoor or indoor antenna range, in either the near-field or far-field of the Device Under Test (DUT) (Balanis, 1997). In the far-field measurements, the DUT is illuminated by a uniform plane wave. This requirement is achieved when the distance between the DUT and Tx, included distance R, meet the far-field criterion given by Equation (5.1). This is also called the Rayleigh distance, where D is the largest dimension of the DUT as viewed from the measurement point.

$$R \geq 2\frac{D^2}{\lambda} \tag{5.1}$$

In general, there are two basic types of far-field antenna ranges such as reflection and free space ranges (Wiley-Interscience, 1979). Of these, the most accurate far-field antenna range is an indoor anechoic chamber (Evans, 1990). The reflection errors are minimized by lining the walls of the chamber with radar absorbing material, and its shielding properties prevent external RF energy to enter the chamber. Nevertheless, the usage of this far-field chamber is limited by the physical size of the DUT and the lowest usable frequency. In this thesis, because the DUT is an antenna for a mobile base station, it has a much larger dimension than the general antenna, the far-field range is a long space. Of these, the durable far-field antenna range is the bare area (outdoor). The reflection errors are moderately occurred by the other base station.

To measure the performance of an antenna, we focused on four fundamental parameters such as the radiation pattern, the HPBW, the polarization, and the gain of the antenna (DUT).

5.5.2 Radiation pattern

The antenna radiation pattern is the display of the far-field radiation properties of the antenna in spherical coordinates at a constant radial distance and frequency. This pattern is usually three-dimensional, however, because it is not pragmatic to measure this, a number of two-dimensional patterns, or cuts plane, are recorded by fixing one angle and varying the other (Balanis, 1997).

The testing of the dual and circularly polarization polarized resonator using the bare area in an outdoor environment, is depicted in Figure 5.7. The maximum antenna dimension of the proposed antennas are 950 mm, thus the far-field conditions are met as Equation (5.1) of 12.63 m. At the outdoor area, a transmitting conventional dipole antenna at 2.1 GHz is fixed at a certain position, while the dual or circularly polarization polarized resonator is in receiving mode. The DUT is installed on a turntable with the Raleigh distance R far from transmitting antenna. Pending the measurements, the proposed antennas were illuminated with uniform plane wave and their receiving characteristic were measured. Elevation plane measurements, or H-plane patterns in this configuration, were taken as previously appeared in Figure 5.7. Specifically, θ was fixed at 90° and ϕ was varied from 0° to 360°. Consideration of Figure. 5.7 that is the measurement set up of the proposed antenna which is installed on turntable wood pillar for measurement.
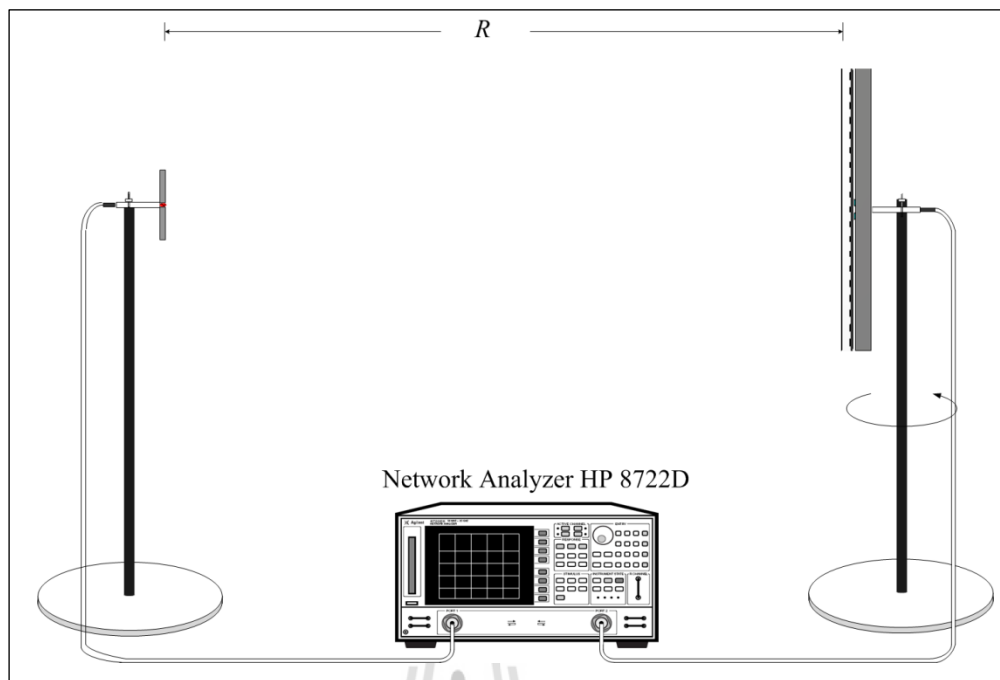
Figure 5.7 Measurement set up of the radiation pattern.

5.5.3   Gain

The power gain of an antenna in s given direction is the radio of the power radiated by the antenna in that direction to the power which would be radiated by a lossless isotropic radiator with the same power accepted as input. This is the reason why the antenna gain is specified as "dBi" in antenna datasheets - "dB" refers the ratio or gain and "i" signifies relative comparison to an isotropic antenna. An isotropic antenna is a hypothetical antenna that radiates with equal intensity in every direction without any losses. There are two basic methods to measure the gain of antenna: absolute gain and gain comparison technique (Balanis, 1997). For either method, the theory is based on the Friis transmission formula Equation (5.2), which can be applied when two polarizations matched antennas aligned for the maximum

directional radiation, and separated by a distance R that meet the far-field criteria, are used for the measurement.

$$\frac{P_r}{P_t} = G_t G_t \left(\frac{\lambda}{4\pi R} \right)^2 \tag{5.2}$$

where

P_r is the measured power received (W)

P_t is the measured power transmitted (W)

G_r is the gain of the receiving antenna

G_t is the gain of the transmitting antenna

$\left(\dfrac{\lambda}{4\pi R} \right)^2$ is the free space propagation loss

R is the far-field distance

The absolute gain method requires no a priori of the transmitting or receiving antenna gain. If the receiving and transmitting antennas are identical, only one measurement is required and Equation (5.2) can be clarified to Equation (5.3).

$$G_{r_{dB}} = G_{t_{dB}} = \frac{1}{2} \left[20\log\frac{4\pi R}{\lambda} + 10\log\frac{P_r}{P_t} \right] \tag{5.3}$$

The gain comparison method, or direct comparison method, commonly used in antenna ranges. Since ideal isotropic antennas mostly do not exist, recalibrated standard gain antennas are used to determine the absolute gain of the DUT. With this manner, two identical regular dipoles are used as transmitting and receiving antennas. The received signal level is plotted over the operating frequency, and, since the two

dipoles are identical, the result of Equation (5.3). Secondly, the receiving standard gain is replaced by the DUT and the measurements resume using the same geometrical arrangement and power level.

5.5.4 Bandwidth

The bandwidth of an antenna is classified actually as the range of utilizable frequencies within which the performance of the antenna conforms to a specified standard and may be limited by impedance mismatch or pattern degeneration. Even though, there are new bandwidth enhancement techniques to overcome the limited operational bandwidth of the patch antenna. The bandwidth can be the range of frequencies on either side of a center frequency where the antenna characteristics such as input impedance, pattern, beamwidth, polarization, side lobe level, gain, beam direction or radiation efficiency, are within an acceptable value of those at the center frequency (Balanis, 1997).

The fractional bandwidth of an antenna is a measure of how wideband the antenna is. If the antenna operates at center frequency f_c between lower frequency f_{lower} and upper frequency f_{lower} (where f_c=(f_{lower} + f_{lower})/2), then the fractional bandwidth FBW is given by Equation (5.4).

$$\text{Bandwidth (\%)} = \left[\left(f_{upper} - f_{lower} \right) / f_c \right] \times 100\% \tag{5.4}$$

The bandwidth of the antennas in this thesis is specified by the standard of mobile communication system.

5.5.5 Polarization

To perform the measurement, the DUT is used as the source. Then a linearly polarized antenna is used (typically a half-wave dipole antenna) as the receive antenna. The linearly polarized receiver antenna will be rotated, and the received power recorded as a function of the angle of the receive antenna. In this manner, the information on the polarization of the test antenna could be obtained. This received information only applies to the polarization of the test antenna for the direction in which the power is received. For a complete description of the polarization of the DUT, the test antenna must be rotated so that the polarization can be determined for each direction of interest. The basic setup for polarization measurements is shown in Figure 5.8. Suppose now that DUT was radiating a circularly polarized wave, the normalized (make the peak output power equal to one for simplicity) output power would resemble circle. Because a circularly polarized wave has equal amplitude components in two orthogonal directions, the received power is constant for a rotated linearly polarized antenna. Note also that the received power is the same whether or not the test antenna is left hand (LHCP) or right hand (RHCP). As a result, this method can determine the type of polarization, but cannot determine the sense of rotation for the polarization.
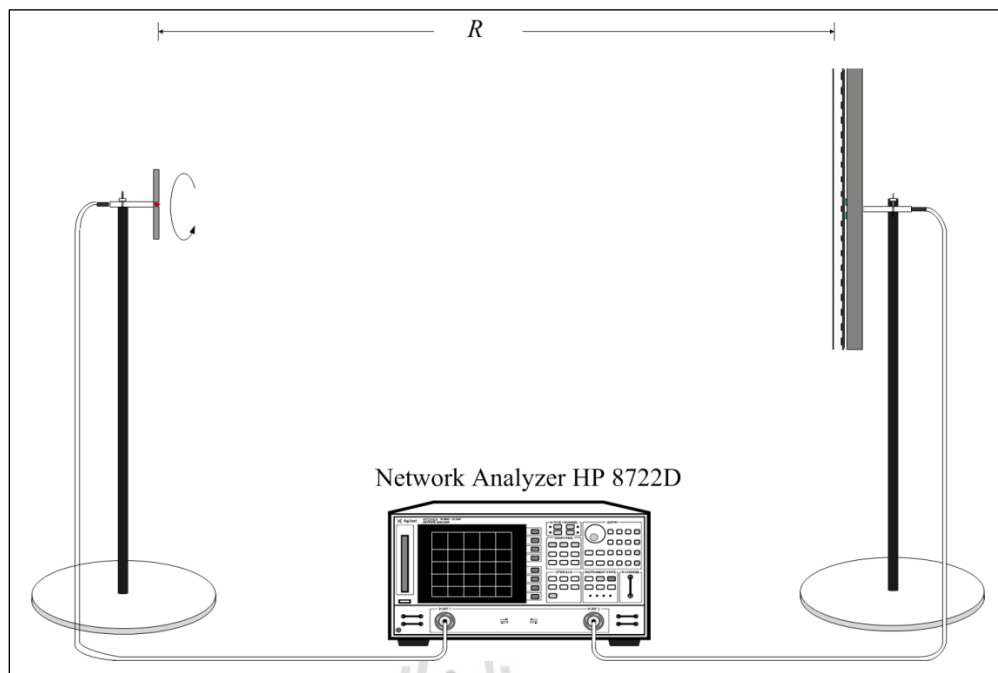
Figure 5.8 Measurement set up of the circularly polarization.

5.6   Experimental results

The measured results is divided into four parts as an upturned curved strip dipole, the radiating element on U-shaped, the dual polarized resonator antenna, and circularly polarized resonator antenna. The above mentioned details are the procedure of the antenna characteristic measurement, also, in this section is determined the performance of our proposed antennas.

5.6.1   An upturned curved strip dipole

The measured S_{11} and SWR of the curve strip dipole antenna are shown in Figures 5.9(a) and (b), and the match frequency for L_d = 53.38 mm is less than 2.1 GHz. Therefore, the antenna is trimming both ends a few while the center frequency is 2.1 GHz, the excellent return loss of -17.42 dBi. The frequency bandwidth is covered 1.92 GHz to 2.32 GHz that is sufficient for mobile

communication systems. Figures 5.9(c) shows impedance, denoted the higher than 51

ohm. Moreover, the measured far-field patterns in E- and H-planes for a curved strip

dipole antenna at the resonant frequency of 2.1 GHz are illustrated in Figures 5.9(d)

and (e). This figure shows the comparison with the simulated patterns and measured

patterns. The half power beamwidth in E- plane is 96.2 degree and the maximum gain

is 1.47 dBi. The measurement is performed in the simulation results.
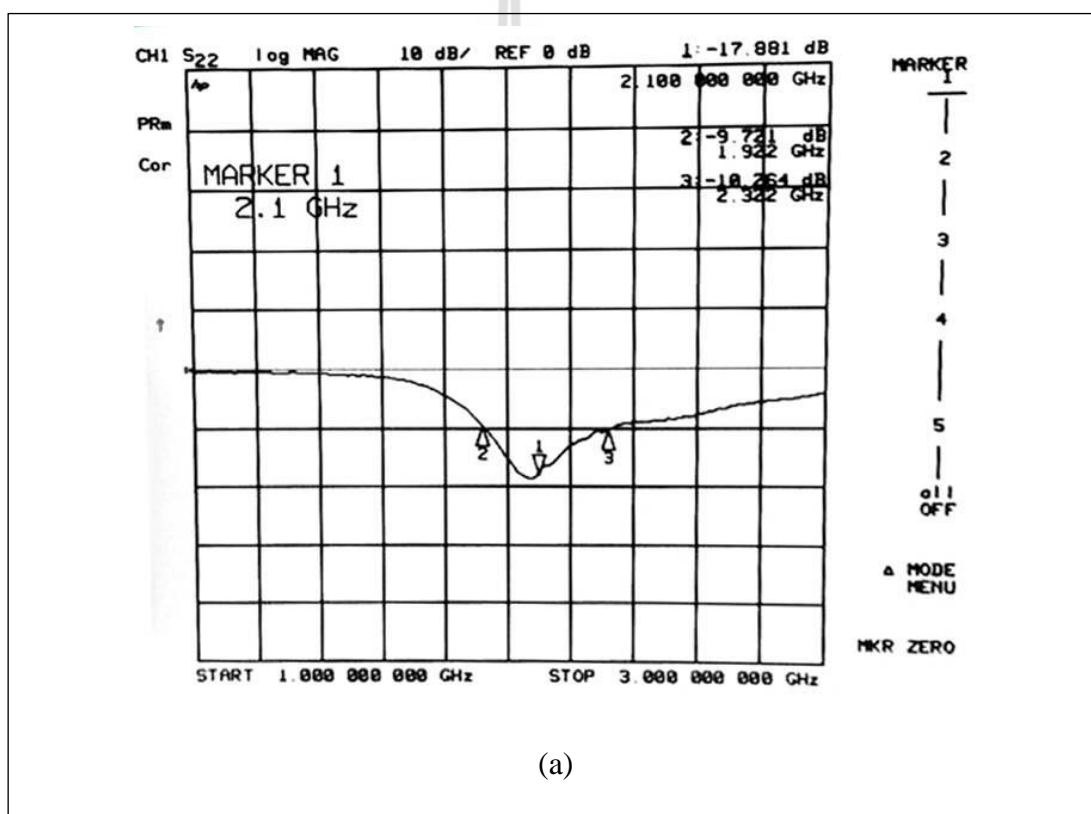
(a)

Figure 5.9 Measured results of an upturned curved strip dipole antenna (a) S_{11},

(b) SWR, (c) smith chart, (d) E-plane, and (e) H-plane.

(b)

(c)

Figure 5.9 Measured results of an upturned curved strip dipole antenna (a) S_{11},

(b) SWR, (c) smith chart, (d) E-plane, and (e) H-plane (cont.).

(d)

(e)
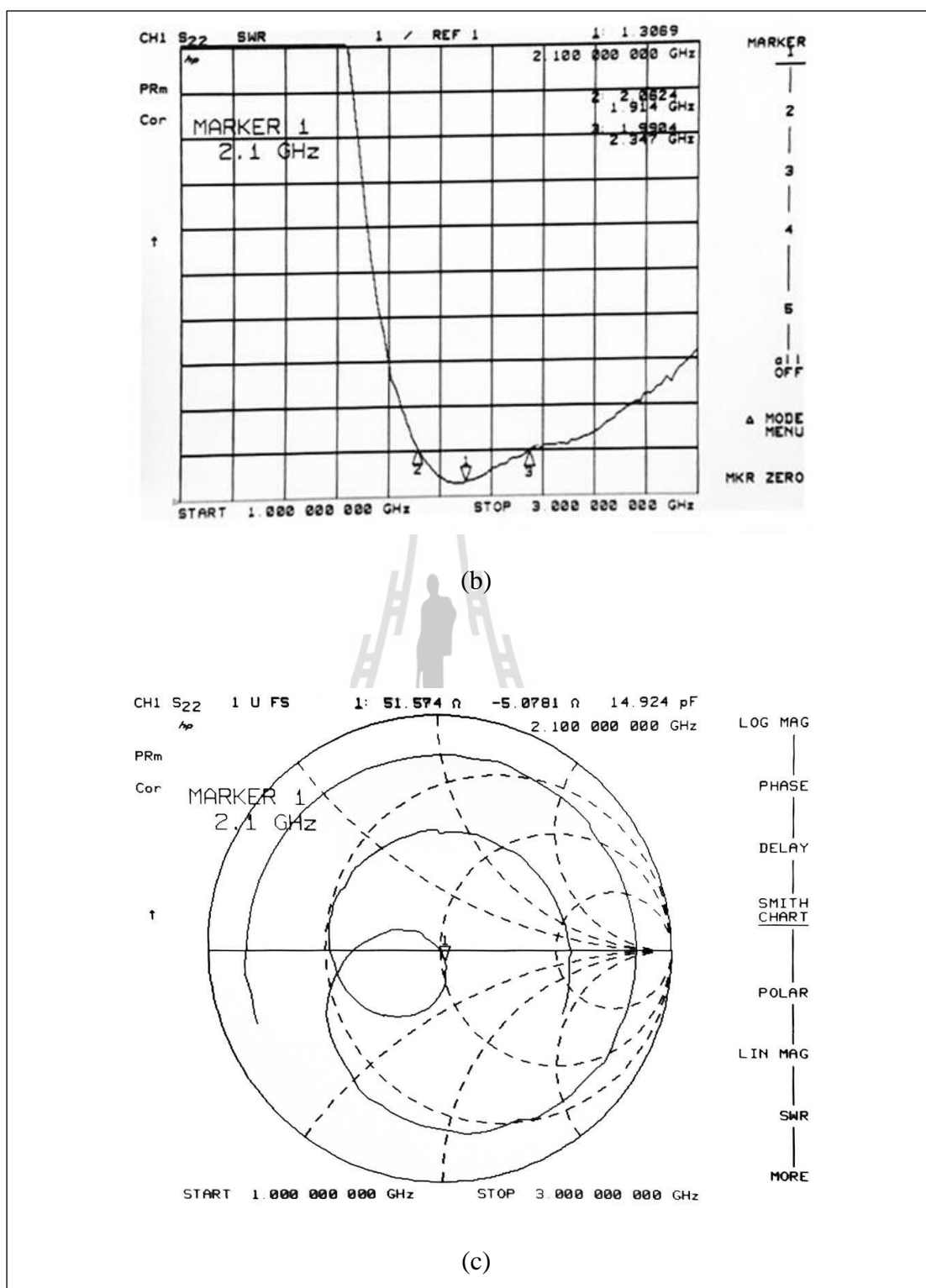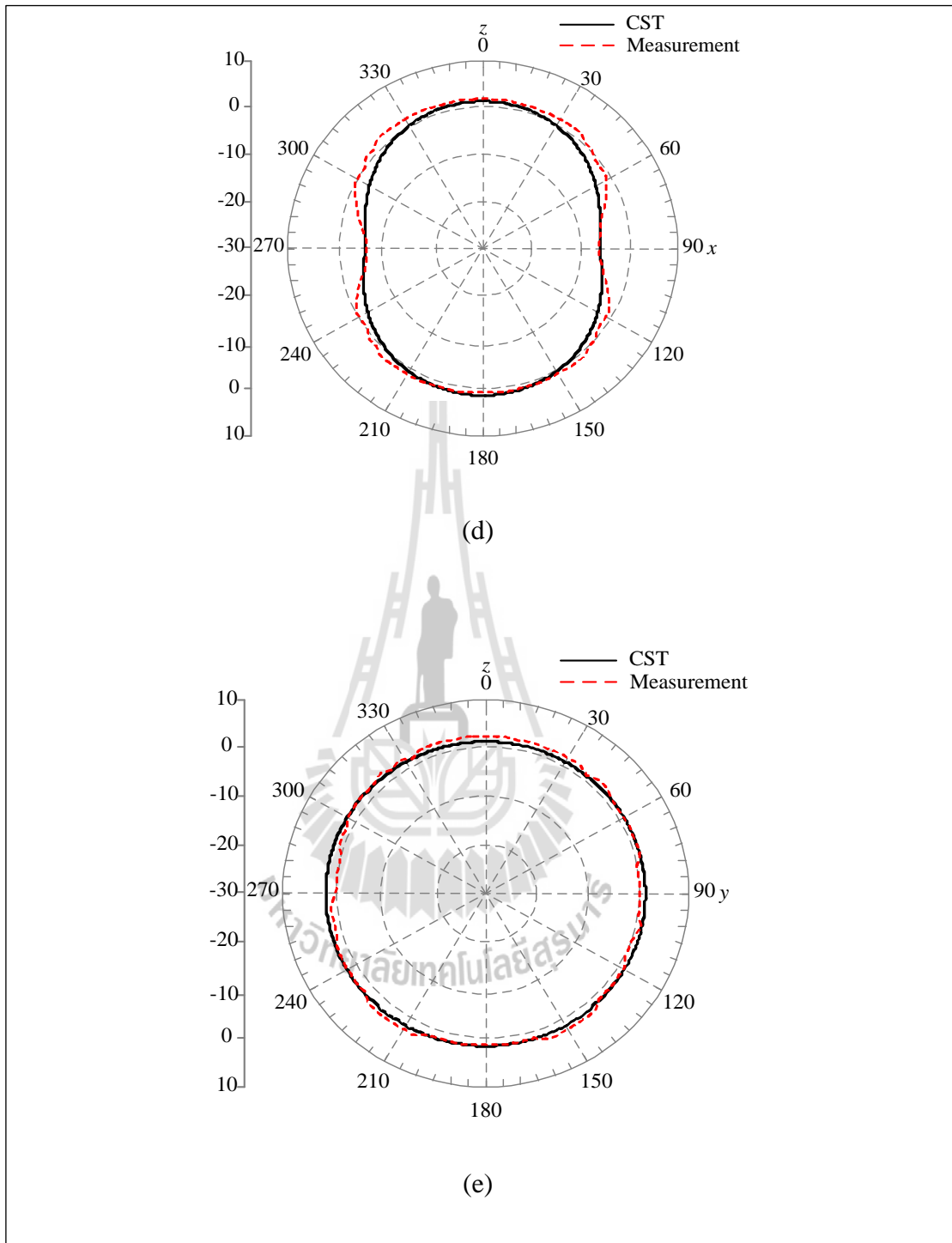
Figure 5.9 Measured results of an upturned curved strip dipole antenna (a) S_{11},

(b) SWR, (c) smith chart, (d) E-plane, and (e) H-plane (cont.).

5.6.2   The radiating element on U-shaped reflector plane

When a curved strip dipole antenna is tested, it is mounted over the U-shaped reflector plane and fed from the center of the curved strip dipole to the back side of the reflector at a quarter wavelengths. The return loss, SWR and impedance are measured as shown in Figures 5.10(a) to (c). As a result, the return loss is about 16.84 dB, SWR is about 1:1.3, and impedance is about 47.9 ohm. This means that this antenna can work very well in practice. Figures 5.10(d) and (e) show the comparison of the theoretical results with measurements for the total far-field radiation patterns on the resonant frequency of 2.1 GHz, while the resulting of the half power beamwidth in E- and H-plane are about 87.2 and 94.3 degree, respectively. The maximum gain is 7.8 dBi that it is satisfied with the antenna model form CST software.
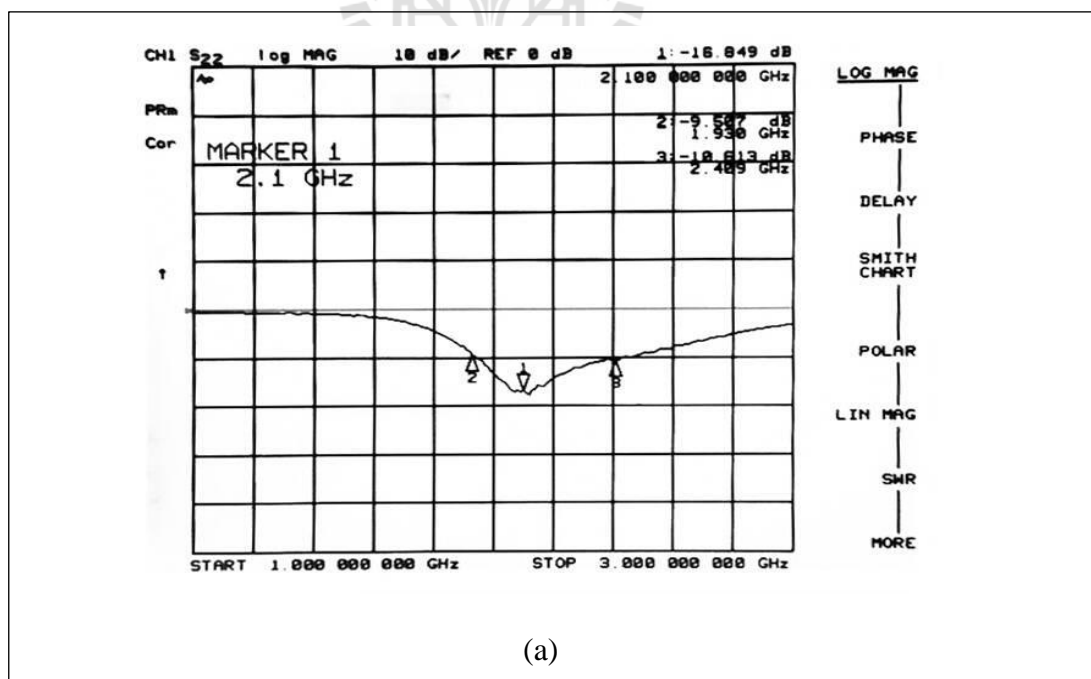
(a)

Figure 5.10 Measured results of feeding antenna on U-shaped reflector (a) S_{11}, (b) SWR, (c) impedance, (d) E-plane, and (e) H-plane.

(b)

(c)

Figure 5.10 Measured results of feeding antenna on U-shaped reflector (a) S_{11},

(b) SWR, (c) impedance, (d) E-plane, and (e) H-plane (cont.).

(d)

(e)
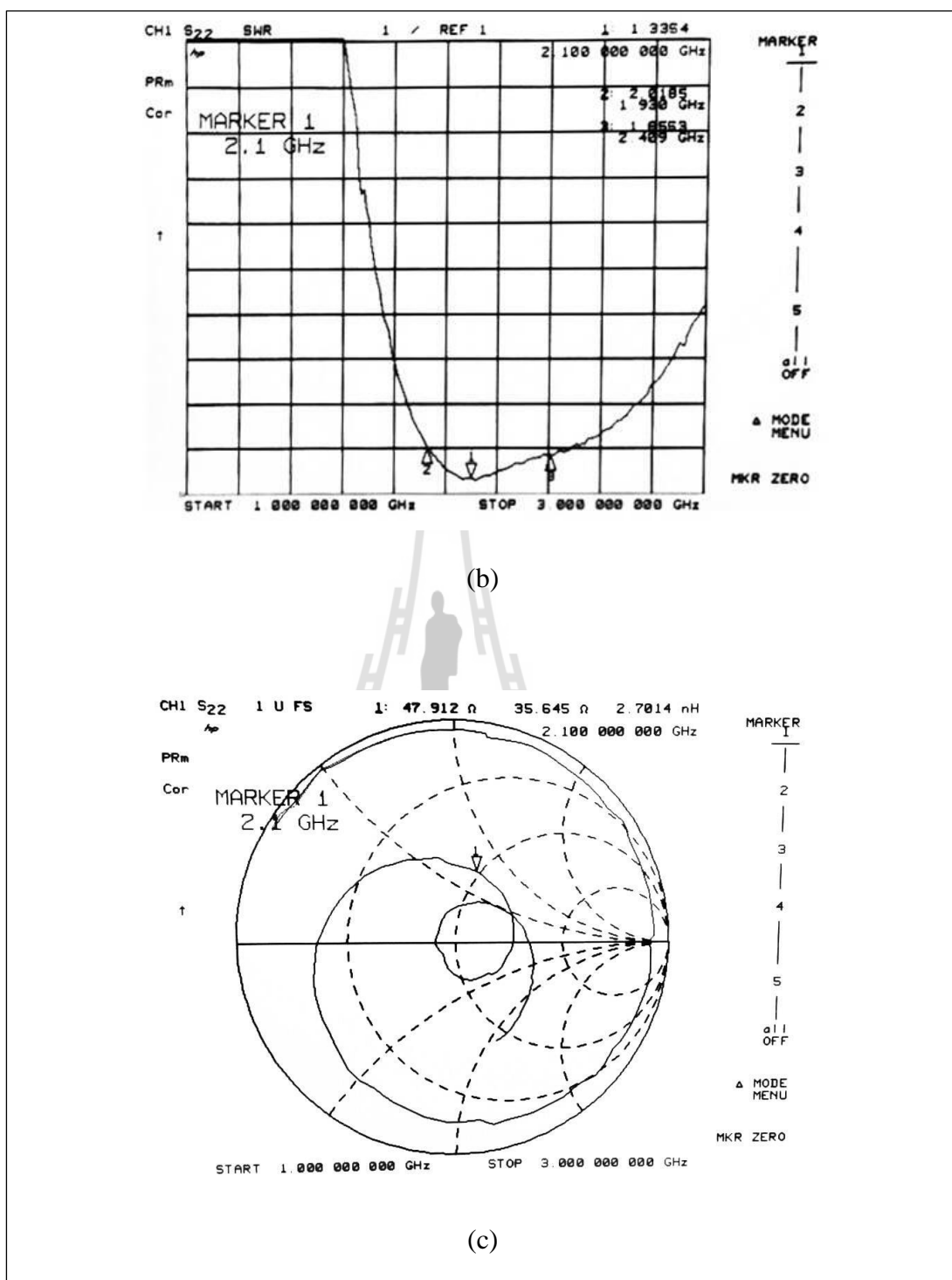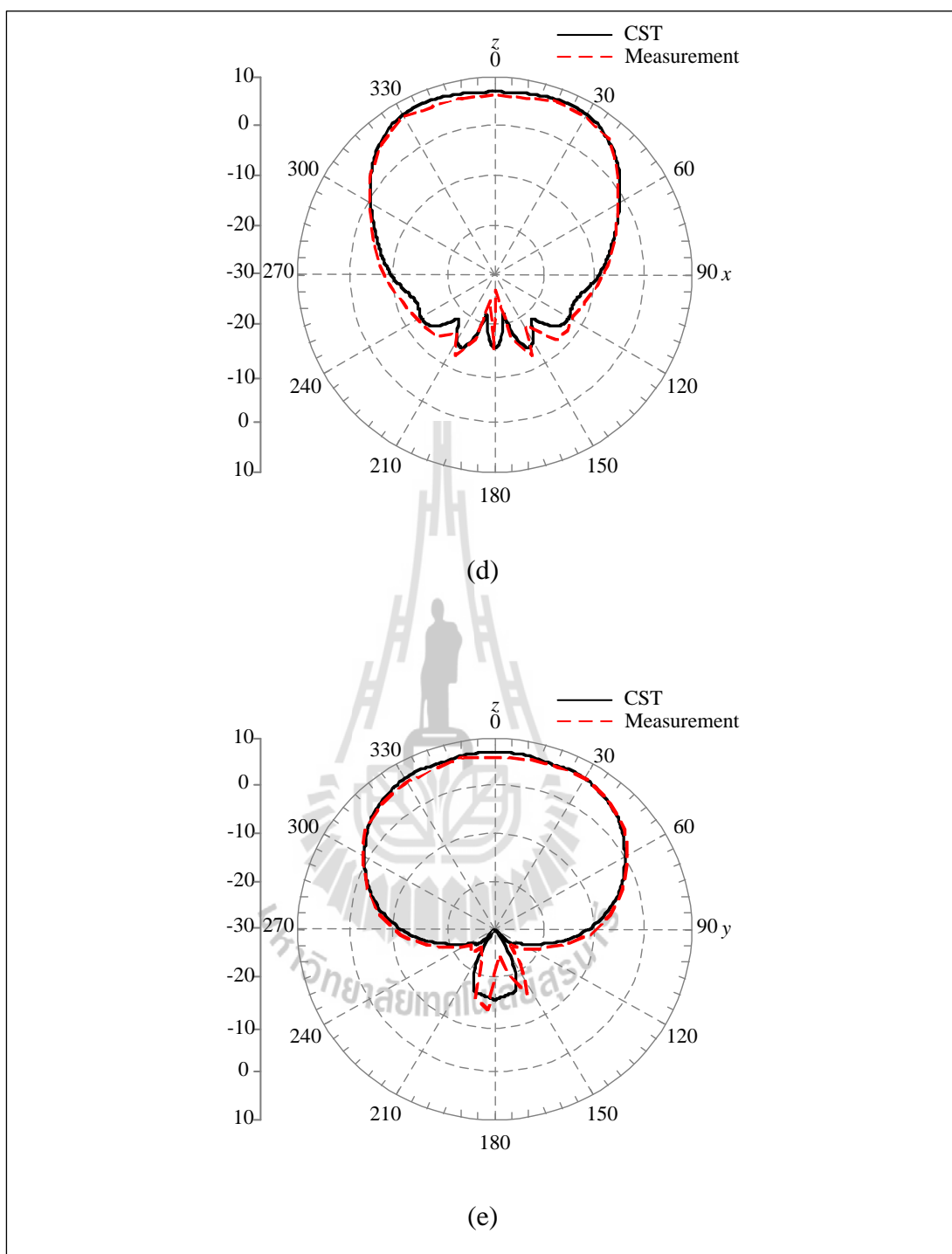
Figure 5.10 Measured results of feeding antenna on U-shaped reflector (a) S_{11},

(b) SWR, (c) impedance, (d) E-plane, and (e) H-plane (cont.).

5.6.3 Dual polarized sector antenna

Figure 5.11(a) shows the measured gain of the proposed antenna. It can be seen that the gain of the antenna is around 14 dBi for either polar V or polar H at working range of frequency. The similar radiation and gain enhances the efficiency of mobile communication systems. In this manner, the normalized output power would be resembled in Figs. 5.11(b) and (c). This plot shows the agreement between the measured and the simulated results in both horizontal and vertical plane patterns. The measured HPBWs in horizontal and vertical plane are 60° and 17.9° at 2.1 GHz, respectively. The half-power beamwith in horizontal plane is suitable for mobile base stations.
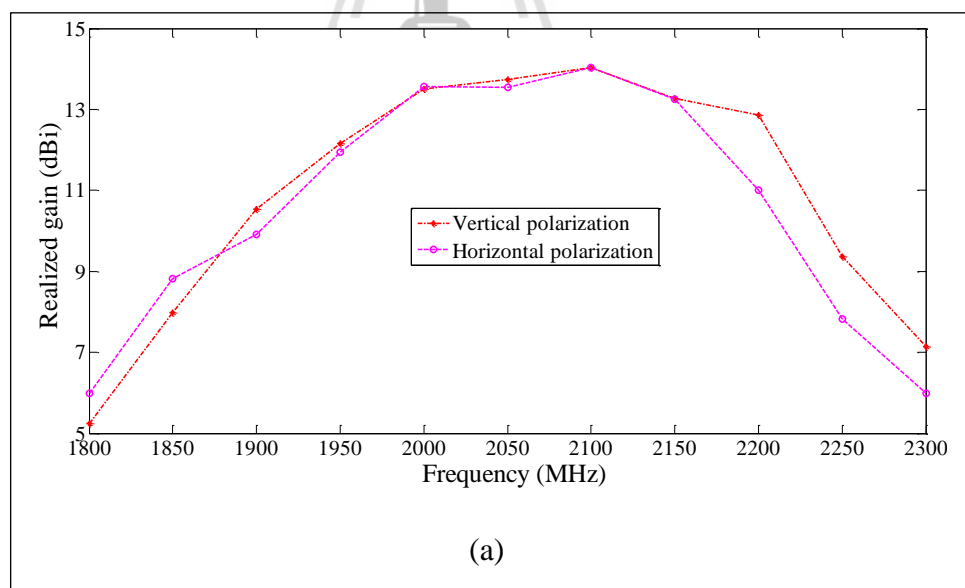
(a)

Figure 5.11 Measured results of dual polarized sector antenna (a) realized gain

(b) horizontal plane, and (c) vertical plane.
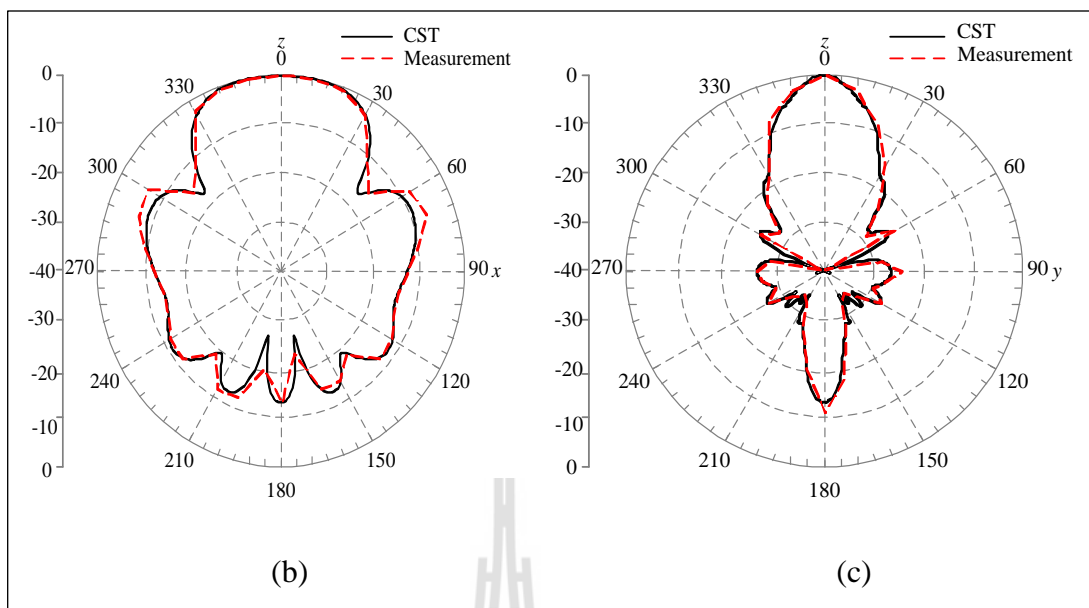
Figure 5.11 Measured results of dual polarized sector antenna (a) realized gain

(b) horizontal plane, and (c) vertical plane (cont.).

5.6.4 Circularly polarized sector antenna

The evaluation of the key antenna parameters such as radiation pattern, polarization, and gain were measured by using Network Analyzer. Figure 5.12(b) illustrates an axial ratio close to 0 dB at the resonant frequency band, covering the uplink and downlink band of mobile base station. Figure 5.12(a) shows the measured gain of the proposed antenna. It can be seen that the gain of the antenna is around 15.11 dBi at working range of frequency. Furthermore, the measured realized gain and AR are continually measured to confirm the antenna performance. After that the proposed antenna is rotated and the measured radiation pattern of the antenna is plotted together with the simulated pattern as shown in Figs. 5.12(c) and (d), respectively. This plot shows agreements between the measured and simulated results both in horizontal and vertical plane patterns. The similar radiation and gain enhance the efficiency of mobile communication systems. When the transmitted antenna

(dipole) is rotate 360° clockwise, the normalized output power would resemble that of Figure 5.12(e). Note that the test antenna was radiating as a circularly polarized waves.
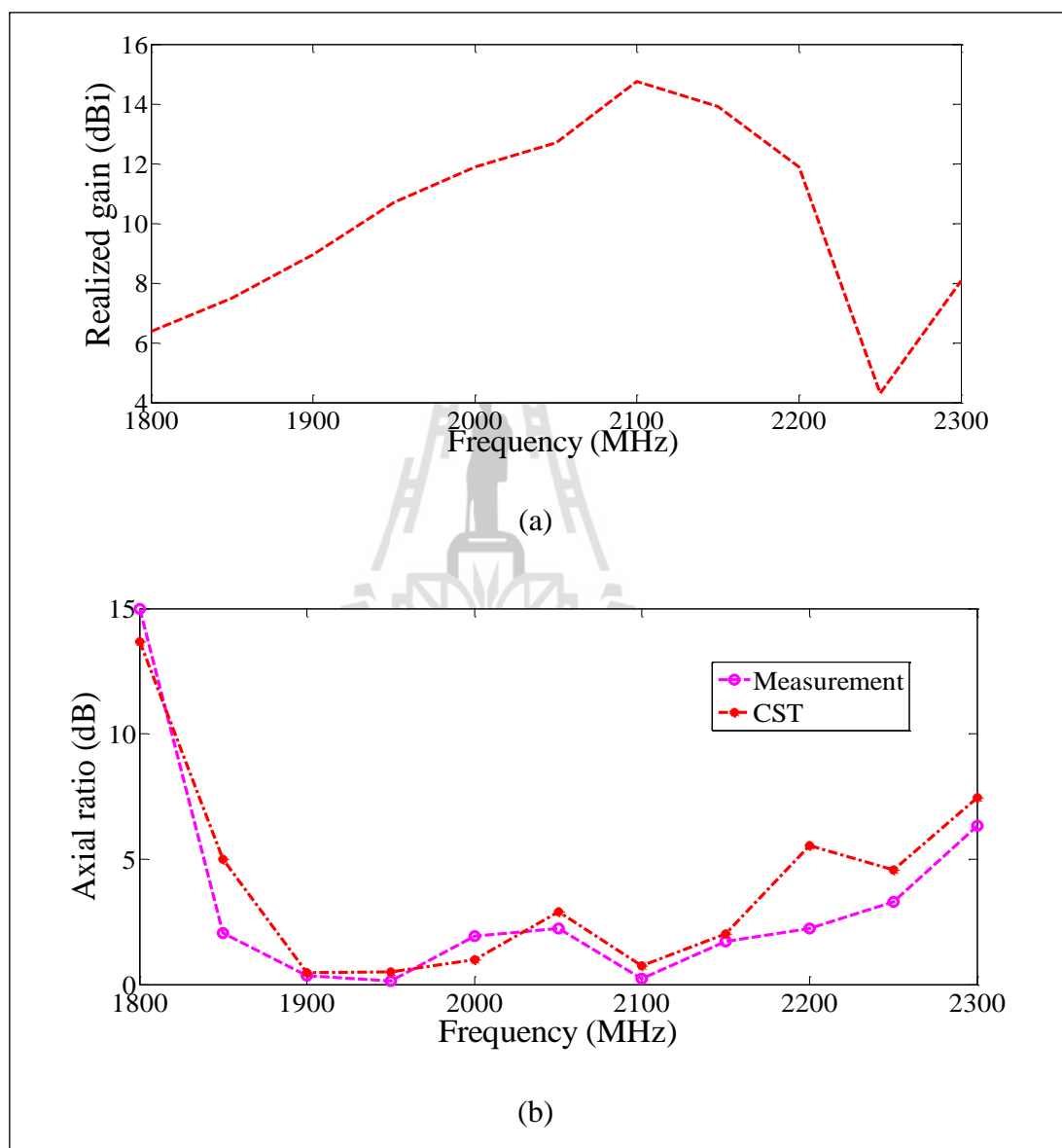
(a)

(b)

Figure 5.12 Measured results of circularly polarized sector antenna (a) realized gain, (b) AR, (c) horizontal plane, and (d) vertical plane (e) output of measurement when the test antenna is circularly polarized.
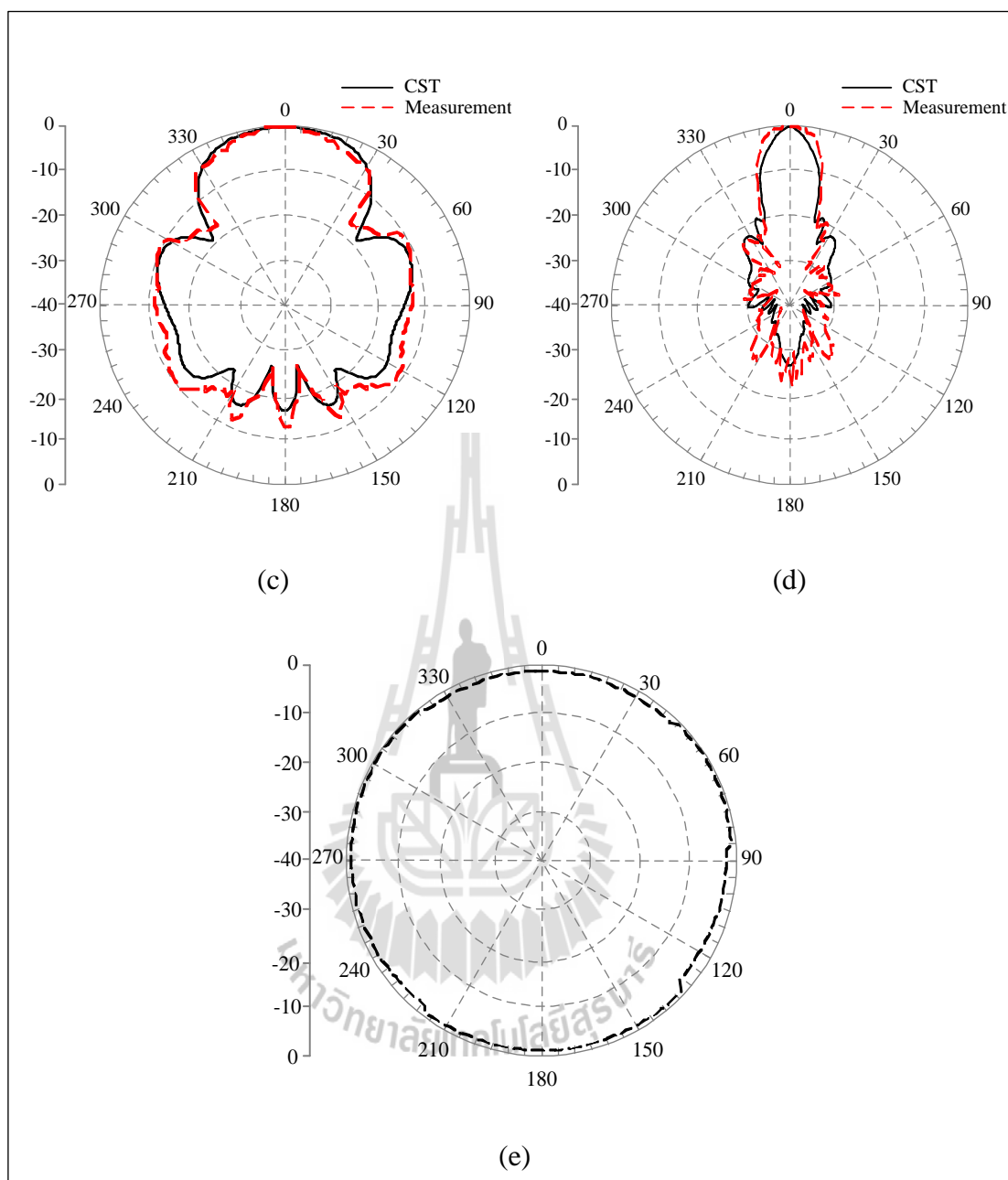
Figure 5.12 Measured results of circularly polarized sector antenna (a) realized gain,

(b) AR, (c) horizontal plane, and (d) vertical plane (e) output of

measurement when the test antenna is circularly polarized (cont.).

5.7   Chapter summary

In this chapter, the antenna prototype was fabricated on aluminium to verify the antenna performance. The beam patterns, gain, and AR are measured according to the BS antenna currently utilized nowadays. All above results can conclude that a 45° oriented curved strip dipole fed between the muti layers EBG and the U-shaped reflector plane produce the circularly polarization and the sectoral radiation pattern (HPBW around 60°) can be obtained by reducing the size of the antenna in *xz* plane. Good agreement between simulated and measured results is achieved.

CHAPTER VI

THESIS CONCLUSION

6.1 Conclusion

Nowadays wireless communications have been developed for the entertainment, education, economic, health, and industry. Mobile technology is the most popular wireless communication which has progressed rapidly from 1G to 4G. The development of antennas with new performances becomes currently imperatively essential for the new services and network of telecommunication. Therefore, the purpose of this thesis is to design a high gain antenna for a mobile base station. Also, the antenna requirements are as follow

- Sector antenna gain : 13 – 18 dBi

- Sector antenna half power beamwidth : 60 - 65 degree

- Impedance : 50 Ohm

As the demands of cellular networks have been dramatically increased, the performance of the sector antenna is concentrated by antenna engineering. Consequently, an analysis of a sector antenna for base station of mobile phone is studied in this thesis. A curved strip dipole is applied for the feeding antenna, placing on U-shaped reflector plane at 45˚ angle and increasing its gain by using double layers metallic rod EBG. New technique to generate the circularly polarization is to add a metallic rod EBG polarizer for differing in phase by 90° of two orthogonal electric fields. The CST Microwave Studio is used to simulate the proposed antenna for details on the design and analysis is discussed in Chapter 5. Furthermore, Table 6.1

summarizes the characteristic of the antenna design. It seems that good agreement between simulated and measured results is achieved.

Table 6.1 Specification of the proposed antenna.

Antenna type	Simulation results		Measurement results	
	Dual Polarized Sector Antenna	Circularly Polarized Sector Antenna	Dual Polarized Sector Antenna	Circularly Polarized Sector Antenna
Material	Aluminium	Aluminium	Aluminium	Aluminium
Frequency band (MHz)	2100 (1920-2170)	2100 (1850-2230)	2100 (1920-2200)	2100 (1870-2170)
HPBW (degree)	H:60 V:17.9	H:60.1 V:12.3	H:60 V:20	H:60 V:14.4
Gain (dB)	15	15.53	14.06	15.11
Antenna size (mm)	950×300×71	950×300×99	950×300×71	950×300×99
Antenna weight (kg)	-	-	2.7	3.3

6.2   Remark for future studies

For future work, the allowed bandwidth can be increased by the use of a new kind of EBG material combining the similar polarization. The combination of multi-layers of metallic rod EBG in the upper interface of the resonator antenna, with respect to some criteria such as the partially reflective surface nature and the distance

between EBG has been shown advantageous in term of bandwidth. In particular, the option of a low layer EBG more reflective than the EBG display in the high layer can participate to the information of a double layer material with positive slope reflection phase. The increased phase profile realized in a local frequency band will allow satisfaction of the resonance condition of the EBG cavity in a wide frequency band, consequently increasing the antenna radiation bandwidth. In addition, the antenna has been improved the radiation bandwidth by the use of broadband primary radiating such as a magneto-electric dipole. It is a kind of complementary antenna which has excellent electrical characteristics including wide impedance bandwidth, low cross polarization and low back lobe radiation.
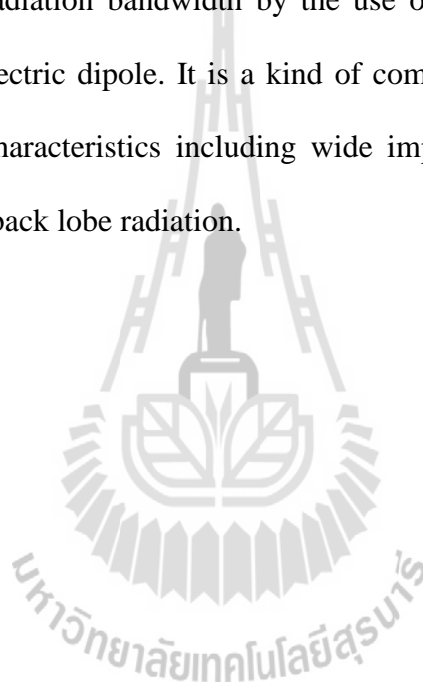
REFERENCES

Abas A., Asrokin A., Basri R.H., and Jamlus N. (2010). Dual-polarized dipole array antenna for CDMA 450 base station application. **IEEE Asia-Pacific Conference on Applied Electromagnetics.** 1 – 4.

Abkenar, M.R. and Rezaei, P. (2011). Design of a Novel EBG Structure and its Application for Improving Performance of a Low Profile Antenna. **Iranian Conference on Electrical Engineering.** 1 – 5.

Agi K., Mojahedi M., Minhas B., Schamiloglu E., and Malloy K.J. (2002). The effects of an electromagnetic crystal substrate on a microstrip patch antenna. **IEEE Transactions on Antennas and Propagation.** 50(4) 451 – 456.

Azad M. Z. and Ali M. (2008). Novel wideband directional dipole antenna on a Mushroom Like EBG structure. **IEEE Transactions on Antennas and Propagation.** 56(5): 1242-1250.

Balanis, C.A. (1997). **Antenna Theory Analysis and Design.** J. Wiley & Sons.

Debogovic T., Perruisseau-Carrier J., and Bartolic J. (2010). Partially Reflective Surface antenna with dynamic beamwidth control. **IEEE Antennas and Wireless Propagation Letters.** 9: 1157-1160.

Fhafhiem N., Krachodnok P., and Wongsan R. (2009). A Shorted-End Curved Strip Dipole on Dielectric and Conducting Plane for Wireless LANs. **International Symposium on Antenna and Propagation.** 835 – 838.

Fhafhiem N., Krachodnok P., and Wongsan R. (2010). Curved strip dipole antenna on EBG reflector plane for RFID applications. **WSEAS Transection on Communications.** 6(9) 374 – 383.

Fhafhiem N., Krachodnok P., and Wongsan R. (2012). Gain improvement of curved strip dipole using EBG resonator. **Progress In electromagnetics research symposium proceedings.** 1631 – 1634.

Fan Yang and Yahya Rahmat-Samii (2005). A low profile single dipole antenna radiating circularly polarized waves. **IEEE Transactions on Antennas and Propagation.** 53(9) 3083 – 3086.

Farahani H.S., Veysi M., Kamyab M., and Tadjalli A. (2010). Mutual coupling reduction in patch antenna arrays using a UC-EBG superstrate. **IEEE Antennas and Wireless Propagation Letters.** (9) 57 – 59.

Grelier M., Djoma C., Jousset M., Mallegpl S., Lepage A. C., and Begaud X. (2012). Axial ratio improvement of an archimedean spiral antenna over a radial AMC reflector. **Apply Physic A.** 1081 – 1086.

Hajj M., Chantalat R., Jecko B. (2009). Design of a dual-band sectoral antenna for Hiperlan2 application using double layers of metallic electromagnetic band gap (M-EBG) materials as a superstrate. **International Journal of Antennas and Propagation.** 1 – 5.

Hajj M., Monediere T., Jecko B., and Chantalat R. (2010). A novel design of circularly polarized sectoral M-PRS antenna. **International Symposium on Antenna Technology and Applied Electromagnetics & the American Electromagnetics Conference.** 1 – 4.

Huan Yi and Shi-Wei Qu. (2013). A novel dual-band circularly polarized antenna based on electromagnetic band-gap structure. **IEEE Antennas and Wireless Propagation Letters.** (12) 1149 – 1152.

Ka-Ming M., Hang W., and Luk, Kwai-Man (2007). A shorted bowtie patch antenna With a cross dipole for dual polarization. **IEEE Antennas and Wireless Propagation Letters.** 6: 126-129.

Lin Peng, Cheng-Li Ruan, and Li Zhi-Qiang. (2010). A novel compact and polarization-dependent mushroom-type EBG using CSRR for dual/triple-band applications. **IEEE Microwave and Wireless Components Letters.** 20(9) 489 – 491.

Liping H., Runbo M., Xinwei C., and Wenmei Z. (2012). Compact dual-band dipole antenna fed by a coplanar waveguide. **International Conference on Microwave and Millimeter Wave Technology.** 1 – 3.

Moghadas H., Daneshmand M., and Mousavi P. (2011). A dual band high-gain resonant cavity antenna With orthogonal polarizations. **IEEE Antennas and Wireless Propagation Letters.** (10) 1220 – 1223.

Nakano H., Kikkawa K., Kondo N., Iitsuka Y., and Yamauchi J. (2009). Low-Profile equiangular spiral antenna backed by an EBG reflector. **IEEE Transactions on Antennas and Propagation.** 57(5) 1309 – 1318.

Pirhadi A., Hakkak M., Keshmiri F., and Baee R.K. (2007). Design of compact dual band high directive electromagnetic bandgap (EBG) resonator antenna using Artificial Magnetic Conductor. **IEEE Transactions on Antennas and Propagation.** 55(6) 1682 – 1690.

Qi Wu, Scarborough C.P., Martin B.G., Shaw R.K., Werner D.H., Lier E., and Wang X. (2013). A ku-band dual polarization hybrid-mode horn antenna enabled by printed-circuit-board metasurfaces. **IEEE Transactions on Antennas and Propagation.** 61(3) 1089 – 1098.

Rodes E., Diblanc M., Arnaud E., Monediere T., and Jecko B. (2007). Dual-band EBG resonator antenna using a single-layer FSS. **IEEE Antennas and Wireless Propagation Letters.** (6) 368 – 371.

Thumvichit A. and Takano T. (2006). Ultra low profile dipole antenna with a simplified feeding structure and a parasitic element. **IEICE Transactions Communications.** 576 – 580.

Trentini G.V. (1956). Partially reflecting sheet array. **IRE Transactions on Antennas and Propagation.** 57(5) 1309 – 1318.

Weily A.R., Horvath L., Esselle K.P., Sanders B.C., and Bird, T.S. (2005). A planar resonator antenna based on a woodpile EBG material. **IEEE Transactions on Antennas and Propagation.** 53(1) 216 – 223.

Wu Di, Yin Yingzeng, Guo Minjun, and Shen Renqiang. (2005). Wideband dipole antenna for 3G base stations. IEEE International Symposium on Microwave, Antenna, Propagation and EMC Technologies for Wireless Communications. 454 - 457.

Yang F. and Rahmat-Samii Y. (2008). **Electromagnetic Band Gap Structures in Antenna Engineering**. Cambridge University Press, Cambridge.

Ying Liu, Hao Yi, u-Wei Wang, and Shu-Xi Gong (2013). A novel miniaturized broadband dual-polarized dipole antenna for base station. **IEEE Antennas and Wireless Propagation Letters.** (12) 1335 – 1338.

Yong-Xin Guo, Kwai-Man Luk, and Kai-Fong Lee (2002). Broadband dual polarization patch element for cellular-phone base stations. **IEEE Transactions on Antennas and Propagation.** 50(2) 251 – 253.

Young Ju Lee, Junho Yeo, Mittra R., and Wee Sang Park. (2005). Application of electromagnetic bandgap (EBG) superstrates with controllable defects for a class of patch antennas as spatial angular filters. **IEEE Transactions on Antennas and Propagation.** 53(1) 224 – 235.

Yue Hui Cui, RongLin Li, and Peng Wang (2005). Novel Dual-Broadband Planar Antenna and Its Array for 2G/3G/LTE Base Stations. IEEE Transactions on Antennas and Propagation. 61(3) 1132 – 1139.

Yuehe Ge, Esselle K.P., and Bird T.S. (2012). The use of simple thin partially reflective surfaces With positive reflection phase gradients to design wideband, low-Profile EBG resonator antennas. **IEEE Transactions on Antennas and Propagation.** 60(2) 743 – 750.

Zhan L. and Rahmat-Samii Y. (2000). PBG, PMC and PEC ground plane: A case study of dipole antenna. **IEICE Transactions Communications.** 674 – 677.

Zhijun Z., Iskander M.F., Langer J.C., and Mathews J. (2004). Wideband dipole antenna for WLAN. **International Conference on Microwave and Millimeter Wave Technology.** 1963 – 1966.

Zhou R., Zhang H., and Xin H. (2010) Metallic Wire Array as Low-Effective Index of Refraction Medium for Directive Antenna Application. IEEE Antennas and Propagation, 58(1) 79 - 87.
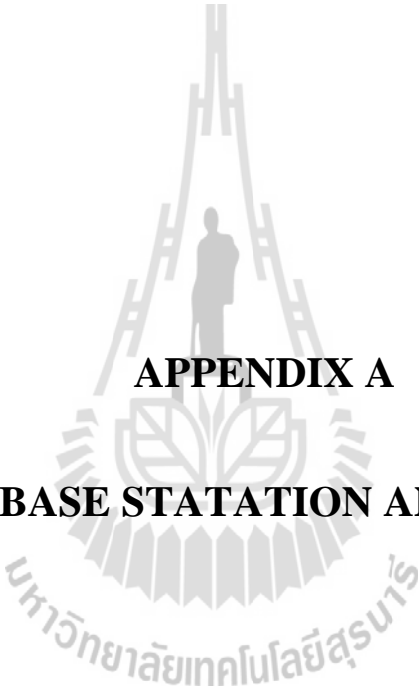
APPENDIX A

3G BASE STATATION ANTENNA

A.1 3G 1710-2170MHz 15dBi Sector Antenna/Repeater

Antenna/Base Station Antenna (GW-SA1710-2170-15D)

Figure A.1 Base station antenna model : GW-SA1710-2170-15d.

Product Feature:

ELECTRICAL			
Frequency Range	1710-1880-MHz	1850-1990-MHz	1920-2170-MHz
Bandwidth	170-MHz	140-MHz	250-MHz
Gain	14.5-dBi	14.5-dBi	15-dBi
Beamwidth	H:68° E:16°	H:65° E:15°	H:62° E:14°
VSWR	≤1.5		
Polarization	Vertical		
Max power	100 -W		
Nominal Impedance	50 -Ω		
MECHANICAL			
Dimension	550×180×80-mm		
Weight	3-KG		

* SHENZHEN GREETWIN TECHNOLOGY CO., LIMITED

A.2   1710-1880/1850-1990/1920-2170 MHz 65°X-Pol

(Model:PB17/21-18-65XT0)

Figure A.2 Base station antenna model : PB17/21-18-65XT0.

Product Feature:

ELECTRICAL			
Frequency Range	1710-1880-MHz	1850-1990-MHz	1920-2170-MHz
Bandwidth	170-MHz	140-MHz	250-MHz
Gain	18-dBi		
Beamwidth	H:68° E:9°	H:65° E:8°	H:63° E:7°
VSWR	≤1.5		
Polarization	±45˚		
Max power	100 -W		
Nominal Impedance	50 -Ω		
MECHANICAL			
Dimension	1300×180×100-mm		
Weight	8-KG		

* http://www.nhmicrowave.com/
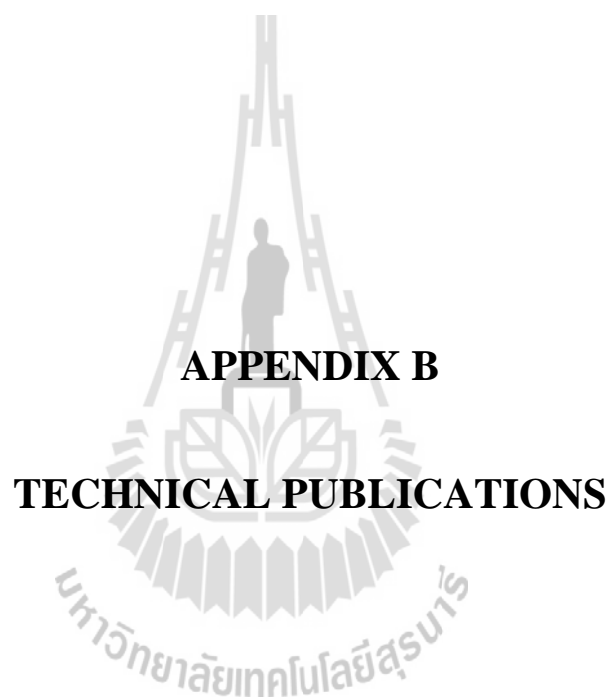
APPENDIX B

TECHNICAL PUBLICATIONS

List of publications

International Journal Paper

Fhafhiem N., Krachodnok P., and Wongsan R. (2014). Design of a Dual Polarized Resonator Antenna for Mobile Communication System. **World Academy of Science, Engineering and Technology** (WASET), International Journal of Electrical, Robotics, Electronics and Communications Engineering, 8(7): 896-903. (International Science Index, ISSN: 1307-6892).

Krachodnok P., Wongsan R., and Fhafhiem N. A Circularly Polarized Sector Antenna for Mobile Base Station Using Single Feed with Metallic Rod EBG. **Open Journal of Antennas and Propagation** (OJAPr). (Received)

International Conference Paper

Fhafhiem N. and Krachodnok P. (2014). A High Gain Omnidirectional Antenna Using Metamaterial Rods. **Electrical Engineering/Electronics, Computer, Telecommunications and Information Technology (ECTI)**.

Fhafhiem N., Krachodnok P., and Wongsan R. (2013). The Effective Directivity of Resonator Antenna Using Curved Strip Dipole. **Asia-Pacific Microwave Conference (APMC).**

Fhafhiem N., Krachodnok P., and Wongsan R. (2012). The Circularly Polarized Resonator Antenna Using Double Polarizing Metallic EBG. **Asia-Pacific Conference on Antennas and Propagation (APCAP).**

Fhafhiem N., Krachodnok P., and Wongsan R. (2012). Gain Improvement of Curved Strip Dipole Using EBG Resonator. **Progress in Electromagnetics Research Symposium (PIERS).**

Fhafhiem N., Krachodnok P., and Wongsan R. (2011). The Positional Effect of Array Curved Strip Dipole On Electromagnetic Band Gap Reflector Plane. **International Symposium on Antennas and Propagation (ISAP).**

Fhafhiem N., Krachodnok P., and Wongsan R. (2011). The 2x2 curved strip dipole antenna array on EBG reflector plane. **Electrical Engineering/Electronics, Computer, Telecommunications and Information Technology** (**ECTI).**

Design of a Dual Polarized Resonator Antenna for Mobile Communication System

N. Fhafhiem, P. Krachodnok, R. Wongsan

Abstract—This paper proposes the development and design of double layer metamaterials based on electromagnetic band gap (EBG) rods as a superstrate of a resonator antenna to enhance required antenna characteristics for the mobile base station. The metallic rod type metamaterial can partially reflect wave of a primary radiator. The antenna was designed and analyzed by a simulation result from CST Microwave Studio and designed technique could be confirmed by a measurement results from prototype antenna that agree with simulation results. The results indicate that the antenna can also generate a dual polarization by using a 45° oriented curved strip dipole located at the center of the reflector plane with double layer superstrate. It can be used to simplify the feed system of an antenna. The proposed antenna has a bandwidth covering the frequency range of 1920 – 2200 MHz, the gain of the antenna increases up to 14.06 dBi. In addition, an interesting sectoral 60° pattern is presented in horizontal plane.

Keywords—Metamaterial, electromagnetic band gap, dual polarization, resonator antenna.

I. INTRODUCTION

DUAL polarization antennas with sector-shaped radiation pattern are often required for the mobile communication systems. To radiate the dual polarized wave, two dipole antennas need to be used with dual feeding. They are placed on a reflector plane at ±45° angle and arrayed to improve the gain [1]-[4]; however, it is hard to fabricate the feed system. Even though the dipole antenna is still interesting in wireless communication systems, it has elementary structure, simple concept, and broadband characteristics [5]-[7]. One solution to enhance the gain of an antenna is using metallic reflector plane as shown in Fig. 1 (a). The metallic reflector is located at the back of a dipole antenna with gap as a quarter wavelength. Usually, the main disadvantage of an antenna on metallic plane is making the overall size of the antenna too big and bulky for the low frequency range of operations. Moreover, the reflector plane cannot suppress the surface wave, so an antenna gain and efficiency will then be greatly decreased [8]-[10]. Figs. 2 (a) and 3 (a) show radiation patterns of a curved strip dipole on reflector plane. Due to a 45° oriented primary radiator located over the reflector plane, its polarized waves values are equal in both x (horizontal) and y (vertical) axis with the maximum gain of 7.6 dBi at 2100 MHz. In this case, when a 45° oriented curved strip dipole on reflector plane has a positive effect on the pattern, it is leaving

N. Fhafhiem, P. Krachodnok, and R. Wongsan are with the School of Telecommunication Engineering, Suranaree University of Technology, Nakhonratchasima 30000, Thailand (e-mail: m5140732@g.sut.ac.th, priam@sut.ac.th, rangsan@sut.ac.th, respectively).

the beam at its centre.

In recent years, metamaterials based on electromagnetic band gap (EBG) structures have been widely investigated in the antennas domain to enhance gain and radiation efficiency. The metamaterials classified by a permittivity and permeability are primarily dependent on the geometrical properties of an inclusion shape and mutual distance between the lattices constant. EBG is not only used to a reflector plane [11]-[13], but also adapted for a superstrate of the primary radiator with reflector plane [14]-[17]. The main advantage of the EBG resonator is enhancing gain and efficiency. To confirm the advantage of the EBG resonator, we presented the radiating curved strip dipole antenna with cavity wall which is composed of single layer EBG as a superstrate and metallic reflector [18]. Unfortunately, few papers were proposing the EBG structures for polarization adjustment [19], [20].

In this paper, the metallic rods are used to a partially reflective surface (PRS) of a 45° oriented curved strip dipole located at the center of the reflector plane. The horizontal polarized partially reflective surface (PRS polar H) is placed above a primary radiator as shown in Fig. 1 (b). Not only it can improve the gain in horizontal polarization (as seen in Fig 2 (b)), but also the gain in vertical polarization is improved by using the vertical polarized partially reflective surface (PRS polar V) as shown in Figs. 1 (c) and 2 (c). A part from this, both of superstrate layers contribute to symmetrical radiation pattern of the antennas demonstrated in Figs. 2 (b), 2 (c), 3 (b) and 3 (c). Two layers of metallic rod type metamaterials, horizontal and vertical polarizations, are combined for dual polarization with high gain. However, the square antenna is not suitable and does not meet the requirements of the sector antenna element, in this paper; the antenna is reduced in size and added the vertical walls in yz plane for wide beamwith in horizontal plane.

II. PARTIALLY REFLECTIVE SURFACE STRUCTURE

In this paper, we firstly simulate the unit cell of metamaterial, a unit cell defined by parameters a_0, g_0, and t_0, shown in Fig. 4 (a). Aluminium rod is surrounded by four periodic boundaries. This model can be used to estimate the transmission and the reflection of the aluminium rods structure. The resonant frequency is determined by the parameter of the aluminium rod structure, especially by the width and thickness of rod structure. An aluminium rod structure is divided into polarized groups which are PRS horizontal polarization (PRS polar H) and PRS vertical polarization (PRS polar V). The PRS polar H and V structures resonating at 2100 MHz are designed and denoted in Figs. 4 (b) and 4 (c). The parameters

are optimized by using CST microwave studio. The aluminium rods are 1 mm and 6 mm thick, respectively, and the parameters are as follows: A_1 = 13.26 mm, A_2 = 3.85 mm, g_1 = 29.83 mm, g_2 = 46.42 mm and t_1 = t_2 = 530 mm. The S-parameters of the unit cell are simulated and then the S_{11} and S_{21} can be plotted in Fig. 5 (a). These results indicate that PRS structure is partially reflective surface, as shown in Fig. 5 (b).

Whenever the electromagnetic band gap becomes one of the several aluminium rods' functions, it works as a medium in the form of a superstrate. Figs. 5 (b) and 5 (c) demonstrate the propagation of electromagnetic fields which is passed through the medium. When the electromagnetic field propagates on the medium, the reflection and refraction wave occur.
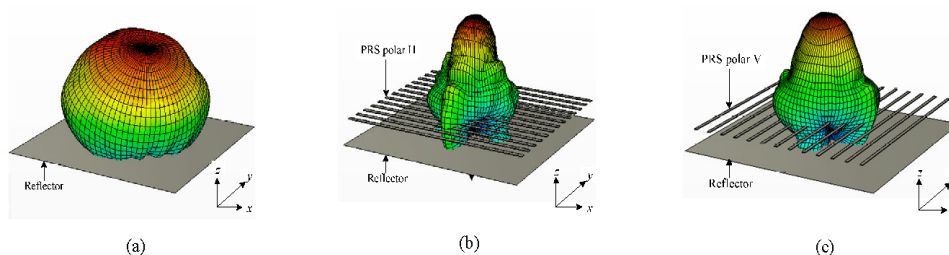

Fig. 1 3 D radiation patterns and structures of a 45° oriented curved strip dipole placed (a) over reflector plane with quarter wavelength, (b) between reflector and PRS polar H, and (c) between reflector and PRS polar V

Fig. 2 The xz plane of a 45° oriented curved strip dipole placed (a) over reflector with quarter wavelength, (b) between reflector and PRS polar H, and (c) between reflector and PRS polar V

Fig. 3 The yz plane of a 45° oriented curved strip dipole placed (a) over reflector with quarter wavelength, (b) between reflector and PRS polar H, and (c) between reflector and PRS polar V

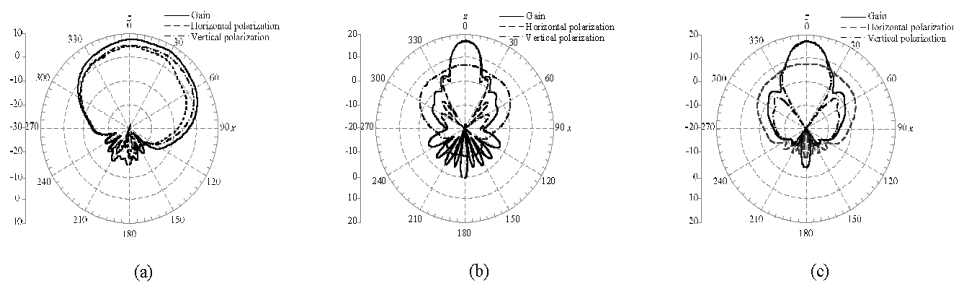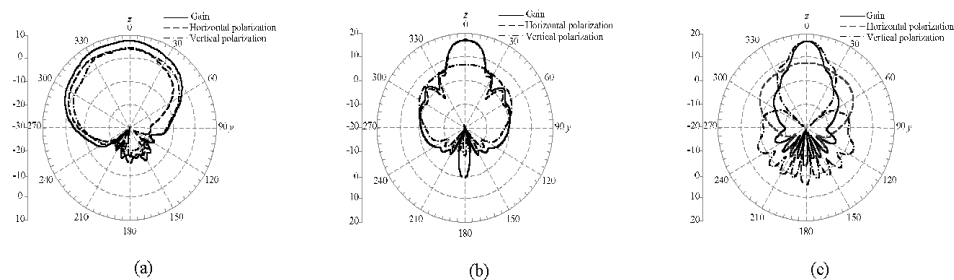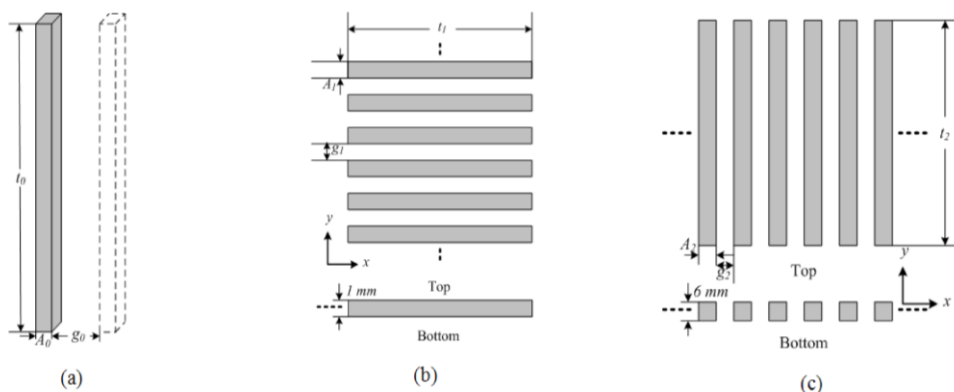Fig. 4 (a) Unit cell of PRS rod structure, (b) PRS polar H, and (c) PRS polar V
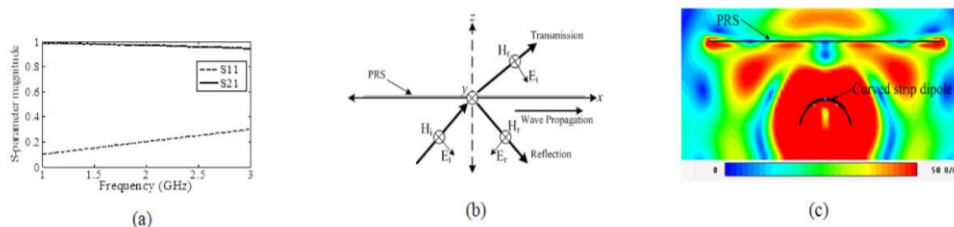

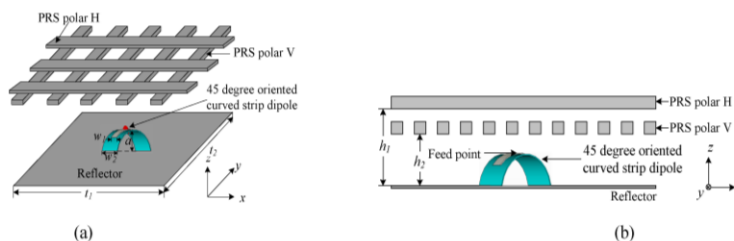Fig. 5 (a) the S-parameters of PRS, (b) wave propagation of PRS, and (c) near-field distribution

Fig. 6 Antenna configurations (a) 3D view and (b) side view of dual polarization square antenna. The center point of antenna is defined as the origin of coordinates
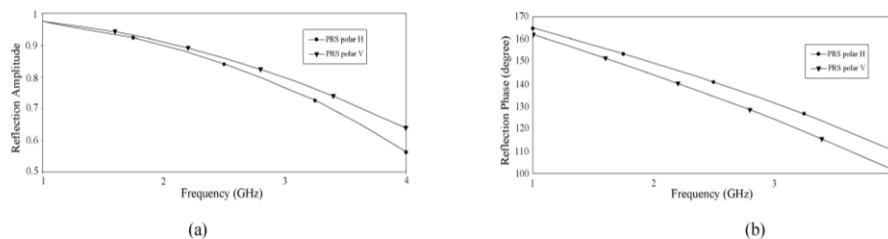

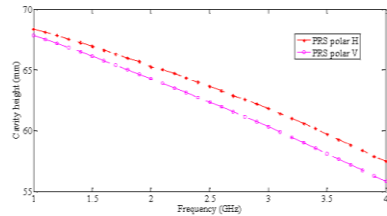Fig. 7 The reflection (a) amplitude and (b) phase of PRS

Fig. 8 Cavity height between the ground plane and superstrate

III. DESIGN OF DUAL POLARIZED RESONATOR ANTENNA

Fig. 6 shows the dual polarized resonator antenna which is excited by a curved strip dipole. It is oriented along $\phi = 45°$ direction and placed over the reflector plane with the height (a) of 0.2λ. The antenna is designed to work at 2100 MHz which is the same resonant frequency of PRS design in the last section. The appropriate parameters are $w_1 = 15$ mm, $w_2 = 30$ mm, $a = 34$ mm, and $L = 82.81$ mm. Besides, the cavity wall consisting of the reflector plane and double PRS layers in polar V and H, is necessary for the two transmitted components to process the equally amplitude. The reflection coefficient amplitude and phase of the PRS polar H and V versus the frequency are shown in Fig. 7. The cavity height (h) depends on the frequency which can be obtained through following relations (1),

$$h = \frac{c}{2f}\left[\frac{\phi_{EBG} + \phi_{PEC}}{360°}\right]. \tag{1}$$

where, the variables $c, f, \phi_{PEC},$ and ϕ_{EBG} are the speed of light, resonant frequency, and the reflection coefficient phase of reflector and EBG, respectively. Due to the relationship

between the reflection phase and (1), so the height h_1 is chosen to be 67 mm for the resonant frequency of 2100 MHz. According to our expectations of the dual polarized antenna, PRS polar V is added to the lower reflective wall with fix the cavity height (h_2) of 63 mm. If the cavity height (h parameter) is changed, Fig. 8 denotes that the resonant frequency is varied.

IV. RESULTS AND DISCUSSION

This section presents that there is a relation between a curved strip dipole with double PRS layers and the electric field level in x- and y-axis is presented. The antenna therefore can radiate the dual polarization. Almost all the parameters are taken from the antenna constructed for the experiment. Only the reflector plate size is assumed to be infinite. The calculated current is weak enough on the peripheral area out of $3\lambda \times 3\lambda$. As the simulated gain, it is around 18.52 dBi at the frequency of 2100MHz as shown in Fig. 9 (a). In addition, over the whole frequency band (2040 – 2180 MHz), the -3 dB directive gain could be obtained. The near-field distribution behavior on the PRS surface of the dual polarization square antenna is studied and indicated in Fig. 9 (b). Studying the electric field behavior between superstrate and primary radiator with reflector plane reveals that waves are refracted and reflected by PRS surface; therefore, the antenna can generate the high electric field level. The simulated radiation pattern of square resonator antenna is shown in Figs. 9 (c) and 9 (d), which has low side lobes. Because of the high requirements on base station antenna in cellular network, the most popular choices are the antennas with horizontal half power beamwidth of 60°. The optimum horizontal and vertical beamwidth is decided by the network architecture and propagation environment.
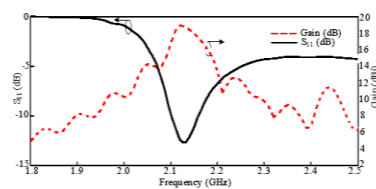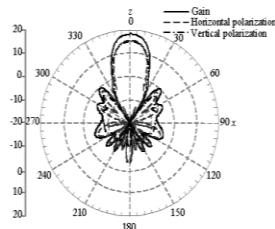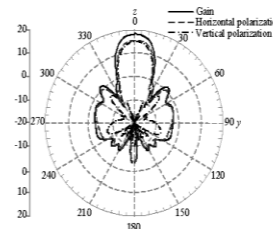

(a)
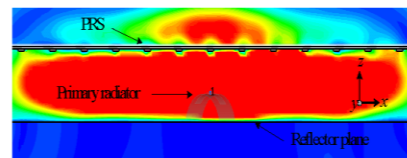
(b)

(c)

(d)

Fig. 9 Simulated results of square resonator antenna (a) gain and S_{11}, (b) near-field distribution, (c) radiation pattern in xz plane, and (d) radiation pattern in yz plane

TABLE I
SIMULATED RESULTS WHEN t_1 IS VARIED

t_1 (mm)	Gain (dBi)	HPBW (degree)
400	16.1	33.7
350	14.8	48.9
300	14.0	58.9
250	12.5	67.9

TABLE II
SIMULATED RESULTS WHEN t_2 IS VARIED

t_2 (mm)	Gain (dBi)	HPBW (degree)
530	13.3	58.9
650	14.2	56.2
750	14.3	57.5
850	14.1	60.1
950	15.0	59.0
1050	14.2	59.6

Consideration of Fig. 10 (a) concludes that if the square resonator antenna is reduced of t_1 = 400 mm, the pattern is rather symmetric and the beamwidth is wide. Therefore, t_1

parameter is reduced and has an effect on HPBW in horizontal plane, as shown in Fig. 10 (b). Because of the finite size of surface waves generated by the antenna on reflector plane, the maximum gain of the antenna is lower than square resonator antenna. Simulated gain and HPBW in xz plane are concluded in Table I. Although the pattern is symmetric at t_1 = 400 mm, the HPBW is not sufficient for the base station antenna. Therefore, the horizontal HPBW of 58.9° when t_1 = 300 mm is used. A side from this the yz radiation pattern is plotted in Fig. 10 (c); it has been already symmetric. To solve a problem in xz plane with h = 50 mm, vertical walls are installed in yz plane as shown in Fig. 11 (a). The parameters of PRS structure are described in section II. Five and nineteen metamaterial rods of PRS polar H and V structure, respectively, are used for a superstrate on reflector plane with vertical walls. To improve the directive gain, the length of antenna in y axis (t_2) is increased. Figs. 11 (b) and 11 (c) show the radiation pattern when t_2 is varied. It illustrates that the HPBW and the gain are suitable for the sector antenna, when t_2 is 950 mm, the simulated gain and HPBW in xz plane are concluded in Table II.
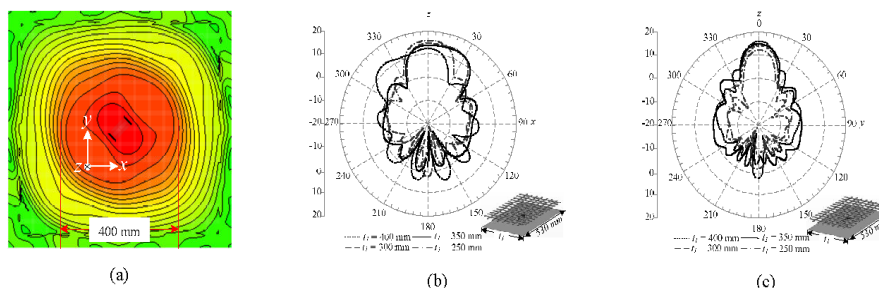

Fig. 10 Simulated results (a) current distribution on reflector plane at 2100 MHz, (b) radiation pattern in xz plane, and (c) yz plane when t_1 is varied
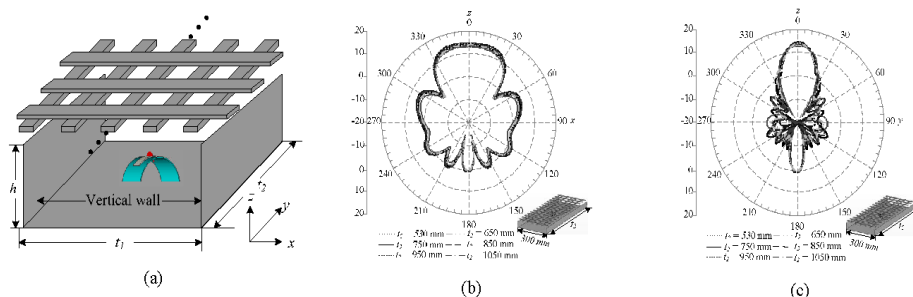
Fig. 11 (a) the geometry of sector antenna, (b) radiation pattern in xz plane, and (c) yz plane at 2100 MHz when t_2 is varied
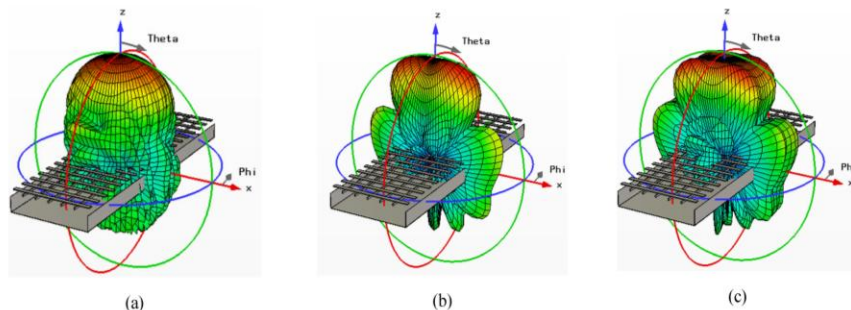
Fig. 12 3D simulated radiation patterns of dual polarization antenna with vertical walls at (a) 1920 MHz, (b) 2100 MHz, and (c) 2170 MHz

Fig. 13 The *xz* plane simulated radiation pattern of dual polarization antenna with vertical walls at (a) 1920 MHz, (b) 2100 MHz, and (c) 2170 MHz.

Fig. 14 The *yz* plane simulated radiation pattern of dual polarization antenna with vertical walls at (a) 1920 MHz, (b) 2100 MHz, and (c) 2170 MHz

Fig. 15 Simulated gain and S_{11} of the antenna with vertical walls

Fig. 16 Near-field distribution of the proposed antenna

901

Fig. 17 Photographs of the fabricated antenna

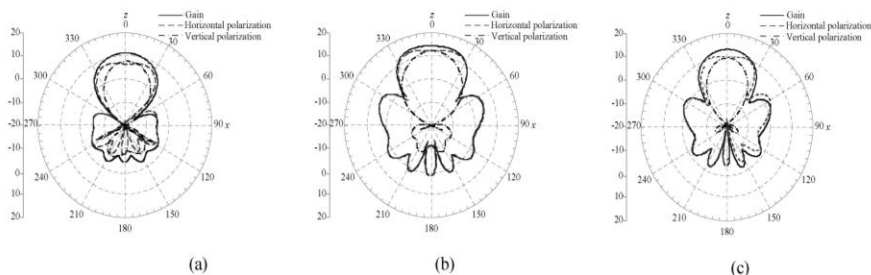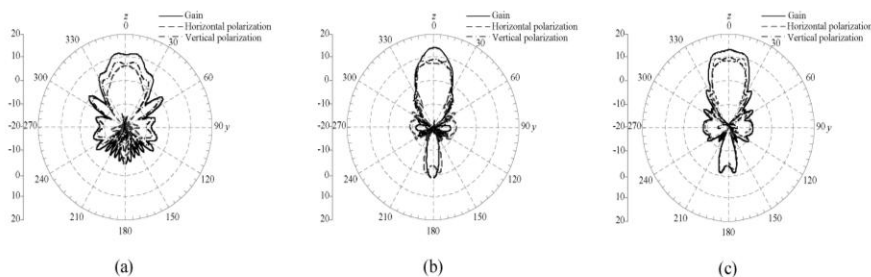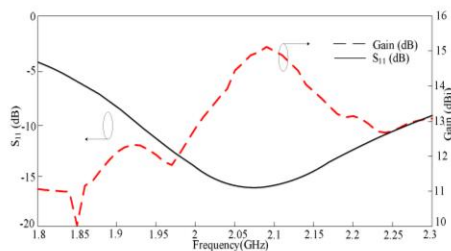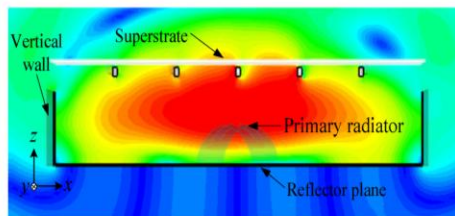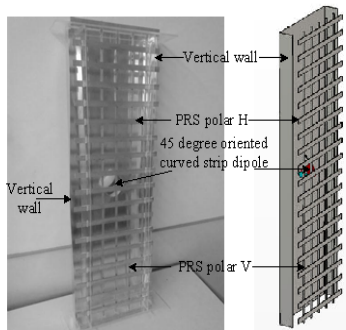To reveal the radiation characteristic of dual polarization antenna in the whole operating bandwidth, the 3D radiation patterns of the proposed antenna at 1920 MHz, 2100 MHz, and 2170 MHz are also simulated and shown in Figs. 12-14. The antenna beam in horizontal plane (xy plane) is wide. These results illustrate the excellent sectoral properties of the antenna. In the vertical plane the radiation is directive with low side lobe, and in the horizontal plane these figures present an interesting sectoral pattern of 60°. The simulated gain is around 15 dBi at the frequency of 2100 MHz as shown in Fig. 15. In addition, over the whole frequency band (1920–2170 MHz), the -3 dB directive gain could be obtained. Moreover, the vertical walls can control the surface wave at the edge and corner, therefore the wave is redirected to the z direction, as shown in Fig. 16.

To verify the performance of the antenna, an antenna prototype has been fabricated as shown in Fig. 17. Corresponding radiation patterns and realized gains of the proposed antenna were measured in the anechoic antenna chamber located at the Suranaree University of Technology (SUT). In this manner, the normalized output power would be resembled in Fig. 18. This plot shows the agreement between the measured and the simulated results in both horizontal and vertical plane patterns. The measured HPBWs in horizontal plane are 51.1°, 60°, and 50° at 1920 MHz, 2100 MHz, and 2170 MHz, respectively. Moreover the measured HPBWs in vertical plane are 30.8°, 17.9°, and 32.5° at 1920 MHz, 2100 MHz, and 2170 MHz, respectively. The half-power beamwith in horizontal plane is suitable for 3G mobile base station. Fig. 19 shows the measured gain of the proposed antenna. It can be seen that the gain of the antenna is around 14 dBi for either polar V or polar H at working range of frequency. The similar radiation and gain enhance the efficiency of mobile communication systems.

In addition, some specifications from experiment are compared with the ones from simulation as shown in Table III. As we can see, the experiment results have a good agreement with the ones from simulation results. Also, the proposed antenna obtained half-power beamwidth in horizontal and vertical planes and directive gain.

TABLE III
SPECIFICATION OF THE PROPOSED ANTENNA

Electrical Data	Simulation	Measurement
Material	Aluminium	Aluminium
Frequency band (MHz)	2100 (1920-2170)	2100 (1920-2200)
Polarization	dual	dual
HPBW (degree)	H:60 V:17.9	H:60 V:20
Gain (dBi)	15	14.06
Antenna size (mm)	950×300×50	950×300×50
Antenna weight (kg)	-	2.7
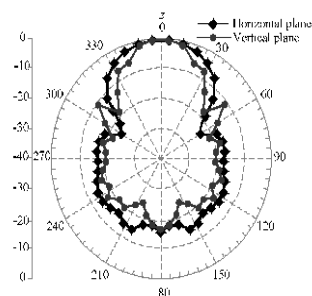
(a)
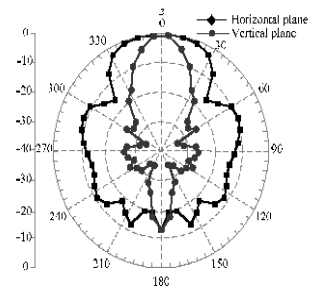
(b)
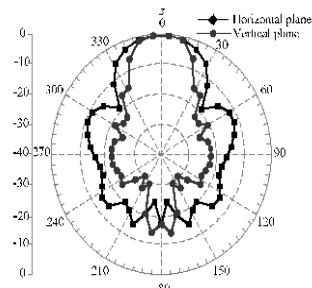
(c)

Fig. 18 Measured radiation pattern of the proposed antenna with vertical walls at (a) 1920 MHZ, (b) 2100 MHz, and (c) 2170 MHz
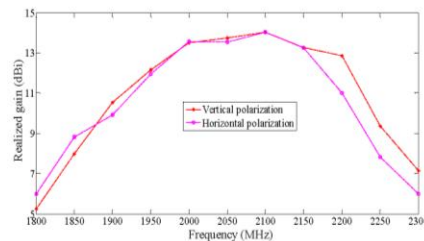
Fig. 19 Measured gain of the proposed antenna

V. CONCLUSIONS

Dual polarized resonator antenna using double polarizing metallic EBG layers with reflector plane and the vertical wall have been developed. It is found that using the double layer of metallic rod type metamaterials above a $45°$ oriented curved strip dipole provides a dual polarization antenna with the gain of 14.06 dBi. Attractively, if vertical walls are placed along yz plane, a symmetrical and sectoral radiation pattern (HPBW around $60°$) can be obtained. Moreover, the proposed antenna has a simple structure and low cost, it is generally required in mobile communication systems.

ACKNOWLEDGMENT

REFERENCES

[1] Y. Liu, A.-T. Bu, E. S. Li, D. M Fu, L. Y. Xiao, "A new dual polarization dipole antenna." *International Conference on Microwave and Millimeter Wave Technology*, pp. 5-7. 2004
[2] K. M. Mak, H. Wong, K. M. Luk, "A shorted bowtie patch antenna with a cross dipole for dual polarization." *IEEE Antennas and Wireless Propag.* Lett. 6, pp. 126 – 129. 2007.
[3] A. Abas, A. Asrokin, R. H. Basri, N. Jamlus, "Dual-polarized dipole array antenna for CDMA 450 base station application." *IEEE Asia-Pacific Conference on Applied Electromagnetics (APACE)*, pp. 1-4. 2010.
[4] Y. Liu, H. Yi, H. Liu, S. Gong, "A novel dual-polarized dipole antenna with compact size for wireless communication." *Progress In Electromagnetics Research C*, 40, pp. 217-227. 2013.
[5] L. Han, R. Ma, X. Chen, W. Zhang, "Compact dual-band dipole antenna fed by a coplanar waveguide." *International Conference on Microwave and Millimeter Wave Technology (ICMMT)* pp. 1-3. 2012.
[6] M.Z. Azad, M. Ali, "Novel Widebawd directional dipole antenna on a mushroom like EBG structure." *IEEE Trans. on Antennas and Propag.* Vol. 5(56), pp. 1242 – 1250. 2008.
[7] Z. Zhang, M.F. Iskander, J.C. Langer, J. Mathews, "Wideband dipole antenna for WLAN." *IEEE Antennas and Propagation Society International Symposium*, pp. 1963-1966. 2004.
[8] A. Thumvichit, T. Takano, "Ultra low profile dipole antenna with a simplified feeding structure and a parasitic element." *IEICE Trans. Communications*, E89-B(2), pp. 576-580. 2006.
[9] L.Zhan, Y.Rahmat-Samii, "PBG, PMC and PEC ground plane: A case study of dipole antenna." *IEICE Trans. Communications*, pp. 674–677. 2000.
[10] N. Fhafhiem, P. Krachodnok, R. Wongsan, "A shorted-end curved strip dipole on dielectric and conducting plane for wireless LANs," *International Symposium on Antenna and Propagation (ISAP)* pp. 835-838. 2009.
[11] N. Fhafhiem, P. Krachodnok, R. Wongsan, "Curved strip dipole antenna on EBG reflector plane for RFID applications," *WSEAS Transection on Communications*, 6(9), pp. 374-383. 2010.
[12] F.Yang, Y.Rahmat-Samii, "Electromagnetic band gap structures in antenna engneering." *USA by Cambridge University Press,* New York 2009.
[13] M. Grelier, C. Djoma, M. Jousset, S. Mallegpl, A. C. Lepage, X. Begaud, "Axial ratio improvement of an archimedean spiral antenna over a radial AMC reflector." *Appl. Phys. A* 109(3), pp. 1081-1086. 2012.
[14] S. Chaimool, C. Rakluea, P. Akkaraekthalin, "Mu-near-zero metasurface for microstrip-fed slot antennas." *Appl. Phys. A* 112(3), pp. 669-675 2013.
[15] E. Rodes, M. Diblanc, E. Arnaud, T. Monediere, B. Jecko, "Dual-band EBG resonator antenna using a single-layer FSS." *IEEE Antennas and Wireless Propag.* Lett. 6, pp. 368–371. 2007.
[16] M. Hajj, R. Chantalat, B. Jecko, "Design of a dual-band sectoral antenna for Hiperlan2 application using double layers of metallic electromagnetic band gap (M-EBG) materials as a superstrate." *International Journal of Antennas and Propag.*, pp. 1 – 5 2009.
[17] G. V. Trentini, "Partially reflecting sheet array." *IRE Trans. on Antennas and Propag.* 4(4), pp. 666 – 671. 1956.
[18] N. Fhafhiem, P. Krachodnok, R. Wongsan, "Gain improvement of curved strip dipole using EBG resonator." *Progress In electromagnetics research symposium proceedings (PIERS)* pp. 1631 – 1634. 2012.
[19] L. Peng, C. L. Ruan, L. Z. Qiang, "A novel compact and polarization-dependent mushroom-type EBG using CSRR for dual/triple-band applications." *IEEE Microwave and Wireless Components Letters*. 20(9), pp. 489 – 491. 2010.
[20] Q. Wu, C.P. Scarborough, B.G. Martin, R.K. Shaw, D.H. Werner, E. Lier, X. Wang, "A ku-band dual polarization hybrid-mode horn antenna enabled by printed-circuit-board metasurfaces." *IEEE Trans. on Antennas and Propag.* 61(3), pp. 1089 – 1098. 2013.

Nuchanart Fhafhiem received the B.Eng. and M. Eng. degrees in telecommunication engineering from Suranaree University of Technology in 2007 and 2009, respectively. At present, He Studying doctoral's degree in telecommunication engineering at Suranaree University of Technology, Thailand. Research interests include antenna design.

Piyaporn Krachodnok graduated with the Bachelor Degree of Engineering in Telecommunication Engineering in 1996 from Suranaree University of Technology (SUT), Thailand, M.Eng. (Electrical Engineering), Chulalongkorn University, Bangkok, Thailand in 2001, and D.Eng.(Telecommunication Engineering), Suranaree University of Technology (SUT), Thailand in 2008 and had worked at this University for a year. Experiences & Expert are Electromagnetic Theory, Microwave Engineering, and Antenna Engineering.

Rangsan Wongsan received B.E. degree in Electronic Engineering from Rajamongala Institute of technology, Theves, and M.E. degree in Electrical Engineering from King Mongkut's Institue of Technology, North Bangkok, Thailand, in 1989, in 1994, respectively. He is currently working toward the Ph.D. degree in Electrical Engineering of King Mongkut's Institute of Technology, Ladkrabang, Thailand. In October 1994 he joined the school of Telecommunication Engineering, Institute of Engineering at Suranaree University of Technology (SUT), Thailand. His research focus is on electromagnetic theory and antenna system for several applications.

The Circularly Polarized Resonator Antenna using Double Polarizing Metallic EBG

N. Fhafhiem, P. Krachodnok, and R. Wongsan
School of Telecommunication Engineering, Institute of Engineering,
Suranaree University of Technology, Nakhon Ratchasima, Thailand
E-mail: m5140732@g.sut.ac.th, priam@sut.ac.th, and rangsan@sut.ac.th

Abstract—The high gain circularly polarized antenna has been investigated, using double polarizing metallic EBG and excitation with a 45° oriented curved strip dipole placed on a ground plane. The electromagnetic band gap (EBG) characteristic is partially reflecting surface (PRS) in x and y axis, which is improved on the electric field of the both polarizes. In this paper consisted in improving the antenna design and characteristics. Ultimately, an antenna was studied at 2.5 GHz with the 19.04 dB gain. The axial ratio remains lower than 3 dB at the resonant frequency.

Keywords-curved strip dipole; circularly polarized antenna; cavity wall; electromagnetic band gap

I. INTRODUCTION

With the rapid development of the wireless communication, the requests for circularly polarized antenna have increased. Many different designs of circularly polarized antenna have already been studied and there are currently developed in antenna research laboratories. To design the circularly polarized antenna the traditional antenna type is designed by the classic theory of microstrip antenna with two feed probes [1]. Moreover, the dipole can be oriented along $\phi = 45°$ direction on EBG ground plane [2] or with polarizer and metallic EBG antenna [3]. In this paper, the double polarizing metallic EBG layers and conductor plane are used for the cavity model of the curved strip dipole antenna, improving the radiation field in Polar V and Polar H.
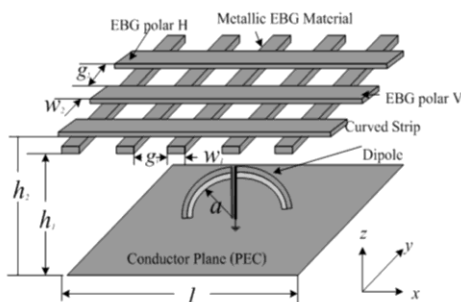

Figure 1.   The proposed antenna.

II. THE CIRCULARLY ANTENNA DESIGN

The radiation mechanism of the circularly polarized resonator antenna which is excited by a curved strip dipole is shown in Fig. 1, the dipole is oriented along $\phi = 45°$ direction and its height of 0.2λ over the PEC ground plane is vary small. Furthermore, the analysis model of the cavity wall consists of the PEC ground plane and double EBG layers in polar V and polar H. This half EBG material has to fulfill the necessary conditions to obtain a polarizing effect and an EBG effect at the same time. Another one is necessary for the two transmitted components to process the same amplitude. The metallic EBG Polar H is made up of 13 metallic rods of $591 \times 13.3 \times 10$ mm^3 and the gap between rods is 29.8 mm. The metallic EBG polar V is composed of 13 metallic rods of $8.4 \times 591 \times 10$ mm^3 and the gap between rods is 34.6 mm. Finally, the cavity height which is the distance between the upper and the lower reflective wall of 55-mm is illustrated in Fig. 3.

III. SIMULATION AND DISCUSSION

In this work, we used an excitation of a 45° oriented curved strip dipole cooperated double polarizing metallic EBG to design the circularly polarized antenna as illustrated in Fig. 1. Because the metallic EBG redirect the partially of field, moreover, the partially of fields are transmitted, so it is optimized at center frequency to have a high directivity and the total field is very well.

When the 45° oriented curved strip dipole antenna is positioned in the center of the PEC ground plane and the single layer of the EBG polar V is used to the upper partially reflective wall, the reflection coefficient phase of the EBG polar V versus the frequency are shown in Fig. 2. The cavity height depend on the frequency can be obtained through following relations (1),

$$h = \frac{c}{2f}\left[\frac{\phi_{EBG} + \phi_{PEC}}{360^o}\right]. \qquad (1)$$

So, the height h_2 is chosen to be 57 mm for the resonant frequency of 2.5 GHz. According to our expectations of the circularly polarized antenna, EBG polar H is added to the upper reflective wall, which we fix the cavity height (h_1) of 55 mm. Therefore, the reflection phase of EBG polar H is calculated of 143° and then the upper wall is designed. With the self-

polarizing EBG, it is possible to generate a 90° phase shift after transmission through the structure and the two transmitted components are processed the same amplitude thus generating circular polarization from the linear one. The simulated antenna gain is shown on Fig. 3. As desired, it is around 19.04 dB at the frequency of 2.45 GHz. On the same figure, the S_{11} is dreadful, as can be expected with this kind of antenna. It is therefore absolutely necessary to use a matching system which won't affect the electromagnetic characteristics. In addition, Fig. 4 shows the axial ratio of the antenna. Over the whole frequency band (2.43-2.61 GHz), the 3 dB axial ratio could be obtained. The E- and H-plane radiation patterns at 2.5 GHz are shown in Fig. 5, which the HPBW in the vertical and horizontal planes are around 18°and 18.5°, respectively. The patterns have low side lobes, so we can estimate that the antenna is circularly polarization.

IV. CONCLUSION

The simulation results of a 45° oriented curved strip dipole using the cavity wall, double polarizing metallic EBG layer and PEC ground plane, for circularly polarized antenna is presented improvably directive gain. It is successful to improve the gain of 19.04 dB because of the qualifications of cavity wall. The EBG polar V and polar H redirect the partially of field, moreover, the partially of fields are transmitted, so the total field is very well.
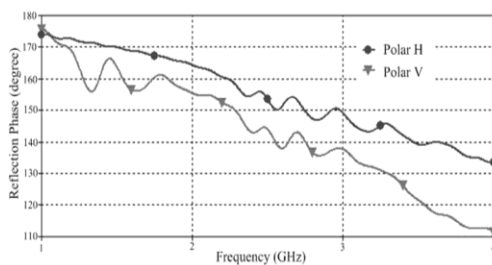

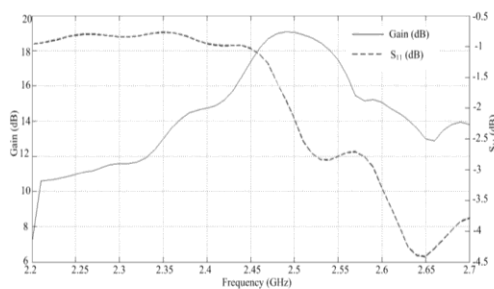Figure 2. The reflection phase of the EBG polar H and polar V.
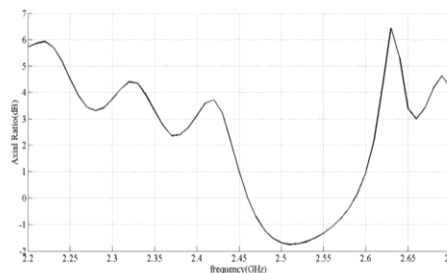

Figure 3. Simulated antenna gain and S_{11}.

Figure 4. Axial Ratio.

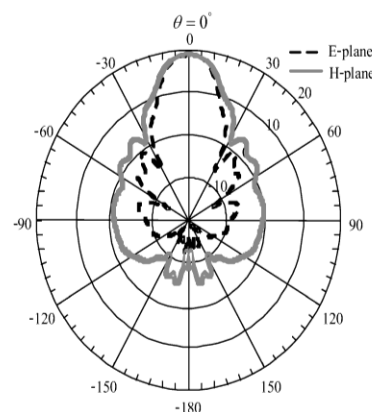Figure 5. Radiation Patterns.

REFERENCES

[1] M. Hajj, T. Monediere, B. Jecko and R. Chantalat, "A novel design of circularly polarized sectoral M-PRS Antenna," Antenna Technology and Applied Electromagnetics & the American Electromagnetics Conference (ANTEM-AMEREM), 2010 14th International Symposium, Canada, pp. 1–4, July 2010.

[2] Y. Fan and Y. Rahmat-Samii., "A low profile single dipole antenna radiating circularly polarized waves,"*IEEETran. Antennas Propag.*, Vol. 53, pp. 3083–3086, September 2005.

[3] E. Arnaud, R. Chantalat, M. Koubeissi, T. Monediere M. Thevenot and B. Jecko, "Improved Self Polarizing Metallic EBG Antenna," Antennas and Propagation, EuCAP 2009. 3rd European Conference, Germany, pp.3813–3817, 2009.

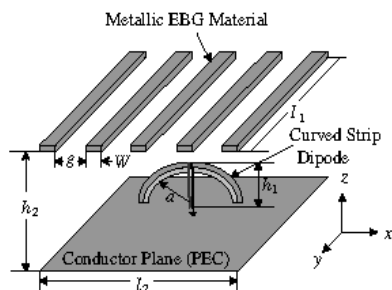PIERS Proceedings, Kuala Lumpur, MALAYSIA, March 27–30, 2012

Figure 1: Configuration of the curved strip dipole using EBG resonator.
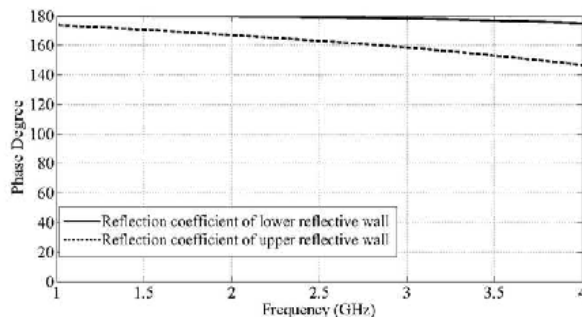

Figure 2: The reflection coefficient.

Table 1: The data of the curved strip dipole using EBG resonator.

Parameter	Size (λ)
w_1	0.082λ
w_2	0.25λ
L_d	0.425λ
a	0.159λ
W	0.075λ
g	0.179λ
$h1$	0.248λ
$h2$	0.627λ
l_1	1.141λ
l_2	1.164λ

3. NUMERICAL SIMULATIONS RESULTS

The objective of this paper is to increased directive gain of the curved strip dipole for application in RFID technology at 2.45 GHz. From optimized analysis, the good matching of this antenna could be obtained. As the resulting, the curved strip dipole antenna has a low gain of 1.5 dB and the HPBW in E-plane is 95.3°. It has omnidirectional radiation pattern, so the power may be loss to unnecessary place.In order to solve such problems, the cavity wall is used for improve the gain of the curved strip dipole antenna. The first step consists in designing an EBG with a resonant frequency corresponding to the microwave band around 2.45 GHz. Fig. 2 is illustrated the reflection coefficient phase of the upper and lower reflective wall by using the periodic boundary condition [7]. The cavity height has a relations with reflection coefficient of cavity wall, where is based on the following reaction (1)

$$h = \frac{c}{2f} \left[\frac{\phi_{PEC} + \phi_{EBG}}{360°} \right] \tag{1}$$

where, the variables c, f, ϕ_{PEC}, and ϕ_{EBG} are the speed of light, resonant frequency, and the reflection coefficient phase of PEC and EBG, respectively. Because the combination of phase should be $2n\pi$, so the cavity height could be obtained. Fig. 3 shows the height variations versus the frequency. It appears that a cavity height of 56.8-mm is proper resonant frequency which complies with the requirements of RFID reader for ETC.

We can calculate the h parameter is 56.8-mm because the upper and the lower reflective wall are simulated separately by using the periodic boundary condition. Fig. 4 shows the return loss at $h = 56.8$-mm, which is mismatch between the curved strip dipole antenna and the cavity. In case of the specialty dipole, the effect of reflection coefficient phase is not only in almost feed center but also in two arms of dipole, the h parameter is adjusted the gain as shown in Table 2. The cavity height of 76.8-mm has the most directive gain of 9.3 dB. In Fig. 4, we found that the proposed
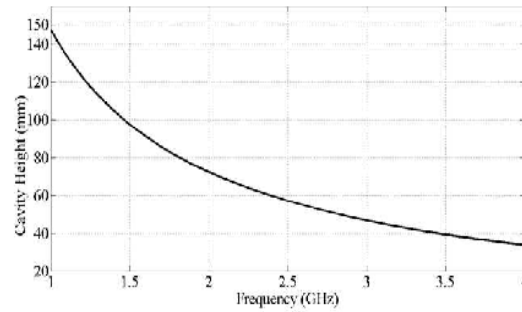
Progress In Electromagnetics Research Symposium Proceedings, KL, MALAYSIA, March 27–30, 2012 1633

Figure 3: Calculation of cavity height.
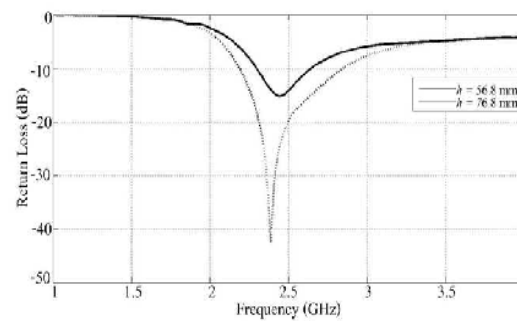

Figure 4: Return loss.
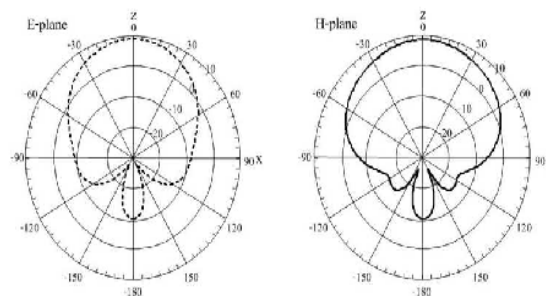
Figure 5: Radiation pattern.

Table 2: The optimizing of cavity height.

h (mm)	Gain (dB)	HPBW (degree)	
		E-plane	H-plane
56.8	7.6	77.1	104.8
61.8	8.13	72.7	91.1
66.8	8.6	67.8	80.9
71.8	9.1	62.8	74.1
76.8	9.3	59.1	71.4
81.8	9.2	57.1	71.3

antenna still exhibits a return loss batter than $-10\,$dB in resonant frequency band. The E- and H-plane radiation patterns at 2.45 GHz are shown in Fig. 5, which is directive. The patterns have low side lobe, so we can estimate that the structure volume is will dimensioned.

4. CONCLUSION

The simulation results of curved strip dipole by using the cavity wall for improve the gain have been presented in this paper. It is utilized to place at the RFID reader for checkpoint at high-way that collects fees from many cars at 2.45 GHz. Then the modeling software (CST Microwave Studio), it is successful to improve the gain of 9.3 dB because of the qualifications of cavity wall. The PEC redirects half of the radiation into the opposite direction. In addition, the EBG wall increases the gain and redirects the radiation too, as far as the radiation can be radiate to the user's zone. Moreover, it has been structure uncomplicated and inexpensive that demand on equipment for wireless communication system. The band of frequency is covered 2.2–2.58 GHz in microwave frequency band.

ACKNOWLEDGMENT

REFERENCES

1. Xianming, Q. and N. Yang, "2.45 GHz circularly polarized RFID reader antenna," *The Ninth International Conference ICCS*, 1189–1192, Krakow, Poland, Jun. 2004.
2. Lei, C., S. Yan, and H. Yang, "Study and design of modified fractal antenna for RFID application," *ISECS International Colloguium*, 8–11, Vancouver, Canada, Aug. 2009.
3. Fhafhiem, N., K. Piyaporn, and W. Rangsan, "High directive gain antenna using shorted-end curved strip dipole on electromagnetic band gap," *PIERS Proceedings*, 840–844, Xi'an, China, Mar. 22–26, 2010.
4. Fhafhiem, N., K. Piyaporn, and W. Rangsan, "A shorted-end curved strip dipole on dielectric and conducting plane for wireless LANs," *The International Symposium on Antenna and Propagation*, 835–838, Bangkok, Thailand, Oct. 2009.
5. Rodes, E., M. Diblanc, E. Arnaud, T. Monediereand, and B. Jecko, "Dual-band EBG resonator antenna using a single-layer FSS," *IEEE Antenna and Wireless Propagation Letter*, Vol. 6, 368–371, 2007.
6. Hajj, M., E. Rodesand, and T. Monediere, "Dual-band EBG sectoral antenna using a single-layer FSS for UMTS application," *IEEE Antenna and Wireless Propagation Letter*, Vol. 6, 368–371, 2007.
7. Fan, Y. and Y. Rahmat-Samii, *Electromagnetic Band Gap Structure in Antenna Engineering*, USA Cambridge University Press, New York, 2009.

BIOGRAPHY

Miss Nuchanart Fafiem was born in Lopburi, Thailand, in 1986. She graduated with the Bachelor Degree and Master Degree of Engineering in Telecommunication Engineering in 2007 and 2010 respectively from Suranaree University of Technology, Nakorn Ratchasima, Thailand. Then she is currently pursuing her Ph.D program in Telecommunication Engineering, School of Telecommunication Engineering, Suranaree University of Technology. Her current research interests concern the design, simulation, and testing of resonator antenna, electromagnetic band gap, and metamaterials.